Up-regulation of Hedgehog signalling in satellite cells and skeletal muscle regeneration

By:

Kamalliawati Mohd Imran

A thesis submitted in partial fulfilment of the requirements for the degree of
Doctor of Philosophy

The University of Sheffield
Faculty of Science
Department of Biomedical Science

Submitted on the 1st of November 2018

Abstract

About half of the human body mass is comprised of skeletal muscles, a component of the musculoskeletal system involved in maintaining body posture, gait and locomotion. Additionally, skeletal muscles have essential function in glucose metabolism and thermoregulation. Thus, maintenance of skeletal muscle homeostasis is critical for the health of organisms. Satellite cells are muscle-specific stem cells responsible for postnatal growth, regeneration upon injury, and maintenance of skeletal muscle homeostasis. Satellite cell's activity is regulated by a sophisticated network of signalling pathways, which act in a combinatorial manner to regulate satellite cell expansion and differentiation, and to preserve a pool of stem cells during the life course of skeletal muscles. Many of these signalling pathways are known to operate during embryonic myogenesis and are re-activated in adult myogenesis. One such signalling pathway, Sonic hedgehog (Shh) signalling, controls several aspects of myogenesis in the embryo and previous studies have indicated that it plays a role in adult myogenesis. However, it remains unclear whether Shh signalling acts upon satellite cells or non-myogenic resident cells. This study builds on previous work in the lab showing that Shh signalling is cell-autonomously required in satellite cells for efficient muscle regeneration. Through a combination of *ex vivo* and *in vivo* genetic approaches, I demonstrated that up-regulation of Shh signalling increased the proliferation of satellite cells by accelerating their entry into cell cycle and progression through the cycle program. Up-regulation of Shh signalling in satellite cells altered also the balance between self-renewal and differentiation, by promoting asymmetric cell division at the expense of symmetric cell division. Given the involvement of Shh signalling in tumour development in other systems and in skeletal muscle tumours i.e. Rhabdomyosarcoma (RMS), the present study may provide novel insights into the role of Shh signalling in the pathogenesis of RMS through the deregulation of satellite cell homeostasis.

Acknowledgement

Bismillahirrahmanirrahim……

First, I would like to say Alhamdulillah (All praise to Allah) for his grace and mercy on me throughout this beautiful yet impossible journey for 4 years. This journey, achievement, thesis and dedication were possible only and solely just because of you Papa, and just for you. The valuable lessons you thought, fearless, focus, determination, confidence, honesty, and staying true were the recipe of this Ph.D. The sacrifices you did for love (me) will be embedded always in this piece of work. Yes Pa, education is indeed priceless! It would be a different experience if you were here of course, but I am sure you can feel it. I missed you so very much, especially when the days seem unbearable.

I would like to express my gratitude to my Honours project's supervisor in Melbourne, Dr Jarrod Church, for spotting that capacity in me and sparked the interest on doing a PhD 6 years ago.

I am very much thankful to Dr Anne-Gaelle Borycki for being the kind of supervisor, boss, colleague and listener I never could have imagine. What would I do with my 4-years PhD without you, Anne-Gaelle. If I am able to come to the stage of writing acknowledgement now, it's only because of you.

I also would like to say thanks to my PhD advisors, Prof Steve Winder and Dr Matt Towers for the suggestions and useful insights on my project. Thanks also to Dr Marysia Placzek and Dr Andy Furley for the technical assistance and sharing the facilities in the lab. I'm also glad throughout these 4 years I got to meet good friends around the department that makes life in the lab less stressful.

The biggest thanks also has to go to the Malaysian people, government and MARA for the scholarship paid to make this journey possible from I was 16 years old. Long 14 years of association and living on your money is definitely significant.

I also want to thank all previous members of the Borycki Lab Hayyati Jaafar, Daniele Ranaldi and special mention to Dr Sara Cruz for the invaluable coaching, training, support and assistance during my early days in the lab. Sara Cruz was my PhD mentor indeed.

To the masters and undergraduate students: Ubaidillah, Hira Khan, Sophie Oakley, Kistina Mohamed, Rebecca Williams, James Sellar, Jack Henry, Constantinos Demetriou, Joe Woodley, Aisya Wahid and Oishee Rahman.. Thank you for the respect, jokes, trust, warmth and acknowledgement you guys gave me. I learnt a lot by being a mentor too!

Life in Sheffield would be very dull and intolerable without the Malaysian community and friends here. Thanks to PMPMS and SMSA for the community events held and Malaysian food! I need to say a huge thanks to my Malaysian friends here. Mira you will always be the UK housemate forever. The Telekong Cakap-Cakap (Nad, Harz, Ella, Zati, Mun, Asdya,

Ejok, TIqah, kak Nor, Fatin, Dhiya) you guys are the most supportive, sporting, chill, entertaining, accommodating, chatty and hilarious bunch of cracked PhD students I can never live without. To my Greenian buddies, the love, care and support I got from you guys kept me going in a positive vibe. Thanks so much peeps!

To Akim, the journey to the UK for PhD started with you, and now ending with you too! I don't even know how did we become this 'PhD buddies' but yes the journey wouldn't be possible without you being 'the friend'. I am lucky to have you with me like a team from start to finish.

Kak Sue, thanks so much for your love and care, thanks to all the confidence and support you and your family gave to me that I can actually make the dream comes true!

Last and most importantly, thank you so very much to my big big family! Pathi, Sitpa, Sinemma, Jsri, Govi, Kayshu and the Palani's, you guys are the amazing people I am priviledged to call family. Abang and Kak Elmy, thanks for the trust and confidence in me. Ma, thanks a lot.

To my husband, the word thank you is too small compared to your contributions in my PhD. Thanks for being on-board! It would definitely be a different journey if I did not have you around. I am sorry I dragged you into this suicide attempt but you pulled us out with dignity. I am sure my dad would have said many thanks to you for sustaining the torture we both started

Table of Contents

List of Figures

List of Tables

List of Abbreviation

β-gal	- Beta galactosidase
α-SG	- Alpha-sarcoglycan
β-TrCP	- Beta-transducin-repeat containing protein
4EBP1	- Eukaryotic translation initiation factor 4E (eIF4E)-binding protein 1
AJ	- Adhesive junction
Akt	- Protein kinase B
AMPK	- AMP-activated protein kinase
ANGPT1	- Angiopoietin 1
aPKC	- Atypical protein kinase C
AraC	- Cytosine beta D-arabinofuranoside
ARF	- ADP ribosylation factor
aRMS	- Alveolar rhabdomyosarcoma
ASPA	- Animals (Scientific Procedures) Act 1986
ATP	- Adenosine Triphosphate
BCC	- Basal cell carcinoma
bFGF	- Basic fibroblast growth factor
BMP	- Bone morphogenetic protein
BMPR	- Bone morphogenetic protein receptor
Boc	- Brother of Cdo
Boi	- Brother of Ihog

BrdU - Bromo-deoxyuridine

Brm - Bharma

c-Met - Tyrosine-protein kinase Met

Ca^{2+} - Calcium ion

CalcR -Calcitonin receptor

CD - Cluster of differentiation

CDC6 - cell division cycle 6

Cdk - Cyklin-dependent kinase

CDKN - Cyclin-dependent kinase inhibitor

Cdo - Cell-adhesion molecule-related, down-regulated by oncogenes

CEP164 - entrosomal protein of 164 kDa

Ci - cubitus interruptus

CiA - Ci activator

CiR - Ci repressor

CK - Creatine kinase

CK2 - Casein kinase 2

CKI - Cyclin kinase inhibitor

Ckm - Creatine kinase (muscle)

CRC - Colorectal cancer

CRD - Cysteine-rich domain

CreERT2 - Cre-Estrogen receptor type 2

CSA - Cross sectional area

CTX - Cardiotoxin

CXCR - Chemokine receptor

DAPC - Dystrophin-associated protein complex

Dhh - Desserted hedgehog

Dll1 - Delta-like ligand 1

DMD - Duchenne Muscular dystrophy

DNA - Deoxyribonucleic acid

DPI - Days post-injury

DTA - Diphtheria toxin fragment A

DTR - Diphtheria toxin receptor

ECM - Extracellular Matrix

EDL - Extensor digitorum longus

EdU - 5-Ethynyl-2´-deoxyuridine

ER - Endoplasmic reticulum

ERK - Extracellular signal-regulated kinases

eRMS - Embryonal rhabdomyosarcoma

FACS - Fluorescence-activated cell sorter

FADD - Fas-associated protein with death domain

FAP - Fibroadipogenic cell

FBS - Foetal bovine serum

FGFR - Fibroblast growth factor receptor

FN - Fibronectin

FoxO1 - Forkhead box protein O1

Fu - Fused

FUCCI2- Fluorescent ubiquitylation-based cell cycle indicator

Gαi2 - Adenylyl cyclase inhibitor 2

GANT-61 - Gli antagonist 61

GAP - Growth-associated protein

GBS-GFP - Gli Binding site-green fluorescent protein

GDF - Growth differentiation factor

GFP - Green Fluorescent protein

Gli - Glioma-associated protein

GliA - Gli activator

GliR - Gli Repressor

GNP - Granular neuron progenitor cells

GPI - Glucose phosphate isomerase

GRMD - Golden Retriever muscular dystrophy

GSK-3β - Glycogen synthase kinase-3 beta

HDACi - Histone deacetylase Inhibitor

HHAT - Hedgehog Acyltransferase

HINGS - Heat-inactivated goat serum

HSC - Hedgehog signalling complex

HSC - Hemopoietic stem cell

HSPG - Heparan sulphate proteoglycan

IFN-γ - Interferon gamma

IFT - Intra-flagellar transport

IGF-1 - Insulin-like growth factor 1

Ihh	- Indian hedgehog
Ihog	- Interference hedgehog
IL	- Interleukin
iPSC	- Induced pluripotent stem cell
JNK	- c-Jun N-terminal kinase
KIF	- Kinesin-like protein
LacZ	- Lactose operon Z
LRC	- Label-retaining cell
M-line	- Middle line
MAPK	- Mitogen-activated protein kinases
MARK2	- Microtubule affinity-regulating kinase 2
MASTR	- Myocardin family of transcriptional activator
MB	- Medulloblastoma
MD	- Muscular dystrophies
MDC1A	- Muscular dystrophy type 1A
MEF2	- Myocyte enhancer factor 2
MEK	- Mitogen-activated protein kinase kinase
miR	- MicroRNA
MKK	- Mitogen-activated protein kinase kinase
MLC	- Myosin light chain
MLC3F	- Myosin light chain 3F
MLL	- Mixed lineage leukemia protein-1
MMP	- Matrix metalloproteinase

MPC - Myogenic progenitor cell

MRF - Myogenic regulatory factor

MRF4 - Myogenic regulatory factor 4

MRTF-A - Myocardin-related transcription factor A

MSC - Mesenchymal stem cell

mTORC1 - Mammalian target of rapamycin complex 1

Myf5 - Myogenic factor 5

MyHC - Myosin heavy chain

MyoD - Myoblast determination protein 1

NBCCS - Nevoid basal cell carcinoma syndrome

NCAM - Neural cell adhesion molecule

NF-κB - Nuclear factor kappa B

NICD - Notch1 intracelullar domain

NMJ - Neuromuscular Junction

NO - Nitric oxide

ODF2 - Outer dense fiber protein 2

OSM -Oncostatin M

PAR - Proteinase-activated receptor

Pax3 - Paired box protein 3

Pax7 - Paired box protein 7

PBS - Phosphate-buffered saline

BSA - Bovine serum albumin

PBST - Phosphate-buffered saline-Tween

PCNA - Proliferating cell nuclear antigen

PCP - Planar cell polarity

PDGF - Platelet-derived growth factor

PDGRα - Platelet-derived growth factor receptor A

PFA - Paraformaldehyde

PH3 - Phospho-histone 3

PHT - PBS-HINGS-Triton

PI3K - Phosphoinositide 3-kinase

PIC - PW^+ interstitial cell

Pitx2 - Paired like homeodomain 2

PKA - Protein kinase A

PRMT - Protein arginine methyltransferase

Ptc - Patched (*Drosophila*)

Ptch - Patched (mammalian)

R26R - ROSA26

RB1 - Retinoblastoma protein 1

RBP-Jκ - Recombination signal binding protein for immunoglobulin kappa J region

RBPJ - Recombination signal binding protein for immunoglobulin kappa J region

RMS - Rhabdomyosarcoma

ROS - Reactive oxygen species

RT - Room temperature

SAG - Smoothened agonist

SC - Satellite cell

Sca-1 - Stem cell antigen 1

SDF-1 - Stromal cell-derived factor 1

SDH - Succinate dehydrogenase

SEM - Standard error of mean

Sema3A - Semaphorin-3A

SEMA3B - Semaphorin 3B

Shh - Sonic hedgehog

Smo - Smoothened

Smo -M2- constitutively active smoothened

SP - Side population

SR - Sarcoplasmic reticulum

SSD - Sterol-sensing domain

SuFu - Supressor of Fused

SW1/SNF - Switching defective/sucrose non-fermenting complex

TA - Tibialis Anterior

TAK1 - Transforming growth factor-activated kinase 1

Tg - Transgenic

TGF-β - Transforming growth factor beta

TNF-α - Tumour necrosis factor-alpha

TRAF6 - Tumor necrosis factor receptor-associated factor 6

Vangl2 - Van Gogh-like protein 2

VCAM - Vascular cell adhesion molecule

VEGF - Vascular endothelial growth factor

WIF - Wnt inhibitor factor

WNT - Wingless/intergrated

WT - Wild type

YFP - Yellow fluorescent protein

ZPA - Zone of polarising activity

1 INTRODUCTION

1.1 Skeletal muscle: Structure and Function

1.1.1 Overview of the structure of skeletal muscles

Skeletal muscle represents up to 40% of the total human body mass. It is a contractile tissue within the musculoskeletal system responsible for maintaining body posture, motion and movement. Skeletal muscles also possess important roles in thermoregulation and metabolism by regulating glucose and amino acid storage (Richter et al., 1982; Argiles et al., 2016).

Skeletal muscles attach to bones via connective tissue structures known as tendons (Fig 1.1). Each muscle has an origin (the proximal end) and an insertion (the distal end), although many muscles have more than one site of insertion and result in multiple movements from a single contraction. At a microscopic level, the architecture of skeletal muscle demonstrates a remarkable degree of organisation. A connective tissue, which is continuous with tendons and makes up the outer layer enclosing a muscle is called the epimysium (Lieber, 2002) (Fig 1.1). Encapsulated in the epimysium, lie numerous muscle bundles termed fascicles, each surrounded by the perimysium (Lieber, 2002) (Fig 1.1). The space between the perimysium and fascicles is filled with blood vessels, lymphatic vessels and motor neuron axons (Saladin, 2018). Fascicles contain the muscle fibres enclosed by another layer of connective tissue called the endomysium (Fig 1.1). Many other non-myogenic cells reside also in the muscle fascicles, including fibroblasts, endothelial cells and immune cells (Pannerec et al., 2012; Gopinath and Rando, 2008). Muscle fibres (also called myofibres) are multinucleated cells surrounded by a cellular membrane called the sarcolemma (Fig 1.1). They consisting mostly of densely packed protein bundles named myofibrils, which are the functional contractile unit of muscles (Hanson and Huxley, 1953). Thus, nuclei are pushed at the periphery of the fibre, adjacent to the sarcolemma. Neuromuscular junctions (NMJs) are specialised regions where neuron axon terminals connect with muscle fibres to allow

electrical and chemical stimulation from the nervous system to be transduced to the myofibre, in a process called excitation-contraction coupling (McElhanon and Bhattacharya, 2018).

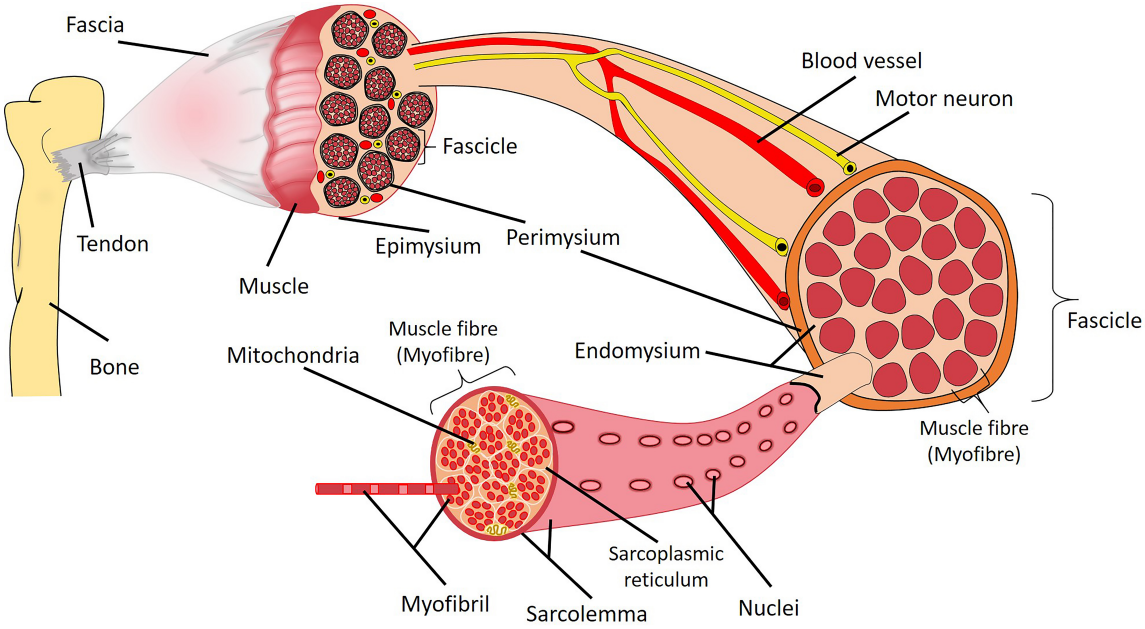

Figure 1.1: Structural organisation of skeletal muscle.
Skeletal muscles are attached to the bone via tendon that extends to a dense connective tissue layer called fascia. Skeletal muscles are surrounded externally by a collagenous layer called the epimysium. The internal muscle bundles (fascicles) are packed together by the perimysium and supplemented with blood vessels and neurons. Myofibres consist of myofibrils that are intercepted by sarcoplasmic reticulum and covered by sarcolemma internally and surrounded by the endomysium externally.

The sarcolemma acts as a barrier separating intracellular content from the extracellular environment, including the basement membrane, a specialized mesh-like extra-cellular matrix (ECM) structure. Dystrophin-associated protein complex (DAPC) is a crucial transmembrane protein complex embedded within the sarcolemma that maintains the integrity of the sarcolemma during muscle contraction by linking the intracellular cytoskeleton to the basement membrane. Genetic mutations in genes coding for DAPC components result in muscular dystrophies (MD) characterised by the progressive weakness and loss of muscle tissue (Emery, 2002). Duchenne muscular dystrophy (DMD) is the most common dystrophy, and represents more than 50% of all dystrophy cases (Towler et al., 2004). DMD is a X-linked recessive disease caused by the mutation in gene coding for Dystrophin (Emery, 2002).

1.1.2 The myofibre contractile machinery

Myofibrils within myofibres are held together and anchored to other organelles including the sarcolemma and mitochondria by intermediate filaments. Desmin is the main protein in intermediate filaments, and it functions in providing a structural support to allow an efficient mechanical coupling and force transduction between myofibrils (Capetanaki et al., 2007). Myofibrils are wrapped around by a specialised form of endoplasmic reticulum called sarcoplasmic reticulum (SR), which functions as storage compartment for calcium ions (Ca^{2+}). Upon depolarization of the sarcolemma, Ca^{2+} is released from the sarcoplasmic reticulum to induce muscle contraction (Lehman et al., 2009). Myofibrils length could extend up to 30cm (an entire muscle cell length) and are arranged in a series of basic contractile units known as sarcomeres, approximately 10, 000 sarcomeres in a myofibril (Fig 1.2) (Martini et al., 2015). A mammalian sarcomere has an average length of 2µm and can shorten about 70% of its length during contraction (Au, 2004).

A sarcomere is divided into few regions; the darker, central region is called the A-band flanked by lighter regions I-band (Fig 1.2). The A-bands contain myosin filaments and the I-bands have actin filaments starting at the Z-disk and overlap at the end of the myosin filaments in the A-band. The H zone is the central part of A-band that does not have actin filaments (Fig 1.2) (Squire, 2016). During contraction, the length of A-band remains constant but the I-band and H-zone shorten. Sarcomeres contains two basic structures that are responsible for muscle contraction, the actin (thin) filament and the myosin (thick) filament (Fig 1.2) (Huxley and Hanson, 1959). Actin and myosin filaments are arranged in anti-parallel manner between two Z-disks, giving skeletal muscle its striated appearance (Squire, 2016). This orientation allows the sliding of actin filaments along myosin filaments to generate contraction. Myosin is tethered in the middle of a sarcomere to the M-line by a protein called titin, whereas actin is anchored to the Z-disk by α-actinin (Fig 1.2) (Au, 2004). Titin is an elastic filament that extends through half of a sarcomere from Z-disk to M-line, functions as an elastic spring that regulate the physiological range of sarcomere stretching during sarcomeric contraction by poising Myosin filament back to the center of sarcomere after a contraction cycle (Martini et al.,

2015). Titin binds to Z-disk via nebulin, α-actinin and telethonin and attaches to M-line by myosin binding protein C, myomesin and few inserted sequences with Titin-kinase domains (Fig 1.2) (Kotter et al., 2014; van der Ven and Furst, 1997).

A contraction begins when an ATP is bound to the myosin head and hydrolysed to ADP and inorganic phosphate. This causes the myosin head to extend and attach to its binding site on actin, forming a cross bridge. An action called power stroke is triggered, allowing myosin to pull the actin filament towards the M-line thereby shortening the sarcomere (Huxley, 1957). Muscle contractions are regulated by Ca^{2+}. The actin filaments are associated with regulatory protein called troponin and tropomyosin. When muscles are relaxed, tropomyosin blocks the myosin binding sites on actin. When Ca^{2+} level is above threshold and ATP is present, Ca^{2+} binds to troponin which then displaces tropomyosin, exposing the myosin binding site on actin (Wakabayashi, 2015).

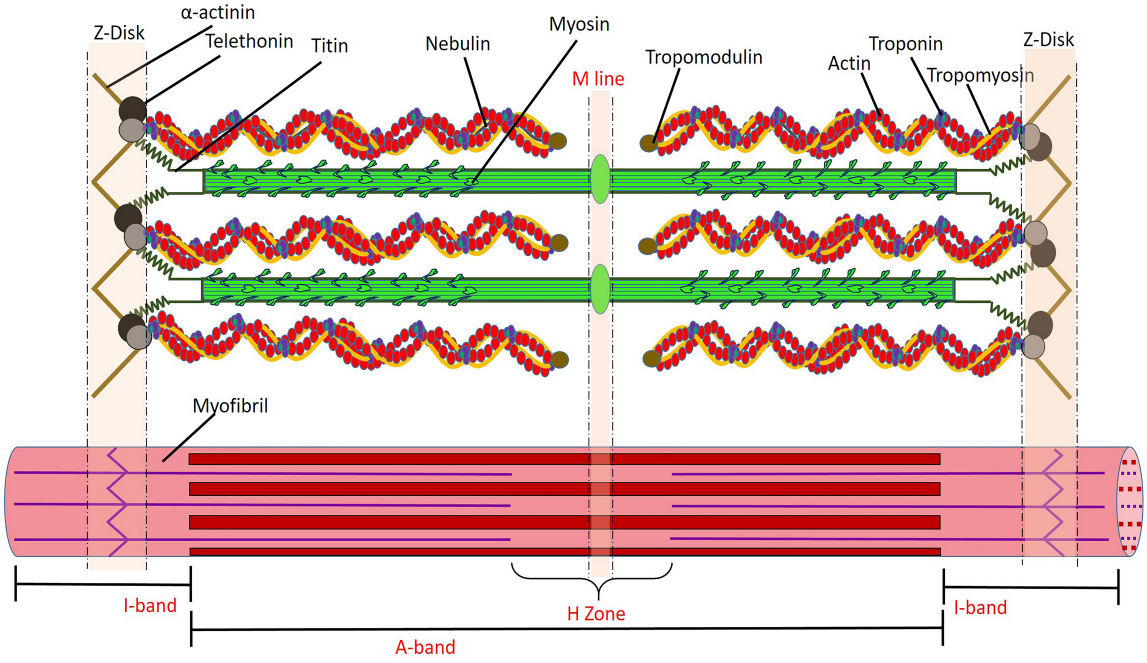

Figure 1.2: Sarcomere is the basic contractile unit of myofibril.
Sarcomere is made of thin filaments of Actin and thick filaments of Myosin, and extends between two Z-disks made of α-Actinin and Telethonin. The thin filaments are attached to the Z disk via Nebulin and contain Troponin and Tropomyosin that regulate Actin binding to Myosin head. Myosin are arranged in anti-parallel pattern and attached to the M line. Titin functions in connecting the M line to the Z-disk. The A-band refers to the area containing Myosin and the I-band refers to the two adjacent sarcomeres that only contain Actin filaments. The H zone is the mid line area where thick and thin filaments do not overlap.

1.1.3 Muscle fibre types dictate the electro-physiological status of muscles

The heterogeneity in muscle fibres is predominantly caused by the different isoforms of myosin heavy chain (MyHC) they express. Four types of muscle fibres exist, which are slow-oxidative (type I), fast-oxidative type (IIa), fast-glycolytic (type IIb) and intermediate (type IIx). They differ in their function, metabolism, contractility and molecular aspects. Type I fibres are fatigue-resistant, slow twitch fibres that contain high levels of Succinate dehydrogenase (SDH) enzymes, representing oxidative metabolism (Khodabukus and Baar, 2015) The high content of mitochondria and myoglobins due to denser capillaries in type I fibres give then their 'red' appearance. Their lower speed of shortening during contraction with lower force partially contributes to their higher resistance to fatigue in addition to its metabolism. Type I-containing muscles are generally implicated in sustained vital activities such as breathing (diaphragm muscle) (Schiaffino and Reggiani, 2011). All type II fibres are fast twitch fibres and carry out activities that require higher speed and stronger muscle contraction such as limb muscles. Type IIa fibres are fast twitch fibres that contain a mixture of both oxidative and glycolytic enzymes, whereas type IIb fibres contain mostly glycolytic enzymes. Type II fibres have lower amount of mitochondria and myoglobin (blood vessels) due to their glycolytic metabolism and they appear 'white'. This type of fibres has lower resistance to fatigue (Schiaffino and Reggiani, 2011). Type IIx fibres have an intermediate phenotype in between Type IIa and IIb in terms of their contraction force, speed and fatigue resistance (Schiaffino and Reggiani, 2011).

The distribution of fibre types within an organism is determined post-natally according to the activity of associated motor neurons. However, fibre type is also influenced by other factors, such as hormones, exercise, aging, weight and diseases like diabetes. For instance, upon endurance training like long distance running, fast-twitch fibres switch from glycolytic type IIb fibres to oxidative type IIa fibres (Qaisar et al., 2016). This modulation of fibre types by physical activity is termed muscle plasticity.

1.1.4 Many distinct cell types populate skeletal muscles

Skeletal muscles are rich in blood vessels, capillaries, and nerve terminals. In addition, other non-myogenic cells reside in skeletal muscles, including immune cells namely neutrophils, mast cells, macrophages and dendritic cells (Fig 1.3). The interstitial space is also filled with a variety of cells such as endothelial cells, pericytes, mesoangioblasts, $PW1^{+}$ interstitial cells (PICs) and fibrogenic cells including fibroblasts and fibro-adipogenic progenitors (FAPs), and endothelial cells (Fig 1.3) (Kharraz et al., 2013).

Non-myogenic muscle resident cells have essential role in supporting myofibres during normal physiological conditions. They have also a critical function during injury and muscle repair, the detail of which will be described later. For instance, mast cells patrol within the interstitium as a sensor for distress or damage and dendritic cells are antigen-presenting cells that capture and process foreign antigen during septic injury to activate T lymphocytes (Wiendl et al., 2005; Bentzinger et al., 2013a). Neutrophils are the first type of immune cells to dominate the injury site and stimulate necrosis by releasing factors such as TNF-α (Peake et al., 2017). Macrophages and neutrophils play an important role by removing debris after injury. In addition, macrophages release chemokines and cytokines that attract immune cells from the circulatory system to initiate muscle repair and stimulate satellite cell function (Bentzinger et al., 2013a).

Cells from the vasculature including endothelial cells, pericytes and mesoangioblasts support muscle plasticity during repair and growth by secreting factors such as VEGF to stimulate the formation of both new capillaries and new myofibres (Fig 1.3) (Christov et al., 2007). Pericytes and mesoangioblasts have a unique ability to differentiate into endothelial cells and myocytes to support skeletal muscle regeneration. However, in some disease setting such as diabetes, their function is impaired (Hayes et al., 2018). Fibroblasts and FAPs play an important function in building the ECM. Fibroblasts secrete ECM proteins like Collagen and Fibronectin that are deposited in the ECM (Charge and Rudnicki, 2004). FAPs are progenitor cells historically known for their ability to differentiate into fibroblasts and adipocytes. Thus, they contribute to fat deposition in muscular dystrophies and sarcopenia (Pagano et al., 2018). However, recent studies have shown that FAPs differentiation into adipocytes

can be prevented by disrupting primary cilia, and this improves the recovery of skeletal muscles after injury (Kopinke et al., 2017; Arrighi et al., 2017).

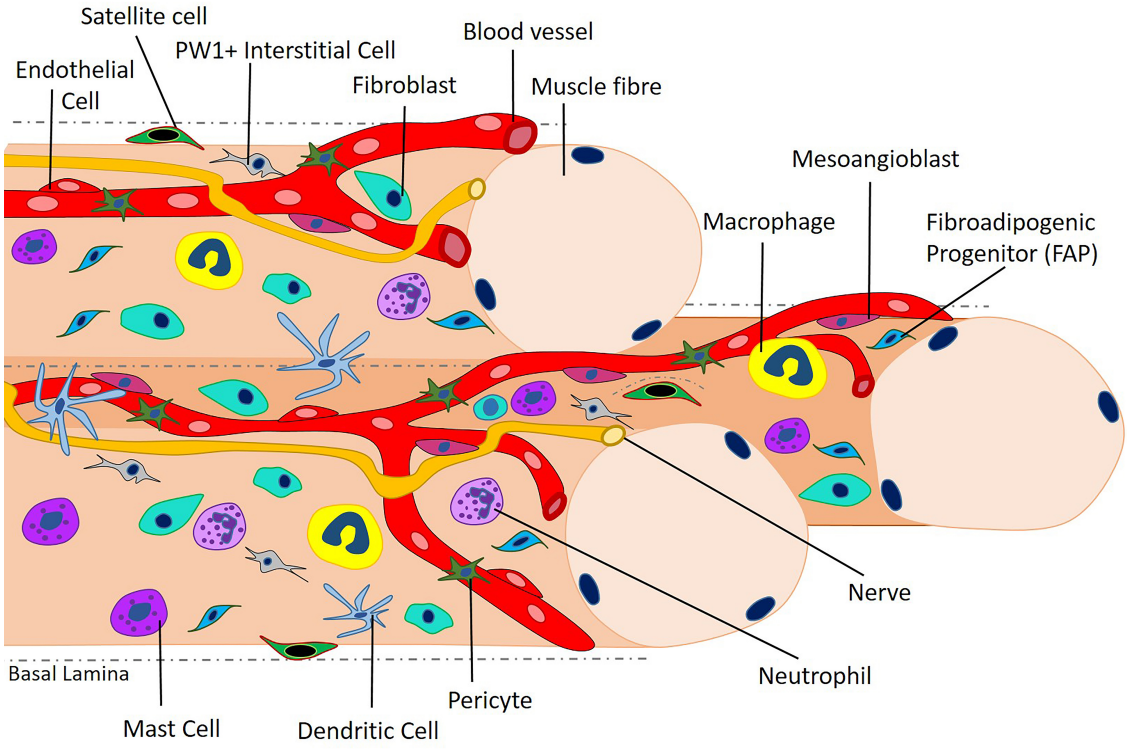

Figure 1.3: Different types of cells reside within the skeletal muscle.
Skeletal muscle tissue is made up of multinucleated muscle fibres that harbour myogenic stem cells called satellite cells beneath their basal lamina. Blood vessels and nerves are inserted in the interstitial space in between the fibres and are associated with other cells types including endothelial cells, mesoangioblasts and pericytes. Interstitial space is also filled with PW1+ interstitial cells, fibroblasts, fibroadipogenic progenitors (FAPs) and immune cells (macrophages, neutrophils, dendritic cells and mast cells).

1.2 Satellite cells are indispensable for skeletal muscle repair

1.2.1 The cellular characteristics of satellite cells in skeletal muscle

Alexander Mauro first described satellite cells (SC) in 1961 using electron microscopy of a tibialis anticus (TA) muscle of a frog. SCs are located at the periphery of muscle fibres, sandwiched between the plasma membrane (sarcolemma) and the basement membrane of the muscle fibre, which contributed to their name, 'satellite'. SCs are mononucleated cells with an elongated spindle-like shape in normal muscles. SCs are distinguishable from myonuclei because of their large nucleus with small cytoplasmic volume relative to the nucleus (Mauro, 1961). Freshly isolated SCs contain few mitochondria suggesting a low metabolic activity consistent with their dormant state during physiological homeostasis (Schultz et al., 1978). SCs in adult myofibres are identified by the expression of Pax7, a member of the paired box transcription factor family responsible for the specification of myogenic progenitor cells (MPCs) in embryos to the satellite cell lineage (Seale et al., 2000). SCs are sparsely scattered throughout muscle fibres, with 5-7 cells per fibre observed. SCs consist of only 2-5% of the total nuclei in adult muscles, albeit accounting for about 30% of sublaminar cells at birth (Charge and Rudnicki, 2004). However, the number of SCs varies with the muscle type, fibre type, age, and species (Bischoff and Heintz, 1994; Charge and Rudnicki, 2004). Slow-twitch muscles such as soleus muscle have at least twice more SCs compared to fast-twitch muscles like extensor digitorum longus (EDL) muscle (Zammit et al., 2002). Despite being just a small fraction of the muscle cell population, SCs have the ability to robustly proliferate and differentiate into functional myocytes to repair damaged muscles following traumatic injuries, degenerative diseases such as dystrophy, and exercise.

1.2.2 The origin of satellite cells during embryogenesis

Skeletal muscle arises from the paraxial mesoderm, a thick band of mesodermal cells flanking the neural tube (Buckingham, 2001). It forms the cranial mesoderm in the cranial region, the source of cranio-facial muscles. In the trunk region, the paraxial mesoderm forms somites in an antero-posterior manner (Buckingham, 2001). Somites are sphere-shaped groups of cells that give rise to the sclerotome (precursor of cartilage) and the dermomyotome (precursor of the dermis and myotome). The sclerotome gives rise to cartilage and bones of the axial skeleton, and the dermomyotome forms the dermatome and myotome (Chal and Pourquie, 2017). The myotome gives rise to skeletal muscles of the trunk, while limb muscles are derived from the lateral compartment of the dermomyotome. Somitic cells are initially multipotent and become committed to specific lineages in response to signals from surrounding tissues such as the dorsal ectoderm, neural tube, the notochord and lateral mesoderm (Buckingham, 2001). For instance, Sonic hedgehog (Shh) a morphogen produced by the notochord and floor plate induces ventral somitic cells to a sclerotomal lineage by downregulating *Pax3* and upregulating *Pax1* and *Nkx3.2* expression (Murtaugh et al., 1999), and simultaneously acts on dorsal somitic cells to induce a myogenic cell fate by inducing *Myf5* expression, an early myogenic differentiation factor (Borycki et al., 1999).

Epithelial cells in the dermomyotome express Pax3, a paired-box transcription factor that labels muscle progenitor cells in the somite, and some express a closely related paired-box transcription factor, Pax7 (Fig 1.4) (Relaix et al., 2005). During primary myogenesis (E10.5-E12.5 for mouse and E3-E7 in chick), Pax3-positive muscle progenitor cells induce the sequential expression of the myogenic regulatory factors (MRFs), beginning with Myf5 and subsequently followed by MyoD and then MRF4 and Myogenin (Fig 1.4) (Chal and Pourquie, 2017). The first evidence of myogenesis during embryonic development is the activation of Myf5 by the *Pax3*-expressing cells in dorsomedial lip of the somites. These cells give rise to myocytes, a differentiated muscle cells expressing myogenic cytoskeletal proteins including *Myh7, Myh3, Acta1*, *MyHC and Desmin* (Lyons et al., 1990). A subset of the Pax3/Pax7-expressing muscle progenitor cells do not engage with myogenesis and instead contribute to the pool of muscle-

specific adult stem cells –the satellite cells (Fig 1.4) (Relaix et al., 2006). Two studies using Pax3-GFP/+:Pax7-LacZ/+ reporter mice reported dividing β-gal^{+}/GFP^{+} cells that did not express myogenic markers as early as at stage E.10.5 in the central domain of the dermomyotome, and by E.15.5 these Pax3^{+}/Pax7^{+} progenitor cells localised along differentiated myofibres and became surrounded by a basal lamina (Kassar-Duchossoy et al., 2005; Relaix et al., 2005). Between E16.5 and E18.5, Pax3+/Pax7+ cells were observed in a satellite cell position outside the muscle fibres and under the basal lamina (Kassar-Duchossoy et al., 2005; Relaix et al., 2005). Together, these data evidenced that SCs arise from uncommitted Pax3^{+}/Pax7^{+} progenitor cells located in the central dermomyotome during embryogenesis, and in the course of secondary myogenesis (E14.5-E17.5 in mouse and E8+ in chick) they home to their final niche location, outside the muscle fibre under the basal lamina.

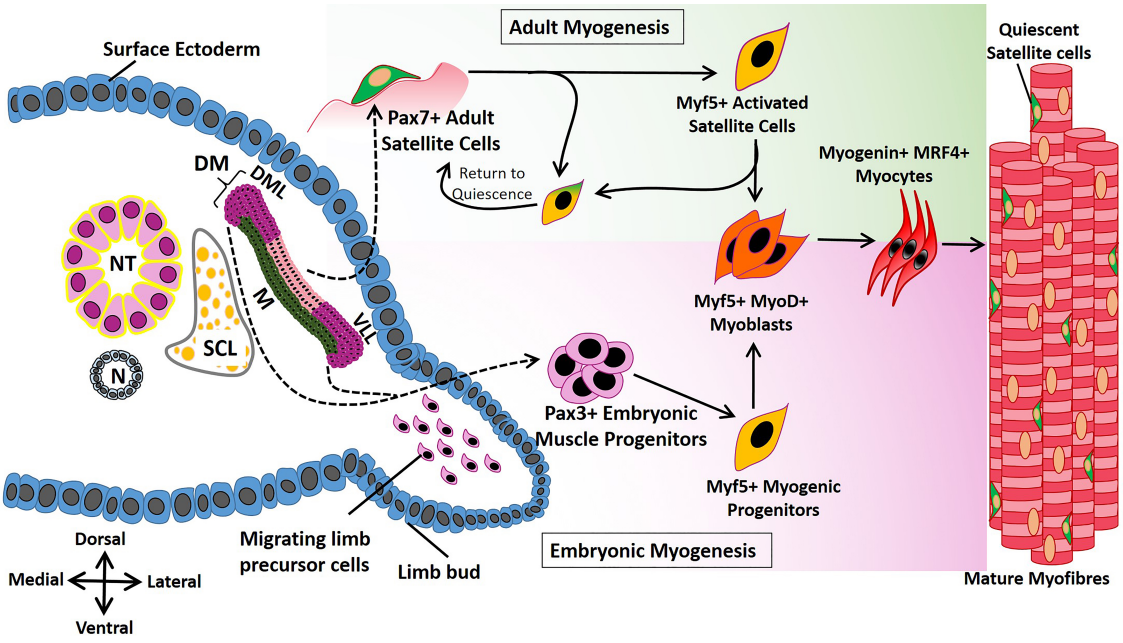

Figure 1.4: Schematic representation of embryonic and postnatal adult myogenesis.
During embryogenesis, somites subdivide to give rise to sclerotome (SCL) and dermomyotome (DM) that further differentiate into dermatome and myotome (M) in response to signaling molecules from the neural tube (NT) and the notochord (N). Precursor cells from dorsomedial lip (DML) migrate to form the epaxial muscles and ventrolateral lip (VLL) migrate towards the limb bud to form limb muscles. Pax7+ satellite cells arises among the Pax3+/Pax7+ progenitor cells that downregulate their Pax3 and enter quiescence during secondary embryonic myogenesis. Both type of cells follow the same dynamic process during myogenesis into becoming differentiated myocytes that contribute to muscle growth and regeneration. Both cell population activate Myf5 and MyoD expression to engage to the myogenic lineage and subsequently express Myogenin and MRF4 during differentiation to form myofibres.

1.2.3 Evidence of satellite cell requirement in muscle repair

In normal and healthy muscles, satellite cells are maintained in quiescence in their niche beneath the basal lamina. Early reports showed that SCs are capable of proliferating upon muscle damage *in vivo* and in vitro as well as of fusing to form myotubes (Reznik, 1969; Bischoff, 1975). Furthermore, injecting SCs associated with their myofibre into irradiated dystrophic muscle is sufficient to trigger muscle repair with evidence of proliferation and new multinucleated myofibres (Collins et al., 2005). This indicates that despite reports of the contribution of other cell types, including bone-marrow stem cells and muscle-resident cells (reviewed in section 1.2.6), satellite cells are critical for muscle regeneration upon injury. Genetic studies have confirmed that successful muscle repair is exclusively dependent on SCs availability. A conditional mouse model expressing human diphtheria toxin fragment A (DTA) receptor (DTR) in Pax7-expressing cells ($Pax7^{DTR}$) which allow the specific ablation of SCs following DTA intra-muscular injection demonstrated that skeletal muscle repair was diminished upon muscular damage. The condition was only rescued upon transplantation of Pax7+ cells (SCs) (Sambasivan et al., 2011). Other studies using similar experimental designs ($Pax7^{iCreERT2/+}$: $R26R^{DTA/+}$ (83-91% ablation), $Pax7^{iCE/+}$: $R26R^{DTA/+}$ (over 90% ablation) or $Pax7^{CreERT2/+}$: $R26R^{GFP\text{-}DTA/+}$ (100% ablation)) to ablate SCs from skeletal muscles by conditionally inducing DTA expression in Pax7-expressing SCs prior to muscle injury reached the same conclusions (Lepper et al., 2011; McCarthy et al., 2011; Murphy et al., 2011). Impaired regeneration in SCs-ablated muscles presented also with deregulated fibroblast function and increase ECM deposition (Murphy et al., 2011). However, injured muscle fibres with ablated SCs showed some degree of functionality due to hypertrophy possibly caused by an expansion of the myonuclear domain (McCarthy et al., 2011). Nonetheless, the presence of functional SCs is utmost crucial to ensure complete and efficient muscle repair.

1.2.4 Satellite cells reside in a niche

The activity and maintenance of adult stem cells require structural and biochemical signals emitted from their surrounding microenvironment, termed the stem cell niche. Maintaining SC in its quiescent state during homeostasis is crucial as non-physiological activation of SCs would result in exhaustion of SC pool and impaired homeostatic maintenance such as in sarcopenia. The immediate SC niche components are the myofibre and basement membrane overlying SCs, and at a distance the niche also includes resident cells within the interstitium. Indeed, SCs face the myofibre on their apical side and the basement membrane on their basal side.

Bischoff in 1990 had shown in *in vitro* experiment that SCs lost its quiescence and start proliferating in response to mitogenic environment when myofibres were killed pharmacologically using Marcaine (Bischoff, 1990b). SCs are anchored to the myofibres via cadherin-based adhesive junction in adult muscle. While m-cadherin is exclusively expressed by SCs, muscle-specific myoblasts and mature myofibres, n-cadherin is expressed by uncommitted progenitor cells, MPCs and young myofibres during embryonic myogenesis but re-expressed again during adult myogenesis (Cifuentesdiaz et al., 1993; Moore and Walsh, 1993). M-cadherin is localized in the apical membrane of SCs thus retaining a direct contact with m-cadherin from sarcolemma (Goel et al., 2017). This contact is crucial to maintain SCs in quiescence as mutation or disruption in m-cadherin anchorage leads to activation and proliferation of SCs (Bischoff, 1990b; Goel et al., 2017). Other than protein anchoring interaction, ligand signalling from muscle fibre also play role in maintaining SCs behaviour. For example, elevated Fgf-2 expression from myofibres in aged mice, which otherwise maintained in low levels during tissue homeostasis, causes a downregulation of Sprouty1 (*spry1*) in SCs (Chakkalakal et al., 2012). Sprouty1 is expressed at high levels to maintained SCs quiescence and its downregulation leads to entry into the cell cycle (Chakkalakal et al., 2014).

The basement membrane is a specialised ECM that functions in maintaining the integrity of muscle fibre and its associated SCs. It consists of two layers, the basal lamina and the reticular lamina. The reticular lamina is connected to the endomysium and is

composed mainly of collagens, whereas the basal lamina is adjacent to the sarcolemma. The basal lamina of the basement membrane contacting the basal side of SCs has also essential role in the SC niche. The elementary structure of basal lamina appears to contain a distinct network of collagen type-IV and laminins, predominantly laminin-α2β1γ1 in uninjured adult muscle. The collagen polymers are cemented by covalent cross-links and are bound to laminins by non-collagenous glycoproteins including entactin and nidogen, and also heparin sulphate proteoglycans (mainly perlecan in skeletal muscle) thus creating an integrated structure (Hohenester and Yurchenco, 2013; Thomas et al., 2015). Components of ECM and basal lamina are also subject to degradation by a group of enzymes called matrix metalloproteinases (MMPs) (Carmeli et al., 2004).

A functional basement membrane is crucial in providing mechanical reinforcement to the sarcolemma and protecting myofibres against contraction-induced damage, which is the primary cause of muscle wasting in muscular dystrophies. Mutations in the gene encoding for laminin-α2 cause congenital muscular dystrophy type 1A (MDC1A), the most common childhood congenital muscular dystrophy in Europe accounting for 30%-50% of all muscular dystrophy cases (Holmberg and Durbeej, 2013). In this disease, laminin-α2 deficiency leads to high susceptibility to membrane breakage upon muscle contraction, which in turn causes repeated degeneration-regeneration cycles, chronic inflammation and fibrosis. Although the defect is associated with the up-regulation of laminin-α4, it is inadequate to restore laminin-α2 function since it is unable to polymerise and bind to receptors (Yurchenco et al., 2017). Study using laminin-α2 null mutant mice (*dy^{3K}*/ *dy^{3K}*) revealed a growth retardation and severe dystrophic muscles with muscle degeneration starting as early as postnatal day 9 (Yurchenco et al., 2017). In homeostatic conditions, laminin receptors anchor to the actin cytoskeleton of myofibres via α-dystroglycan binding and α7/β1-integrins, (Mayer et al., 1997; Montanaro et al., 1999). Because the dystrophic phenotype of *dy^{3K}*/ *dy^{3K}* mice is not aggravated when Integrin-α7 is genetically ablated (*dy^{3K}*/ *Itgα7*), it suggests that Integrin-α7 operates in the same pathway as α-dystroglycan (Gawlik and Durbeej, 2015).

Integrin-α7 is also abundantly expressed by quiescent SCs (Dumont et al., 2015b). However, recent studies in the lab demonstrated that a dynamic remodeling of the basal lamina occurs during muscle regeneration, with the deposition of laminin-α1 and laminin-α5 in addition to laminin-α2 to support SC proliferation and self-renewal (Rayagiri et al., 2018). Moreover, laminin-α1 signalling during myogenesis was mediated by integrin-α6, which is highly expressed in embryonic muscles, instead of the Integrin-α7. MMP2 and MMP9 catalyzed this remodeling, since blocking their activities inhibited SC-mediated myogenesis (Rayagiri et al., 2018). Thus, an intact plasma membrane and basal lamina is essential to provide structural support and signalling cues to maintain SC function.

1.2.5 Immune response during skeletal muscle injury

Adult skeletal muscle is a stable tissue with little turnover of nuclei in physiological condition. However, upon damage caused by trauma such as sport injury and by diseases as in muscular dystrophy, a repair programme is induced to repair skeletal muscles. Muscle repair comprises of two major phases, the degeneration or necrosis phase and the regeneration or myogenesis phase (Chazaud, 2014). Inflammatory cells play sequential roles throughout the muscle repair process by regulating the degeneration of damaged fibres during the necrosis phase upon injury and by releasing growth factors and cytokines during the myogenesis phase (Fig 1.5) (Chazaud, 2014). The interplay between these two phases is fundamental for muscle repair, and any disruption in this balance may result in defective repair. For example, prolonged inflammation impacts on the ability to generate new functional muscle fibers in Duchenne muscular dystrophy (DMD), while delayed regeneration results in excessive ECM deposition and fibrosis.

The nature and degree of injury/degeneration is the main determinant of the scale of immune response. Upon injury, disrupted sarcolemma and loss of membrane integrity of the muscle fibres cause an increase of cytosolic content such as creatine

kinase (CK) in the serum. Concomitantly, sarcolemmal damage leads to calcium influx into muscle fibres and causes an imbalance of calcium content, thus resulting in calcium-dependent proteolysis (Kharraz et al., 2013). This activates resident inflammatory cells to release chemotactic signals to attract circulatory immune cells to migrate out from vasculature and infiltrate the damaged site (Fig 1.5). There are two waves of inflammatory response that take place during muscle repair. During the first 6 hours after the onset of muscle injury, monocytes and neutrophils are among the first immune cells recruited from the circulation to invade the injured area (Fig 1.5) (Fielding et al., 1993). This marks the onset of the first wave of inflammatory response with the release of pro-inflammatory cytokines and phagocytosis of debris from foreign particles and damaged fibres. Neutrophils play a significant role during muscle repair by releasing reactive oxygen species (ROS) and proteases to cause secondary damage, which in turn facilitate the recruitment of monocytes from the circulatory system (Fig 1.5) (Kharraz et al., 2013). Differentiated monocytes are called macrophages and they are categorised into different subpopulations according to the expression level of Ly-6C (also known as GR1). Ly-6C+ macrophages, termed M1 macrophages, release important pro-inflammatory cytokines including TNF-α, IFN-γ, IL-1β and IL-6 that activate satellite cell proliferation (Fig 1.5) (Chazaud, 2014). The maturation of Ly-6C+ pro-inflammatory M1 macrophages into Ly-6C- anti-inflammatory M2 macrophages is triggered by the phagocytosis action and begins from day 2 post-injury in Notexin-induced acute injury (Arnold et al., 2007). M2 macrophages release anti-inflammatory cytokines, including IL-4, IL-10, IL-13, and TGF-β to support myogenic differentiation and fusion into myotubes (Fig 1.5) (Arnold et al., 2007).

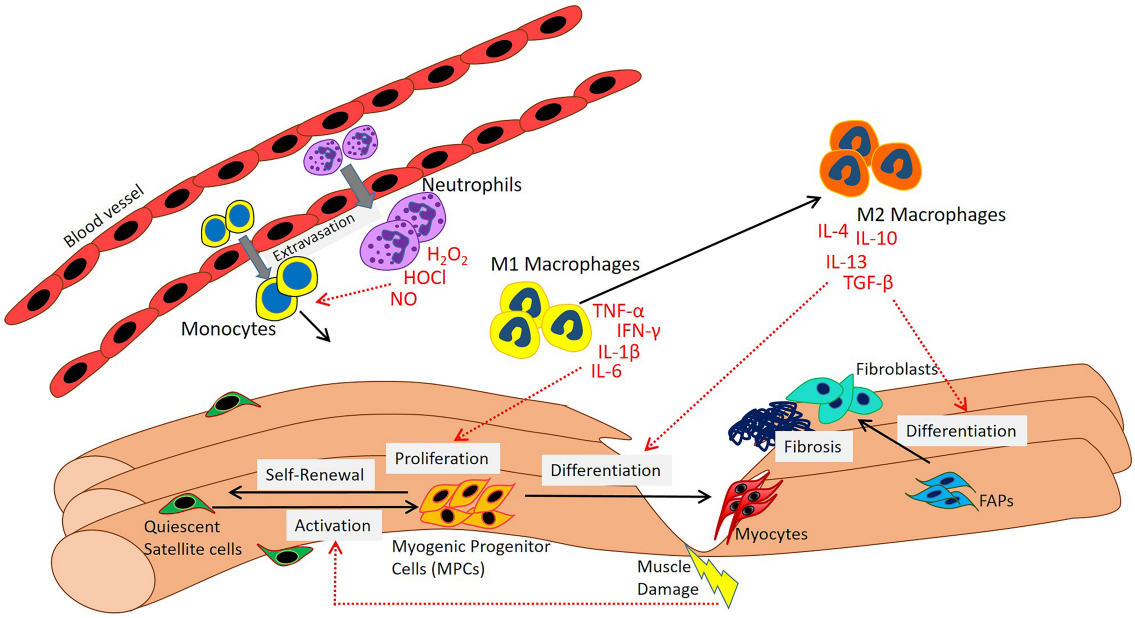

Figure 1.5: Cellular dynamics and immune response during skeletal muscle repair.
Upon injury, damaged myofibres releases cellular contents into interstitial space particularly creatine kinase (CK) that activates satellite cells and attract neutrophils and monocytes to the injury site. Neutrophils release reactive oxygen species (ROS) (H_2O_2, HOCl and NO) and protease to attract more monocytes. At an early stage of regeneration upon migration of immune cells into the injury site, monocytes differentiate into M1 macrophages and release proinflammatory cytokines TNF-α, IFN-γ, IL-1β and IL-6 to promote myogenic proliferation. At a later stage of regeneration, macrophages polarise into M2 macrophages and release anti-inflammatory cytokines IL-4, IL-10, IL-13, and TGF-β to support myogenic differentiation. M2 macrophages also support fibroadipogenic progenitors (FAPs) to differentiate into fibroblasts and support muscle repair by secreting ECM components and metalloproteases (MMPs) to promote the remodeling of muscle tissue.

Immune cells also play a pivotal role in the pathogenesis in chronic degeneration diseases such as in muscular dystrophies, where chronic inflammation and continuous cycles of myofibre degeneration-regeneration are evident (Porter et al., 2002). Macrophages are the most abundant leucocytes and both M1 and M2 subtypes are present in dystrophic muscles. Pro-inflammatory cytokines related to M1 macrophages (TNF-α, IL-1β and IL-6) are found to be elevated in DMD patients, in addition to another pro-inflammatory cytokine, IL-17 which induces the release of the mentioned cytokines (De Paepe and De Bleecker, 2013). However, M2 macrophages are also vital in dystrophic muscle pathology because of their pro-fibrotic effects via the release of TGF-β (Kharraz et al., 2014). M2 macrophages also increase muscle fibrosis through arginase-mediated hydrolysis of arginine that drives ornithine production which then metabolises

to produce proline for collagen production (Wang et al., 2015). The shifted balance of FAPs differentiation from myogenic to fibrotic also exacerbates the disease by replacing functional muscle fibres with fibrous and adipose tissue (Contreras et al., 2016). Taken together, these studies demonstrate that a tightly synchronised transient inflammatory response is crucial to regulate muscle regeneration.

1.2.6 Contribution of non-myogenic cells to muscle repair.

In addition to Pax7+ satellite cells, other cell types have been shown to contribute to muscle repair. The ability of these cells to differentiate into myoblasts and fuse to regenerate myofibers depends on the cellular context. Non-myogenic stem cells that have been tested in muscle regeneration include hematopoietic stem cells (HSCs), mesenchymal stem cells (MSCs) and side population (SP) cells. In addition, other muscle-resident cells, including pericytes, mesoangioblasts and FAPs, have shown regenerative capacity in muscles.

1.2.6.1 Hematopoeitic stem cells (HSCs)

Transplantation of bone-marrow derived stromal cells (not purified hematopoietic stem cells) via intravenous injection, as well as directly transplanting whole bone-marrow, has demonstrated a degree of incorporation of bone-marrow cells into regenerating fibres upon damage. A study using bone-marrow from ML3CF-*nlacZ* (lacZ gene under the myosin light chain 3F promoter) transgenic mice showed that lacZ-positive myogenic cells derived from bone-marrow hematopoietic stromal stem cells were observed in cardiotoxin (CTX) injured muscles (Ferrari et al., 1998). However, the contralateral muscle of the same recipient mice, which had received SCs instead of bone-marrow hematopoietic stromal cells displayed better engraftment. These cells migrated into the damaged muscle area and participated in muscle regeneration when injected in the peripheral circulation (arterial transplantation) (Ferrari et al., 1998). In another study, FACS purified bone marrow-derived hematopoietic stem cells (HSCs) injected into the tail vein of irradiated *mdx* mice contributed to regenerating myofibres

(Gussoni et al., 1999). However, the incorporation rate of donor nuclei was only 10-30%, and dystrophin expression in myofibres was decreased gradually from 9% at the first week to less than 1% at 5 weeks post-transplantation (Gussoni et al., 1999). Similarly, HSCs isolated from myogenic reporter mice (*Myf5*$^{nlacZ/+}$ and *C57/MlacZ*) were shown to undergo myogenic reprograming and express the myogenic markers *Myf5*, *Mlc* and *Mhc* when co-cultured with myoblasts *(Xynos et al., 2010).* Although unable to fuse with myoblasts, the reprogrammed cells were able to fuse among themselves to form myotubes. Another study using GFP-labeled bone marrow-derived cells transplanted into irradiated mice found that donor cells were detected at a sublaminar location in regenerating myofibres 7 days post-transplantation, suggesting a longer-term benefit for muscle homeostasis (LaBarge and Blau, 2002). However, this observation is controversial as subsequent studies by other groups failed to report the same effect and claimed that engrafted cells lacked proliferative or self-renewal capacity (Xynos et al., 2010). Collectively, these data suggest that although HSCs could be programmed to the myogenic lineage and participate in muscle regeneration, their engraftment efficiency is limited.

1.2.6.2 Mesenchymal stem cells (MSCs)

Mesenchymal stem cells (MSCs) are multipotent stem cells isolated from bone marrow stroma. MSCs are able to differentiate into osteoblasts (bone), chondrocytes (cartilage), adipocytes (adipose tissue) and myoblasts (muscle) under stimulation by specific factors. Myogenic-differentiated MSCs have the ability to avoid immune response from T lymphocytes during allogeneic transplantation, making them a potential candidate for stem cell therapy (Joo et al., 2014)

Differentiation towards the myogenic lineage is induced by basic- Fibroblast growth factor (bFGF), Forskolin, Platelet-derived growth factor (PDGF), and Neuregulin followed by transfection with *Notch1 intracellular domain* (*NICD*) gene (Galli et al., 2014). Although HSCs fusion with host myoblasts during myogenesis is debatable, human-derived MSCs fuse efficiently when co-cultured with primary myoblasts and C2C12, a myogenic cell line widely used to study myogenesis (Shi et al., 2004; Kulesza et al., 2016). Combined transplantation of MSCs and myoblasts were also shown to have mutual

advantages since MSCs had increased oxidative stress resistance and migration capacity when cultured in myogenic-conditioned media, even though they were unable to acquire a myogenic phenotype and fuse into myotubes. Also, myoblasts cultured with MSC-conditioned media increased their proliferation but were not protected against oxidative stress (Kulesza et al., 2016). Transplantation of human MSCs into cardiotoxin-injured Tibialis anterior (TA) muscle of immune-deficient mice showed incorporation of human nuclei in regenerating myofibres at 7-days post injury (Shi et al., 2004). Furthermore, allogeneic transplantation of MSCs following repeated crush injury showed an increase in myofibre cross-sectional area (CSA) and strength in functionality test. MSCs grown in Matrigel were able to directly incorporate into regenerating myofibres (Andrade et al., 2015). However, no functional improvement was observed when *Pax3* transfected MSCs (to acquire myogenic lineage) were transplanted into dystrophin-deficient *mdx* mice even though they were able to fuse with regenerating myofibres (Dezawa et al., 2005; Gang et al., 2009). The isolation, expansion and myogenic programming protocols for MSCs has been established and their incorporation efficiency is promising. However, their benefits in improving muscle functionality are still dubious which reduces their therapeutic value for translational medicine.

1.2.6.3 Side population (SP) cells

SP cells are derived from the hematopoeitic lineage and are present in many adult tissues including the brain, lungs, spleen and skeletal muscle. SP cells in skeletal muscle express CD45 and Sca-1 and are characterized by the exclusion of Hoechst 33342 dye during cell sorting (Gussoni et al., 1999; Asakura, 2012). They can re-establish the entire hematopoietic repertoire if transplanted into lethally irradiated mice (McKinney-Freeman et al., 2002). Although SP cell lineage-tracing studies indicate that they do not originate from the Pax7-positive cells that give rise to SCs (Asakura et al., 2002; Schienda et al., 2006), they can be induced to contribute to the myogenic lineage when co-cultured with myoblasts. Furthermore, when injected into injured muscles, SP cells incorporate into new fibres (Asakura et al., 2002). In addition, intravenous transplantation of human SP cells into *mdx* mice partially restores *Dystrophin* expression

with donor-nuclei identified in myofibres (Muskiewicz et al., 2005). However, a recent study demonstrated that although SP cells are readily reprogrammed to the myogenic lineage, their cell fate shifts towards FAP-like behaviour and they differentiate into fibroblasts and adipocytes in dystrophic and damaged muscles (Penton et al., 2013). This suggests that SP cells are not suitable for cell transplantation therapy and could instead contribute to the scarring of the muscle upon damage.

1.2.6.4 Pericytes

Non-myogenic stem cells derived from the skeletal muscle interstitium have also the ability to fuse with regenerating myofibres during muscle repair. Pericytes are smooth muscle cells isolated from the microvasculature. Pericytes have the ability to differentiate into several cell lineages including smooth muscle, osteoblasts, adipocytes and myocytes (Wong et al., 2015). During postnatal growth, pericytes are closely associated with SCs in newly formed fibres and stimulate myogenic differentiation by releasing Insulin-like growth factor-1 (IGF-1) and by promoting SC quiescence through the expression of Angiopoietin-1 (ANGPT1) (Kostallari et al., 2015). Culturing pericytes with myogenic-conditioned medium or co-culturing with myoblasts improves the efficiency of differentiation into myocytes (Dellavalle et al., 2007). Laminin, a component of the basal lamina, promotes myogenic differentiation of pericytes (Gautam et al., 2017). Pericytes transplanted into *scid-mdx* mice can contribute to regenerating myofibres and enhance dystrophin expression (Dellavalle et al., 2007). Therefore, pericyte function during muscle repair makes this cell type a good candidate for supporting myogenesis during muscle repair.

1.2.6.5 Mesoangioblasts

Mesoangioblasts are progenitor cells found in blood vessels with dual potential to differentiate into endothelial or mesenchymal cells including myogenic cells, and contribute to skeletal muscle growth and repair (De Angelis et al., 1999). Mesoangioblasts transplantated in vivo adopt the myogenic program and integrate into growing muscle fibres, and Pax3 has been shown to be crucial in orchestrating this process (De Angelis et al., 1999; Messina et al., 2009). Moreover, the dual lineage of

mesoangioblasts holds some advantages over other type of stem cells especially in terms of reproducibility and migratory capacity (Sampaolesi et al., 2003). Indeed, if injected into arteries, mesoanglioblasts can extravasate the circulation to colonise the muscle tissue (Sampaolesi et al., 2003). This migratory capacity relies on the inflammation profile of the tissue and is more efficient when cells are pre-treated with chemokine stromal-derived factor-1 (SDF-1) and cytokines TNF-α (Galvez et al., 2006). Mesoangioblast survival and myogenic differentiation upon colonising the muscle tissue is supported by the release of cytokine IL-10 by polarized M2 macrophages (Bosurgi et al., 2012). Cellular therapy to treat muscular dystrophies using mesoangioblasts has shown some promising responses. Mesoangioblasts expressing α-sarcoglycan (α-SG) isolated from wild-type mice were able to restore protein expression in novel myofibres and ameliorate the dystrophic phenotype when transplanted into α-Sarcoglycan null mice (a Limb Girdle muscular dystrophy model) (Sampaolesi et al., 2003). Autologous transplantation of genetically corrected mesoangioblasts using lentiviral transduction of α-Sarcoglycan is also achievable using similar transplantation methodology, but with a lesser efficiency (Sampaolesi et al., 2003). Importantly, a study on a golden retriever muscular dystrophy (GRMD) model showed an improvement in muscle morphology and function, with prolonged mobility of the animal up to 13 months of age whereas untreated animals developed mobility defects at 8 months of age (Sampaolesi et al., 2006). Recent developments include the use of induced-pluripotent stem cells (iPSCs) derived from fibroblasts and myoblasts and induced to differentiate into mesoangioblast-like cells to restore α-Sarcoglycan in null mice (Tedesco et al., 2012). Taken together, mesoangioblasts hold a therapeutic value in cellular therapy approaches for treating muscular disease.

1.2.6.6 Fibroadipogenic progenitors (FAPs)

Ectopic fat deposition and replacement of contractile myofibres with adipose tissue are characteristics of aged and diseased muscles such as DMD. Fibroadipogenic progenitors (FAPs) are muscle-resident cells expressing Platelet-derived growth factor receptor-α (PDGFRα+), and responsible for the increase in fibroblasts and adipocytes in response to injury (Uezumi et al., 2010). FAPs do not undergo myogenic differentiation,

but promote myogenic differentiation in SCs-mediated regeneration (Joe et al., 2010). FAPs proliferation and effect on myogenesis are induced by cytokines IL-4 and IL-13 released by Type 2 immune cells (Heredia et al., 2013). Conversely, FAPs adipogenic differentiation is inhibited by both cytokines and regenerating myofibres (Uezumi et al., 2010; Heredia et al., 2013). In old *mdx* mice, FAPs repress SC-mediated regeneration and impede the effect of HDAC inhibitor (HDACi), which normally has beneficial effects on the dystrophic phenotype of young *mdx* mice (Mozzetta et al., 2013). Gene expression and micro-RNA analyses revealed that two genes, MyoD and BAF60C, and two miRNAs, miR-133 and miR-206, can reverse FAPs repression by HDACi and improve myogenic regeneration in *mdx* mice (Saccone et al., 2014). While it is important to regulate FAPs differentiation to limit the adipocyte population in regenerating fibres, its expansion and fibrogenesis differentiation is vital to ensure efficient muscle repair (Fiore et al., 2016).

1.3 Satellite cells in adult myogenesis

1.3.1 An overview of satellite cell-mediated myogenesis in adult skeletal muscles

SCs in adult myofibres are usually quiescent and identified by the expression of Pax7, a member of paired box transcription family (Seale et al., 2000). Skeletal muscle regeneration is mediated by SCs through the interplay between inflammatory responses (reviewed previously in 1.2.5) and the myogenic programme controlled by a family of regulatory factors termed the myogenic regulatory factors (MRFs), which includes Myf5, MyoD, Myogenin, and MRF4 (Charge and Rudnicki, 2004).

Upon injury, Pax7-expressing SCs become activated and induce Myf5 expression. They then enter the cell cycle and divide either symmetrically to produce two daughter cells of the same fate (self-renewing or differentiating) or asymmetrically to produce one self-renewing SC and one differentiating SC (Fig 1.7). Self-renewing SCs return to quiescence and a stem cell fate, and are responsible for the long-term maintenance of the SC pool. Committed myoblasts express Myf5 and MyoD, and undergo terminal

differentiation into myocytes following myogenin and MRF4. Myocytes either fuse together into myotubes or fuse with existing myofibres, thus completing the regeneration process (Fig 1.8). Maturing myotubes will begin expressing muscle contractile proteins such as Desmin and MyHC (reviewed previously in 1.1.2). Every stage of SC-mediated postnatal myogenesis from quiescence, activation, proliferation, self-renewal to differentiation will be explained in this section, including the signaling pathways involved in regulating these processes.

1.3.2 Satellite cells are quiescent in adult skeletal muscles

A subset of stem cells, including SCs in skeletal muscles, is maintained in their niche in a dormancy state to restrict their exhaustion over the lifespan. Quiescence is a state where cells are maintained in a reversible G0 state of the cell cycle (Fig 1.6). It differs from cell cycle exit during terminal differentiation since the cells are able to re-enter the cell cycle and undergo proliferation upon injury (Montarras et al., 2013). Stem cell quiescence is also related to another cell behaviour, self-renewal whereby stem cells give rise to daughter cells that retain their stemness to replenish the quiescent stem cell pool. The self-renewal program will be reviewed in details in section 1.3.5.

1.3.2.1 Intrinsic regulation of SC quiescence

During quiescence, the maintenance of SCs in G0 requires active regulation of the cell cycle mainly through the expression of high levels of cyclin kinase inhibitors (CKIs) namely cyclin-dependent kinase inhibitor 1A (*Cdkn1a/p21Cip1*), 1B (*Cdkn1b/p27Kip*) and 1C (*Cdkn1/p57Kip2/p57*) (Thomas et al., 2000; Chakkalakal et al., 2014). In addition, other cell cycle regulators are also highly expressed in quiescent SCs such as the tumor suppressor protein retinoblastoma protein (*Rb1*), G-protein signaling regulator 2 and 5 (*Rgs2* and *Rgs5*), peripheral myelin protein 22 (*Pmp22*) and FGF signaling inhibitor Sprouty homolog 1 (*Spry1*) (Fig 1.8) (Dumont et al., 2015b). A study using temporally-inducible lineage tracing genetic model (*Pax7-CreER^{tm}; R26R-LacZ*) to follow SCs cell fate demonstrated that SCs expressed high level of *Spry1* in uninjured muscle, down-regulated it during the proliferative phase and re-expressed it in Pax7+ cells in

regenerated muscles (Shea et al., 2010). Deletion of *Spry1* in cycling SCs prevents them from returning to quiescence and causes apoptosis (Shea et al., 2010). This suggest that Sprouty 1 plays an important role in maintaining SC quiescence, and its re-expression at the end of myogenesis may be crucial for SC self-renewal.

1.3.2.2 Extrinsic signals essential for SCs quiescence

Immediately after injury, SCs make a transition into an intermediate state between G0 and G1, known as G(Alert) that primes quiescent SCs to cell cycle entry (Fig 1.6) (Rodgers et al., 2014). This priming into G(Alert) is under the control of mammalian Target of rapamycin complex-1 (mTORC1) mediated by HGF signaling through the *c-Met* transmembrane receptor. Although SCs in G(Alert) show characteristics of SCs in G1 such as increased cellular content, higher metabolic activity and increased affinity towards cell cycling, they retain a quiescent SC signature, including stemness and engraftment efficiency (Rodgers et al., 2014).

SCs are enriched with cell surface and cell adhesion molecules, including Tyrosine kinase receptor c-Met, caveolin-1, NCAM-1, integrin-α7/β1, VCAM-1, calcitonin receptor (CalcR), sialomucin surface receptor CD34, frizzled-7, notch, notch co-receptor syndecan-3, syndecan-4 and m-cadherin. These proteins interact with the SCs niche (reviewed previously in 1.2.4) to transmit both mechanical and molecular cues from the microenvironment to regulate SCs function including quiescence. For instance, although m-cadherin is expressed in myoblasts and its loss has no effect on myogenesis, a recent study revealed that conditional deletion of n-cadherin (mostly involved in embryonic myogenesis) and m-cadherin in SCs caused a 2-fold increase in the amount of Pax7+ cells in uninjured muscle and myofibre culture (Hollnagel et al., 2002; Goel et al., 2017). The loss of cadherin caused a partial disruption of adhesive junctions (AJs) between SCs and myofibres, which triggers SCs to be in a transition state between quiescence and activation, termed SC_{DAN} for 'diminished-adhesive-niche'. However, this state is different from G(Alert) (Fig 1.6) since SCs in G(Alert) have a lower proliferative efficiency and do not express MyoD, suggesting the state as being closer to quiescence (G0). Interestingly, SC_{DAN} does not affect the self-renewal capacity of SCs and mice maintain an effective regeneration after multiple injuries (Goel et al., 2017).

The role of immune cells and their related cytokines during muscle repair has been extensively studied (reviewed in 1.2.5). Although traditionally macrophage-related cytokines have been linked to proliferation and differentiation of SCs, a recent study by Sampath et al., highlighted a role of oncostatin M (OSM) (member of IL-6 family of cytokines) in maintaining SC quiescence (Sampath et al., 2018). OSM is released by healthy muscle fibres and induces SC reversible cell cycle exit, thus maintaining their stemness. Conditional deletion of OSM receptors leads to the exhaustion of the SC pool and impaired tissue repair (Sampath et al., 2018). Collectively, these data portray the fragility of the quiescence state of SCs that requires a tight regulation by their niche to maintain their status.

5.1.1.1.1 Notch signalling is the main regulator of SC quiescence

Quiescent SCs express high levels of Notch receptors and their target genes, including *Notch1*, *Notch2*, *Notch3*, *HeyL* and *Hesr3* (Fukada et al., 2011; Bjornson et al., 2012). As Notch signaling is down-regulated upon SC activation, it suggests that it plays a role in maintaining SCs quiescence (Bjornson et al., 2012). Notch receptors (1-3) expressed on the surface of quiescent SCs bind to Delta-like 1 (Dll1) (transmembrane ligand) expressed by associated myofibres (Fukada et al., 2007). Subsequently, Notch undergoes protease-mediated cleavage to release the Notch intracellular domain (NICD), which translocates to the nucleus and binds to recombining binding protein suppressor of hairless (Rbpj). The NICD-Rbpj complex then activates the transcription of Notch target genes, including *Hey* and *Hes* genes (Mourikis et al., 2012b). Interestingly, a study using SC-specific constitutive overexpression of NICD (Pax7-NICD^{OE}) mice demonstrated that Notch signaling also regulates Pax7 through direct interaction with RBP-Jκ (Wen et al., 2012). Similarly, double mutant mice for the Notch target genes Hesr1/3 have a reduced Pax7+ SC pool, with premature SC differentiation and defective muscle regeneration that is age-dependent (Fukada et al., 2011). Therefore, Notch signaling has a dual role in maintaining SC quiescence directly through its target genes and indirectly through its regulation on Pax7 expression.

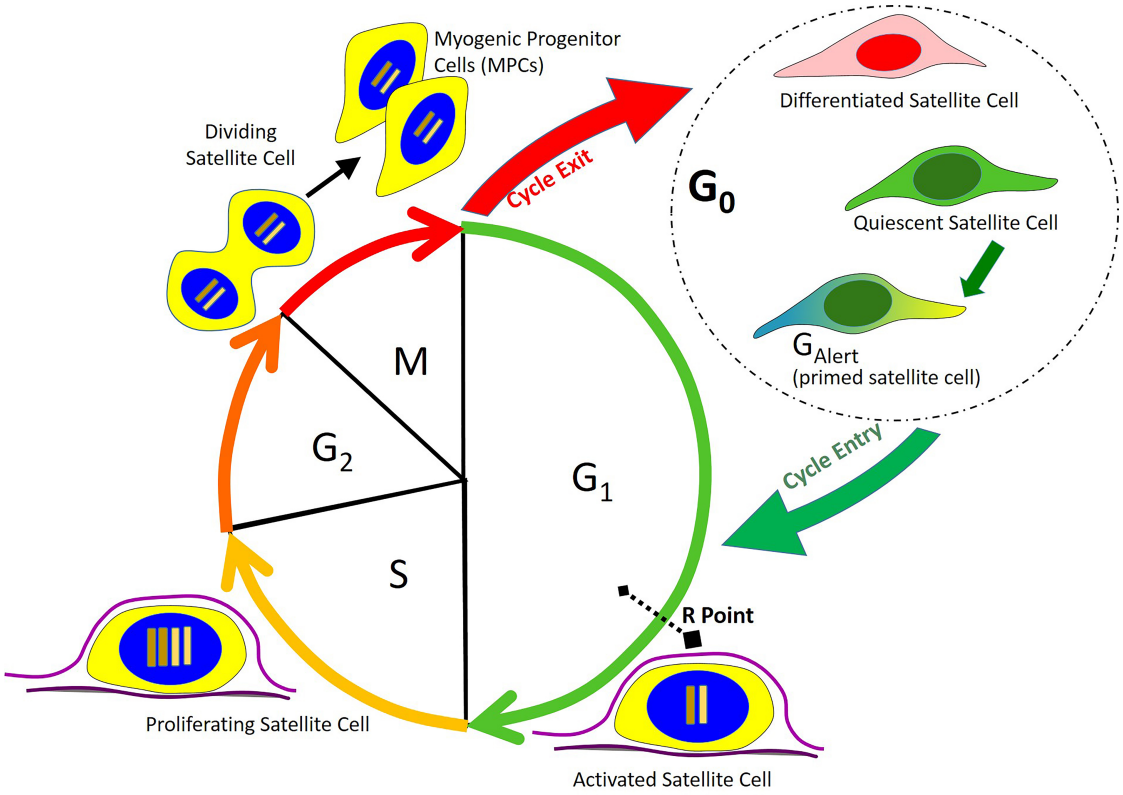

Figure 1.6: The satellite cell cycle program.
Quiescent satellite cells are maintained in a reversible G0 state. Upon muscle damage, satellite cells enter an intermediate state called the G(Alert) state that primes them to the cell cycle program. Then, satellite cells become activated and committed to the cell cycle by entering the mitogen-dependent G1 phase and transitioning through the R point. The Cyclin D-Cdk4/6 complex is implicated in the R point transition. Satellite cells subsequently enter the S phase where they replicate their DNA and this transition is mediated by Cyclin E-Cdk2 complex. After replication, satellite cells transit to G2 phase and the process is mediated by Cyclin A- Cdk1/2 complex. Satellite cells next enter mitosis to divide and generate two daughter cells termed myogenic progenitor cells (MPCs) and the G2-M transition is regulated by Cyclin B-Cdk1 complex. Upon this stage, MPCs will either continue another cell cycle to divide more, or exit the cell cycle and differentiate, or enter reversible G0 state and become quiescent satellite cell.

1.3.3 Satellite cell activation upon injury

Satellite cells are activated in response to many triggers including traumatic injuries, muscle denervation, aging, exercise, and muscular diseases like cancer cachexia and muscular dystrophies. The diversity in stimuli that activates the same process suggests that different pathways crosstalk to regulate SC activities. Quiescent SCs are stimulated by mitogens released by damaged fibres to re-enter cell cycle and undergo adult myogenesis (Bischoff, 1990a). Activation of SCs is indeed the transition period from G0 (quiescent) to G1 (proliferation) (Bischoff, 1990a). Previously described G(Alert) is a pre-activation state where SCs are primed to enter the cell cycle, characterized by increased cell metabolism and upregulation of cell cycle genes (Rodgers et al., 2014). When the activation stimulus is the mechanical trauma caused by single fibre isolation, the first division of SCs is relatively longer, usually between 28.5-33 hours compared to the subsequent cell divisions (Siegel et al., 2011; Rocheteau et al., 2012). The time taken by SCs at G0 to perform the first division is relatively slower than the subsequent divisions because of the additional steps needed to exit the quiescent state (Fig 1.6) (Dumont et al., 2015b). As discussed previously, quiescent SCs expressed significant level of *Cdkn1a, Cdkn1b and Cdkn1c,* which inhibit the formation of Cyclin D-CDK4/6 complexes required to mediate cell cycle entry upon activation (Mohan and Asakura, 2017). SC activation is also characterized by an increase in MRFs required for myogenic commitment, initially Myf5 and shortly after MyoD, or both (Fig 1.8) (Cooper et al., 1999). Further investigation also showed that 98% of Pax7+ cells express My5 prior to expression of MyoD at 24 hours of stimulation (Zammit et al., 2002). Indeed, studies using the C2 myoblast cell line showed that Myf5 and MyoD are mutually exclusive during the cell cycle (Zammit, 2017). Myf5 is highly expressed in G0 but reduced significantly during early G1, before reappearing at the end of G1. In contrast, MyoD is not expressed in G0 but its expression peaks at G1 before being down-regulated at G1/S phase and gradually increasing in S and M phase (Kitzmann et al., 1998; Lindon et al., 1998). Therefore, the entry into the cell cycle regulated by Cyclin D-CDK4/6 complex marks the activation of SCs and the induction of Myf5 and MyoD expression.

1.3.3.1 Signalling pathways regulating SC activation

Quiescent somatic stem cells can reversibly oscillate between G0 and G1 before they reach the restriction point (R point) (Fig 1.6) (Cheung and Rando, 2013). Restriction points in cycling cells function to determine their cell fate whereby cells can either reverse back to quiescence or become committed and progress through mitosis after this point. R point occurs before DNA synthesis, is situated between G1 and S phases, and is sensitive to the levels of growth factors in the environment. Several factors have been identified as regulating SC activation upon muscle injury, including hepatocyte growth factor (HGF), fibroblast growth factor (FGF2), and insulin-like growth factor (IGF-1) (Fig 1.8).

1.3.3.1.1 HGF signalling

Quiescent SCs express the HGF receptor c-Met (tyrosine protein kinase Met) (Tatsumi et al., 1998), and blocking antibodies prevent SC activation (Allen et al., 1995), indicating a role for HGF/c-Met signaling in SC activation. HGF is bound to the ECM through heparin-like glycosaminoglycans as an inactive precursor referred to as pro-HGF (Gonzalez et al., 2017). The release of nitric oxide (NO) by injured muscles and filtrating neutrophils activate MMPs to digest the ECM, which releases HGF (Yamada et al., 2006). The downstream signaling cascade of HGF is not entirely understood, but a recent study has demonstrated that HGF signals through the phosphorylation of mitogen-activated protein kinases (MAPK/ERK) (Gonzalez et al., 2017). HGF also activates SCs through its effect on Semaphorin 3A (Sema3A), which regulates the expression of Pax7, Myf5, MyoD and Emerin (nuclear membrane protein) (Qahar et al., 2016).

1.3.3.1.2 FGF signalling

Two FGF receptors, FGFR-1 and FGFR-4, and their co-receptors Syndecan 3 and Syndecan 4 are expressed by quiescent SCs (Cornelison and Wold, 1997). FGF2 is also found in the connective tissue overlying SCs, is released in response to muscle injury, and found abundantly up-regulated in the damaged fibre sarcoplasm 3-6 hours after injury (Anderson et al., 1995). FGF-mediated activation of SCs is also associated with the activation of MAPK signalling (Yablonka-Reuveni et al., 1999). FGF2 stimulates SC activation by acting on the transition from G1 to S phase through the activity of Raf-

MKK1/2 on ERK1/2 (Jones et al., 2001a). Furthermore, the activation of p38α/MAPK pathway occurs in parallel with SC activation and functions in regulating SC differentiation by inducing MyoD expression, suggesting that MAPK signalling act as a molecular switch for SC activation (Jones et al., 2005; Troy et al., 2012). Indeed, SCs remained quiescent when treated with MAPK blocking agent SB203580 (Jones et al., 2005).

1.3.3.1.3 IGF-1 signalling

IGF-1 has been known for its activity in stimulating proliferation, differentiation and myotube maturity in myogenic cell lines (Engert et al., 1996; Sandri, 2008). In adult myogenesis, IGF-1 downregulates Cdk1b (p27) expression, which releases SCs from cell cycle inhibition (Chakravarthy et al., 2000). The process is mediated through the activation of phosphoinositide 3-kinase/Akt (PI3K/Akt) pathway which phosphorylates Ser256 to inactivate Forkhead transcription factor FoxO1, independently of MAPK signalling (Chakravarthy et al., 2000; Machida et al., 2003). Blocking IGF-1 signalling in turn inhibits Cyclin E-Cdk2 kinase activity, phosporylation of pRb and dowregulates Cyclin A expression (Chakravarthy et al., 2000). IGF-1 signaling also activates SCs through the phosporylation of mTOR and its downstream target S6 kinase and 4E-binding protein 1 (4EBP1), but this is still controversial (Han et al., 2008). Quiescent SCs have elevated expression of *Igbp6* transcripts, which function in sequestering IGFs. Igbp6 is also an effector for SEMA3B, a tumor supressor implicated in G0/G1 phase associated in SC activation (Pallafacchina et al., 2010).

Taken together, the data suggest that multiple growth factors are released upon muscle tissue damage to regulate cell cycle-related proteins and MRFs expression via both MAPK/ERK pathway and PI3K/Akt pathway in order to activate SCs.

1.3.4 Proliferation of SC-derived myoblasts

1.3.4.1 Markers expressed by proliferating muscle progenitor cells (MPCs)

Once SCs are activated and have entered the cell cycle, the proliferation phase commences whereby the SC population expands in cell number as a result of repeated cell divisions to produce transit amplifying cells or muscle progenitor cells (MPCs). Since activation allows SCs to exit G0 and to reach R point, proliferating MPCs are cells that have successfully passed the R point and committed to cell division (Fig 1.6). Pax7 continues to be expressed throughout SC activation and proliferation, and will only be down-regulated upon differentiation as it plays a role in promoting proliferation and cell survival (von Maltzahn et al., 2013; Zammit et al., 2006). Proliferative MPCs express Myf5 and begin to express high levels of MyoD, a myogenic regulatory factor crucial in determining myogenic commitment and promoting cell cycle exit (Cornelison and Wold, 1997; Cooper et al., 1999). Peak MyoD expression induces myogenin expression, and thus induces cells to terminally differentiate (Fig 1.8) (Charge and Rudnicki, 2004). Loss of MyoD results in the accumulation of cycling MPCs that fail to fuse and form myotubes (Megeney et al., 1996). Although MPCs from *MyoD*-null mice are morphologically normal *in vivo*, they form abnormal branched myofibres, possibly due to an inefficient fusion mechanism (Megeney et al., 1996; Cornelison et al., 2000).

Besides the hallmarks of proliferating SCs mentioned above, MPCs also express markers commonly used to label proliferation of other cell types, including Ki67, which is expressed by all cycling cells, Proliferating Cell Nuclear Antigen (PCNA), which is expressed by cells in S phase, and phospho-Histone 3 protein (PH3) expressed by cells undergoing mitosis. Proliferating MPCs in S phase are also identified through the incorporation of the thymidine analogs 5-bromo-2-deoxyuridine (BrdU) or 5-ethynyl-2deoxyuridine (EdU) (Salic and Mitchison, 2008).

1.3.4.2 Signalling pathways regulating myoblast proliferation

Growth factors promoting SC activation generally promote also myoblast proliferation. Indeed, in primary culture 100% of Pax7-expressing cells enter the cell cycle and incorporate BrdU (Troy et al., 2012). In all experimental settings used so far (*in vitro, ex vivo and in vivo*), an heterogeneity in SC response to stimuli has been noted. For instance, SC mitotic divisions are not synchronised, and occur between 24 and 48 hours after stimuli or trauma (Rocheteau et al., 2012; Siegel et al., 2011). Levels of Pax7 in SCs are one of the factors associated with this heterogeneous response (Rocheteau et al., 2012). A study using transgenic mice *Tg: Pax7-nGFP* showed that while Pax7-nGFP^{Low} had higher metabolic status and started dividing earlier (25.5 hours), Pax7-nGFP^{Hi} cells were less active and had their first division at 33 hours *in vitro* (Rocheteau et al., 2012). Several pathways have been identified in mediating proliferation of MPCs in postnatal myogenesis, including Wnt, Transforming growth factor-β (TGF-β), Sonic hedgehog (Shh) signalling, and microRNAs (Fig 1.8).

1.3.4.2.1 Wnt pathway

Both the canonical and non-canonical Wnt signalling pathways have been implicated in MPC expansion during adult myogenesis. Components of the canonical Wnt/β-catenin signalling pathway are absent in quiescent SCs but activated in SCs in 24-48 hours post-culture *ex vivo* (Otto et al., 2011). Wnt ligands including Wnt1, Wnt3, Wnt5, Wnt6 and Wnt11 are expressed by these proliferative MPCs, and exogenous treatment with Wnt1, Wnt3 and Wnt5 increases MPC proliferation *ex vivo* (Otto et al., 2011), in contrast to the anti-proliferative effect of Wnt1 and Wnt3a in *in vitro* C2C12 myoblast cultures (Kuroda et al., 2013).

Non-canonical Wnt pathways is independent of β-catenin and is instead mediated by intracellular Ca^{2+} and JNK pathway (Gomez-Orte et al., 2013). The most studied non-canonical pathway is perhaps the planar cell polarity (PCP) pathway, a pathway involved in cell migration, orientation of cell division and asymmetric distribution of cellular components during cell division (will be further discussed in 1.3.5.2) (Gomez-Orte et al., 2013). Van Gogh-like protein 2 (Vangl2), a component of the PCP pathway is expressed by Pax7+/Myf5+ MPCs, suggesting an involvement of the non-

canonical Wnt signalling pathway (Buono et al., 2012). Frizzled-7 (Fzd7) and co-receptor Syndecan 4, the receptors involved in PCP pathway are also expressed by quiescent SCs and involved in accelerating activated myoblasts both *ex vivo* and *in vivo* (Le Grand et al., 2009; Bentzinger et al., 2013b). Fzd7 has been shown to bind to Wnt7, which is upregulated in myogenic regeneration, and to the ECM associated glycoprotein, Fibronectin (FN) (Le Grand et al., 2009; Bentzinger et al., 2013b). Therefore, these data demonstrate the involvement of Wnt signalling in driving MPC proliferation possibly through Wnt/β-catenin pathway and PCP pathway

1.3.4.2.2 Sonic hedgehog signalling

Sonic hedgehog (Shh) signalling is well known for its mitogenic effect on myoblasts during embryonic development (Duprez et al., 1998). So, it is not surprising that it also has an effect on adult MPCs. Administration of recombinant Shh protein to cultures of the C2C12 myoblast cell line increases cell proliferation and this effect is attenuated upon treatment with cyclopamine, a potent inhibitor of the Shh signalling pathway (Elia et al., 2007; Straface et al., 2009a). The effect on proliferation was proposed to be mediated via MAPK/ERK pathways and phosphoinositide 3-kinase (PI3K)/Akt phosphorylation (Elia et al., 2007). Interestingly, IGF-1 was reported to have a combinatorial function with Shh signalling in SC proliferation, as blocking of IGF-1 receptors reduced Shh-dependent Akt phosphorylation (Madhala-Levy et al., 2012).

1.3.4.2.3 TGF-β signalling

TGF-β signalling in SCs has been extensively studied due to its dual role in regulating myogenesis through its impact on myoblast proliferation and differentiation. Activated SCs contain TGF-β transducer proteins called Smad, including Smad2, Smad4 and Smad5 and express membrane receptors for TGF-β signalling, suggesting that it functions during proliferation (Delaney et al., 2017; Ono et al., 2011). Bone morphogenetic proteins (BMP) are member of the TGF-β family, and BMP Receptor type 1A (BMPR-1A), which is not expressed in freshly isolated SCs, is upregulated in Pax7+ cells thereafter (Ono et al., 2011). Furthermore, BMP4 which has been reported to promote proliferation and inhibiting differentiation when added exogenously *in vitro* (Ono et al., 2011). Smad2-mediated TGF-β signalling causes PCNA localisation into nucleus which increases proliferation rate by inhibiting cell cycle exit (Delaney et al.,

2017). Recently, TGF-β-activated kinase 1 (TAK1) has been shown to increase myoblast proliferation via NF-κB/JNK pathway (Ogura et al., 2015). Conditional ablation of TAK1 in SCs causes precocious cell cycle exit and differentiation of SCs (Ogura et al., 2015). Interestingly, a mechanism independent of TGF-β ligand-receptor interaction is also affecting SC proliferation through the physical interaction of Smad7 and MyoD, which blocks the inhibitory effect of MAPK kinase (MEK) has on MyoD (Miyake et al., 2010).

The release of SCs from cell cycle arrest during early proliferation is mediated by TGF-β signalling through AMPK/mTOR. The mTOR pathway regulates SC entry into the cell cycle by activating the transcription of *Cyclin D1* (Jash et al., 2014). SCs go through the S phase where DNA synthesis and replication occur. Upon cell cycle entry, the G1-S transition is inhibited by the expression of *p21,* upregulated by myostatin, a member of the TGF-β family (McPherron et al., 1997). Myostatin was discovered due to the phenotype of *Myostatin*-null bull called the 'Belgian Blue bull' characterised by the extremely lean and overgrown muscular features. In laboratory, *Myostatin*-null mice are known for the increased muscle mass and size due to hypertrophic fibres and hyperplasia (Reisz-Porszasz et al., 2003). The resultant muscle hyperplasia is caused by an increased in activated and proliferating SCs upon inhibition of *p21*, which blocks the activity of Cyclin E-Cdk2 complex during the S phase (McCroskery et al., 2003). Another member of the TGF-β family, Growth/Differentiation factor-11 (GDF11) has redundancy function with Myostatin (McPherron et al., 2009). Interestingly, GDF11 has been named as the most potent anti-aging factor that was able to reverse stem cell-related frailty (Sinha et al., 2014). However, subsequent screening performed on extracellular protein sample from aged muscle claimed otherwise, and it was later discovered that the earlier study (Sinha et al., 2014) was poorly designed (Hinken et al., 2016). In summary, these data emphasize the role of TGF-β signalling in promoting SC proliferation via its control on MyoD expression and cell cycle regulators.

1.3.4.2.4 MicroRNAs

Micro RNAs (miRNAs or miRs) are small non-coding RNA molecules that bind to specific coding mRNAs to inhibit their translation or tag the mRNA for degradation (Winbanks et al., 2011). For instance, miR-29 and miR-206 repress the translation of histone deacetylase (HDAC), which is a key myogenic differentiation inhibitor, therefore

affecting proliferation. HDAC function in inhibiting SC differentiation is TGF-β-dependent, and can be repressed by miR-29 and miR-206 via their inhibition on Smad3 (Winbanks et al., 2011). Another pathway affected at the post-transcriptional level by miRNAs is the heterotrimeric G-protein alpha subunit Gαi2 (Minetti et al., 2014). MicroRNAs including miR-1, miR-27b, and miR-206 inhibit SC proliferation by repressing Gαi2 activity in a HDAC-dependent manner. Moreover, miR-15b, miR-23b, miR-106b and miR-503 were found to be inhibited by the expression of transcription factor Pitx2 in Myf5+ SCs, which result in their expansion (Lozano-Velasco et al., 2015). Therefore, miRNAs are capable of regulating SC proliferation by affecting proteins involved in TGF-β signalling and G-protein receptor-mediated pathway.

1.3.4.3 Cyclins and cell cycle regulators

The cell cycle comprises four phases, G1, S, G2 and M. While G1 is sensitive to external stimuli from mitogens and growth factors discussed earlier, cell cycle progression beyond the R point is regulated by cyclin dependent kinases (CDKs) and cyclin kinase inhibitors (CKIs) (Fig 1.6) (Mohan and Asakura, 2017). A number of cyclins, including Cyclin A2, B1, D1, D3 and E, has been reported to regulate SC proliferation.

The release of SCs from cell cycle arrest during early proliferation was shown to be mediated by the AMPK/mTOR pathway. The mTOR pathway regulates SC entry into the cell cycle by activating the transcription of *Cyclin D1* (Jash et al., 2014). SCs go through the S phase where DNA synthesis and replication occur. However, the G1-S transition is inhibited by the expression of *p21,* upregulated by myostatin (reviewed previously in 1.3.4.2.3) (McPherron et al., 1997). Although cyclin D is well known to be regulating early G1 phase, a recent study showed that *Cyclin D3*-null myoblasts fail to progress through S phase (De Luca et al., 2013). As a result, myoblasts accumulated at G0/G1 and G2/M phases, and differentiated precociously (De Luca et al., 2013). Subsequently, the Cyclin A2-Cdk2 complex accumulates at early S phase and mediates the phosphorylation of a cell cycle-specific protein called the cell division control protein 6 (CDC6). CDC6 is responsible for checking that DNA replication only occurs once in every cell cycle (Bendris et al., 2011). *In vitro*, the transient knock-down of the tumor

suppressor gene mixed lineage leukemia 5 (MLL5) upregulates *Cyclin E* and *Cyclin A2* suggesting that it mediates SC entry and exit from S phase (Sebastian et al., 2009).

Cyclin B1, which associates with Cdk1, is the main cell cycle regulator at the G2/M phase; it accumulates at G2 and is expressed significantly during metaphase. Protein arginine methylation is a common post-translational modification carried out by protein arginine methyltransferase (PRMT) family (Zhang et al., 2015). Interestingly, a study on histone arginine methyltransferase PRMT5 and PRMT7 demonstrated that conditional deletion of Pmrt5 in SCs results in the up-regulation of *p21*, a negative regulator of Cyclin B1-Cdk1 complex (Blanc et al., 2016; Zhang et al., 2015). This result in SCs entering cell senescence prematurely thus impairing muscle regeneration *in vivo* (Blanc et al., 2016). These data collectively suggest that the regulation of SC proliferation is mainly performed through the sophisticated control of the cell cycle program by multiple signalling pathways.

1.3.5 Self-renewal underlies satellite cell long-term tissue regenerative capacity.

Adult stem cells including satellite cells have a unique ability to generate progenitor cells that retain their stem cell characteristics via a process called self-renewal (Fig 1.8). Self-renewing SCs also termed satellite stem cells, maintain Pax7 expression and do not express the myogenic markers upon division in order to return to quiescence to maintain a SC pool (Chakkalakal et al., 2014). Early evidence of SC self-renewal showed that 10% of sublaminar Pax7+ cells have never expressed Myf5 during their lifespan using Myf5-Cre; Rosa26-YFP mice (Kuang et al., 2007). One of the mechanism by which the SCs self-renew is by segregating template-DNA strands selectively into self-renewing daughter cell via asymmetric cell division (Shinin et al., 2006).

Using TetO-H2B-GFP reporter mice, which indicate the cell proliferative history because proliferating cells termed non-label retaining cells (non-LRCs) lose GFP, whereas 'reserved' stem cells retain the label (LRCs), it was shown that SCs are label retaining cells (Chakkalakal et al., 2014). These label-retaining cells that inherit

template-DNA strands also express higher level of Pax7 compared to the proliferative SCs (Rocheteau et al., 2012). Self-renewing SCs have a low metabolic status and are slow dividing cells but have a higher capability in forming secondary colonies after passaging *in vitro* or generating myogenic progenitors after serial transplantation *in vivo* (Ono et al., 2012; Rocheteau et al., 2012). Maintenance of the self-renewal program is thought to involve the cell cycle inhibitors *Cdk1a* and *Cdk1b* (Chakkalakal et al., 2014).

1.3.5.1 Role of Notch signalling in the self-renewal program

Notch signalling is implicated in regulating the self-renewal program as evidenced by the reduced number of quiescent SCs in degenerating disease such as DMD and in aging in the absence of Notch signalling. Restoring Notch signalling such as in Rosa26^{NCID}/*mdx* (constitutive active Notch in the *mdx* mouse model) is sufficient to rescue the self-renewal defect in *mdx*-derived SCs (Jiang et al., 2014; Day et al., 2010). Interestingly, a study using SC-specific constitutive overexpression of NICD (Pax7-NICD^{OE}) mice demonstrated that Notch signaling also regulates Pax7 through direct interaction with RBP-Jκ (Wen et al., 2012). Furthermore, blocking Rbpj function in SCs through the conditional deletion of *Rbpj* in adult satellite cells (Pax7$^{CreERT2/+}$: RBP-J$^{flox/flox}$) results in severe exhaustion of the Pax7+ SC pool and impaired regeneration upon injury (Bjornson et al., 2012; Mourikis et al., 2012b). The depletion of SCs in Rbpj-deficient mice is not caused by cell apoptosis, but is due to SC spontaneous activation, differentiation and fusion causing fibre hypertrophy. Most of Rbpj-null SCs are not proliferating and dividing, suggesting that they are precociously differentiating. Together, these data propose that Notch signaling regulates SC self-renewal by controlling Pax7 expression through RBP-Jκ.

1.3.5.2 Role of Pax7 in SC self-renewal

The ability of SCs to maintain long-term skeletal muscle homeostasis relies on the balance between self-renewal and differentiation during myogenesis. A lineage-tracing study suggests that high Pax7 SCs (Pax7-nGFP$^{(Hi)}$) commit to self-renewal as they are restricted at undifferentiated state (Rocheteau et al., 2012). High expression of Pax7

inhibits differentiation of myoblast by downregulating the expression of MyoD thus preventing the induction of myogenin expression (Olguin and Olwin, 2004). Pax7 expression stimulates cell cycle exit in myoblasts and directs them to re-enter quiescence (von Maltzahn et al., 2013).

SCs self-renewal is negatively regulated by Pax7 degradation by both proteasomes and ubiquitin ligases. Proteasome-dependent degradation of Pax7 in differentiating SCs is promoted by ubiquitin-ligase Nedd4 (Gonzalez et al., 2016). Moreover, casein kinase 2 (CK2)-dependent Pax7 phosphorylation at serine residues 201 (S201) correlates with Pax7 ubiquitination in proliferating myoblasts (Gonzalez et al., 2016). Pax7 protein is also subject to degradation by caspase 3 cleavage (Dick et al., 2015). Stimulation of caspase 3 *ex vivo* leads to premature differentiation and down regulation of Pax7 target genes. In contrast, reduced caspase 3 activity or blocking of caspase 3-mediated cleavage of Pax7 by CK2 result in increased self-renewing SCs (Dick et al., 2015; Gonzalez et al., 2016). SCs self-renewal is also promoted by another protein, the TNF receptor-associated factor 6 (TRAF6) which is an E3 ubiquitin ligase (Hindi and Kumar, 2016). TRAF6 function via MAPK signalling to activate both ERK1/2 and JNK1/2 pathway downstream, which stimulate c-JUN to bind to Pax7 promoter and increase Pax7 expression. TRAF6 also indirectly downregulates microRNAs related to SCs myogenic commitment including miR-1 and miR206 (Hindi and Kumar, 2016). Together, this suggests an important role for Pax7 in driving SC self-renewal to maintain the SCs pool.

1.3.5.3 Symmetric and asymmetric cell division

During cell division, SCs can generate self-renewing cells by dividing symmetrically or asymmetrically, although symmetric division is often associated with producing transit-amplifying cells that differentiate. Pax7-expressing cells can also generate two daughter cells with distinct cell fate through asymmetric cell division, a preferred division pattern in repair program (Fig 1.7) (Shinin et al., 2006). However, in extreme conditions, SCs can perform a symmetric cell division to generate two identical stem cells (Rayagiri et al., 2018). Upon SC activation, SCs divide in a planar orientation along the axis of the myofibre with both daughter cells associated with the basal lamina,

or in apico-basal orientation perpendicular to the fibre axis with one daughter cell associated with the basal lamina and another one associated with the myofibre (Fig 1.7) (Kuang et al., 2007). Symmetric cell divisions usually occur in a planar orientation and are associated with the Planar Cell Polarity (PCP) pathway, giving rise to two identical self-renewing SCs (Le Grand et al., 2009). Both fibronectin and Wnt7a are able to stimulate frizzled-7 and syndecan-4 receptors on SC to induce polarized distribution of the PCP effector Vangl2 to promote symmetric cell division (Fig 1.7) (Le Grand et al., 2009; Bentzinger et al., 2013b). Treatment of SCs *ex vivo* with Laminin-111 also mediates self-renewal in adult myogenesis through planar symmetric cell division, probably through the interference of extrinsic signalling from basal lamina (Rayagiri et al., 2018).

Asymmetric cell division involves an unequal distribution of cell size, protein content and stem cell fate determinants (Shinin et al., 2006; Knoblich, 2008). Template DNA-strands form mother cell are also segregated asymmetrically in self-renewing SCs along with proteins associated with stemness including Pax7*, CXCR4*, *CD34*, and Numb (Fig 1.7) (Shinin et al., 2006; Rocheteau et al., 2012). An apoptosis related protein Fas-associated death domain (FADD) has also been shown to regulate cell fate decision and is asymmetrically located in self-renewing SCs (Cheng et al., 2014). The phosphorylated form of FADD is usually accumulated in uncommitted myoblasts that expresses stem cell markers (Cheng et al., 2014).

The primary cilium is a cellular microtubule-containing organelle that contains receptors for many cellular signalling pathways including Shh and Wnt pathways. Around 70% of quiescent SCs present a primary cilium anchored in the cytoplasm to the basal body containing the mother centriole (Jaafar Marican et al., 2016). Upon entry into the cell cycle, the primary cilium is disassembled to allow the duplication of centrioles, and is re-assembled after cell mitosis. A study in the lab has shown recently that primary cilia are selectively re-assembled in SCs committed to self-renewal, and asymmetrically inherited by SCs, which express high Pax7 and do not express Myogenin (Fig 1.7) (Jaafar Marican et al., 2016).

SC asymmetric cell divisions usually occur in the apico-basal orientation with self-renewing SCs associated with the basal lamina (Kuang et al., 2007; Dumont et al., 2015c). Apico-basal cell divisions are driven by the differential distribution of proteins related to

cell polarization and mitotic-spindle orientation (Morin and Bellaiche, 2011; Troy et al., 2012). Asymmetric accumulation of a group of proteins called the partitioning-defective proteins (PAR complex) at the apical side of the cell during mitosis activates p38α/β MAPK in the apical daughter cell, which induces MyoD expression and myogenic differentiation (Fig 1.7) (Troy et al., 2012). The PAR complex is composed of few polarity-regulating proteins including Par-3, Par-6 and atypical protein kinase C (aPKC) (Dumont et al., 2015c). Another polarity protein, microtubule affinity–regulating kinase 2 (Mark2) also known as Par-1 is localized at the basal side of SC where it interacts with dystrophin. MARK2 mediates cell polarity by directly phosphorylating Par-3, causing the accumulation of Par-3 at the apical side of SC. Loss of dystrophin in SCs prevents Par-3 apical distribution and causes loss of polarity with impaired mitotic spindle orientation. As a result, SC cell division appears to be abnormal in terms of centrosome amplification (Dumont et al., 2015c). Thus, SC self-renewal is associated with asymmetric cell division driven by cell polarity determinants and communication with the basal lamina.

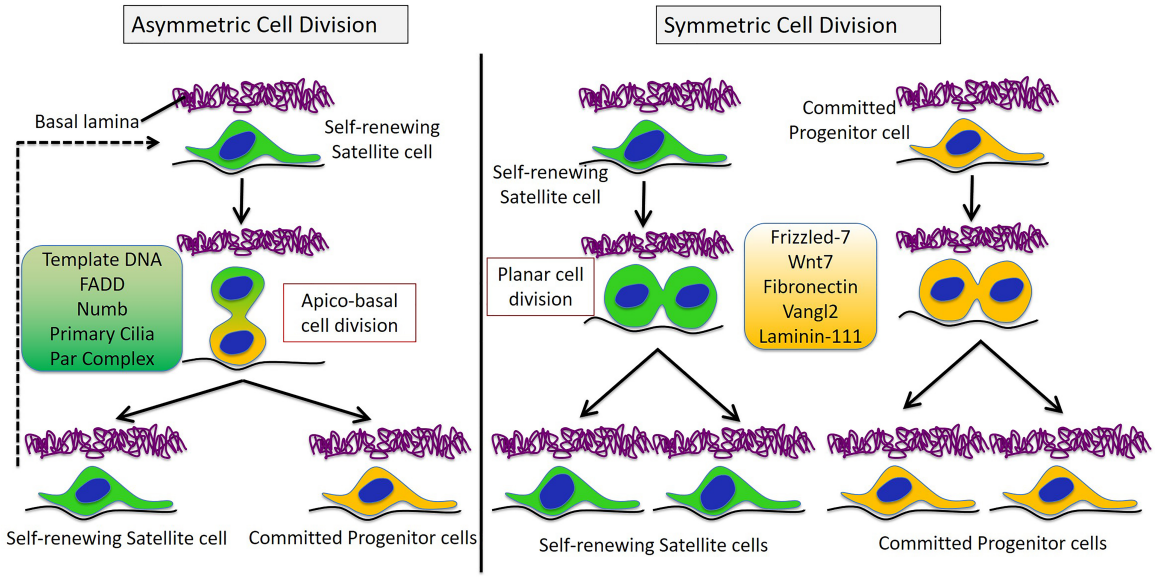

Figure 1.7: Asymmetric and symmetric cell fate during satellite cell division.
In asymmetric cell division, self-renewing satellite cells have unequal distribution of cellular contents and align in a perpendicular orientation called apico-basal plane to give rise to one committed progeny (yellow) and one self-renewal progeny (green). Self-renewal progeny is associated with the basal lamina and inherits the template DNA strands and other stem cell markers. On the other hand, during symmetric cell division satellite cells have a planar orientation parallel to the muscle fibre with both progenies associated with the basal lamina. Both progenies can either self-renew or differentiate and have equal distribution of cellular contents.

1.3.6 Differentiating satellite cells reset tissue homeostasis after injury

Differentiation of SCs occurs upon cell cycle exit when myoblasts begin to express high levels of myogenin and MRF4, members of MRFs necessary for terminal differentiation. Upon injury of muscle *in vivo*, *Myogenin* mRNA transcription peaked at 2 days post injury and declined at 8 days post injury (Ground 1992). However, the protein expression peaked at around 4 days post injury and 72 hours in myofibre culture (Rayagiri et al., 2018). Importantly, myogenin expression is induced when MyoD is at its highest level. Myogenin is one of MyoD target genes and is induced upon formation of the MyoD-Pbx1 complex on the *Myogenin* promoter (Rudnicki et al., 2008). Both Myogenin and MRF4 induce the transcription of gene coding for muscle machinery proteins including MyHC, myosin light chain (MLC), and creatine kinase (Ckm) (Rudnicki et al., 2008; Molkentin and Olson, 1996). In parallel to the induction of myogenin expression, differentiating SCs turn off Pax7 expression, as the two proteins are mutually exclusive (Olguin and Olwin, 2004). Indeed, Pax7 overexpression inhibits myogenin expression directly and through post-transcriptional repression of microRNAs miR-1, miR-186 and miR-206 (Antoniou et al., 2014; Chen et al., 2010a). However, despite the overlapping functions between MyoD, myogenin and MRF4, MyoD fail to rescue the muscle phenotypic loss in *Myogenin*-null myoblasts (Myer et al., 2001).

Regulatory proteins associated with the maturation of myocytes and with building contractile structures are elevated during differentiation. This includes the myocardin family of transcription factors MASTR and MRTF-A (Mokalled et al., 2012). Conditional loss of *MASTR* in SCs results in impaired myogenic regeneration and inhibited expression of Desmin, an intermediate filament protein found in sarcomere. MASTR and MRTF-A also function in up-regulating MyoD expression, a critical event in SC proliferation and myogenic commitment (Mokalled et al., 2012). Myocyte enhancer factor (MEF2) also plays important role during myoblast differentiation as the conditional ablation of MEF2 in Pax7-expressing SCs compromised muscle regeneration *in vivo (Liu et al., 2014)*. Furthermore, *in vitro* culture of MEF2-deficient cells display a reduced expression of differentiation markers including MRF4, Ckm, MyHC1 and MyHC4

(Liu et al., 2014). Thus, advance MRFs including Myogenin and MRF4 are the master regulators driving SCs preparation towards fusion and myotubes formation.

1.3.6.1 Regulation of satellite cells differentiation

Similar to SC self-renewal, the differentiation program requires cells to exit the cell cycle. Therefore, cell cycle inhibitors p21 and p57 are up-regulated to induce irreversible cell cycle arrest (Almeida et al., 2016). Retinoblastoma protein (pRb1) is also implicated in SC terminal differentiation by mediating mitotic arrest and maintaining cell viability (Burkhart and Sage, 2008). Inhibition of pRb1 in primary myoblast-derived myotubes *in vitro* leads to a reversal of differentiation and re-entry into the cell cycle associated with upregulated $p19^{ARF}$ expression (Pajcini et al., 2010). Moreover, Inhibition of cell cycle regulator *Cyclin D1* by Brahma (Brm), a catalytic subunit of the SW1/SNF chromatin remodelling complex causes precocious cell cycle exit (Albini et al., 2015).

Wnt signalling has been reported to regulate SC differentiation. Exogenous administration of Wnt3a to primary myoblasts or myofibre cultures increases myoblast differentiation while blocking Wnt signalling reduces the number of Desmin+ myoblasts (Brack et al., 2008). A study found that kindlin 2, an integrin-associated protein also induce differentiation by acting upstream of Wnt to regulate myogenin expression (Yu et al., 2013). Shh signalling, which is known for its mitogenic effect on myoblasts also regulates their differentiation. Treatment of C2C12 cells with Shh recombinant protein increased the expression of MyHC. The effect was mediated through the MAPK/ERK and PI3K pathways activated upon Akt phosphorylation (Elia et al., 2007). p38α MAPK pathway has also been shown to be regulating myogenin expression, suggesting Shh might have (Liu et al., 2012b).

Taken together, SC-mediated myogenesis involves sophisticated and overlapping signals from growth factors such as IGF, FGF, TGF-β and extrinsic signalling pathways including Notch, Wnt, Shh to regulate every step of myogenesis from activation up to differentiation. It is equally important to ensure that there is a balance between generating progenitors and maintaining the stem cell pool via self-renewal so long-term tissue homeostasis can be guaranteed.

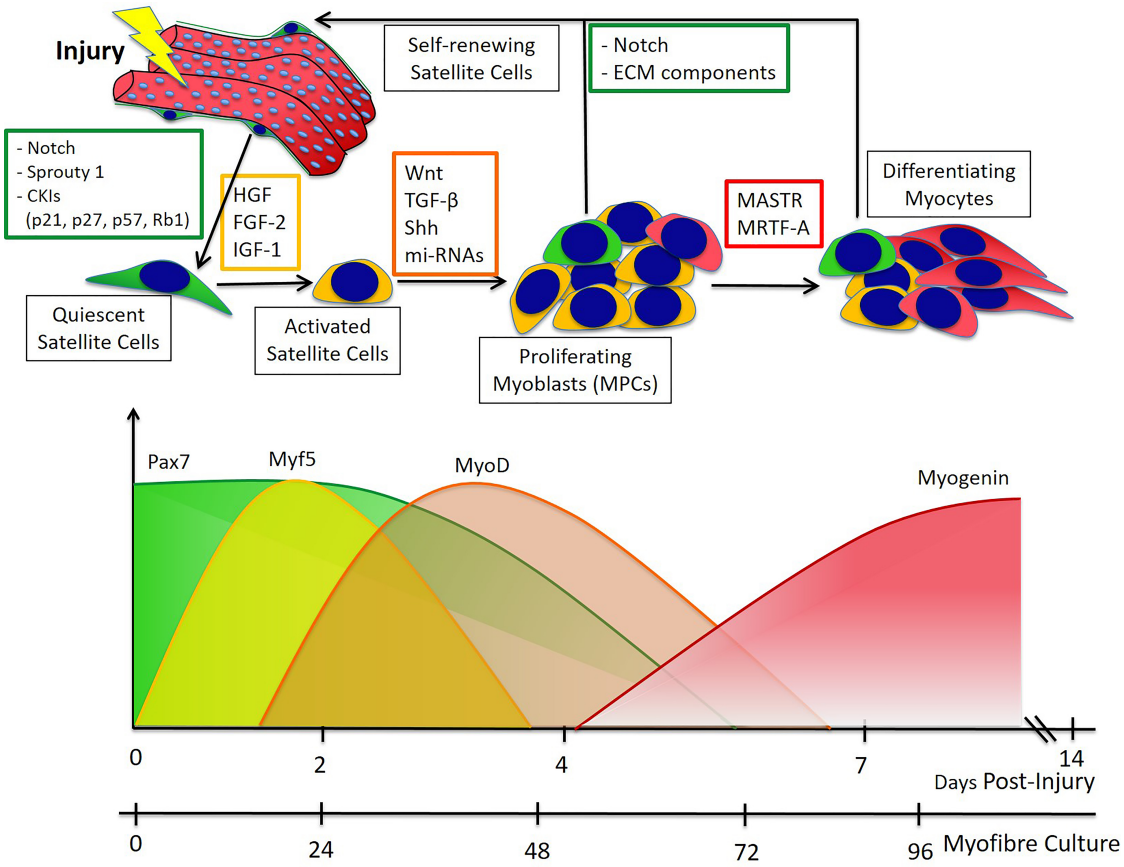

Figure 1.8: The satellite cell-mediated myogenesis program.
In physiological conditions, quiescent satellite cells express high level of Pax7 and are maintained by c-Met, Notch and cyclin kinase inhibitors (CKIs). Upon muscle injury, satellite cells become activated and express early myogenic regulatory factors (MRFs) Myf5 and MyoD. The activation signals are transmitted by growth factors including HGF, FGF-2 and IGF-1. Activated satellite cells then begin to proliferate under the regulation of Wnt, TGF-β, Shh and several mi-RNAs. Proliferating satellite cells are also termed as myoblasts or myogenic progenitor cells (MPCs). Then, MPCs start to express Myogenin and differentiate into myocytes under the control of MASTR and MRTF-A. Small population of MPCs become self-renewing satellite cells and do not express Myogenin while maintaining high level of Pax7 to return to quiescence under the control of Notch signalling and cues from ECM.

1.4 The Hedgehog (Hh) signalling pathway

1.4.1 Hedgehog ligands and their function

The name Hedgehog (Hh) was given upon the observation of a 'spiked' phenotype of the cuticle of *Drosophila* larvae carrying a mutation in the *hh* gene (Nusslein-Volhard and Wieschaus, 1980). Nusslein-Volhard and Wieschaus in 1980 first discovered mutations in the *hh* gene in a large screen for mutations that cause abnormal or impairment in *Drosophila* larval body segmentation during development. Components of the Hh signalling pathway are conserved in vertebrates and invertebrates (Ingham and Placzek, 2006). Although *Caenorhabditis elegans* (roundworms) do not have a *hh* ortholog, they contain several homologs of the hh receptor *Ptc*, which carry important functions in cytokinesis and osmoregulation of *C. elegans* (Varjosalo and Taipale, 2008). While *Drosophila* has a single *hh* gene, mammals have three homologs, *Sonic Hedgehog* (*Shh*), *Indian Hedgehog* (*Ihh*) and *Desert Hedgehog* (*Dhh*) and zebrafish have five homologs of the *hh* gene due to genome duplication, *shha* and *shhb*, *ihha* and *ihhb*, and *dhh* (Cruz-Migoni Sara and Borycki, 2014).

Hh proteins play important roles in almost all tissues, including but not limited to the brain, neural tube, eyes, bones, kidneys, lungs, limbs and gut. Among the three Hh genes, Dhh is the gene with the most restricted expression in the gonads including testis (sertoli cells) and ovaries (granulosa cells) (Varjosalo and Taipale, 2008). Consistent with this expression pattern, targeted mutations in *Dhh* cause an absence of mature sperm in male mice (Bitgood et al., 1996). Ihh is expressed in a limited number of tissues, including the gut, primitive endoderm and prehypertrophic chondrocytes in growing bones (Alman, 2015). *Ihh*-null mice have a high lethality (50%) due to a failure in the yolk-sac vascular development (Varjosalo and Taipale, 2008). In addition, severe defects in cortical bones and atypical chondrocyte development in long bones are observed in surviving *Ihh*-null embryos (Colnot et al., 2005). A conditional knockout mouse line with loss of Ihh in limb mesenchymal cells ($Prx1^{Cre}$;$Ihh^{fl/fl}$) showed a complete loss of secondary ossification centre and growth plate, but unaffected osteoblast differentiation and bone formation (Amano et al., 2015). In humans, homozygous hypomorphic mutations in *IHH* cause acrocapitofemoral dysplasia, a rare disease

characterised clinically by short stature, short limbs, abnormally shorter digits and narrow thorax (Hellemans et al., 2003).

Of all *Hh* genes, *Shh* is the most broadly expressed gene during mammalian embryogenesis (Briscoe, 2009). Shh proteins are produced by the notochord, floor plate of the neural tube and the limb bud (at the zone of polarising activity (ZPA)) in early embryogenesis (Briscoe, 2009). However, as a long-range signalling protein, Shh diffuses away from its source (Briscoe, 2009). Shh functions as a morphogen, establishing a concentration gradient in the neural tube and limb bud. Concentration and duration of signal then dictate particular cell fates. Shh regulates the proliferation, differentiation, patterning, and survival of various tissues including the brain, neural tube, eyes, limb bud, axial skeleton and skeletal muscles. Consequently, *Shh*-deficient mice are embryonic lethal, have cyclopia, and severe defects in somite and foregut patterning, complete loss of neural tube ventral cell types, and truncated fore and hindlimbs (Chiang et al., 1996). Interestingly, similar defects are observed in mice with germline mutation in Smoothened (Smo), a transmembrane protein that transduces Shh signals (Varjosalo and Taipale, 2008). Some tissues like the foregut express more than one Hh protein, which display functional redundancy (Varjosalo and Taipale, 2008).

Hh signalling plays crucial role in regulating patterning, morphogenesis, proliferation and survival during embryonic development. As with other signalling pathways active during embryogenesis, Hh signalling is also reactivated in adulthood to modulate tissue regeneration. Thus, deregulation of Hh signalling has been implicated in tumorigenesis. For instance, aberrant activation of Shh signalling has been found to be driving tumour growth in various tissues including brain, skin, lungs, intestine and skeletal muscles (Skoda et al., 2018).

1.4.2 Biosynthesis and release of Hh ligands

Upon translation of Hh protein by Hh expressing cells, several post-translational modifications are required in order to produce the active form of the ligand. Initially, the 45kDa Hh precursor protein generated in the endoplasmic reticulum (ER) is subjected to autoproteolytic cleavage at its C-terminal domain between two conserved glycine and

cysteine residues (Porter et al., 1996). This creates a 19kDa N-terminal fragment called N-Hh that is responsible of all signalling activities. Next, the N-Hh fragment is subjected to addition of an ester cholesterol at its C-terminus and a palmitate at its N-terminus (Pepinsky et al., 1998). This modification is essential to boost Hh protein secretion by *skinny hedgehog* (*ski*) for *Drosophila* and Hh acyltransferase (HHAT) in mammalian tissues (Buglino and Resh, 2008).

The release of Hh ligand as a paracrine molecule requires another 12-span transmembrane protein called Dispatched (Disp) and a glycoprotein Scube2 (Tukachinsky et al., 2012). Both proteins bind to separate domains of the cholesterol molecule on the ligand and promote its secretion. Once released from the membrane, Hh proteins are stabilised at the cell surface and prepared for diffusion with the support of heparin sulphate proteoglycans (HSPGs) (Jakobs et al., 2016). Several assisting molecules present during Hh secretion are the glypicans, a glycosylphosphatidylinositol (GPI)- linked HSPGs that facilitate the formation of Hh ligand clusters using lipid rafts (Jakobs et al., 2016). For long-range transport of Hh ligands, two other molecules called *division abnormally delayed* (*dally*) and *dally-like protein* (*dlp*) function in promoting N-Hh cluster formation into lipoprotein (Yan et al., 2010). In addition, they also interact with another protein *shifted* (*shf*) in *Drosophila* and Wnt inhibitory factor -1 (WIF-1) to couple Hh with HSPGs and mediate its distribution (Sanchez-Hernandez et al., 2012). The interactions between HH ligands with different molecules along the process starting from its translation up to its release from Hh secretory cells are important to ensure Hh stability and efficient transportation in the extracellular space.

1.4.3 Hh signalling at the cell membrane

In *Drosophila*, Hh signalling is initiated by the binding of Hh proteins to the co-receptors Ihog and Boi (homolog proteins in vertebrates are Cdo and Boc) found at the plasma membrane of responding cells (Yao et al., 2006; Tenzen et al., 2006). Hh ligands bind to these transmembrane proteins via conserved fibronectin domains to increase the potential of Hh ligands to bind to its receptor, Patched (Ptc) (Yao et al., 2006). In response to active Hh signalling, the expression levels of both Cdo and Boi are down-

regulated, indicating a negative feedback loop to restrict Hh signalling activity (Varjosalo and Taipale, 2008).

While *Drosophila* has a single *ptc* gene, there are two *Ptch* genes in amniotes, *Ptch1* and *Ptch2* (Skoda et al., 2018). Hh ligands bind to both Ptch1 and Ptch2 with similar affinity to activate Hh signalling cascade downstream (Gailani et al., 1996). Ptch is a 12-transmembrane protein containing a sterol-sensing domain (SSD) within its extracellular loop that interacts with cholesterol on Hh (Ingham, 2000). SSD domain also functions in mediating the internalisation and trafficking of Ptc upon Hh binding (Strutt et al., 2001).

Ptc receptors are localised in intracellular vesicles in *Drosophila* but in vertebrates they are localised at the surface of primary cilia (Rohatgi et al., 2007). Primary cilia function as sensory organelles at the cell surface, which harbour receptors for many signalling pathways including Hedgehog pathway. Primary cilia are rode-like microtubule-containing structures that are anchored to the basal body in the cytoplasm (Sasai and Briscoe, 2012).

Ptch1 and *Ptch2* are expressed differentially during embryonic development with *Ptch1* generally expressed more broadly than *Ptch2*, whose expression is limited to skin basal cells and testicular epithelial cells only (Veenstra et al., 2018). This differential expression of Ptch receptors is probably the reason for the mild phenotype of *Ptch2*-deficient mice compared to the lethal phenotype of *Ptch1*-deficient mice (Nieuwenhuis et al., 2006). Loss of *Ptch1* also causes abnormally high expression of Hh target genes, indicating that the receptor acts as a negative regulator of Hh signalling, despite being the key receptor of the ligand (Taipale et al., 2002). *Ptch1*-deficient cells are still responsive to Hh signalling in a ligand dependent manner since blocking Shh with 5E1 antibody reduced the response. This is because loss in *Ptch1* was compensated by *Ptch2* expression, at least in early embryonic development (Alfaro et al., 2014). Mutations in *Ptch1* or loss of one copy of *Ptch1* are prevalent in some cancers including Gorlin syndrome, a familial disease with predisposed risk of developing skin, brain and skeletal muscle malignancies (Varjosalo and Taipale, 2008). Interestingly, *Ptch1* is also a transcriptional target gene of Hh pathway once activated. Therefore, activated Hh signalling increased the expression levels of *Ptch1* thus creating a negative feedback loop to inhibit the pathway (Varjosalo and Taipale, 2008). Another negative feedback

mechanism was identified in a study on *Drosophila* larval wing imaginal disc whereby increased Hh signalling results in sequestering of Hh ligands by ptc thus limiting the range of signalling (Johnson et al., 2000).

In *Drosophila*, the absence of Hh ligand triggers ptc to maintain smo in an unphosphorylated state (Zhao et al., 2007). Unphosphorylated smo is removed from the plasma membrane by endocytosis and processed through lysosomal degradation (Zhao et al., 2007). In vertebrates, Ptch1 is localised at the ciliary membrane when Hh proteins are absent and maintains the signalling pathway in an inactive or "off" state (Kim et al., 2015a). Ptch1 is doing so by inhibiting the translocation of vesicle-bound Smo into primary cilia (Kim et al., 2015a). The mechanism by which Ptch1 inhibits Smo activity has not been confirmed, but it was suggested that it is done via Ptch1 SSD domain since specific mutation at the site eradicates the inhibitory effect on Smo (Taipale et al., 2002). Another possibility would be an indirect regulation of another ligand modulating Smo function since Ptc is able to sequester lipophorin (Lpp) lipids causing its accumulation at the membrane of endosomes and blocking Smo translocation to the plasma membrane (Khaliullina et al., 2009). The *Smo* gene is conserved in both *Drosophila* and mice and *Smo*-deficient mice are not viable and die before birth (Alcedo et al., 1996; Huangfu and Anderson, 2005). However, small molecules known to block or activate Smo in vertebrates do not function in *Drosophila*, indicating that the mechanisms of Smo action in *Drosophila* are different (Varjosalo and Taipale, 2008). Smo is a 7-pass transmembrane protein and has a similar structure to G protein-coupled receptors with a cysteine-rich domain (CRD) that is crucial for its function (Rana et al., 2013).

Initial binding of Hh ligand to Ihog/Cdo or Boi/Boc and subsequently Ptc/Ptch1 results in Ptc/Ptch1 internalisation into endocytic vesicles (Torroja et al., 2004). Then, Smo is released from its inhibition, translocates to the base of primary cilia and is trafficked to the tip of primary cilia through the action of intraflagellar transport proteins (IFTs) (Huangfu and Anderson, 2005).

1.4.4 Intracellular Hh signalling transduction

In *Drosophila* and vertebrates, intracellular Hh signalling downstream of Smo is associated with microtubules. However, while in *Drosophila* microtubules are cytoplasmic, in vertebrates they are localised in primary cilia (Varjosalo and Taipale, 2008). Hh signalling transduction post-Smo activation involves the processing of the zinc-finger transcription factor *cubitus interruptus* (*Ci*) in *Drosophila* (Alexandre et al., 1996). There are three *Ci* homologs in vertebrates, called glioma-associated oncogene Gli1, Gli2 and Gli3 (Hui et al., 1994). Full-length Ci, or CiA, acts as a transcriptional activator and is the predominant form during active Hh signalling. (Aza-Blanc et al., 2000). Ci is cleaved into its repressor form CiR and blocks the transcription of Hh target genes in the absence of Hh ligands (Aza-Blanc et al., 2000). Like Ci, Gli2 and Gli3 are bi-potential transcription factors cleaved into repressor forms (GliR) in the absence of Hh and maintained as full-length transcriptional activators (GliA) in the presence of Hh. Gli1 lacks the cleavage site and thus exists only as a full-length form that functions to potentiate Gli2 activity (Varjosalo and Taipale, 2008).

When the pathway is inactive, the *Drosophila* kinesin-like protein Costal-2 (Cos2) or Kif7 in vertebrates functions as a scaffolding protein to attract cytoplasmic proteins including Protein kinase A (PKA), Glycogen synthase kinase-3β (Gsk-3β), Casein kinase Ia (CKIa) and Fused kinase (Fu) to form a complex called hedgehog signalling complex (HSC) (Chen et al., 1999; Jia et al., 2002; Robbins et al., 1997). In Drosophila, the complex is associated with microtubule and function to hyperphosphorylate Ci, which becomes the target of the ubiquitin E3 ligase Slimb to promote its proteosomal degradation into CiR (Smelkinson et al., 2007). Similarly, vertebrates Gli2 and Gli3 are phosphorylated by the HSC complex and recognised by β-transducin-repeat containing protein (β-TrCP), which mediates the proteolytic cleavage into the truncated repressor forms (Skoda et al., 2018).

Upon activation of Hh signalling, Smo is phosphorylated by the HSC kinases including PKA, CKIa, and CK2 with the association of G-protein coupled receptor kinase-2 (Gprk2) (Chen et al., 2010b). Stabilised Smo accumulates at the membrane or at the tip of primary cilia and associates with Cos2/Kif7 phosphorylated by Fu (Corbit et al., 2005). This process promotes Fu-dependent phosphorylation of Suppressor of Fused

(SuFu) and the release of the full-length activator forms of Ci/Gli2/Gli3, which translocate to the nucleus for the activation of Hh target genes (Humke et al., 2010; Aza-Blanc and Kornberg, 1999).

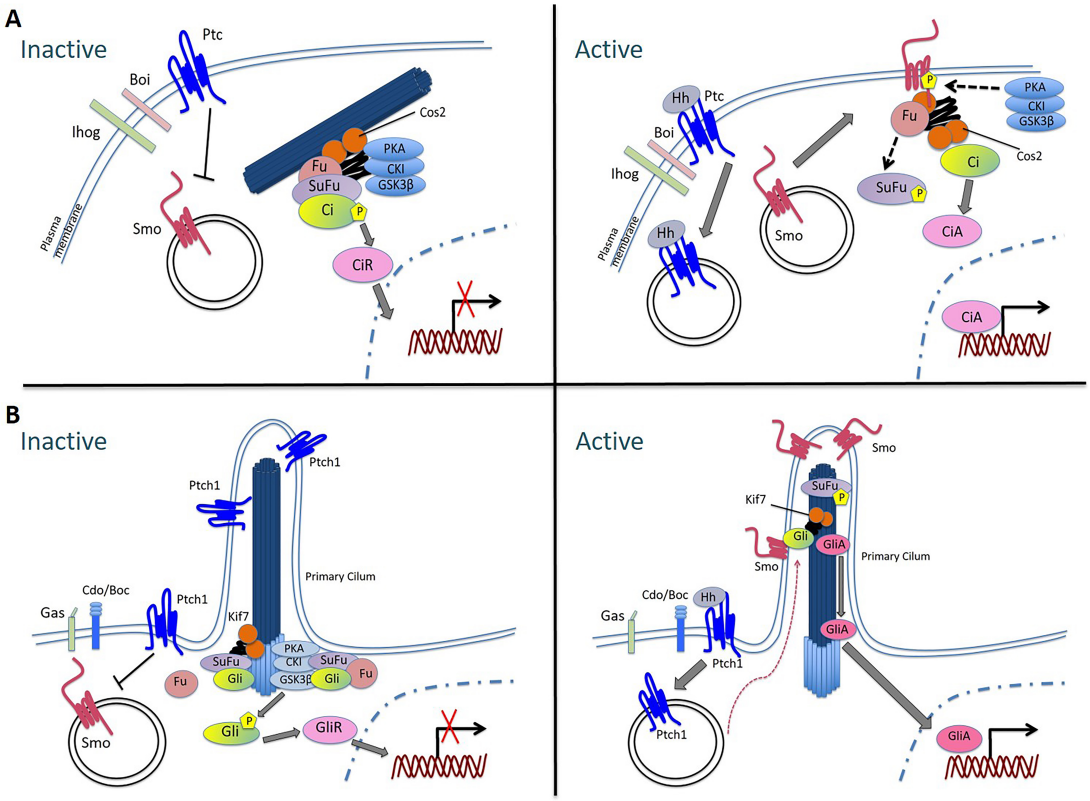

Figure 1.9: Intracellular transduction of HH signalling.
A) When HH ligands are absent in D. melanogaster (Inactive), Ptc receptors on the membrane constitutively inhibit the vesicle-associated Smo and promote its degradation. Consequently, the HSC complex comprised of PKA, CKI, GSK3β, Fu and Ci becomes associated with the microtubule. HSC complex then phosphorylates Ci to be cleaved into its repressor form (CiR). When HH ligands are available (Active), they are associated with Ihog and Boi to increase their affinity to bind to Ptc which release Smo from its repression. Smo then transported to the plasma membrane and phosphorylated by PKA, CKI and Gprk2. This lead to the phosphorylation of Cos2 and SuFu by Fu and thus HSC complex are dissociated to release Ci in their activator form (CiA). **B)** In the vertebrates, HH signalling is transduced via a microtubule-based organelle called a primary cilium. When Hh ligands are absent (Inactive), Ptch receptors accumulate along and at the base of primary cilia to inhibit the translocation of Smo into the organelle. This in turn causes Kif7 to accumulate in the base of primary cilia and promotes the recruitment of HSC kinases. Therefore, Gli2 and Gli3 are phosphorylated and cleaved into their repressor form (GliR) which is translocated into nucleus. When HH ligands are present (Active), their binding to Ptch receptor is assisted by co-receptors Gas, Cdo and Boc. This causes Ptch receptors to exit the primary cilia and release their inhibition on Smo, allowing Smo to be translocated into the tip of primary cilia. HSC kinases phosphorylates Smo and SuFu to induce the release of full-length Gli activator proteins (GliA) from the complex, and translocate into nucleus to activate transcription of its target genes.

1.5 Rhabdomyosarcoma: a childhood tumour of skeletal muscle origin

1.5.1 Disruption in Sonic hedgehog signalling is associated with several cancers

Although the Hedgehog pathway is mainly inactive in adult tissues, it is reactivated to support several homeostatic processes including tissue healing and maintenance of somatic stem cell pluripotency (Skoda et al., 2018). Embryonic development and tissue healing share common characteristics with tumorigenesis. Aberrant activation of SHH signalling is a common feature in a rare hereditary disease called the Gorlin Syndrome or Nevoid basal-cell carcinoma syndrome (NBCCS), characterised by an increased risk of developing a group of tumours including basal cell carcinoma (BCC), medulloblastoma (MB) and rhabdomyosarcoma (RMS) (Hahn et al., 1998; Skoda et al., 2018).

Abnormal Shh signalling activation is not limited to Gorlin syndrome, as it has also been described in sporadic tumours including non-small cell lung cancer, prostate cancer, pancreatic cancer and colorectal cancer (CRC)(Choudhry et al., 2014). This is probably due to the mitogenic function of the pathway adapted during normal embryogenic tissue development (Ruiz i Altaba et al., 2002). Sporadic Shh-responsive tumours are ligand-dependent tumours that respond to Hh in an autocrine or juxtacrine manner caused by the overexpression of Shh or ectopic expression of pathway components such as *Ptch1* or *Gli1* (Ruiz i Altaba et al., 2002). In addition, a paracrine activation of Hh pathway in surrounding stromal cells has also been reported in the growth of sporadic cancers (Arsic et al., 2007). For instance, Shh ligands secreted by tumour cells bind to Ptch1 receptors on stromal cells surrounding them, hence activating the pathway. This in turn leads to the release of growth factors such as VEGF, PDGF, IGF, Wnt and BMP to promote tumour cell expansion and differentiation (Jiang and Hui, 2008). While sporadic tumours were usually linked to the availability of the ligands, Gorlin syndrome occurs in a ligand-independent manner due to mutations in Hh pathway components.

1.5.2 Rhabdomyosarcoma and the Gorlin Syndrome

Gorlin Syndrome is a familial autosomal disease in humans caused by a germline mutation of *PTCH* associated with a high incidence of several types of tumours including basal cell carcinoma (BCC), medulloblastoma (MB) and rhabdomyosarcoma (RMS) (Gorlin, 1995). RMS is a tumour of skeletal muscle origin and the most common soft tissue sarcoma in children, often diagnosed with poor prognosis (Pappo et al., 1995). Sporadic BBC, the most common tumour in humans are predominantly caused by gene mutations, which lead to constitutive activation of the Hh pathway. Indeed, 85% of BBCs possess an inactivating mutation in the *PTCH1* gene (Johnson et al., 1996). In addition, mutations in *SMO* that result in its constitutive activation and loss of sensitivity to Ptch1 inhibition account for 10% of BBC cases (Reifenberger et al., 2005). A lower prevalence of BBC cases have mutations in *SUFU*, also an inhibitor of the Hh pathway although studies in mice demonstrated that loss of one allele of *Sufu* does not result in tumour formation (Lee et al., 2007).

RMS are divided into 2 subtypes based on their clinical presentation, histological features, distinct molecular markers and prognosis (Dagher and Helman, 1999). Embryonal RMS (eRMS) constitutes 75% of total RMS incidence and is more common in infants and young children (Malempati and Hawkins, 2012). Alveolar RMS (aRMS) is more common in adolescents and young adults, and is often associated with chromosomal translocations which cause a fusion between *PAX3* or *PAX7* and the forkhead transcription factor *FOXO1* (Merlino and Helman, 1999). Though the cellular origin of aRMS has been linked with terminally differentiated muscle fibres during postnatal life, the cellular origin of eRMS remains a debated issue. Several studies have reported that SCs or myogenic precursor cells expressing either Pax7 only or in combination with MyoD to be the cellular origin of eRMS (Tiffin et al., 2003; Blum et al., 2013). Young *Ptch1* heterozygous mice displayed a high incidence of RMS, and neoplastic cell histological observations resembled an eRMS-like morphology, thus indicating that *Ptch1* mutation could be involved in eRMS etiology (Hahn et al., 1998). Consistent with this, a study using several Cre driver lines, including M-Cre (Pax3), Pax7Cre, Myf5-Cre, and MRF4-Cre to generate conditional knockout of p53 in a $Ptch1^{+/-}$ background found that although eRMS arose in all cases in $Ptch1^{+/-}$ mice, the

concomitant loss of p53 increased the incidence of eRMs even from terminally differentiated muscle cells (Rubin et al., 2011; Kikuchi et al., 2011).

Previous studies have reported that Hedgehog (HH) signalling components including *SHH, PTCH, SMO, GLI* genes were overexpressed in human muscle tumour biopsies and human RMS cell lines (Hahn et al., 1998). Investigations in tumour biopsies of sporadic eRMS revealed that there is a haploinsufficiency of HH-mediated tumour suppressor genes *PTCH* and *SUFU* in the samples (Hahn et al., 1996). A study on mouse embryos has found that upon deletion of one copy of *Ptch1* allele, embryos at early stage (E9.5) are more susceptible to develop eRMS with 88% incidence, compared to later stages at E11.5 (44%) and E13.5 (12%) (Nitzki et al., 2011). Further, a study by Rajurkar et al. attempted to elucidate the impact of Hh/Gli de-regulation on tumourigenesis and the cellular origin of eRMS *in vivo* using *Shh* and *Gli1* cre lines to drive the expression of a mutated constitutively active *Smo* (*SmoM2*) in mice. They found that postnatal activation of Hh signalling leads to eRMS formation (Rajurkar et al., 2014). Additionally, treatments using Shh inhibitors cyclopamine and GANT-61 inhibit tumour cell proliferation *in vitro* and reduce tumour xenografts growth *in vivo*. The inhibition of proliferation was associated with disruption of the cell cycle due to the reduction of cyclins D1/2/3 and E expression, and the induction of p21 expression (Srivastava et al., 2014).

1.5.3 Cellular origin of Embryonal Rhabdomyosarcoma

Few studies have addressed the relationship between Shh-dependent RMS development and myogenesis, although Zibat et al. reported that *Myod1* expression was significantly attenuated in eRMS and fusion-negative aRMS, thus leading to the theory that HH-dependent RMS had an embryonic origin caused by a defect in myogenic differentiation (Zibat et al., 2010). However, a study by F Nitzki et al. has demonstrated that eRMS tumour incidence was reduced by 10-fold when *Ptch* allele was deleted in Myf5-expressing cells, compared with *Ptch* deletion in the whole organism (Nitzki et al., 2011). Therefore, it is possible that eRMS originates from a progenitor cell population that has not yet acquired a myogenic cell fate during embryonic development. However,

the satellite cell origin of eRMS was disputed in the Rajurkar et al. study showing that constitutive *Smo* and *Gli1* activation in Pax7^{+} SCs *in vivo* (Pax7^{CreER}; R26^{SmoM2}, Pax7^{CreER}; R26^{Gli1}, Pax7^{CreER}; R26$^{Gli2\Delta N}$ and Pax7^{CreER}; R26^{Gli1}; R26$^{Gli2\Delta N}$ mutants) failed to cause eRMS after 360 days (Rajurkar et al., 2014). Instead, Hh signalling was found to be more prominent in Sca1^{+} cells residing in the interstitial region outside basal lamina. Nonetheless, this study did not show that cells responding to Hh signalling were negative for the myogenic precursor cell markers Pax7, Myf5 or MyoD. In addition, mRNA analysis of isolated myogenic cells from the mutant mice showed an up-regulation of *MyoD* expression in eRMS cells compared to myogenic progenitors, suggesting that a more committed population of SCs is involved in eRMS formation. Thus, existing evidence of a satellite cell origin of eRMS in Ptch1$^{+/-}$ mice remains controversial, with current studies leaning towards a hypothesis of a non-myogenic origin of eRMS.

1.6 Sonic hedgehog (Shh) signalling in adult skeletal muscles

1.6.1 Sonic hedgehog signalling pathway in embryonic myogenesis

The onset of myotome development is marked by the formation of the epaxial myotome whereby Pax3-positive progenitor cells from the dorso-medial region of the dermomyotome start expressing *Myf5* and migrate into the myotomal space (Deries and Thorsteinsdottir, 2016). The epaxial (medial) and hypaxial (lateral) myotomal regions contribute to epaxial muscles which consist of the deep muscles of the back, and hypaxial muscles which include body wall and limbs muscles, respectively (Cheng et al., 2004). Embryonic myogenesis of the epaxial and hypaxial progenitor cells is dynamically regulated by MRFs which coordinate the cell fate and terminal differentiation of muscle progenitor cells (MPCs) into contractile myofibres (Pownall et al., 2002). Myogenesis and activation of MRFs expression in the myotome is controlled by signalling pathways from surrounding tissues, including Wnts, BMPs and Shh (Deries and Thorsteinsdottir, 2016). Indeed, the specification and fate determination of epaxial MPCs rely on signals

from adjacent notochord and neural tube while hypaxial MPCs depend on signals from ectoderm and lateral plate mesoderm.

During embryonic development, Shh is secreted by the notochord and floor plate of neural tube. A study using avian embryos showed that treatment of presegmental plate mesoderm explants with Shh and Wnt *in vitro* induced myogenic differentiation by stimulating the expression of myogenic markers like MyoD and Myosin Heavy Chain (Munsterberg et al., 1995). Moreover, it was demonstrated that bead implantation containing recombinant Shh was adequate to replace the function of notochord in quail embryos as it induces the expression of MyoD in dorsal somites (Borycki et al., 1998). Conversely, antisense oligonucleotides to knock-down Shh expression inhibited the transcription of *Myf5* and *MyoD* in somites (Borycki et al., 1998; Borycki et al., 1999). Further studies using mouse embryos revealed that Shh is essential for *Myf5* activation in epaxial MPCs, and that Shh controls embryonic myogenesis by directly regulating *Myf5* transcription in MPCs via the binding of Gli2/Gli3 to an epaxial *Myf5* enhancer (Borycki et al., 1999; McDermott et al., 2005). The non-canonical Shh pathway was also shown to be regulating Myf5 expression and epaxial differentiation via the regulatory effect of β-catenin on Gli proteins, which are the effectors of Shh (Borello et al., 2006).

All Shh, Wnts and BMPs regulating epaxial muscle development are also expressed in limb mesenchyme and ectoderm, suggesting their role in regulating limb morphogenesis (Deries and Thorsteinsdottir, 2016). Shh transcripts are expressed in the zone of polarising activity (ZPA) in the posterior limb mesenchyme (Riddle et al., 1993). *Shh*-mutant embryos have defective limb muscle formation, although initially no effect on *Myf5* expression was reported (Kruger et al., 2001). Nevertheless, Shh overexpression experiments using Shh-coated beads or engraftment of Shh-expressing cells in developing limb buds increases the expression of Pax3 and MyoD and results in muscle hypertrophy (Duprez et al., 1998; Johnson and Tabin, 1997). In agreement with this, conditional deletion of Smo in Pax3-expressing cells ($Pax3^{Cre}$; $Smo^{flox/flox}$) in mice leads to a delay in the induction of *Myf5* and *MyoD* expression and the specific loss of ventral limb muscles (Anderson et al., 2012; Hu et al., 2012). Shh signalling directly regulates *Myf5* transcription in ventral limb MPCs via the interaction of Gli2/3 with a *Myf5* limb enhancer (Anderson et al., 2012).

A final role for Hh signalling in embryonic myogenesis is in muscle patterning via the control of components of the myotomal basal membrane. The myotomal basal membrane is a specialised extra-cellular matrix structure made of several components including Collagen type IV, Laminins (Laminin-111 and Laminin-511), Nidogen and proteoglycans (Borycki, 2013). During early embryonic myogenesis, MPCs upregulate the expression of Integrin α6β1 (a Laminin receptor) and Dystroglycan as they migrate from the dermomyotome to form the myotome (Anderson et al., 2009). This initiates the onset of myotomal membrane assembly. Shh signalling regulates the assembly of the myotomal basal membrane by stimulating *Lama1* gene expression, which encodes Laminin-α1 protein, an important component of myotomal basal membrane (Pickering et al., 2017; Anderson et al., 2009). Thus, in addition to cell fate specification, Shh signalling also regulates embryonic myogenesis by controlling myotomal membrane assembly, which is important in mediating MPCs function.

1.6.2 Sonic Hedgehog signalling is recapitulated in adult myogenesis

The multiple roles of Shh signalling in embryonic myogenesis suggested that it may also function in adult myogenesis, since SCs are derived from the dermomyotome during embryogenesis. There is as yet no confirmation of the source of Hedgehog ligands in adult skeletal muscles, it has been suggested to act in an autocrine manner in SCs and/or interstitial mesenchyme al fibroblasts (Elia et al., 2007; Pola et al., 2003; Straface et al., 2009b). Early studies on Shh effects on adult muscle-derived cells were carried out by treating C2C12 cells, a myoblast cell line, with either recombinant Shh proteins to activate the pathway or the Smoothened inhibitor cyclopamine to inhibit the pathway (Elia et al., 2007; Koleva et al., 2005a; Li et al., 2004; Madhala-Levy et al., 2012; Straface et al., 2009b). Similar studies have also been carried out on primary myoblasts derived from chick, frog and mouse muscles (Elia et al., 2007; Koleva et al., 2005a; Yamane et al., 2011). *In vivo* studies have also been performed in wild-type (WT) mice and transgenic mice with *LacZ* reporter gene under the control of the *Ptch1* promoter (NLS-Ptch1-LacZ) (Straface et al., 2009b). Collectively, these studies established that quiescent cells or freshly isolated myoblasts do not display signs of Shh pathway activity (Elia et al., 2007;

Koleva et al., 2005a; Straface et al., 2009b), although expression of *Smo* suggests that the cells are capable of responding to the pathway (Elia et al., 2007). Indeed, the transcription of the Shh signalling target genes *Ptch1* and *Gli1* is upregulated in myoblasts cultured in growth medium (Elia et al., 2007; Koleva et al., 2005a). Upregulation of the reporter gene was also observed in crush or cardiotoxin-injured NLS-Ptch1-LacZ reporter mice, although no evidence was provided of the muscle-resident cell types displaying *Ptch1* expression (Straface et al., 2009b). These reports are therefore indicative of a possible Hedgehog response in adult myogenesis, although clear evidence of Hh signalling in satellite cells in vivo has been lacking so far.

1.6.3 Sonic hedgehog signalling promotes muscle progenitor cell proliferation and differentiation in adult muscles

Ptch1 up-regulation in primary myoblast cultures suggested that Hh signalling may play a role in adult myogenesis. Several *in vitro* studies using C2C12 cells and primary myoblasts reported that treatment with Shh or N-Shh increased myoblast proliferation, as assayed by measuring cell count, BrdU labelling and Ki67 expression (Elia et al., 2007; Koleva et al., 2005a; Li et al., 2004; Straface et al., 2009b). Moreover, the size of limb skeletal muscles in developing embryos was increased upon ectopic implantation of Shh-expressing cells (Li et al., 2004). However, Shh administration has also been suggested to affect myoblast differentiation, due to increased mRNA levels of cell cycle regulators *p21*, *p27* and *pRb* (Elia et al., 2007) and increased levels of differentiation markers including Myf5, MyoD, Myogenin and MyHC in Shh-treated myoblast cultures (Elia et al., 2007; Li et al., 2004; Straface et al., 2009b). Consistent with this, a recent study using primary myoblasts suggested that Shh signalling is required for myoblast commitment and early differentiation, although it must be down-regulated to allow terminal differentiation as expression of *Smo*, *Gli1*, *Gli2* and *Gli3* decreased with differentiation (Fu et al., 2014). Finally, Shh treatment was also found to reduce cell apoptosis by inhibiting Caspase-3 activity, suggesting another role in cell survival (Koleva et al., 2005a). In all cases, the effects of Shh on myoblast proliferation and differentiation

were shown to be dose-dependent, and attenuated by cyclopamine treatment (Koleva et al., 2005a; Straface et al., 2009b).

Therefore, conflicting findings have emerged from these previous studies, with Shh signalling possibly implicated in myoblast proliferation, differentiation and cell survival. These divergent views result most likely from different culture conditions and cell types used. While primary myoblast and cell line cultures are widely used to study skeletal muscle regeneration, they do not faithfully represent the behaviour of native satellite cells, which is largely influenced by the microenvironment. This may explain the discrepancies between the Koleva et al. and Elia et al. studies. Therefore, the single fibre culture system introduced by Bischoff in 1985, which has been the gold standard technique to examine satellite cells in their niche (Pasut et al., 2013), must be used to address the role of Shh signalling in satellite cells. The myofibre culture system allows also to observe the behaviour of satellite cells from quiescence, since satellite cells are spontaneously activated once detached from their niche (Dhawan and Rando, 2005).

Thus, it remains unclear whether Hh signalling is acting directly or indirectly on satellite cells and muscle regeneration, and whether it controls proliferation or differentiation of satellite cells, or other aspects of adult myogenesis.

1.7 Previous work leading to this project

Previous work carried out in the laboratory by Sara Cruz-Migoni (PhD student) has shown that the expression of the Shh components *Smo*, *Ptch1*, *Gli1*, *Gli2* and *Gli3* is up-regulated in cultured myofibres (Cruz Migoni, 2015). Investigation using transgenic reporter mice expressing GFP under the control of Gli binding sites (Tg(GBS-GFP)) as indicator of Shh response revealed that SCs are unresponsive to Shh signalling during quiescence. However, upon activation and during the proliferation and differentiation phases, SCs become responsive to Shh signalling. Consistent with this observation, Ptch1 expression is significantly increased during SCs proliferation, suggesting a role for Shh signalling in the regulation of the cell cycle, which is important in tumour formation. Moreover, pharmacological inhibition of Shh signalling using GANT61 causes a decline

in SC number and proliferation, and a concomitant delay in differentiation. Flow cytometry analyses, combined with studies of myofibre cultures from FUCCI2 mice, revealed that GANT61-treated satellite cells were arrested at the G1/S transition compared to control satellite cells, suggesting that Shh signalling controls SC progression through the cell cycle. Consistent with these findings, muscle regeneration following cardiotoxin-mediated injury was impaired (Cruz Migoni, 2015).

1.8 Conclusion and aims of the thesis

Thus, although the effect of Shh signalling on skeletal muscle regeneration was examined in previous studies, the exact mechanism by which Shh signalling activation alters SCs behaviour during skeletal muscle regeneration is not fully understood. Furthermore, the effect of Shh upregulation on satellite cell quiescence, activation, proliferation, self-renewal and differentiation, and skeletal muscle regeneration and tumour formation has yet to be elucidated.

Therefore, I hypothesised that aberrant activation of Shh signalling in satellite cells alters their behaviour during myogenesis and may play a role in tumour formation or promote tumour expansion in skeletal muscles, particularly the embryonal type of RMS. The aims of this project were:

1. To investigate the effects of upregulating Shh signalling in satellite cells *ex vivo*
2. To conditionally delete *Ptch1* in Pax7-expressing satellite cells to study the impact of deregulated Shh signalling on muscle regeneration *in vivo*
3. To investigate the possibility that deregulating Shh signalling in satellite cells contributes to eRMS tumorigenesis.

The implication of Shh signalling in various tumours and growing evidence of Shh signalling role in satellite cells makes it a good candidate and molecular target whose de-regulation would support a stem cell theory for the cellular origin of eRMS. Thus, unravelling the pathogenesis of eRMS would provide novel strategy for a targeted treatment to combat this disease, which affects predominantly young children.

2 Materials and methods

2.1 Mouse Models Utilised

2.1.1 C57BL/6

The maintenance of the C57BL/6 mice and all subsequent mouse models were carried out according to the UK Home Office regulation compliance to the UK Animals (Scientific Procedures) Act 1986 (ASPA) under a valid UK Home office project licence (PPL). Subsequent mouse lines in this project were maintained on a C57BL/6 background, referred to as wild-type (WT) mice thereafter. Animal care and husbandry of all the mouse lines in this study were carried out at the Biological Services Western Bank Division at The University of Sheffield.

2.1.2 Tg: Pax7-nGFP

The transgenic mouse line Tg: Pax7-nGFP, thereafter referred as Pax7GFP was generated in the Tajbakhsh lab, as described in (Sambasivan et al., 2011). The line contains a non-targeted insertion of a BAC transgene containing ~200kb of mouse genomic DNA with the locus encoding *Pax7* gene that drives the nuclear expression of EGFP (nGFP). This construct resembles the endogenous expression of Pax7 during both developmental and postnatal stages (Sambasivan 2009).

2.1.3 Inducible Cre line Pax7$^{CreERT2/+}$

The inducible mouse line Pax7Cre$^{ERT2/+}$ was generated by (Lepper et al., 2009) by inserting a modified *Cre* recombinase allele (knock-in) adjacent to the *Pax7* locus. The *Cre* is modified by fusing a mutated Estrogen binding-site of the Estrogen receptor (ERT2) that binds to tamoxifen, but not Estrogen in high affinity. Cre recognises a 34-bp site

called *loxP* site and efficiently catalyses DNA recombination between pairs of *loxP* sites by excision or inversion.

I. Ptch1$^{flox/flox}$; Pax7Cre$^{ERT2/+}$ were generated at the Biological Services Western Bank Division, The University of Sheffield by crossing Ptch1$^{flox/flox}$ mice (Goodrich 1997; Uhmann 2007) with Pax7Cre$^{ERT2/+}$ as described above. Homozygous mutant mice (Ptch1$^{flox/flox}$;Pax7Cre$^{ERT2/+}$) are thereafter referred as Ptch1^{cKO} and heterozygous mice (Ptch1$^{flox/+}$; Pax7Cre$^{ERT2/+}$) are referred as Ptch1$^{\Delta/+}$. Control WT mice used were either Ptch1$^{flox/flox}$ or Ptch1$^{flox/+}$.

2.1.4 Induction of Cre-mediated recombination

Tamoxifen (TM, Sigma-Aldrich, #Ref: T5648-1G) at 10mg/ml was prepared by dilution in corn oil (Sigma-Aldrich, #Ref: C8267-500ML). Warm tamoxifen (3mg/40g of body weight) was administered to mice via daily intraperitoneal (IP) injection for 4 days using sterile 25G needle (BD Microlance™) with 1ml syringe (BD Plastipak™), followed by Tamoxifen diet (~40mg/kg/day, Harlan Laboratories) from day 5 onwards until sacrifice. Tamoxifen treatment was performed one week before Cardiotoxin injury (explained in 2.4.1). For repeated injury experiments, mice were kept on the tamoxifen chow until 14 day-post-injury (DPI) and maintained with normal chow for the rest of the experimental period.

2.1.5 Mouse genotyping

Mice were ear-clipped at 14-21 day-old to provide tissue samples for genotyping. Samples were digested in 100 µl of 10mM NaOH and heated at high temperature (95°C) on a heating block for 15-20 minutes and neutralised with one volume of 40mM TrisHCl. The genomic DNA was used for gene amplification via polymerase chain reaction (RT-PCR) technique. Amplification products were analysed by gel electrophoresis. Genotyping was performed by Dr. Anne-Gaelle Borycki. Primers used for genotyping were:

Tg:Pax7-nGFP:

SV40pA F3 - Forward: CCACACCTCCCCCTGAACCTGAAACATAAA

Pax7 R10 - Reverse: GAATTCCCCGGGGAGTCGCATCCTGCGG

Size: 500bp

Ptcflox/flox:

PtcFL-Forward: TTC ATT GAA CCT TGG GGA AC

PtcFL-Reverse: AGT GCG TGA CAC AGA TCA GC

wild-type allele: 216bp

floxed allele: 269bp

2.2 *Ex vivo* system: Single Myofibre culture

2.2.1 *Extensor digitorum longus* (EDL) muscle harvesting

Procedure for EDL muscle harvesting tendon to tendon from mouse hind limb is as follows. First, the mouse was sacrificed by cervical dislocation in accordance to Schedule 1 of ASPA. The right hind limb was semi-sterilised using 70% Ethanol and hair was partially shaved using a scalpel. A small incision on the skin was made to grip the skin with toothed forceps and skin was torn upwards. The mouse was pinned on a dissecting board and visualised under a stereo dissecting microscope. Excess skin on the paw was removed to expose the four distal EDL tendons in a cluster and the *Tibialis anterior (TA)* tendon in the interior side of the paw. Both tendons were cut using dissecting scissors and looped out of the connective tissue mesh at the ankle level. Connective tissue covering the TA muscle was removed carefully using forceps (without damaging the TA muscle tissue underneath) starting from the area below the knee and downwards towards the distal tendons. The mouse was positioned with its lateral side facing upwards by pulling its tail to the side. The proximal EDL tendon, observed just at

the lower exterior side of the knee (inserted at the lower part of the knee cap) was slightly looped and cut using dissecting scissors. Then, the distal tendons were separated and only the TA tendon was gripped and carefully pulled away from the limb. Then, the EDL was gripped at its distal tendon and carefully lifted away from the limb until the entire EDL was detached while minimal force applied onto the muscle. EDL muscle were place into the collagenase medium for digestion. The same steps were followed to harvest another EDL from the left hind limb.

2.2.2 Digestion and Isolation of single myofibers from EDL muscle

EDL muscles were digested using Collagenase Type 1 (Sigma-Aldrich, #C0130-500MG) at 2.2 mg/ml in Dulbecco's Modified Eagle's medium (DMEM) supplemented with GlutaMAX™-1 (Gibco, #31966-021) and 1% Penicilin-Streptomycin-Fungizone (PSF) (Sigma-Aldrich, #A5955-100ML) for 80-90 minutes at 37°C. While waiting for digestion, 6 plastic Petri dishes (60 mm diameter, Nunc) labelled 1-6 were coated with filtered (0.2mm syringe filter) 5% Bovine Serum Albumin (BSA) (Sigma- Aldrich, #A1470-100G) in phosphate-buffered saline (PBS) (Fisher Bioreagents, #P399-4) and air-dried. Isolation medium was prepared (DMEM with GlutaMAX™-1 and 1% PSF) and added into petri dishes (5ml/dish). Media dishes were placed in a culture incubator at 37°C. Then, two glass pipettes were prepared and heat-polishing with one having a wider bore (~3-4mm diameter) and another having smaller bore (~1mm). Glass pipettes were coated with 5% BSA. After digestion, EDL muscles were transferred into a pre-warmed 1st isolation dish using the wide-bored glass pipette. Single myofibres were released from tendon attachments and muscle bulk by flushing the media onto the muscle bulk. This was done by partially filling the pipette with isolation media, tilting the dish and flushing that media towards the muscle bulk repeatedly for ≤10 minutes under a clean stereo microscope with transmitted light (from below the stage) at room temperature (RT). Dishes were returned into the incubator to avoid extreme temperature difference. Released and healthy single myofibres were transferred into subsequent isolation dishes using the narrow-bore pipette to wash the myofibres from debris and collagenase residues.

2.2.3 Culture of single myofibres

Nunc Petri dishes (same as above) were coated with filtered 5% BSA in PBS and air dried. Dishes were labelled with mouse line, treatment type, harvesting time point and date. Culture medium was prepared, containing DMEM with GlutaMAX™-1, 10% Horse serum (Gibco, #16050-130), 1% PSF and 0.5% Chicken Embryo Extract (CEE) (SeraLab, #CE-650-J). Washed myofibres were transferred into pre-warmed culture media using the narrow-bore pipette with the total of 30-40 myofibres per dish. Myofibres were cultured at 37 °C and 5% CO_2 in high humidity and sterile environment.

2.2.3.1 Pharmacological agent to up-regulate Shh signalling

Single myofibre cultures were treated with Smoothened agonist (SAG) (Millipore, #566660) at 100nM to up-regulate Shh signalling. SAG was dissolved in Dimethyl Sulfoxide (DMSO) (Sigma-Aldrich, #D8418-100ML) to create a 0.25mM stock solution and 2µl of the stock solution was added into a culture dish. Myofibres in the control group were treated with 2µl of DMSO only.

2.2.3.2 EdU (5-Ethynyl-2'-Deoxyuridine) Assay

EdU assay was performed to detect proliferating satellite cells in S-phase of the cell cycle using the Click-iT™ EdU Imaging Kit (Invitrogen, #C10339) following the manufacturer's instructions. Prior to harvesting, myofibres were incubated with EdU at 10µM for 60 minutes at 37 °C. Then, myofibres were harvested into 2ml sterile Eppendorf tube and fixed with 3.7% formaldehyde (Sigma, #15512) for 10 minutes. Formaldehyde was discarded and myofibres were washed twice with 3% BSA in PBS for 10 minutes. Myofibres were then permeabilised with 0.5% Triton X-100 for 15 minutes, washed again with 3% BSA, and incubated in the EdU detection cocktail for 30 minutes in the dark at RT. After washing for 10min, blocking performed for 30 minutes in 1% of Heat-inactivated goat serum (HINGS) (Gibco, Life Technologies). Subsequent procedures for immunofluorescence staining is described in the next section.

2.3 Immunofluorescence staining for Single Myofibres

Cultured single myofibres were harvested into 2ml Eppendorf tubes using polished glass pipette coated with 5% BSA according to time points decided in experimental design. Excess medium was carefully discarded using a glass pipette using a stereo microscope to avoid discarding floating myofibres. Myofibres were washed once with PBS for 5 and quickly fixed in 400µl 4% paraformaldehyde (PFA) (Sigma-Aldrich, #P6148) (pH ~7.5) in PBS for 6-8 minutes. PFA was discarded and myofibres were washed 3 times in PBS for 5 minutes. At this point myofibres were either kept in PBS at 4 °C for further steps (within 2 weeks) or processed in the same day.

Next, fixed myofibres were permeabilised in 0.25-0.5% Triton X-100 in PBS for 5-7 minutes and washed 3 times for 5 minutes with excess PBS. Then, myofibres were blocked in 20% horse serum in PBS for 30 minutes at RT, before incubation with 250µl of primary antibodies cocktail diluted in PBS overnight with agitation at 4 °C. Primary antibodies were discarded and myofibres were washed 3 times for 5 minutes with PBS and incubated in the secondary antibody solution prepared in PBS for 60 minutes at RT on a shaker and protected from light. Then, myofibres were washed 3 times for 5 minutes in PBS containing 0.025% Tween-20 (PBST) (Sigma, #P1496). Myofibres were transferred onto clean and labelled microscopy slides (Thermo Scientific, Menzel Glaser) using a BSA-coated glass pipette. Myofibres were mounted in mounting solution containing DAPI (VectaSHIELD, #H-1200) and a coverslip was applied for imaging. List of primary and secondary antibodies used in this study are shown in table 2.1 and 2.2

Table 2.1: List of Primary Antibodies

Name	Host	Supplier	Reference	Dilution
Pax7	Mouse monoclonal	DSHB	Pax7	1:20
Myf5	Rabbit polyclonal	Santa Cruz	Sc-302	1:1000
MyoD	Rabbit polyclonal	Santa Cruz	Sc-304	1:2000
MyoD	Rat Monoclonal	Active Motif	3991	1:1000
Myogenin	Mouse monoclonal	DSHB	F5D	1:50
Myogenin	Rabbit polyclonal	Santa Cruz	Sc-576	1:50
Myogenin	Rabbit polyclonal	Novus Biologicals	NBP2-54972	1:500
Caveolin-1	Rabbit polyclonal	Santa Cruz	Sc-894	1:400
GFP	Chicken polyclonal	Abcam	Ab13970	1:600
Ki67	Rabbit polyclonal	Lieca	Ki67	1:300
Ki67	Rabbit polyclonal	Abcam	Ab66155	1:300
PH3	Rabbit polyclonal	Millipore	MC463	1:300
Laminin α-2	Rat monoclonal	Enzo	mAb(4H8-2)	1:300
Laminin	Rabbit polyclonal	Sigma-Aldrich	L9393	1:1000
Collagen-1	Rabbit polyclonal	Millipore	AB765	1:350
ARL13B	Mouse monoclonal	Neuromab	75-287	1:1000
ODF2	Rabbit polyclonal	Abcam	Ab43840	1:100
CEP164	Rabbit polyclonal	Proteintech	22227-1-AP	1:1000

Table 2.1 List of Secondary Antibodies

Name	Host	Supplier	Reference	Dilution
Alexa 594 anti-mouse	Goat	Life Technologies	A11005	1:500
Alexa 488 anti-mouse	Goat	Life Technologies	A10680	1:500
Alexa 594 anti-rabbit	Goat	Life Technologies	A11037	1:500
Alexa 488 anti-rabbit	Goat	Life Technologies	A11034	1:500
Alexa 633 anti-rabbit	Goat	Life Technologies	A21070	1:500
Alexa 594 anti-rat	Goat	Life Technologies	A11006	1:500
Alexa 488 anti-rat	Donkey	Life Technologies	A21208	1:500
Alexa 488 anti-chicken	Goat	Life Technologies	A11039	1:500

2.4 *In vivo* system: Cardiotoxin-induced muscle injury model

2.4.1 Cardiotoxin injections

Mice were induced into unconsciousness using a vaporiser anaesthesia machine supplied with 4% Isoflurane, and maintained under anaesthesia for the duration of the procedure through a mask delivering 3% Isoflurane (Abbott Laboratories). Mice were place on a heated pad with their left hind limb partially flexed inwards and immobilised with a sticky tape to expose the Tibialis anterior (TA) muscle. The lower hind limb was shaved and sterilised with 70% Ethanol wipes. 50µl of Cardiotoxin (CTX) 10µM in sterile PBS purified from *Naja mossambica* were injected into the TA muscle using insulin syringes and spread throughout the muscle by slowly retracting the needle while injecting. Mice analgesic agents by subcutaneous injection (Vetergesic), and kept in a warm incubator until recovery. Injections were carried out by Dr. Anne-Gaelle Borycki. For repeated injury experiments, the same procedure was repeated twice after a recovery period of 28 days (4 weeks). TA muscles were then harvested at the indicated time points after CTX injection (dpi, day post-injury).

2.5 Muscle tissue transverse sections

2.5.1 Tissue harvesting and freezing protocol

Injured TA muscles were harvested in the same way as EDL muscles (described in 2.2.1) and were cut at the knee. For transverse tissue sectioning, TA muscles were fixed using cold 2% PFA with 0.25% Triton X-100 in PBS for 60 minutes at 4°C on a rotator. Muscle tissues were then washed 3 times for 60 minutes with ice-cold PBS on a rotator at 4°C and incubated in 20% sucrose (VWR, #27483.294) in PBS overnight at 4°C on a rotator. Muscles were embedded in O.C.T compound (Thermo Scientific) after being placed vertically in a cylindrical moulding boat and rapidly frozen in cold Isopentane (Fisher, #AC397220010) maintained in liquid Nitrogen. Frozen TA muscles were kept at -80°C for long-term storage.

Frozen muscles were mounted on steel chunk or holder using O.C.T compound on dry ice. Transverse tissue sections were generated at 7-10µm on a Bright cryostat. The specimen temperature was maintained at -16 to -18°C and the chamber temperature was maintained at 22°C. Sections were collected on negatively charged Superfrost™ Plus slides (Thermo Scientific, #J1810AMNT) and were air-dried for 2 hours at RT before immunofluorescence staining or kept at -20°C freezer for further processing.

2.5.2 Immunofluorescence on muscle sections

Fresh or frozen sections are air-dried for 30 minutes. Sections were re-hydrated with excess PBS for 5 minutes and then blocked with blocking solution containing 5% BSA, 0.5% Triton X-100, 1% HINGS, 1% foetal bovine serum (FBS) (Gibco Life Technologies, 10270106) in PBS in a humidified chamber for 60 minutes. The blocking solution was discarded and 350µl of primary antibodies diluted in PHT solution consisting of 1% HINGS and 0.05% Triton X-100 in PBS were gently pipetted onto slides. Slides were incubated in a humidified chamber at 4°C overnight. Slides were washed with PHT 3 times for 10 minutes each and then incubated in secondary antibodies diluted in PHT for 60 minutes in a humidified chamber at RT and protected from light. Sections were washed with PHT 3 times for 10 minutes each and mounted with Vectashield DAPI and covered with glass coverslips.

2.6 Imaging

Sections with immunofluorescence staining were observed under Olympus BX51 microscope using 40X lenses with X-cite 120 illumination system (EXFO, Quebec, Canada). Immunofluorescence images were captured on a Zeiss Apotome with ZEN pro imaging system at 40X and 20X lenses kindly provided by Dr. Marysia Placzek. Images were enhanced and assembled via Adobe Photoshop CC 2017 and Microsoft Office Power Point 2016.

2.7 Doublets scoring method

Immunostained single myofibres were mounted in DAPI (Vectashield, Vector Labs) on clear glass slides under coverslips and were observed under fluorescence microscope (Zeiss Apotome). Doublets were identified as sets of two satellite cells (SCs) expressing SC markers partially attached or situated close to each other with no other SC present near the doublet to be considered for analysis.

The orientation of doublets was determined as planar when cells were observed on the same focal plane and the doublets' nuclei had identical morphology, irrespective of whether the planar doublets' division axis was parallel to the myofibre, perpendicular to the fibre or oblique to the fibre. If the doublets were located at the periphery of the harbouring myofibre, both sister cells needed to make contact with the myofibre.

The orientation of doublets was categorised as apico-basal if one sister cell was in a different focus plane to the other sister cell. This indicated that the doublet cells were on top of each other in 3-dimensional position. If the doublets were located at the periphery of the myofibre, then one sister cell needed to be in contact with the myofibre while the other sister cell needed to not have association with the myofibre but be in close contact with the sister cell (on top of the sister cell from side view).

For cell fate, each sister cells were scored according to the expression of marker genes used for the study. Symmetric cell fate were identified when the markers were expressed/not-expressed by both cells. Asymmetric cell fate was identified when both sister cells displayed different repertoire of marker gene expression.

2.8 Analysis

Myofibres were analysed via manual cell counting technique while observing them under Olympus BX51 microscope using 40X lenses. Muscle sections were analysed via cell counting on images taken on Zeiss Apotome microscope using Adobe Photoshop CC 2017. Analyses for minimum ferret diameter and area fraction of fluorescence were performed using the FiJi (previously ImageJ) software.

2.8.1 Statistical analysis

All graphs were generated using GraphPad Prism 7 software and presented as the mean ± standard error of mean (SEM). A minimum of three biological replicates with on average 15-25 myofibres per culture set for every time point were analysed in *ex vivo* studies. A minimum of three mice (biological replicates) per genotype for every time point with 6-8 sections per muscle were analysed. Statistical analyses were performed using GraphPad Prism 7 on the mean values from different groups using unpaired *t*-test or multiple *t*-test assuming parametric two-tailed distribution.

3 Up-regulation of Shh signalling affects skeletal muscle regeneration.

3.1 Introduction

The role of satellite cells during skeletal muscle repair can be studied using injury models in animals. Muscle repair is characterised by two phases, the degeneration phase and regeneration phase (Charge and Rudnicki, 2004). Muscular degeneration upon injury starts with calcium influx and cell necrosis caused by damaged myofibres and the increase in membrane permeability (Peake et al., 2017). High levels of cytosolic proteins such as creatinine kinases and other chemotactic factors attract the migration of monocytes and other immune cells that support the regeneration phase (De Paepe and De Bleecker, 2013). Monocytes are primed to differentiate into macrophages to assist the regeneration phase (Varga et al., 2016).

During the regeneration phase, satellite cells are activated to expand their population size via proliferation and differentiate into myocytes to generate newly regenerated fibres by fusing to each other (Dumont et al., 2015a). Newly formed myofibres are smaller and are centrally nucleated, compared to mature myofibres that are larger and peripherally nucleated (Whalen et al., 1990). New myofibres continue to grow in size through continued myocyte fusion (secondary fusion) to restore the muscle architecture (Chal and Pourquie, 2017). While acute muscle injuries usually involve only one round of the degeneration-regeneration muscle repair mechanism, chronic muscle injuries consist of multiple rounds of the muscle repair process (De Paepe and De Bleecker, 2013). The most common injury model used to explore chronic muscle injury is the *mdx* mouse, a genetic mouse mutation in the *Dystrophin* locus used as a model for Duchenne Muscular Dystrophy (DMD) (De Paepe and De Bleecker, 2013).

There are several methodologies used to induce acute muscle injuries, including using myotoxins such as bupivacaine, notoxin or cardiotoxin (CTX), which efficiently damage 80%-90% of myofibres while sparing the satellite cells residing in those myofibres (Relaix and Zammit, 2012). $BaCl_2$ injections are used also to severely injure

muscle tissue by causing membrane depolarisation, exocytosis and blocking Ca^{2+} efflux (Relaix and Zammit, 2012). In addition, mechanical injuries such as freezing and mechanical crushing, and physiological intervention such as ischemia and denervation are also adapted to induce acute injury to study muscle regeneration (Charge and Rudnicki, 2004). The myogenesis program in acute injury is different from chronic injury due to several factors including like the degree of the injury (loss of basement membrane or satellite cells), the type of muscle injured, the levels of immune response, and the age and pre-existing pathological status affect the progression and duration of muscle regeneration.

In previous work in the laboratory, Sara B Cruz-Migoni revealed that satellite cells are responsive to Shh signalling upon activation and require intact Shh signalling to support their proliferation (Cruz Migoni, 2015). Blocking Shh signalling in the *ex vivo* myofibre culture system disrupted the myogenic program, in particular the proliferation phase, and impaired skeletal muscle regeneration in *in vivo* genetic model (Cruz Migoni, 2015).

In this chapter, I sought to investigate further the role of Shh signalling in satellite cells *in vivo* using a genetic conditional knockout model adapting the Cre-loxP system (Bouvier and Cheng, 2009). The mouse model I used in this chapter is the $Pax7^{CreERT2}$; $Ptch1^{flox/flox}$ ($Ptch1^{cKO}$), to specifically delete *Ptch1* expression (negative regulator of Shh signalling) and upregulate Shh signalling in adult satellite cells (Lepper et al., 2009; Uhmann et al., 2007).

The Cre-loxP system is an efficient method widely used to generate inducible tissue-targeted gene deletion (Bouvier and Cheng, 2009). The enzyme Cre recombinase recognises a pair of 34-bp of length sequences called the loxP sites and catalyses the DNA recombination of the gene sequence flanked by them. An altered version of this system modifies the Cre recombinase by fusing it to a mutated estrogen receptor (ER) to allow temporal control of the gene deletion upon binding of the ER antagonist, tamoxifen (TM) (Indra et al., 1999). Importantly, estrogen is unable to bind to the receptor and therefore does not affect the recombination (Indra et al., 1999). The system has been verified in the satellite cells by Lepper et. al. 2009 whereby Pax7 expression was conditionally deleted in Pax7-expressing satellite cells (Lepper et al.,

2009). This particular Pax7^{CreERT2} mouse line is a knock-in model whereby the *Cre-ER^{T2}* sequence is inserted adjacent to the *Pax7* promoter after its stop codon the 3' UTR of the gene. This is to not inactivate the *Pax7* gene and ensure a firmly regulated expression since the gene utilizes endogenous 3' UTR (Lepper and Fan, 2012). Since Pax7 is expressed in both the embryonic muscle progenitor cells and adult satellite cells, the inducible Cre system made it possible to study satellite cell function in adulthood by permitting its expression during embryonic stage and deleting it in adult animals (Lepper et al., 2011).

As Shh signalling is crucial for normal skeletal muscle development during embryogenesis (Anderson et al., 2012; McDermott et al., 2005). I used the inducible Cre-Lox system to investigate the effect of upregulating Shh signalling in adult mice by deleting Ptch1 expression in satellite cells and chemically inducing acute muscle injury in the *Tibialis Anterior* (TA) muscle using cardiotoxin injection.

3.1.1 Hypothesis and aim

Given that the loss of Shh signalling in satellite cells impaired skeletal muscle regeneration and inhibited the progression of satellite cells through the cell cycle, I hypothesized that upregulation of Shh signalling in skeletal muscles would enhance skeletal muscle regeneration by promoting satellite cell proliferation upon injury. Hence, the aim of this chapter was to conditionally delete Ptch1 expression in Pax7-expressing satellite cells and investigate the effect of increased Shh signalling during muscle regeneration *in vivo.*

3.2 Method

To investigate the effect of aberrant activation of Shh signalling in adult skeletal muscle, the negative receptor Ptch1 was specifically deleted from satellite cells using the Cre-LoxP system. $Ptch1^{flox/+}$ mice were bred to $Pax7^{CreERT2/+}$ mice to generate double heterozygous $Pax7^{CreERT2}$; $Ptch1^{flox/+}$ mice, which were bred to $Ptch1^{flox/flox}$ mice to generate mutant $Pax7^{CreERT2}$;$Ptch1^{flox/flox}$ mice, also referred as $Ptch1^{cKO}$, heterozygous mice $Pax7^{CreERT2}$;$Ptch1^{flox/+}$ referred as $Ptch1^{\Delta/+}$, and control $Ptch1^{flox/flox}$ or $Ptch1^{flox/+}$ mice (Fig 3.1 A).

The deletion of Ptch1 expression in this conditional knockout model is triggered by the administration of tamoxifen. Insufficient dose of tamoxifen would reduced the efficiency of the gene deletion and excessive of tamoxifen administered would lead to cytotoxicity to the cells. In addition, prolonged administration of tamoxifen for 15 months in *mdx* mice was shown to affect the musculature (Dorchies et al., 2013). It is therefore essential to apply the right dosage to maximize recombination without interfering with the phenotype caused by the gene inactivation. The efficiency of recombination by tamoxifen is affected by factors including the dosage, duration of treatment and mode of administration. Therefore, in my study the experiments were designed for a relatively low dosage for a transient period (not more than 3 weeks) to ensure a high level of DNA recombination. Mice were injected intraperitoneally with tamoxifen dissolved in corn oil at 10mg/ml at a dose of 3mg/40g of mouse weight for four constitutive days and maintained with lower dosage of tamoxifen diet at 40mg/kg/day for up to 3 weeks (Fig 3.1 A). Muscle injuries were performed one week after the first tamoxifen injection using cardiotoxin (CTX) to damage the muscle fibres without affecting the satellite cells (Fig 3.1 A). Injured *Tibialis Anterior* (TA) muscles and control non-injured contralateral muscles were isolated from euthanized animals at 2, 4, 7 and 14 days post-injury.

3.3 Results

3.3.1 Establishment of the tamoxifen-mediated Cre recombination protocol with high DNA recombination efficiency.

To evaluate the efficiency of our tamoxifen-mediated Cre recombination, we generated a Cre recombinase reporter mouse $Pax7^{CreERT2}$;$Smo^{\Delta/+}$;Rosa26-YFP. Although I did not use $Smo^{flox/flox}$ mice, the Cre recombination was mediated by the same mouse line ($Pax7^{CreERT2}$). In this reporter line, efficiency of recombination can be measured by evaluating the expression of the yellow fluorescence protein upon successful DNA recombination. Therefore, $Pax7^{CreERT2}$;$Smo^{\Delta/+}$;Rosa26-YFP mice were injected with tamoxifen and fed with tamoxifen chow as designed in Figure 3.1 A and myofibres from their *Extensor Digitorum Longus* (EDL) muscle were used for analysis. Myofibres were isolated and either fixed immediately to generate samples at 0 hour or cultured for 24 hours and fixed thereafter. Myofibres were analysed via immunofluorescence staining against Caveolin1 as satellite cell marker and YFP protein (Fig 3.1 B). Quantification analysis showed that approximately 83.81% of SCs at 0 hour were expressing YFP protein, and this was increased to 90.50% after 24 hours of culture (Fig 3.1 C). This result parallels that of other studies that adopted the same protocol and reported 80% Cre recombination efficiency using the same $Pax7^{CreERT2}$ mouse line (von Maltzahn et al., 2013). This experimental feature is important in studies involving inducible knockout system as recombination with low efficiency would mask the mutation phenotype and may lead to inconclusive data.

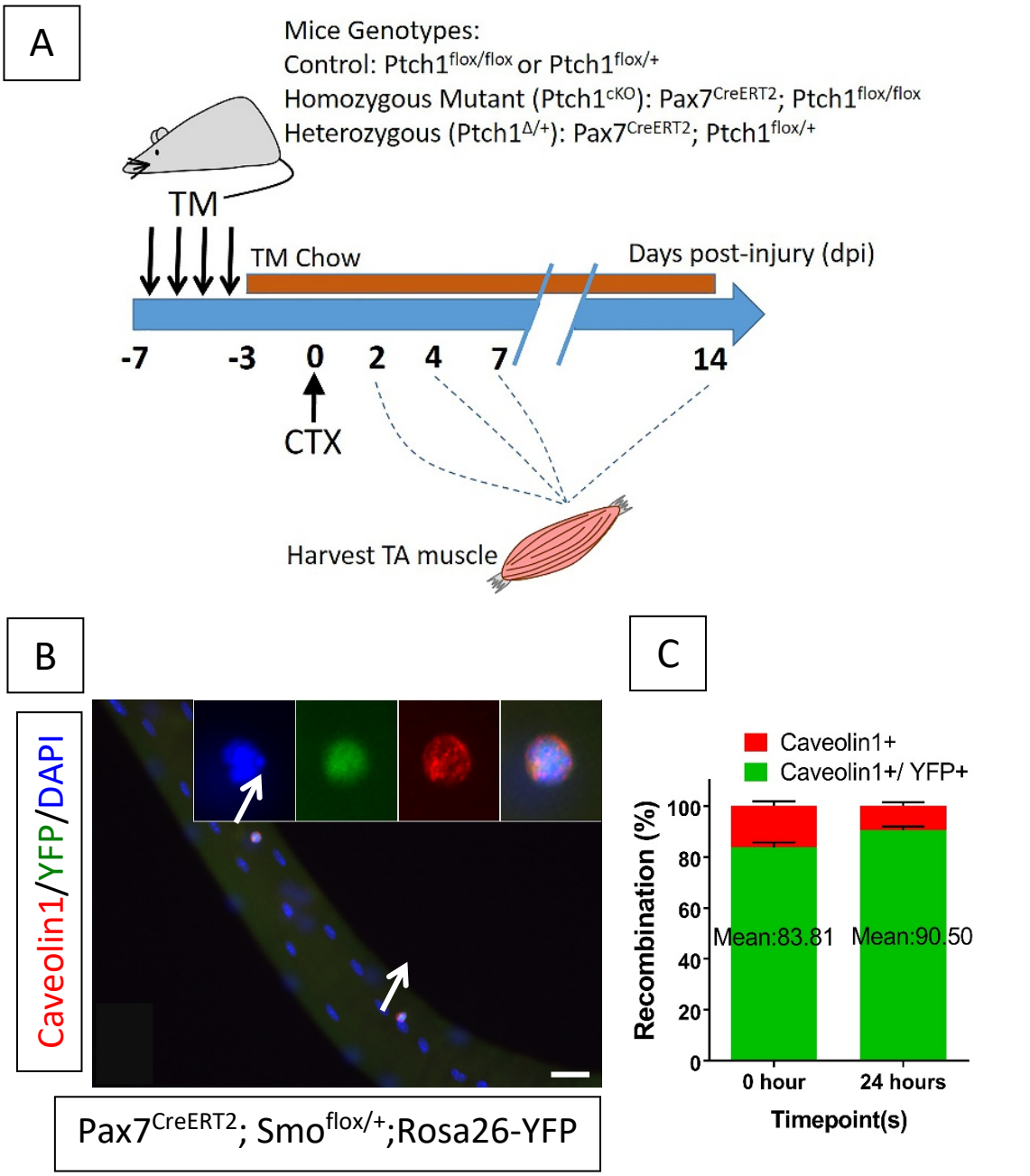

Figure 3.1: The study design and time line for muscle regeneration study using a tamoxifen-mediated Cre-LoxP conditional knockout system.

A) Peritoneal injections of tamoxifen (TM) were performed on mice for four constitutive days and mice were maintained on a tamoxifen chow thereafter until sacrifice. Unilateral TA muscle was injured by a single cardiotoxin (CTX) intramuscular injection under anaesthesia and TA muscles were harvested after euthanasia at 2, 4, 7 and 14 days post-injury (dpi). B) Representative image of a myofibre from Pax7^{CreERT2}; Smo$^{flox/+}$;Rosa26-YFP mice isolated following the study design. Myofibres were isolated from EDL muscle and either fixed immediately (0 hour) or upon culture in growth media for 24 hours. Myofibres were analysed by immunofluorescence using antibodies against Caveolin1 in red, YFP in green and nuclei counterstained with DAPI. High magnification images of single channels of the satellite cell shown in white arrow are on the top corner of the image. Scale bar is 32µm. C) Graph showing the quantification of the recombination percentage in Caveolin1+ satellite cells. Data were from two mice and error bars are mean± SEM.

3.3.2 Up-regulation of Shh signalling transiently increases satellite cell proliferation during muscle regeneration.

Dr Cruz-Migoni observed that inhibition of Shh signalling caused a decrease in SC proliferation in *ex vivo* system and that loss of Shh signalling in SCs *in vivo* using $Pax7^{CreERT2}$; $Smo^{flox/flox}$ mutant mice led to a decrease in the number of MyoD-expressing SCs (Cruz Migoni, 2015). Therefore, I carried out a study to test the effect of up-regulating Shh signalling on SC proliferation *in vivo* in $Pax7^{CreERT2}$;$Ptch1^{flox/flox}$ mice. Current work by another student in the lab using myofibres isolated from $Ptch1^{cKO}$ injected with tamoxifen as described has indeed shown a 3-folds increase in Ptch1 expression after 21 hours of culture. Since Ptch1 is one of the target gene upregulated by the signalling, that data confirm that the recombination was successful in upregulating the signal and its target genes.

Mice were allowed for natural recovery and euthanised at 2, 4 and 7 days post-injury (dpi) before collecting their regenerating TA muscles. Sectioned TA samples were immunostained with antibodies against laminin to visualise the sarcolemma and MyoD as an early differentiation and proliferation marker with nuclei counterstained with DAPI. Representative images shown in Figure 3.2 suggest that the number of SCs expressing MyoD increased in $Ptch1^{cKO}$ compared to control muscles at 2dpi and 4dpi (Fig 3.2 A-B', D-D'). However, at 7dpi the number of MyoD-expressing SCs in $Ptch1^{cKO}$ appeared to return to values similar to control muscles (Fig 3.2 G-H'). In heterozygous $Ptch1^{\Delta/+}$ mice the number of MyoD-positive cells was similar to control mice at 2 dpi, but appeared to be increased at 4 and 7dpi (Fig 3.2 C-C', F-F', I-I'). Quantification analyses showed that although there was a trend towards an increase in the number of MyoD-positive cells in $Ptch1^{cKO}$ mice at 2dpi, the data was not significant (Fig. 3.2 J). However, there was a marked increase in the number of MyoD-positive cells at 4dpi (mean=111.5 cell in $Ptch1^{cKO}$ versus mean=97.19 cell in control) followed by a significant decrease at 7dpi (mean=35.46 cell in $Ptch1^{cKO}$ versus mean=48.61 cell in control) in $Ptch1^{cKO}$ mice (Fig 3.2 J). There was no significant difference in the number of MyoD-positive cells in $Ptch1^{\Delta/+}$ mice compared to control mice at 2 and 4dpi, although there was an increase in the number of MyoD+ cells in $Ptch1^{\Delta/+}$ (mean=61.75 cell) compared to control mice (mean=48.61 cell) at 7dpi (Fig 3.2 J). Therefore, gene inactivation of the *Ptch1* locus,

which is predicted to cause a putative up-regulation of Shh signalling in SCs, results in a transient increase in the number of myogenic progenitor cells during myogenesis *in vivo*. Interestingly, deletion of one allele of *Ptch1* also caused an increase in the number of myogenic progenitor albeit with a different timing than when two alleles of *Ptch1* are deleted.

Table 3.1 Data of the number of MyoD-positive cells in regenerating muscles.

	Experimental Group	Mean value (cell)	S.E.M.	N	Significance p value
2dpi	Control	32.700	8.394	3	
	$Ptch1^{cKO}$	35.287	2.999	3	n.s
	$Ptch1^{\Delta/+}$	29.333	3.387	3	n.s
4dpi	Control	97.190	1.365	4	
	$Ptch1^{cKO}$	111.467	1.695	3	0.0012
	$Ptch1^{\Delta/+}$	99.288	7.076	4	n.s
7dpi	Control	48.610	2.245	3	
	$Ptch1^{cKO}$	35.463	2.844	4	0.019
	$Ptch1^{\Delta/+}$	61.753	3.291	3	0.03

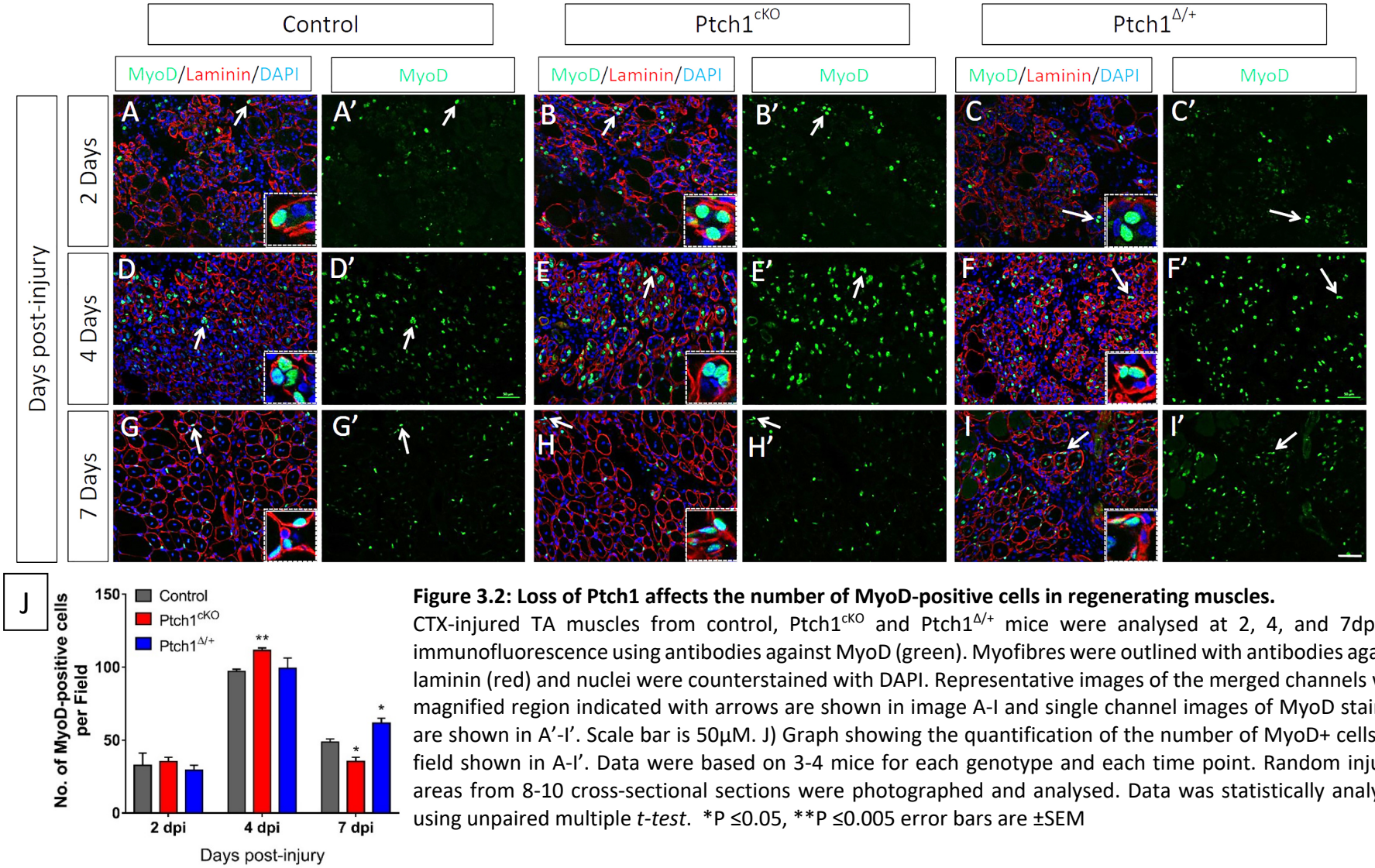

Figure 3.2: Loss of Ptch1 affects the number of MyoD-positive cells in regenerating muscles.
CTX-injured TA muscles from control, Ptch1^{cKO} and Ptch1$^{\Delta/+}$ mice were analysed at 2, 4, and 7dpi by immunofluorescence using antibodies against MyoD (green). Myofibres were outlined with antibodies against laminin (red) and nuclei were counterstained with DAPI. Representative images of the merged channels with magnified region indicated with arrows are shown in image A-I and single channel images of MyoD staining are shown in A'-I'. Scale bar is 50µM. J) Graph showing the quantification of the number of MyoD+ cells per field shown in A-I'. Data were based on 3-4 mice for each genotype and each time point. Random injured areas from 8-10 cross-sectional sections were photographed and analysed. Data was statistically analysed using unpaired multiple *t-test*. *P ≤0.05, **P ≤0.005 error bars are ±SEM

To confirm my observations that loss of Ptch1 results in an increase in the number of muscle progenitor cells and to test whether this is due to a proliferative effect, I used a proliferation marker Ki67 together with MyoD detection to observe the effect of *Ptch1* deletion on SC proliferation. Fixed and frozen TA muscles were sectioned and analysed via immunostaining against MyoD as a myogenic marker and Ki67 as a proliferation marker (Fig 3.3 A). Representative images of $Ptch1^{cKO}$ TA muscle at 2dpi show a moderate increase in the number of Ki67+/MyoD+ cells compared to control muscles (Fig 3.3 A-A', B-B'). In contrast, $Ptch1^{\Delta/+}$ TA muscles displayed a reduced number of Ki67+/MyoD+ cells (Fig 3.3 C-C'). However, at 4 days post-injury there was a marked increase in the number of Ki67-expressing myogenic progenitor cells in both $Ptch1^{cKO}$ and $Ptch1^{\Delta/+}$ TA muscles compared to control muscles (Fig 3.3 D-F'). Interestingly, there was no noticeable increase in the number of Ki67+/MyoD- cells, suspected to be macrophages and immune cells, suggesting that loss of Ptch1 in SCs does not have non-cell autonomous effects on non-myogenic cells. At 7 dpi, there was decrease in the number of Ki67+/MyoD+ cells in $Ptch1^{cKO}$, but not in $Ptch1^{\Delta/+}$, TA muscles compared to control muscles (Fig 3.3 G-I'). Quantitative analyses confirmed that there was no difference in the number of Ki67+/MyoD+ cells between control and $Ptch1^{cKO}$ or $Ptch1^{\Delta/+}$ TA muscles at 2dpi (Fig 3.3 J). However, there was a significant increase in the number of Ki67+/MyoD+ cells in both $Ptch1^{cKO}$ (mean= 32.54 cell) and $Ptch1^{\Delta/+}$ (mean= 28.47 cell) compared to control (mean= 21.59 cell) at 4 dpi (Fig 3.3 J). At 7dpi, there was a trend towards a decrease in the number of Ki67+/MyoD+ cells in $Ptch1^{cKO}$, but not $Ptch1^{\Delta/+}$ muscles, although the data was not statistically significant (Fig 3.3 J). Therefore, I concluded that putative activation of Shh signalling through loss of *Ptch1* had a transient effect on SC proliferation.

Table 3.2 Data of the number of MyoD-positive/Ki67-positive cells in regenerating muscles.

	Experimental Group	Mean value (cell)	S.E.M.	N	significance
2dpi	Control	25.190	4.288	3	
	$Ptch1^{cKO}$	23.583	6.163	3	n.s
	$Ptch1^{\Delta/+}$	15.877	3.314	3	n.s
4dpi	Control	21.59	1.076	4	
	$Ptch1^{cKO}$	32.538	1.164	4	0.0005
	$Ptch1^{\Delta/+}$	28.470	2.589	4	0.0495
7dpi	Control	11.467	1.550	3	
	$Ptch1^{cKO}$	8.375	1.325	3	n.s
	$Ptch1^{\Delta/+}$	11.180	0.680	2	n.s

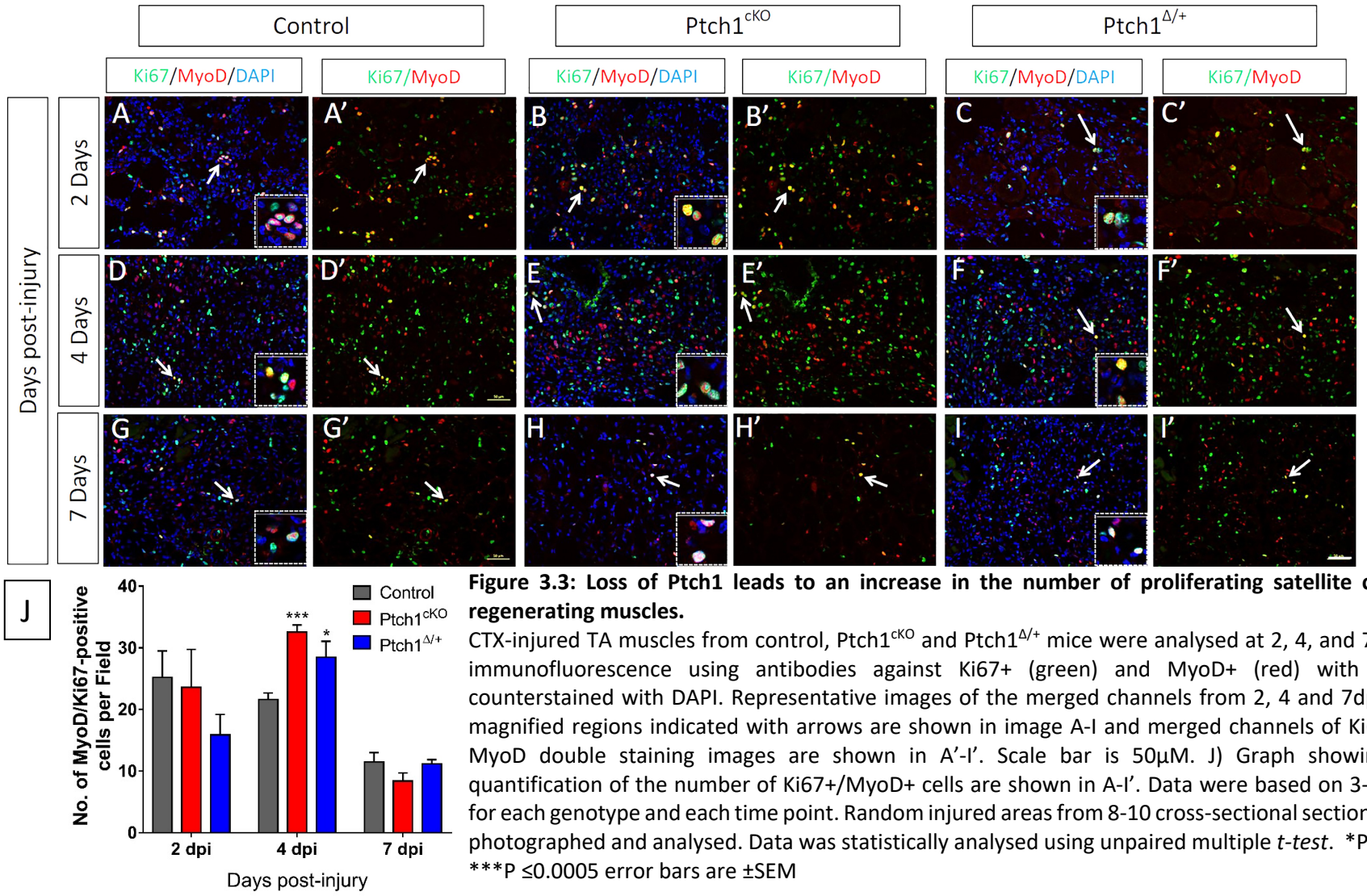

Figure 3.3: Loss of Ptch1 leads to an increase in the number of proliferating satellite cells in regenerating muscles.

CTX-injured TA muscles from control, Ptch1^{cKO} and Ptch1$^{\Delta/+}$ mice were analysed at 2, 4, and 7dpi by immunofluorescence using antibodies against Ki67+ (green) and MyoD+ (red) with nuclei counterstained with DAPI. Representative images of the merged channels from 2, 4 and 7dpi with magnified regions indicated with arrows are shown in image A-I and merged channels of Ki67 and MyoD double staining images are shown in A'-I'. Scale bar is 50µM. J) Graph showing the quantification of the number of Ki67+/MyoD+ cells are shown in A-I'. Data were based on 3-4 mice for each genotype and each time point. Random injured areas from 8-10 cross-sectional sections were photographed and analysed. Data was statistically analysed using unpaired multiple *t-test*. *P ≤0.05, ***P ≤0.0005 error bars are ±SEM

3.3.3 Up-regulation of Shh signalling impairs myogenic differentiation during muscle regeneration.

To assess the effects of Shh upregulation, I next evaluated the effects of SC-specific *Ptch1* inactivation on myogenic differentiation during muscle regeneration *in vivo*. I evaluated SC differentiation by observing the expression of myogenin, a myogenic regulatory factor acting downstream of MyoD in the control of terminal differentiation (Deato et al., 2008; Weintraub et al., 1989). Regenerating TA muscles from control group, $Ptch1^{cKO}$ group and $Ptch1^{\Delta/+}$ were harvested at 2, 4 and 7 days post-injury and immunostained with antibodies against Laminin-α2 to visualise the myofibres' basal lamina and myogenin. Nuclei were counterstained with DAPI. Representative images shown in Figure 3.4 indicate that there was no obvious difference between the three genotypes at 2dpi, an observation supported by the quantitative analysis (Fig 3.4A-C', J). At 4dpi, I observed more myogenin+ cells in $Ptch1^{cKO}$ and $Ptch1^{\Delta/+}$ compared to control muscles, although by 7dpi the number of myogenin+ cells was consistently reduced in $Ptch1^{cKO}$ and $Ptch1^{\Delta/+}$ compared to control muscles (Fig 3.4D-I'). The quantitative analyses confirmed these observations and showed a transient increase in the number of Myogenin+ cells at 4 dpi in $Ptch1^{cKO}$ mice compared to control mice (mean=40.38 cell versus mean=31.77 cell) followed by a significant loss of myogenin+ cells at 7 dpi in $Ptch1^{cKO}$ mice compared to control mice (mean= 19.11 cell versus mean= 50.46 cell) (Fig 3.4J). Loss of one allele of Ptch1 in the heterozygous $Ptch1^{\Delta/+}$ mice had a similar phenotype with the loss of two alleles with a transient increase in the number of myogenin+ cells at 4dpi (mean=37.98 cell versus mean= 31.77 cell), and a trend towards a decrease in the number of Myogenin+ cells at 7dpi although not statistically significant (Fig 3.4J). This may be due to the fact that there was insufficient *n* number (2 biological repeats only) at this time point (Fig 3.4 J).

To conclude, while myogenin expression increased steadily during muscle regeneration in control mice, loss of one or two alleles of *Ptch1* in SCs caused a transient increase in the number of differentiating cells that mirrored the increase in the number of muscle progenitor cells at 4dpi, but this was followed by a sharp impairment of differentiation in mice lacking *Ptch1* function. Whether the inhibition on myogenic differentiation was a direct effect or as a consequence of an effect on proliferation is yet to be explored.

Table 3.3 Data of the number of Myogenin-positive cells in regenerating muscles.

	Experimental Group	**Mean value (cell)**	**S.E.M.**	**N**	**significance**
2dpi	Control	10.277	2.531	3	
	$Ptch1^{cKO}$	4.759	1.751	3	n.s
	$Ptch1^{\Delta/+}$	5.500	0.500	3	n.s
4dpi	Control	31.773	1.028	4	
	$Ptch1^{cKO}$	40.377	2.686	3	0.019
	$Ptch1^{\Delta/+}$	37.978	2.113	4	0.038
7dpi	Control	50.460	1.836	3	
	$Ptch1^{cKO}$	19.105	1.630	4	0.0001
	$Ptch1^{\Delta/+}$	37.517	7.712	3	n.s

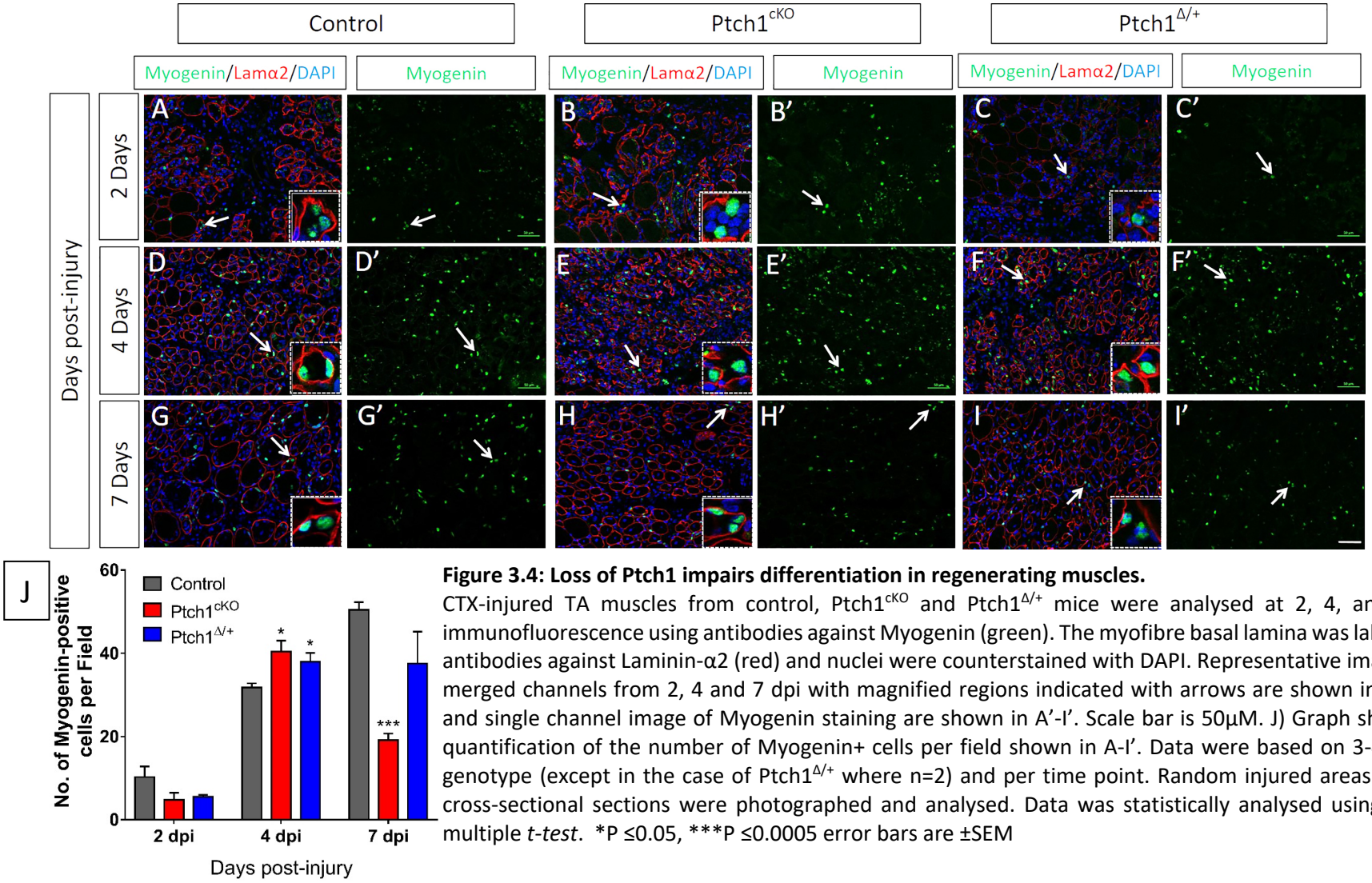

Figure 3.4: Loss of Ptch1 impairs differentiation in regenerating muscles.
CTX-injured TA muscles from control, Ptch1^{cKO} and Ptch1$^{\Delta/+}$ mice were analysed at 2, 4, and 7dpi by immunofluorescence using antibodies against Myogenin (green). The myofibre basal lamina was labelled with antibodies against Laminin-α2 (red) and nuclei were counterstained with DAPI. Representative images of the merged channels from 2, 4 and 7 dpi with magnified regions indicated with arrows are shown in image A-I and single channel image of Myogenin staining are shown in A'-I'. Scale bar is 50µM. J) Graph showing the quantification of the number of Myogenin+ cells per field shown in A-I'. Data were based on 3-4 mice per genotype (except in the case of Ptch1$^{\Delta/+}$ where n=2) and per time point. Random injured areas from 8-10 cross-sectional sections were photographed and analysed. Data was statistically analysed using unpaired multiple *t-test*. *P ≤0.05, ***P ≤0.0005 error bars are ±SEM

3.3.4 Ptch1 deficiency in SCs impairs muscle repair *in vivo*

In the previous section, I reported that, although loss of Ptch1 function caused a transient increase in proliferation and myogenic differentiation at 4dpi, expression of myogenin, a transcription factor controlling differentiation, was severely impaired at 7dpi. This suggests that loss of Ptch1 may prevent differentiation and lead to defective muscle repair. To test this possibility, I carried out analyses at 14 days post-injury to evaluate the effect of Ptch1 deficiency in SCs on muscle repair *in vivo*. Upon cardiotoxin-mediated injury, regenerating TA muscles from control, $Ptch1^{cKO}$ and $Ptch1^{\Delta/+}$ were harvested at 14dpi and immunostained with antibodies against laminin to highlight the fibre membrane and the minimum Feret's diameter of centrally nucleated regenerating myofibres was measured using the FIJI software.

Representative images of muscle transverse sections show that regenerating myofibres in $Ptch^{cKO}$ mice are smaller and more rounded than in control muscles, although the overall muscle architecture does not appear to be affected (Fig. 3.5A,B). In contrast, $Ptch1^{\Delta/+}$ muscles presented obvious defects in regeneration with the presence of large gaps between regenerating myofibres, a high frequency of small myofibres with irregular shapes (Fig. 3.5A,C). In addition, the presence of laminin-positive basal lamina within myofibres suggests that fusion and myofibre maturation are defective in $Ptch1^{\Delta/+}$ muscles (Fig. 3.5A,C). Analysis of the distribution of myofibre size (minimum Feret's diameter) showed no significant trend towards an increase in the percentage of smaller myofibres and a decrease in larger myofibres in $Ptch1^{cKO}$ muscles compared to control muscles (Fig. 3.5D).

Consistent with this observation, the analysis of the number of centrally nucleated nuclei per myofibre cross-sectional area showed that there was a significant decrease in the proportion of myofibres with more than 1 central nucleus, particularly myofibres with 2 central nuclei (mean=20.61 myofibre in control versus mean= 10.83 myofibre in $Ptch1^{cKO}$ muscles) (Fig 3.5E). Instead, there was a non-significant increase in the proportion of smaller fibres containing one central nucleus in the $Ptch1^{cKO}$ muscles. Finally, the quantification of the total number of myofibres per field indicated that the

Ptch1^{cKO} muscles had significantly more myofibres (mean=259.9 myofibre) compared to the control muscles (mean= 190.9 myofibre) (Fig 3.5 F).

Although the data collected for Ptch1$^{\Delta/+}$ muscles is based on n=1 due to a shortage of mice, I observed a similar trend with approximately 70% of myofibres smaller than 10 µM (~35% were less than 5 µM and ~35% in between 5-10 µM) (Fig 3.5 D), an increase in the proportion of smaller myofibres with a single central nucleus and a decrease in the proportion of larger fibres with multiple central nuclei (Fig 3.5E).

Collectively, these data indicate that loss of Ptch1 impairs muscle regeneration. My findings are consistent with the possibility that Ptch1-deficiency impacts on the differentiation and fusion of myogenic progenitor cells, leading to a phenotype of hyperplasia.

Table 3.4 Data of the number of myofibres in regenerating muscles at 14 days post-injury.

	Experimental Group	**Mean value (Myofibre)**	**S.E.M.**	**N**	**significance**
14dpi	Control	190.9	23.01	3	
	Ptch1^{cKO}	259.9	19.9	3	0.0425
	Ptch1$^{\Delta/+}$	199.3	-	1	n.s

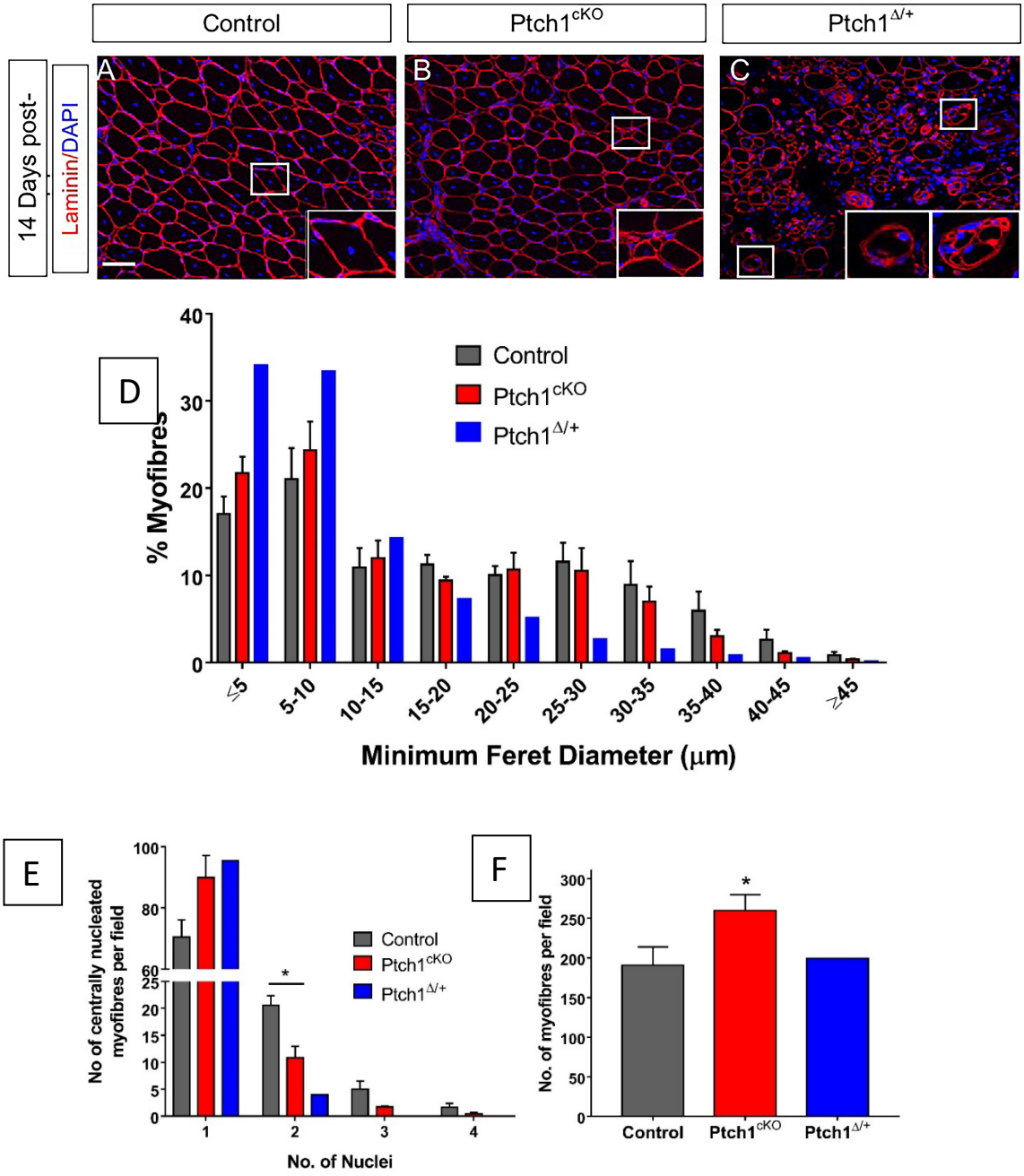

Figure 3.5: Loss of Ptch1 function impairs muscle regeneration.
(A-C) Representative images of regenerating TA muscles from control, Ptch1^{cKO} and Ptch1$^{\Delta/+}$ mice that were analysed at 14dpi by immunofluorescence using antibodies to label myofibres' outline with Laminin (red). Nuclei were counterstained with DAPI. Scale bar is 50μM **D)** Graph showing the quantitative evaluation of the distribution (percentage) of myofibre size (minimum Feret's diameter) ranging from ≤5μM to ≥45μM. **E)** Graph showing the quantitative evaluation of the number of central nuclei harboured by regenerating myofibres in a field. **F)** Graph showing the quantitative evaluation of the number of centrally nucleated regenerating fibres per field. Data were based on 3-4 mice for control and Ptch1^{cKO} but only 1 mouse for Ptch1$^{\Delta/+}$. Random injured areas from 8-10 cross-sectional sections were photographed and analysed. Data was statistically analysed using unpaired multiple t-test. Error bars are ±SEM *P ≤0.05

Because of the apparent defective muscle repair in *Ptch1*-deficient mice, I evaluated collagen disposition and the fibrosis status of regenerating skeletal muscles upon injury, since the development of fibrotic tissue is an indication of a defective repair process. Thus, regenerating TA muscles from control, Ptch1^{cKO} and Ptch1$^{\Delta/+}$ mice were harvested at 14 days post-injury and immunostained with antibodies against collagen Type I and Laminin-α2. Nuclei were counterstained with DAPI. Representative images confirm that Ptch1^{cKO} muscles have little collagen deposition between regenerating myofibres compared to control muscles, in agreement with the maintenance of the muscle architecture (Fig. 3.6A,B). In contrast, Ptch1$^{\Delta/+}$ muscle presented a large area with collagen deposition, indicating the presence of fibrosis (Fig 3.6A,C). Quantification of the levels of fibrosis confirmed that Ptch1^{cKO} are not significantly different from control muscles (Fig. 3.6D). No statistical analysis could be performed on Ptch1$^{\Delta/+}$ muscles due to the low *n* number.

Taken together, the analyses of fibre size distribution and collagen disposition indicate that the reduced number of Myogenin-positive cells in *Ptch1*-deficient mice results in defective differentiation and fibre fusion, leading to an hyperplasia phenotype. Preliminary findings in mice lacking one allele of *Ptch1* are indicative of a worsening phenotype; however, such conclusion would need to be confirmed.

Table 3.5 The percentage of collagen-1 deposition in regenerating muscles at 14 days post-injury.

	Experimental Group	Mean value (%)	S.E.M.	N	significance
14dpi	Control	10.32	0.732	3	
	Ptch1^{cKO}	12.84	1.235	4	n.s
	Ptch1$^{\Delta/+}$	16.58	-	1	n.s

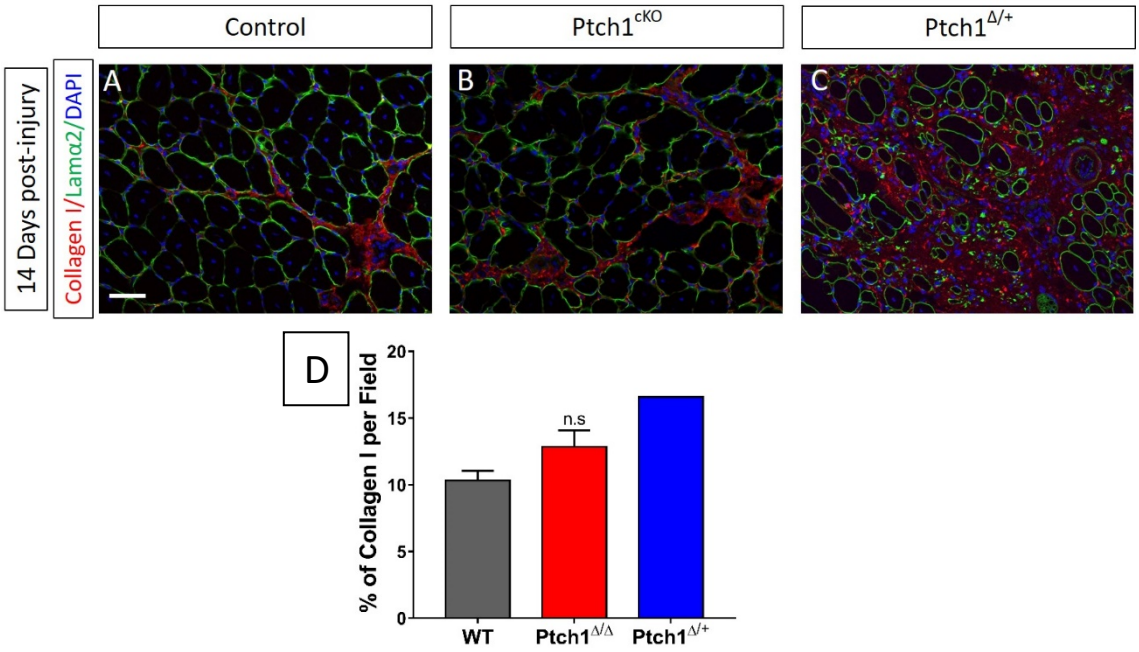

Figure 3.6: Absence of Collagen Type 1 disposition in Ptch1c^{KO} mice.
(A-C) Representative images showing regenerating TA muscles from control, Ptch1^{cKO} and Ptch1$^{\Delta/+}$ mice that were analysed at 14 dpi by immunofluorescence using antibodies against Collagen-1 (red) and Laminin-α2 (green) and nuclei counterstained with DAPI. Scale bar is 50µM **D)** Graph showing the quantification of the percentage of Collagen-1-labeled area per field analysed using FIJI software. Data were based on 3-4 mice for control and Ptch1^{cKO} but only 1 mouse for Ptch1$^{\Delta/+}$. Random injured areas from 8-10 cross-sectional sections were photographed and analysed. Data was statistically analysed using unpaired multiple t-test. Error bars are ±SEM

3.3.5 Ptch1 deletion increases satellite cell self-renewal *in vivo.*

Since Shh signalling has been implicated in the regulation of stem cell self-renewal in embryonic and adult stem cells (Buller et al., 2012), I evaluated the effect of up-regulating Shh signalling on SC self-renewal *in vivo*. SC self-renewal can be determined by examining cells that return to a sublaminal position after the regeneration process is complete at 14 days post-injury (dpi) (Rayagiri et al., 2018). Regenerating TA muscles from control, Ptch1^{cKO} and Ptch1$^{\Delta/+}$ were harvested at 14dpi and immunostained with antibodies against laminin to label the myofibre's basal lamina and MyoD as a marker for SCs (low levels of immunostaining persists in self-renewing cells). Figure 3.7 shows representative images of MyoD+ SCs in sublaminal position in control and Ptch1^{cKO} muscles, but not in Ptch1$^{\Delta/+}$ muscles (Fig 3.7A-C). Interestingly,

more sublaminal SCs were observed in Ptch1^{cKO} muscles than in control muscles (see inserts in Fig. 3.7A-C). I quantified the number of sublaminal SCs and plotted the results on a graph. This shows a significant increase in the number of SCs in sublaminal position in Ptch1^{cKO} (mean= 10.44) compared to control (mean= 7.5) (p= 0.037) muscles (Fig 3.7D). No statistical analysis could be performed in Ptch1$^{\Delta/+}$ muscles, although a similar increase could be observed (Fig. 3.7D).

Thus, it can be concluded that putative up-regulation of Shh signalling in SCs upon Ptch1 gene inactivation resulted in an increase in the number of self-renewing SCs. However, further studies are required to confirm this observation.

Table 3.6 The number of MyoD-positive SCs at sublaminal position in regenerating muscles at 14 days post-injury.

	Experimental Group	Mean value (cell)	S.E.M.	N	significance
14dpi	Control	7.5	0.288	3	
	Ptch1^{cKO}	10.44	0.860	4	0.0376
	Ptch1$^{\Delta/+}$	3.125	-	1	n.s

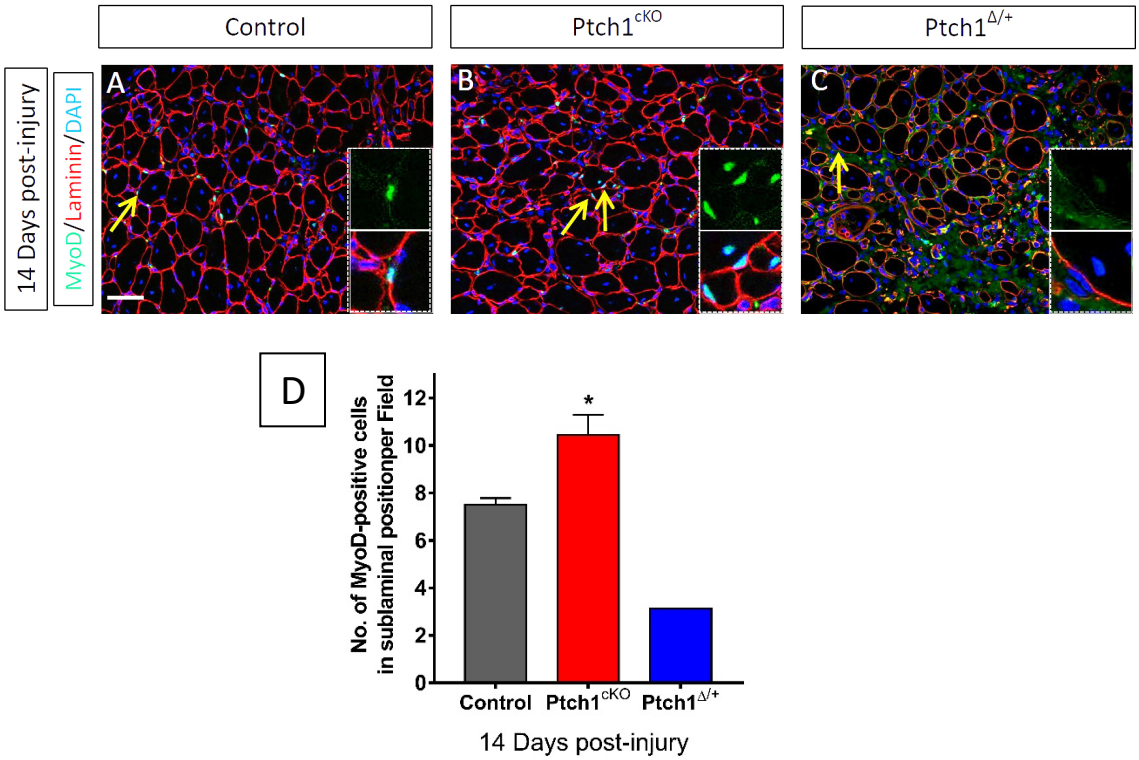

Figure 3.7: The number of self-renewing SCs is increased in Ptch1^{cKO} mice.
(A-C) Representative images showing regenerating TA muscles from control, Ptch1^{cKO} and Ptch1$^{\Delta/+}$ mice that were analysed at 14 dpi by immunofluorescence using antibodies against MyoD (green) and Laminin (red). Nuclei were counterstained with DAPI. Scale bar is 50µM **D)** Graph showing the quantification of the number of MyoD-expressing SCs in sublaminal position per field. Data were based on 3-4 mice for control and Ptch1^{cKO} but only 1 mouse for Ptch1$^{\Delta/+}$. Random injured areas from 8-10 cross-sectional sections were photographed and analysed. Data was statistically analysed using unpaired multiple t-test. Error bars are ±SEM. *P≤0.05

3.4 Discussion

In this chapter, I used the Pax7^{CreERT2}; Ptch1$^{flox/flox}$ mice to conditionally delete the *Ptch1* gene in SCs and investigate the effect on skeletal muscle regeneration upon cardiotoxin-induced injury up to 14 days post injury. The inactivation of Ptch1 is understood to release Smoothened (Smo) from Ptch1 inhibition and activate Shh signalling (Choudhry et al., 2014). Consistent with this prediction, work carried out in the laboratory by another student showed a 3-fold increase in *Ptch1* transcript levels within the first 12 hours of culture in Ptch1^{cKO} compared to control mice. As *Ptch1* itself is a transcriptional target of Hedgehog signalling, this indicates that *Ptch1* inactivation in SCs has indeed caused an up-regulation of Shh signalling. I observed that the

inactivation of *Ptch1* in SCs disrupted muscle regeneration. Ptch1 loss-of-function increased SC proliferation during early myogenesis and caused a defect in terminal differentiation, fusion and maturation of regenerating myofibres at later stages. Interestingly, loss of *Ptch1* promoted also SC self-renewal. Finally, loss of one allele of *Ptch1* appeared to have more significant effect on muscle regeneration than loss of two *Ptch1* alleles ($Ptch1^{cKO}$).

3.4.1 Up-regulation of Shh signalling promotes proliferation of satellite cells upon activation during early myogenesis.

Following cardiotoxin injection, $Pch1^{cKO}$ and $Ptch1^{\Delta/+}$ muscles were initially undistinguishable from control muscles (at 2 dpi), indicating that SC activation was not affected by up-regulation of Shh signalling. However, by 4dpi $Pch1^{cKO}$ and $Ptch1^{\Delta/+}$ muscles presented more MyoD+ progenitor cells and analyses using the proliferation marker Ki67 confirmed that up-regulation of Shh signalling promoted the proliferation of muscle progenitor cells. This observation is consistent with the pro-proliferative effect of Shh signalling reported by others in *in vitro* myogenic cell lines (Koleva et al., 2005a; Elia et al., 2007). Likewise, intra-muscular injections of a human Shh-expressing plasmid in injured aged or dystrophic muscles were also shown to increase the number of activated (Myf5-positive) SCs (Piccioni et al., 2014a; Piccioni et al., 2014b). However, it is worth noting that the plasmid treatment was delivered into the whole muscle tissue and thus may have had a direct effect on SC-mediated myogenesis or an indirect effect by affecting angiogenesis or inflammatory cells (Piccioni et al., 2014a). In the present study, by directly targeting Ptch1 in SC, I ruled out the possibility that the effects observed are solely indirect, and demonstrate that levels of Hedgehog signalling in SC play an important role in the control of SC activity. In agreement with the conclusion that hedgehog signalling is acting in a cell-autonomous manner on SC, previous studies in the lab and by others have shown that SCs from injured muscles were responsive to Shh signalling and expressed the Shh target genes *Gli1* and *Ptch1* (Cruz Migoni, 2015; Piccioni et al., 2014a; Piccioni et al., 2014b). While previous studies investigated the beneficial effect of Shh signalling in dystrophic or aged muscles upon injury, the work reported in this chapter indicates that Hedgehog signalling may have beneficial effects in young and healthy muscles. Interestingly, my work revealed for the first time that loss

of a single allele of *Ptch1* was sufficient to increase proliferation of SCs, and the effect of Shh signalling was dose-dependent. On the contrary, loss of Hedgehog signalling, which impairs SC proliferation, does not appear to be subjected to a dose-dependent response (Cruz Migoni, 2015). This suggests that while low levels of hedgehog signalling are sufficient to permit normal SC proliferation, increasing the levels of Hedgehog signalling above a threshold has an effect on SC proliferation and muscle repair *in vivo* (Straface et al., 2009b; Renault et al., 2013a; Cruz Migoni, 2015).

3.4.2 Timely regulation of Shh signalling is crucial for efficient muscle repair.

Although in this chapter I demonstrated that Shh signalling promoted SC proliferation during early myogenesis, the long-term effects of up-regulating Shh signalling on myogenesis was unexpected as it adversely affected muscle repair at later stages. Indeed, the number of proliferating muscle progenitor cells increased at 4 dpi and was initially accompanied by an increase in the number of MyoD and myogenin-expressing cells, suggesting that up-regulation of hedgehog signalling may have a beneficial effect on muscle repair. However, I found that this initial phase was followed by a drop in the number of cells expressing MyoD and Myogenin at 7dpi. There are two possibilities to explain the decrease in differentiating cells at 7 dpi. First, up-regulation of Shh signalling may have accelerated the myogenic program. In control muscles, differentiation is preceded by a transit-amplifying phase, which aims at producing sufficient progenitor cells for the completion of the repair program. Myogenin-expressing cells and differentiation only gradually increased with time up to 7 dpi. Upon up-regulation of Hedgehog signalling, it is possible that SCs engaged into the myogenic program more rapidly, leading initially to an increase in the number of muscle progenitor cells. However, earlier progression through myogenesis would lead to insufficient numbers of muscle progenitor cells produced and thus over time a decrease in the pool of cells available for differentiation. Such explanation would be supported by the fact that in the absence of Shh signalling, muscle progenitor cells were found to fail to progress through the cell cycle, leading to a prolonged time taken for muscle repair and a delay in myogenesis up to 21 days after injury (Cruz Migoni, 2015). If this were true, adding another time point of analysis before 7dpi would be predicted to show

the conversion of all muscle progenitor cells observed at 4dpi into Myogenin-expressing cells.

A second possibility would be that increasing Hedgehog signalling has pleiotropic effects on myogenesis: Hedgehog signalling may promote SC proliferation, and simultaneously inhibit differentiation, therefore preventing SCs to progress further into the myogenic program after the proliferation phase at 4dpi. This hypothesis is supported by previous studies on the expression pattern of *Shh*, *Ptch1* and *Gli1* mRNA upon muscle regeneration following injury, showing a down-regulation of *Shh*, *Ptch1* and *Gli1* expression after a peak at 4dpi (Straface et al., 2009b; Piccioni et al., 2014a). Piccioni et al. showed that *Gli1* mRNA was down-regulated by at least 3-fold at 7dpi compared to 4dpi in 6 month-old mice following cardiotoxin injury (Piccioni et al., 2014b). This suggests that Hedgehog signalling may need to be dampened for differentiation to occur.

The effects on differentiation were more prominent at 14dpi, and resulted in a reduced number of larger myofibres and an increased number of smaller fibres. In addition, there was a concomitant increase in the number of regenerating myofibres and regenerating myofibres contained on average fewer centrally-located nuclei when Shh signalling was up-regulated. This led me to propose a defect in myocyte fusion. Indeed, another study using the C_2C_{12} myoblast cell line revealed that Shh treatment *in vitro* resulted in the absence of myotubes even after 120 hours of culture (Koleva et al., 2005a). Myogenin was recently found to be a major regulator of myofibre fusion as a defect in myofibre fusion was observed in adult *Myog*$^{-/-}$ zebrafish (Ganassi et al., 2018). However, I did not observe that up-regulation of Hedgehog signalling prevented myogenin expression. This indicates that the fusion defect is likely to be myogenin-independent and since myogenin regulates the expression of several fusion-related proteins including *Myomaker*, *Myomixer* and *Jam3b* (Bi et al., 2018; Millay et al., 2014; Powell and Wright, 2011), it remains possible that Shh signalling acts downstream of myogenin in the control of genes essential for myoblast fusion. However myoblast fusion is a process that involves multiple steps including cell-cell adhesion, lipid bilayer instabilisation, exocytosis and endocytosis (Kim et al., 2015b). It is therefore possible that Shh signalling is implicated in one of these steps. Moreover, a similar morphology in regenerating muscles was observed upon treatment with a Wnt agonist called BIO

(Jones et al., 2015). Since Wnt signalling is a mitogen known to affect SC behaviour, it is a possible that Shh may have similar effect to those observed upon Wnt agonist treatment.

3.4.3 Shh signalling promotes SC self-renewal upon completion of muscle repair.

In this chapter, I have observed for the first time that up-regulation of Shh signalling in SCs promoted their self-renewal, as shown by the increase in sublaminal SCs. Although drawing a conclusion on the basis of a single experimental approach is not sufficient, the effect was sufficiently convincing to incite me to seek additional evidence to support this observation, which I will report in the coming chapters. While my study is the first one to demonstrate a self-renewal effect for Shh signalling in SCs, similar effects have been reported in adult stem cells of the brain, skin, hair follicle and the intestine (Park et al., 2018; Petrova and Joyner, 2014). Therefore, Shh signalling, like other developmental pathways such as Wnt and Notch signalling, regulates stem cell self-renewal (Clevers et al., 2014; Liu et al., 2010). This is important as the control of self-renewal by Shh signalling is thought to play an important role in cancer malignancies, metastases and relapse through the maintenance of cancer stem cells (Ruiz i Altaba et al., 2002).

4 Up-regulation of Sonic hedgehog signalling promotes satellite cell proliferation during adult myogenesis *ex vivo*.

4.1 Introduction

Satellite cell behaviour has been studied extensively by adapting *in vitro* and *in vivo* models. Initially, immortalised cell lines such as the C_2 line and its subclone C_2C_{12} derived from primary mouse myoblasts were widely used as a model to investigate the molecular and cellular characteristics of satellite cells *in vitro*. Its availability, viability, robust proliferation and capacity to differentiate efficiently into myotubes made it a popular model with scientists. However, the cells are tumorigenic and lack any translational value due to cell senescence and low transplantation efficiency (Rando and Blau, 1994). Another *in vitro* model used to investigate satellite cell biology is primary myoblasts culture isolated from adult and juvenile muscles. Primary myoblasts have also robust proliferation and myogenic differentiation capacity like cell lines. Although initially the yield of myoblasts are low due to contaminating fibroblasts, Rando and Blau introduced a technique in 1994 to purify and increase the yield of primary myoblasts in vitro (Rando and Blau, 1994). In addition, primary cultures made it possible to isolate myoblasts from different muscles to explore the heterogeneity of myogenic programs in cells of different embryogenic origin. Nevertheless, primary myoblast cultures do not completely recapitulate adult myogenesis *in vivo* since the stem cell niche components including the basal lamina, the sarcolemma of the myofibre and other non-myogenic cells have been removed from the system (Pasut et al., 2013). More recently, an *ex vivo* system using single myofibre cultures has become a model of choice for studying adult myogenesis and satellite cell biology because it allows satellite cells to be in full contact with their niche micro-environment. The ex vivo system was first described in 1977 by Bekoff and Betz using single myofibres isolated from rat *flexor digitorum brevi* (FDB) muscle and further optimised by Bischoff in 1986 (Bischoff, 1986). Subsequently, the technique was adapted to isolate myofibres from other muscles including soleus, *tibialis*

anterior (TA) and *extensor digitorum longus* (EDL) muscles. Other laboratories have also produced modified and improved versions of the technique on non-adherent whole myofibre cultures (Pasut et al., 2013). Although this system preserves the self-renewal capability of satellite cells during myogenesis, floating myofibres can only be cultured up to 120 hours before hyper-contracting. Hence, this system is not suitable to investigate later stages of myogenesis such as cell fusion and myotube formation.

As reported above, previous work in the lab has demonstrated that SCs are responsive to Shh signalling during muscle regeneration (Cruz Migoni, 2015). Using a loss-of-function approach, we showed that blocking of Shh signalling using pharmacological agents cyclopamine and GANT61, and using $Pax7Cre^{ERT2}$;$Smo^{flox/flox}$ for *in vivo* studies, inhibited SCs proliferation and delayed muscle regeneration, indicating that Shh signalling is necessary for adult myogenesis (Cruz Migoni, 2015). In this chapter, I investigated whether Shh signalling was sufficient to promote adult myogenesis. The effect of up-regulating Shh signalling using a pharmacological agent, smoothened agonist (SAG), was assessed on SCs proliferation and progression through myogenic program *ex vivo.*

SAG is a cell-permeable benzothiophene compound that binds to the functional heptahelical (transmembrane) domain of Smo (Chen et al., 2002). This in turn induces phosphorylation of the Smo cytoplasmic tail, which leads to a structural change that stimulates Smo translocation into the primary cilia (Arensdorf et al., 2016). Smo interacts with ciliary protein complex Ellis van Creveld Syndrome (Evc2) to activate downstream Shh signalling (Arensdorf et al., 2016). SAG concentration at 100nM has been optimised by (Chen et al., 2002) by plotting a dose-response curve of SAG on the Shh-LIGHT2 cell line, which has a Gli-luciferase reporter incorporated into NIH3T3 cells. A proof-of-concept experiment using SAG at 100nM on C_2C_{12} cells had also been performed previously in the lab and shown an increase in *Gli1* expression (Cruz Migoni, 2015).

To further investigate how Shh signalling controlled MPC numbers, I took advantage of the availability of proliferation markers expressed at different stages of the cell cycle to monitor satellite cells entering and progressing through the cell cycle in the presence of SAG and in control conditions (Fig 4.1). Ki67 is a broad proliferation marker expressed in all phases of the cell cycle G1, S, G2, and M. Ki67 is not expressed during cell cycle arrest (G0), and therefore is not expressed by freshly isolated SCs and terminally differentiated SCs. 5-ethynyl-2'-deoxyuridine (EdU) labelling is a method used to label dividing cells in S phase, during DNA synthesis. EdU is a nucleoside analog of thymidine, which is incorporated in the DNA during synthesis and detected using copper-mediated catalysis of fluorescent-labelled azide. Another marker used to mark proliferating cells is antibody against PH3, which label phosphorylated Histone 3. Histone 3 is highly phosphorylated during late G2 to M phase, and marks cells undergoing mitosis.

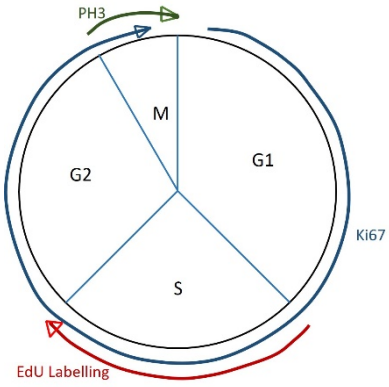

Figure 4.1: Proliferation markers used to label satellite cells at different phases of the cell cycle. Ki67 expression is used to mark all cycling SCs, 5-ethynyl-2'-deoxyuridine (EdU) labels SCs in S phase and phospho-Histone 3 (PH3) is expressed during late G2-M phase.

4.1.1 Hypothesis and Aims

Since loss-of-function approaches showed that disrupting Shh signalling inhibited SC proliferation, I hypothesised that up-regulating Shh signalling in SCs would stimulate SC proliferation and accelerate their progression through the myogenic program. Thus, the aim of this chapter was to increase Shh signalling pharmacologically using SAG in an *ex vivo* culture system and analyse the impact on SC myogenesis and proliferation.

4.2 Methods

Single myofibres were isolated from EDL muscles of 6-10 week-old wild type (C57BL/6) mice. Myofibres were either fixed immediately upon isolation indicated as 0 hour, or cultured in suspension for 24, 48 and 72 hours before being fixed for further immunofluorescence analysis. Cultures were treated with DMSO at 100nM as control or SAG at 100nM in treated group at 0 hour.

4.3 Results

4.3.1 MRF expression in the *ex vivo* system (single myofibre culture) mimicks adult myogenesis.

Myofibres were immuno-stained with antibodies against Pax7 and MRF including Myf5, MyoD and Myogenin to analyse the myogenesis program in standard condition. SCs on fibres at 0 hour are mainly quiescent, as indicated by the sole expression of Pax7 (Fig 4.2 A) ((Seale et al., 2000). Pax7+ cells at 0 hour have a spindle shape. 3 to 8 satellite cells per fibre with a mean value of 4.1 cells (Fig 4.2 E) were observed under the microscope, in agreement with previous reported values (Beauchamp et al., 2000). About 20% of SCs at 0 hour were positive for Myf5, a myogenic regulatory factor (MRF) expressed by activated SCs (Zammit et al., 2002). After 24 hours of culture in non-adherent condition, SCs became activated and expressed both Pax7 and Myf5 (mean= 3.22), although about 11% of SCs (mean=0.38) did not express Myf5 (Fig 4.2 E). The reduction in the number of SCs at 24 hours compared to 0 hours was not significant. Activated SCs were morphologically different and appeared larger than SCs at 0 hour and more spherical in shape (Fig 4.2 B)

After 48 hours of culture, myofibres contained three different cell populations. A small population of SCs are expressing Pax7 only (mean= 3.4 cell) (Fig 4.2 E) and did not expressed MyoD, another MRF protein widely used to mark SCs committed to the myogenic program following Myf5 expression (Zammit et al., 2002). This population of SCs that fail to express Myf5 or MyoD are suggested to be self-renewing SCs (Zammit et al., 2004a). The majority of SCs at 48 hours were positive for both Pax7 and MyoD

(mean= 14.14 cell), indicating that they are engaged in myogenesis. A small number of SCs had down-regulated Pax7 expression but expressed MyoD (mean= 2.64 cell) represents differentiating progenitor cells. SCs at 48 hours had increased more than 3 fold (mean= 20.18 cell), suggesting that they are actively proliferating (Fig 4.2 C, E). Indeed, SCs were observed in groups of 2 cells, also known as doublets, and sometimes in clusters of 3 or 4 cells. Other studies have reported that SCs undergo their first cell division between 25 and 33 hours (Rocheteau et al., 2012; Siegel et al., 2011).

After 72 hours in culture, the number of SCs more than doubled (mean= 57.42 cell) (Fig 4.2 D, E), indicating that SCs continue to proliferate after 48 hours. Importantly, Pax7 expression was not used as a SC marker at this stage since Pax7 was down-regulated in the majority of SCs that enter terminal differentiation and express another MRF protein, myogenin (Zammit et al., 2004b). Instead, I used caveolin-1, which is more consistently expressed at 72 hours (Fig 4.2 D). As shown by immunofluorescence, SCs at 72 hours were present in clusters of more than 10 cells, with different fates co-existing within a cluster: while half of the cluster was made of myogenin+ cells, the remaining cells expressed only caveolin-1. Again, there were three different cell populations found at this time point. Interestingly, a large population of SCs, 46.4% (mean= 26.66 cell) did not express myogenin at 72 hours, suggesting that these cells had not activated myogenin expression yet and expressed MyoD instead, or they were self-renewing cells that do not differentiate and return back to quiescence (Zammit et al., 2004a). However, the majority of cells expressed both caveolin-1 and myogenin (mean= 29.72 cell), while only one cell on average had completely differentiated and down-regulated caveolin-1 expression. This data confirms that the *ex vivo* system mimics adult myogenesis and is a suitable model to study SC behaviour.

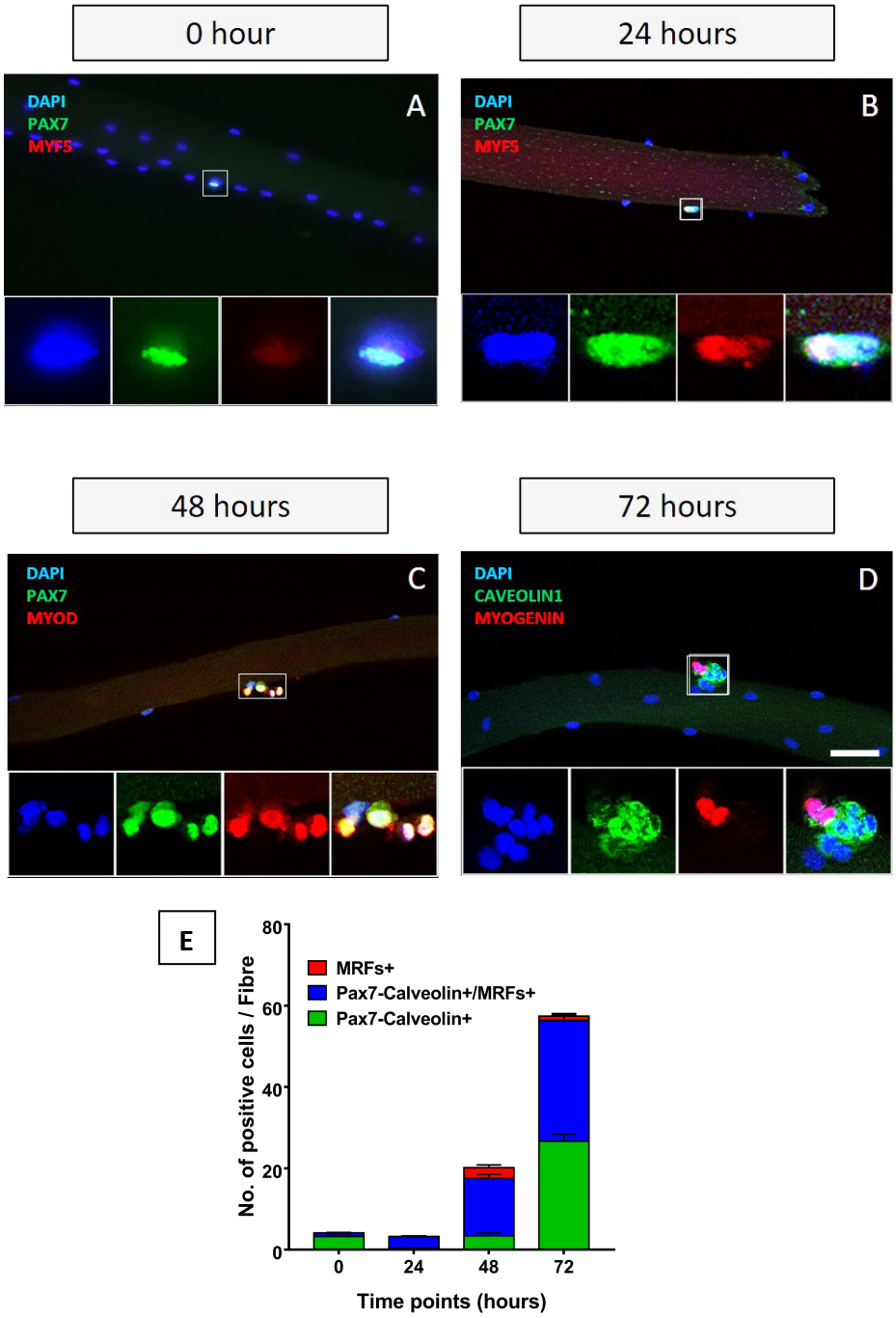

Figure 4.2: Satellite cell markers and Myogenic regulatory factor expression in SCs in the single myofibre culture system.

Single myofibres isolated from mouse EDL were cultured in non-adherent condition up to 72 hours and fixed every 24 hours (0, 24,48 and 72 hours). Myofibres were observed via Immunofluorescence staining against SC marker Pax7 in green **(A-C)** at 0, 24 and 48 hours and Caveolin-1 also in green **(D)** at 72 hours. Myogenesis was monitored through the expression of early myogenic marker Myf5 in red **(A-B)** at 0 and 24 hours, early differentiation marker MyoD in red **(C)** at 48 hours and differentiation marker Myogenin in red **(D)** at 72 hours. Nuclei were counterstained with DAPI (blue). The area magnified is indicated by a box (Scale bar, 50µm). **(E)** Quantification of SCs population expressing SCs markers only (green bar), SCs engaged in myogenic program (blue bar) and differentiated SCs (red bar). Quantification is based on 4 independent experiments and a total of 50 fibres were analysed for each time point. Error bars are ±SEM.

4.3.2 Stimulation of Shh signalling with the Smo agonist SAG increases the number of both committed and uncommitted progenitor cells.

Previous work in the lab has shown that although quiescent satellite cells do not possess any sign of active Shh signalling, activated SCs become responsive to Shh signalling, thus suggesting a role for Shh signalling during adult myogenesis. Therefore, I tested whether up-regulation of Shh signalling using SAG had an effect on the distribution of MRFs expression in SCs in the *ex vivo* myofibre culture system.

The expression of the SC markers Pax7 or caveolin-1 (at 72 hours) with the MRF markers Myf5 at 24 hours, MyoD at 48 hours and myogenin at 72 hours of culture was assayed. Freshly isolated fibres had 6-10 SCs per fibre (mean= 7.43 cell), a value higher than in Fig 4.2 E, but within the normal range of SCs found on a fibre. There was no difference in the number of activated SCs expressing both Pax7 and Myf5 at 24 hours in SAG-treated compared to control cultures, although morphologically SCs in the SAG-treated fibres (Fig 4.3 A, A') appeared to be spherical compared to control fibres, with mean= 7.03 cell for control and 7.32 cell for SAG-treated fibres. At 48 hours, most SCs expressed both Pax7 and MyoD in control and SAG-treated fibres. However, while the control group had cell clusters of 4-6 cells, SAG-treated myofibres had larger clusters of 6-8 cells (Fig 4.3 B, B'). Thus, there was a significant increase in the number of proliferating cells expressing Pax7 and MyoD at 48 hours with mean=21.2 cell for SAG-treated myofibres compared to control (mean= 16.33 cell), although there is no difference in cell percentage (Fig 4.3 D, E). No difference was noticed in control and SAG-treated self-renewing SCs expressing Pax7+ only in green (about 14%, Fig 4.3 D, E). Likewise, there was no difference (14% vs. 13.32%) in the proportion of differentiating SCs expressing MyoD only (MRFs+) (Fig 4.2 D, E). The effect of SAG treatment on SCs was most prominent at 72 hours. While in the representative image the control cultures had 16 cells per cluster with 8 Myogenin+ cells (Fig 4.3 C), SAG-treated cultures had larger cluster with around 20-24 cells with around 12 mygenin+ cells (Fig 4.3 C'). However due to the morphology of SCs at 72 hours where the cells are grouped together in a 3-dimensional manner, the actual number of the cells were underestimated in the images. However, as shown in Fig 4.2 C, C', D, there was a significant increase in the number of cells positive for caveolin-1 only (mean= 31.42 cell in SAG-treated compared to mean=

23.92 cell in control). The number of early differentiating SCs expressing caveolin-1 and myogenin also increased in SAG-treated fibres compared to control (mean= 44.63 cell compared to mean= 38.31 cell), but there was no difference in the number of myogenin+ differentiating SCs (Fig 4.3 D). However, the proportion of caveolin1+/myogenin+ and myogenin+ SCs were decreased at 72 hours at the expense of the increased caveolin1+ SCs. This suggest that SAG treatment had possibly delayed or inhibited differentiation directly. SAG treatment might also indirectly affecting myogenin+ cells by favouring another program during myogenesis. These data suggest that stimulating Shh signalling promotes SC-mediated myogenesis by increasing SC number during their expansion phase.

Table 4.1 The expression of Myogenic regulatory factors (MRF) in SCs upon Shh stimulation ex vivo.

		Pax7-Caveolin1+		Pax7-Caveolin1+ /MRFs+		MRFs+		
Time (h)	**Experimental Group**	**Mean value (cell)**	**S.E.M.**	**Mean value (cell)**	**S.E.M**	**Mean value (cell)**	**S.E.M.**	**N**
24	Control	0.16	0.09	6.87	0.45	0.00	0.00	3
	SAG-Treated	0.09	0.04	7.23	0.51	0.00	0.00	3
48	Control	3.	0.72	16	1.12	3.21	1.03	3

		4 0	. 3 2		
	SAG-Treated	4 0.92 . 4 1	2 1.03 1 . 1 9 *	3.93 1.47	3
72	Control	2 2.55 3 . 9 2	3 1.03 8 . 3 1	3.42 1.84	3
	SAG-Treated	3 0.94 1 . 4 2 *	4 1.04 4 . 6 3 *	2.91 0.83	3

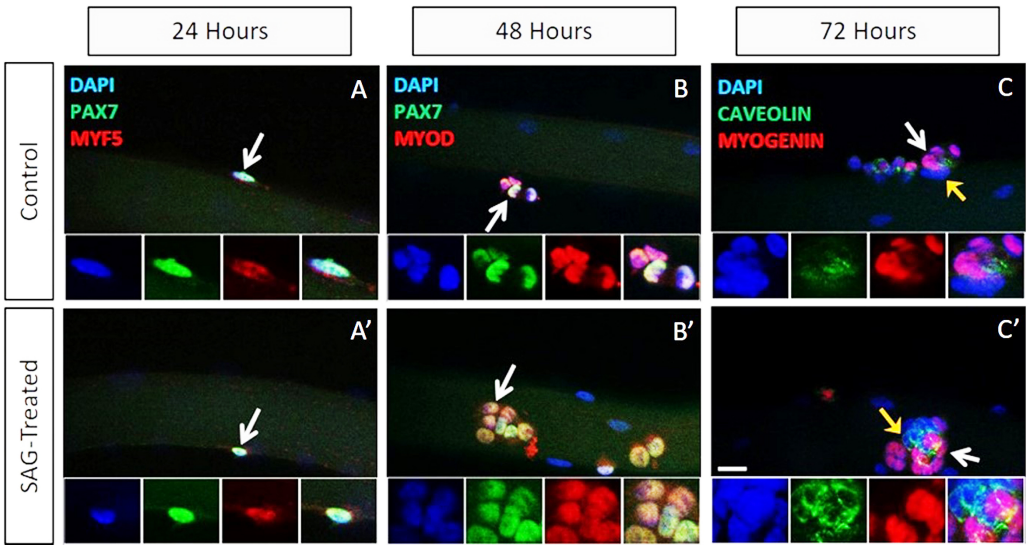

D

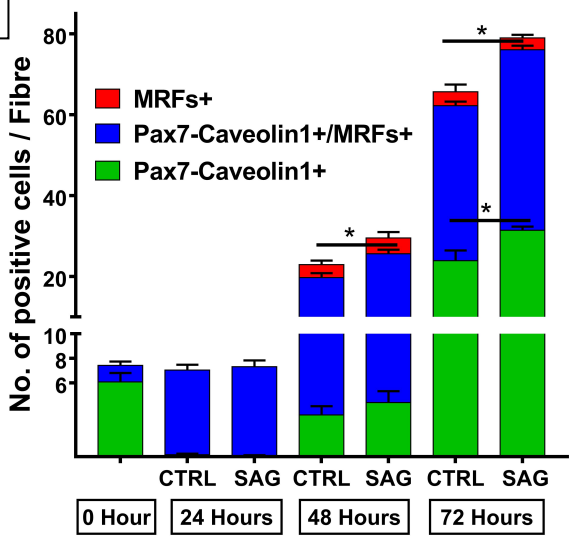

E

Time point	24 hours		48 hours		72 hours	
Cell Population	**Control**	**SAG**	**Control**	**SAG**	**Control**	**SAG**
Pax7-Caveolin1+	2.33%	1.29%	14.82%	14.92%	36.43%	39.79%
Pax7-Caveolin1+/MRFs+	97.68%	98.71%	71.18%	71.76%	58.36%	56.52%
MRFs+	0%	0%	14%	13.32%	5.21%	3.69%

Figure 4.3: Stimulation of Shh signalling with SAG increased satellite cell number *ex vivo*. **A-A'**) Representative immunofluorescence images of control and SAG-treated myofibres cultured for 24 hours expressing Pax7 in green and Myf5 in red. **B-B'**) Representative immunofluorescence images of control and SAG-treated myofibres cultured for 48 hours expressing Pax7 in green and MyoD in red. **C-C'**) Representative immunofluorescence images of control and SAG-treated myofibres cultured for 72 hours expressing Caveolin-1 in green and Myogenin in red. Scale bar= 20μM **D**) Graph showing the quantification of the number of positive SCs expressing Pax7-Caveolin-1 (green), Pax7-Caveolin-1/MRF (blue) and MRF only (red) per myofibre cultured 24-72 hours in control (CTRL) and SAG treatment (SAG). **E**) Table showing the percentage of SCs population per group shown in D. Data were based on 3 independent experiments with 32-69 myofibres analysed per condition. *$P \leq 0.05$, error bars are ±SEM

4.3.3 Stimulation of Shh signalling with Smo agonist SAG increases the number of proliferating SCs

In the previous section, I have shown that there was an increase in the number of SCs expressing MRFs during the expansion phase of adult myogenesis (48 – 72 hours) when myofibre cultures were treated with SAG. This observation suggested that SAG stimulates SC proliferation. To test this possibility, myofibres from EDL muscles isolated from a reported mouse line Tg(Pax7-GFP) which expresses GFP under the control of the Pax7 promoter were cultured for 24 to 72 hours in the presence of SAG at 100nM or treated with DMSO only as control. Fixed muscle fibres were immuno-stained with

antibodies against GFP and a widely used proliferation marker Ki67. After 24 hours of culture, there was no difference in the number of SCs expressing Ki67 in cultures treated with SAG compared to control cultures (Fig 4.4 A-D, A'- D'). However, after 48 hours of culture, there were more SCs expressing Ki67 upon treatment with SAG compared to the control group. While only 1 cell had high ki67 expression and another 2 cells expressed faintly Ki67 in a cluster in control cultures (Fig 4.4 E- H), SAG-treated SCs had 4 SCs in a cluster that were Ki67+ when observed under microscope (Fig 4.4 E'- H'). Indeed, quantification of Ki67-positive SCs showed a significant increase in SCs positive for both GFP and Ki67 in SAG-treated myofibres (mean= 18.65 cell) compared to DMSO-treated control myofibres (mean= 13.22 cell). At 72 hours, while there were 5 Ki67+ SCs in a 7-cell cluster, there were about 10 Ki67+ SCs in a 16-cell cluster identified in the representative images (Fig 4.4 I- L, I'- L'). The quantification of SC after 72 hours culture also showed that there was a significant increase in the number of GFP+/Ki67+ SCs treated with SAG (mean= 50.94 cell) compared to control (mean= 41.41 cell). This data confirms that the increase in the number of SCs in SAG-treated cultures in Fig 4.3 results from the stimulation of SC proliferation mediated by Shh signalling.

Table 4.2 The expression of Proliferation marker Ki67 in SCs upon Shh stimulation ex vivo.

		GFP+		**GFP+/ Ki67+**		
Time (hours)	**Experimental Group**	**Mean value (cell)**	**S.E.M.**	**Mean value (cell)**	**S.E.M.**	**N**
24	Control	5.19	0.45	1.00	0.19	4
	SAG-Treated	5.27	0.29	1.16	0.14	4
48	Control	1.23	0.30	13.22	0.98	4
	SAG-Treated	1.70	0.25	18.65**	0.97	4
72	Control	17.06	0.75	41.42	1.73	4

	SAG-Treated	21.71	3.03	50.94*	2.59	4

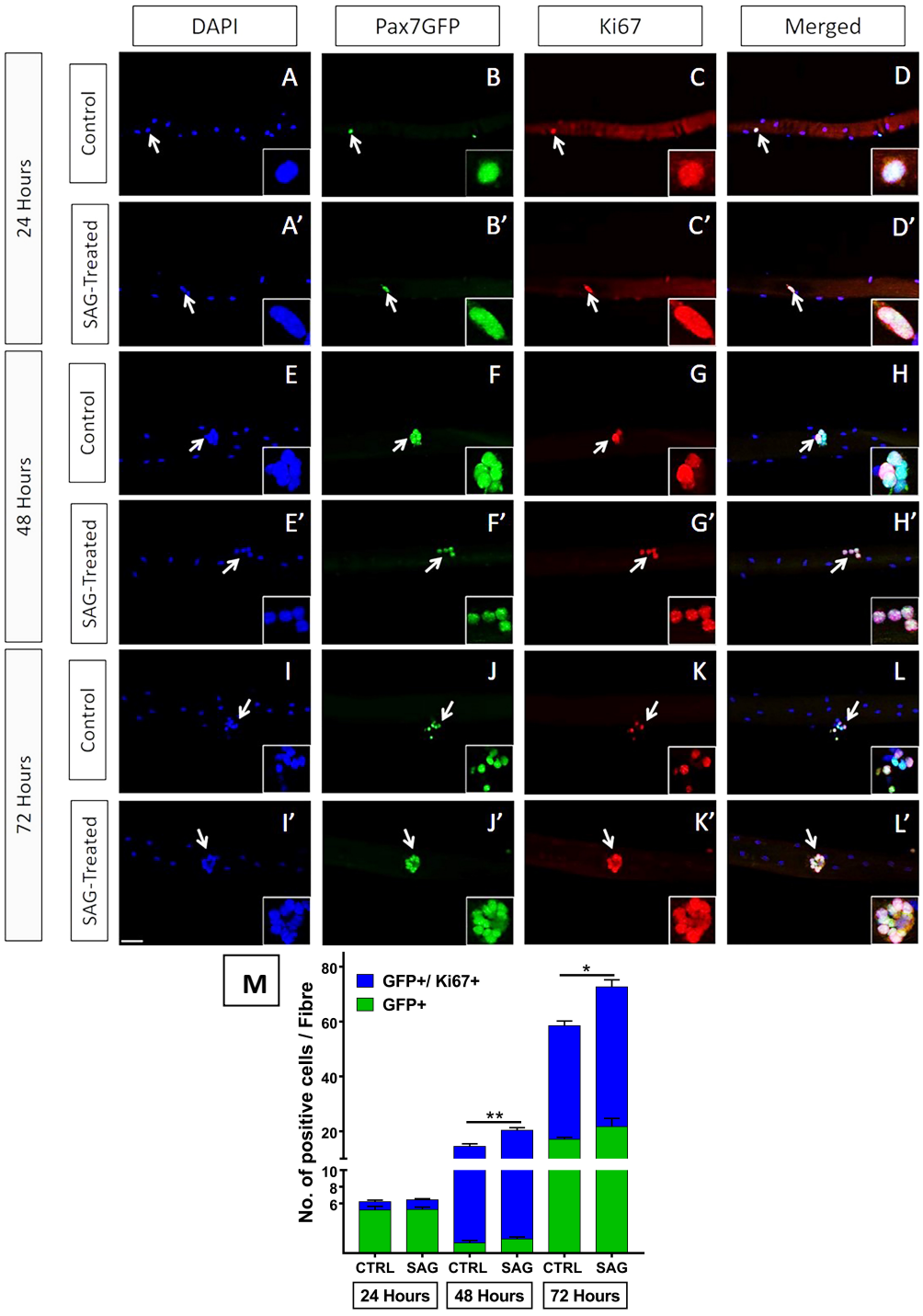

Figure 4.4: Stimulation of Shh signalling with SAG increased satellite cell proliferation *ex vivo*. Representative images of EDL myofibres cultured in the presence of DMSO (Control) or SAG at 100nM for 24 hours **(A-D & A'-D')**, 48 hours **(E-H & E'-H')** and 72 hours **(I-L & I'-L')**. For every

condition, the first panel shows nuclei counterstained with DAPI (blue), Pax7GFP expression (green), Ki67 expression (red) and merged images. Magnified image of SCs indicated with arrow are shown at the bottom of images. Scale bar is 50µM. **M)** Graph showing the quantification of the number of GFP+ SCs (green bar) and GFP+/Ki67+ SCs (blue bar) per myofibre in 24, 48 and 72 hours control (CTRL) or SAG-treated cultures. Data were based on 4 independent experiments with 39-74 myofibres analysed per condition per time point. *P ≤0.05 and **P ≤0.005, error bars are ±SEM

4.3.4 Stimulation of Shh signalling with Smo agonist SAG promotes earlier entry into the cell cycle.

To further characterize how up-regulation of Shh signalling impacts on SC cell cycle, we labelled SCs with the nucleotide analog 5-Ethynyl-2´-deoxyuridine (EdU) in order to monitor cells in S phase. EdU incorporated into divided SCs was detected in combination with immunofluorescence staining using a caveolin-1 antibody to label SCs (Salic and Mitchison, 2008). Interestingly, I observed that 5.30% of SCs were already in S-phase at 24 hours when treated with SAG compared to only 0.57% in the control cultures (Fig 4.5 A- D, A'- D', M- N). At 48 hours, 55.90% of SCs treated with SAG were EdU+ (mean= 14.382 cell) compared to 49.58% (mean= 10.14 cell) of SCs labelled with EdU in control cultures (Fig 4.5 E-H, E'-H', M-N). At 72 hours, 18% of SCs in SAG-treated cultures incorporated EdU while the control group had 15% of EdU+ cells (Fig 4.5 I-L, I'-L'). There was a significant increase in the number of EdU+ SCs treated with SAG with a mean value of 14.08 cell compared to control cultures which had a mean value of 10.57 cell (Fig 4.5 M). This suggests that upregulation of Shh signalling promotes earlier and prolonged SCs entry into the cell cycle. Notably, while EdU+ SCs were very rare at 24 hours, almost 10 times more EdU+ SCs were observed in SAG treated myofibre cultures, suggesting that SCs were driven to enter the cell cycle earlier.

Table 4.3 The data of EdU labelling in SCs upon Shh stimulation ex vivo.

		Caveolin1+		**Caveolin1+ /EdU+**		
Time (hours)	**Experimental Group**	**Mean value (cell)**	**S.E.M.**	**Mean value (cell)**	**S.E.M.**	**N**
24	Control	6.33	0.68	0.04	0.02	4
	SAG-Treated	5.77	0.67	0.32**	0.05	4
48	Control	10.31	1.81	10.14	0.31	4

	SAG-Treated	11.35	0.85	14.38*	1.27	4
72	Control	58.99	0.73	10.57	1.01	4
	SAG-Treated	64.57	2.59	14.08*	0.51	4

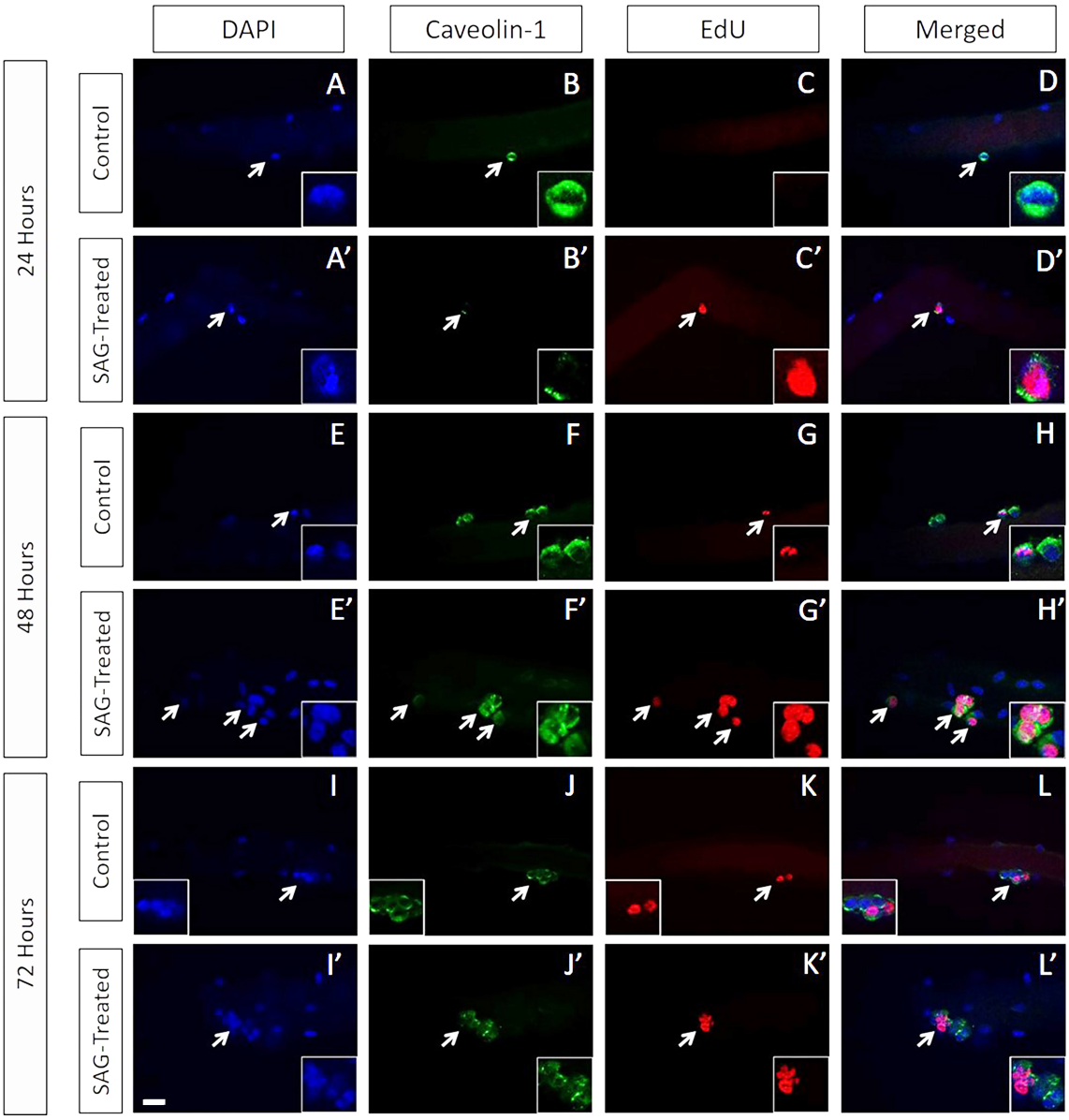

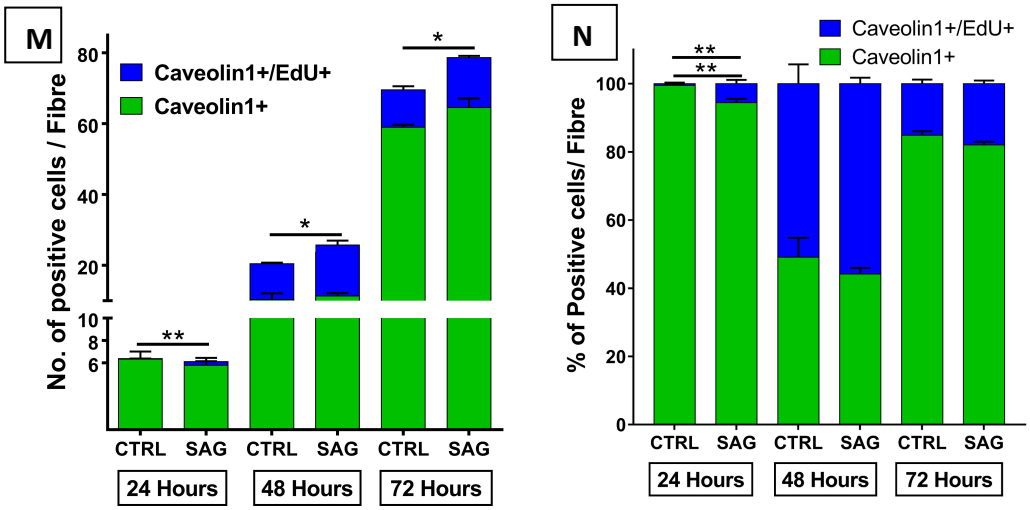

Figure 4.1: Stimulation of Shh signalling with SAG promotes satellite cell entry into the cell cycle.

Representative images of EDL myofibres from Tg (Pax7-GFP) mice cultured in the presence of DMSO (control) or SAG at 100nM for 24 hours **(A-D, A'-D')**, 48 hours **(E-H, E'-H')** and 72 hours **(I-L, I'-L').** From left to right, panels show nuclei counterstained with DAPI (blue), Caveolin-1 expression (green), EdU labelling (red) and merged images. Magnified image of SCs indicated with arrows are shown at the bottom of images. Scale bar is 20µM. **M)** Graph showing the quantification of the number of SCs positive for Caveolin1 only (green bar) and positive for Caveolin1 and EdU (blue bar) at 24, 48 and 72 hours in control (CTRL) or SAG-treated conditions. **N)** Graph of data in M in percentage. Data were based on 4 independent experiments with 69-84 myofibres analysed per condition per time point. *P ≤0.05 and **P ≤0.005, error bars are ±SEM

To assess the effect of up-regulation of Shh signalling on SCs undergoing mitosis, cultured myofibres were immuno-stained with antibodies against phospho-Histone 3 (PH3) and Pax7 as SC marker. This confirmed that upon SAG treatment, SCs entered and progressed faster through the cell cycle, as 9.9% (mean= 0.602 cell) of SCs were PH3+ at 24 hours in SAG treated cultures whereas 2.5% (mean= 0.16 cell) of SCs were PH3+ in control cultures (Fig. 4.6 I, J). Regrettably, I failed to provide representative images for this particular time point due to technical pitfall. At 48 hours, 49.6% (mean= 12.1 cell) of SCs were PH3+ in SAG-treated cultures whereas 32.4% (mean= 6.91 cell) of SCs were PH3+ in control cultures (Fig 4.6 A-D, A'-D', I-J). At 72 hours, 17% (mean= 8.0 cell) of SCs treated with SAG were positive for PH3 whereas 13.6% (mean= 4.6 cell) of SCs were positive for PH3 in control cultures (Fig 4.6 E-H, E'-H', I). This indicates that SAG treatment promotes cell cycle progression and retains SCs mitotically active for up to 72 hours.

Table 4.4 The expression of PH3 in SCs upon Shh stimulation *ex vivo*.

		Pax7+		**Pax7+ /PH3+**		**PH3+**		
Time (h)	**Experimental Group**	**Mean value (cell)**	**S.E.M.**	**Mean value (cell)**	**S.E.M.**	**Mean value (cell)**	**S.E.M.**	**N**
24	Control	6.04	0.10	0.16	0.07	0.00	0.00	4
	SAG-Treated	5.45	0.42	0.60*	0.14	0.00	0.00	4
48	Control	14.45	1.35	6.91	0.57	0.00	0.00	4
	SAG-Treated	12.28	0.82	12.10*	1.59	0.00	0.00	4
72	Control	27.33	2.74	4.60	1.11	1.80	0.65	4

	SAG-Treated	35.98	3.16	7.98*	0.25	3.02	1.17	4

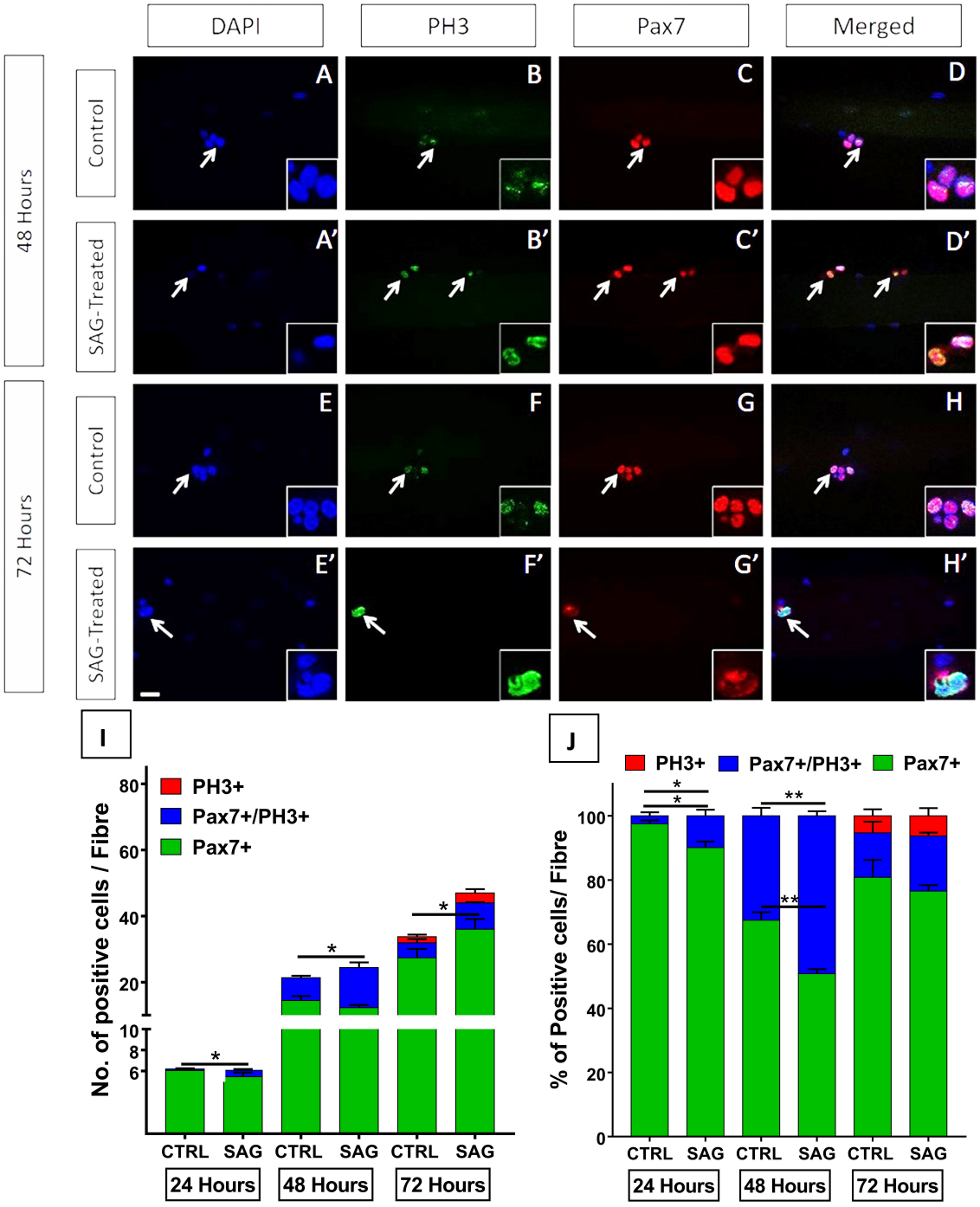

Figure 4.2: Stimulation of Shh signalling with SAG increases the number of satellite cells in the mitotic phase of the cell cycle.

Representative images of C57BL/6 EDL myofibres cultured in the presence of DMSO (control) or SAG tat 100nM for 48 hours **(A-D, A'-D')** and 72 hours **(E-H, E'-H')**. From left to right, panels show nuclei counterstained with DAPI (blue), PH3 expression (green), Pax7 expression (red) and

merged images. Magnified image of SCs indicated with arrows are shown at the bottom of images. Scale bar is 20µM. **I)** Graph showing the quantification of the number of Pax7+ SCs (green bar), of Pax7+/PH3+ SCs (blue bar) and PH3+ SCs (red bar) per fibre cultured for 24, 48 and 72 hours in control (CTRL) or SAG-treated conditions. **J)** Graph of data in M in percentage. Data were based on 4 independent experiments with 61-85 myofibres analysed per condition per time point. *$P \leq 0.05$ and **$P \leq 0.005$, error bars are ±SEM.

4.4 Discussion

4.4.1 Up-regulation of Shh signalling expands the MPCs population during adult myogenesis.

The role of Shh signalling in embryonic myogenesis is well-characterised (Anderson et al., 2009; Borycki et al., 1999; Gustafsson et al., 2002; Hu et al., 2012; Kahane et al., 2013; Kruger et al., 2001; McDermott et al., 2005), but its function in adult skeletal muscles remains obscure. In this study using SAG to up-regulate Shh signalling in myofibres cultured *ex vivo*, I discovered that there was an increase in the number of committed SCs expressing MyoD and myogenin when Shh signalling was up-regulated. This finding parallels previous work in the lab (Cruz Migoni, 2015) which demonstrated that blocking Shh signalling using cyclopamine and GANT61 delayed SC progression through the myogenic program *ex vivo* and resulted in an accumulation of SCs at an uncommitted stage and delayed myogenin expression.

Cyclopamine intra-muscular administration one day prior to injury by CTX *in vivo* has also been shown by others to cause a decreased number of Myf5 and MyoD positive muscle progenitor cells (MPCs) at 4dpi (Straface et al., 2009b), an effect that our lab showed resulted from a direct effect of Shh signalling on satellite cells by examining MyoD and myogenin expression upon CTX injury in a loss-of-function genetic model, $Pax7Cre^{ERT2}$; $Smo^{flox/flox}$ (Cruz Migoni, 2015). An *in vitro* study treating primary myoblasts with Shh recombinant (Elia et al., 2007) and an *in vivo* study using a human Shh plasmid to transfect muscles prior to CTX injury (Piccioni et al., 2014a) also showed a positive impact upon Shh signalling upregulation on myogenesis by increased mRNA expression for *MyoD*, *Mef2* and *MyHC* (Elia et al., 2007) and Myf5 protein at 4dpi (Piccioni et al., 2014a). Thus, there are a number of compelling evidences indicating that modulating Shh signalling can affect how many muscle progenitor cells are generated. However, the

mechanism by which Shh signalling controls adult myogenesis has not been determined. Up-regulation of Shh signalling could result in an increase in the number of MPCs by controlling MPC commitment or survival or proliferation.

Table 4.5: Comparison of the percentage of satellite cells in different phases of the cell cycle at different time points

Time Point	Ki67 Expression (overall cell cycle)			EdU Labelling (S-Phase)			PH3 Expression (G2/M Phase)		
	CTRL (%)	SAG (%)	Increment (%)	CTRL (%)	SAG (%)	Increment (%)	CTRL (%)	SAG (%)	Increment (%)
24 hours	16.2	18.07	2	0.57	5.7	5.1	2.5	9.9	7.4
48 hours	91.49	91.65	0	49.58	55.9	6.3	32.4	49.9	17.2
72 hours	70.83	70.11	0	15	18	3	13.6	17	3.4

I reported that SAG treatment increased the number of Ki67-positive SCs at 48 hours and 72 hours, although the proportion of proliferating SCs does not differ between SAG-treated and control cultures despite a small increase in the proportion of cells expressing Ki67 at 24 hours (Table 4.1). Interestingly, subsequent tests measuring proliferation using EdU incorporation and PH3 expression showed a significant increase in number of SCs in S and G2/M phases when myofibres were treated with SAG compared to control at 24, 48 and 72 hours of culture (Fig 4.5 & 4.6, Table 4.1). Notably, the presence of EdU-positive cells in SAG-treated myofibre cultures when no or few EdU-positive cells were visible in control myofibre cultures suggest strongly that upon Shh signalling SCs exited quiescence and entered the cell cycle rapidly, leading to an increase in the number of cells in S and G2/M phase. These findings support and extend previous data by others that reported an increase in BrdU incorporation in C_2C_{12} cells and primary myoblasts treated with either Shh ligand or recombinant Shh (rShh) in concentration-dependent manner (Koleva et al., 2005a; Straface et al., 2009b). Importantly, treatment of *mdx*-derived primary myoblasts with rShh also increased BrdU incorporation, suggesting that up-regulating Shh signalling may have therapeutic benefit in muscular dystrophies (Piccioni et al., 2014b). The present findings are also consistent with previous findings reported in the lab (Cruz Migoni, 2015) showing that blocking Shh signalling results in a defect in SC ability to progress through the cell cycle and their arrest at the G1/S checkpoint.

An upregulation of *Shh* mRNAs in whole-tissue section has been reported following skeletal muscle injury produced through different methods including ischaemic, mechanical and cardiotoxin-mediated, although without determining precisely the nature of the cells expressing *Shh* (Pola et al., 2003; Renault et al., 2013b; Straface et al., 2009b). One study reported observing the expression of Shh protein co-localised with Pax7 in normal adult skeletal muscles, suggesting a possible cell autonomous signalling (Elia et al., 2007). However, these findings have not be confirmed and in fact work in the lab has shown that there was no *Shh* transcription detected in adult SC collected from single myofibre cultures at any time point (Cruz Migoni, 2015). Nonetheless, work in the lab has shown that despite the absence of Shh response in quiescent and uninjured adult skeletal muscles, activated SCs become responsive to Shh signalling and expressed Gli target genes including Ptch1 and Gli1 *ex vivo* and *in vivo*, confirming p observations by others (Cruz Migoni, 2015; Piccioni et al., 2014a; Piccioni et al., 2014b; Straface et al., 2009b). Shh signalling increases SC proliferation by promoting entry and progression through the cell cycle.

How does Shh signalling control SC entry and progression through the cell cycle remains to be established. It is noteworthy that the time of SC first cell division has been reported to be approximately 25.5-33 hours, followed by shorter cell cycles lasting between 8-10 hours (Rocheteau et al., 2012; Siegel et al., 2011). Therefore, it is likely that cell cycle regulation of SC first cell division differs from that of the subsequent cell divisions. Data shown here suggest that Shh signalling has the power to control both the length of the first cell division and the subsequent short cell divisions. The molecular regulation of the cell cycle program has not been investigated in SCs yet, but has been discussed in other systems, and several molecular components controlling the G1/S transition were indicated including *N-myc, CyclinD1, CyclinE1, Dp1 and E2f1* (Seifert et al., 2010; Towers et al., 2008; Wall et al., 2009). The activation of Shh signalling in postnatal neural stem cell (granule cell precursors – GCPs) promotes cell cycle entry into G1 phase by promoting the expression of *N-myc* (Colvin Wanshura et al., 2011; Liu et al., 2012a). Moreover, Shh signalling control the G1/S transition during cell cycle by regulating the expression of *Cyclin D1*, *Cyclin D2*, *Cyclin E1* and phosphorylated *Rb* in neural GCP cells and retinal stem cells (Duman-Scheel et al., 2002b; Oliver et al., 2003;

Wang et al., 2005). Importantly, Shh signalling has also been implicated in the regulation of *Cyclin D1*, *Cyclin E* and phosphorylated *Rb* (Li et al., 2010). Due to the key functions of Shh signalling in controlling the timely progression of stem cells through cell cycle, its inhibition were found to disrupt cell cycle kinetics and prolonged cell cycle program (Cruz Migoni, 2015; Seifert et al., 2010)

A data collected using EDL-derived SCs reported cell doubling time as 16.4 hours would be closer to my data, but still myofibres and SCs in that study were plated on matrigel-coated dish instead of in floating condition (Zammit et al., 2002). If we are using this information to calculate the amount of cycles the SCs for 72 hours using data from Fig 4.3 (Ki67 staining) as an example, the cell doubling time would be 18.03 hours (1.33 cycle) at 24-48 hours and 5.69 hours (8.44 cycles) at 48-72 hours of culture. While in SAG-treated cultures, cell doubling time at 24-48 hours culture would be 11.07 hours (2.17 cycles) and decreased to 4.66 hours (10.31 cycles). Indeed, this information is parallel to a report by Siegel et al. 2011, who recorded satellite cell division using time-lapse live imaging technique and reported that SCs took 4.8 hours on average to divide (Siegel et al., 2011). However, direct comparison would be impossible as the culture methodology was different and SCs are known to be sensitive to their niche environment. Therefore, data provided in this chapter reports on a pro-proliferative effect of Shh signalling by accelerating cell cycle program during adult myogenesis.

5 Up-regulation of Sonic hedgehog signalling increases SC self-renewal *ex vivo*.

5.1 Introduction

SC self-renewal allows repeated cycles of myogenesis to take place over the life span, by maintaining a SC 'reserve cell pool'(Collins and Partridge, 2005). During myogenesis, a subset of SCs are excluded from undergoing myogenic differentiation and instead continue expressing stem cell-related genes including Pax7 and CDKN1B ($p27^{Kip1}$) (Chakkalakal et al., 2014; Olguin and Olwin, 2004). This subset of cells, termed self-renewing SCs or satellite stem cells are slow dividing SCs that reverted to quiescence at a later stage of myogenesis (Gopinath et al., 2014; Ono et al., 2012). A number of extrinsic and intrinsic cues have previously been shown to drive SC cell fate towards self-renewal and contribute to maintaining self-renewal. These include extra-cellular matrix components such as laminin-111, fibronectin and collagen VI (Rayagiri et al., 2018), signalling molecules such as Notch and Wnt, and intrinsic factors and organelles such as primary cilia (Jaafar Marican et al., 2016; Rayagiri et al., 2018) and cell polarity proteins (Troy et al., 2012). Asymmetric cell division has been described as the preferred method adopted by SCs to generate self-renewing daughter cells, whereby one daughter cell retain the template DNA from the mother cell while the other daughter cell become committed to a myogenic cell fate (Rocheteau et al., 2012; Shinin et al., 2006; Troy et al., 2012; Yennek et al., 2014).

In chapter 3, I demonstrated that stimulating Shh signalling caused an increase in SC proliferation. Interestingly, there was also an increase in uncommitted SCs at the end of

myogenesis *ex vivo*. This led me to ask whether increased proliferation was also accompanied by a change in cell fate choice in favour of self-renewal.

5.1.1 Hypothesis and aim

So, I hypothesized that Shh signalling stimulates SC self-renewal during adult myogenesis. The aim of this chapter was to investigate the effect of Shh up-regulation on SC self-renewal in the *ex vivo* myofibre culture system.

5.2 Method

Single myofibres were isolated from EDL muscles of 6-10 week-old wild type (C57BL/6) mice. Myofibres were cultured in suspension for 48, 72, or 96 hours before being fixed for further immunofluorescence analysis. Cultures were treated with DMSO at 100nM as control or SAG at 100nM in treated group at 0 hour.

5.3 Results

5.3.1 Stimulation of Shh signalling increases the proportion of undifferentiated Pax7-positive SCs in late stage myogenesis.

In chapter 3 (Fig 3.2), I showed that SAG-treatment resulted in a significant increase in the number of undifferentiated SCs negative for myogenin but positive for caveolin-1 at 72 hours. This observation suggests that up-regulation of Shh signalling may stimulate SC self-renewal. However, additional experiments are required because the caveolin1^{+}/myogenin^{-} cell population present at 72 hours also comprise of cells in early differentiation (MyoD^{+}/myogenin^{-}) and terminally differentiated SCs that have down-regulated myogenin.

Myofibres were immuno-stained with myogenin to label differentiating MPCs and Pax7 to identify self-renewing SCs. After 48 hours of culture, there were very minimal changes shown between the control group and SAG-treated group (Fig 5.1 A-D, A'-D'). As shown in Figure 5.1E-H, cell clusters from the control group observed after 72 hours of culture are generally composed of cells expressing either Pax7 or myogenin, either in equal proportion or with slightly more differentiating cells (myogenin$^+$). None of the cells are double positive. However, in the SAG-treated culture at 72 hours, clusters have generally more Pax7$^+$ SCs and fewer myogenin$^+$ cells (Fig 5.1 E'-F'). Quantification analysis of the data showed that despite a trend towards an increase in the number of Pax7$^+$ SCs at 48 hours in SAG-treated compared to control myofibres, the difference was not statistically significant (Figure 5.1 I). However, by 72 hours there was a significant increase in the number of Pax7$^+$ SCs in myofibres treated with SAG (mean= 33.58 cell) compared to control (mean= 23.49 cell). There was no significant difference in the number of Myogenin$^+$ SCs despite the mean numbers indicating a slight increase (mean= 60.33 cell for SAG-treated group and mean= 48.09 cell for control) at 72 hours (Figure 5.1 I). Although an increase in the total number of self-renewing cells was observed in SAG-treated myofibres, there was no difference in the percentage of SCs (Fig 5.1 J), indicating that the increase in cell number did not change the overall distribution of self-renewing and differentiating cells (myogenin$^+$).

Table 5.1 The expression of Pax7 and myogenin in SCs upon Shh stimulation *ex vivo.*

		Pax7+		**Pax7+ /Myogenin+**		**Myogenin+**		
Time (h)	**Experimental Group**	**Mean value (cell)**	**S.E.M.**	**Mean value (cell)**	**S.E.M.**	**Mean value (cell)**	**S.E.M.**	**N**
48	Control	16.46	1.39	2.20	0.41	1.20	0.48	3
	SAG-Treated	19.63	0.84	2.24	0.46	1.41	0.51	3
72	Control	23.49	2.80	0.93	0.13	48.09	5.70	3
	SAG-Treated	33.58*	1.54	0.61	0.10	60.33	2.09	3

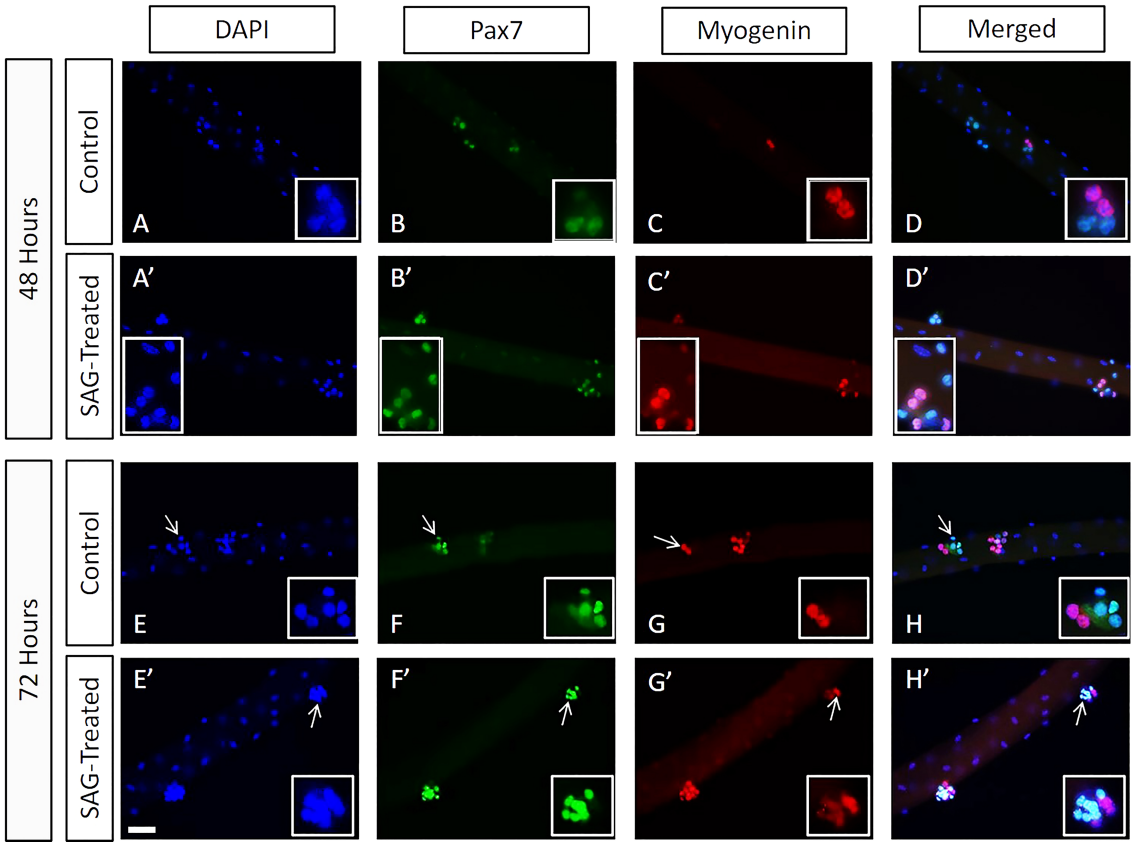
DAPI
Pax7
Myogenin
Merged
48 Hours
72 Hours
Control
SAG-Treated
Control
SAG-Treated
A
B
C
D
A'
B'
C'
D'
E
F
G
H
E'
F'
G'
H'

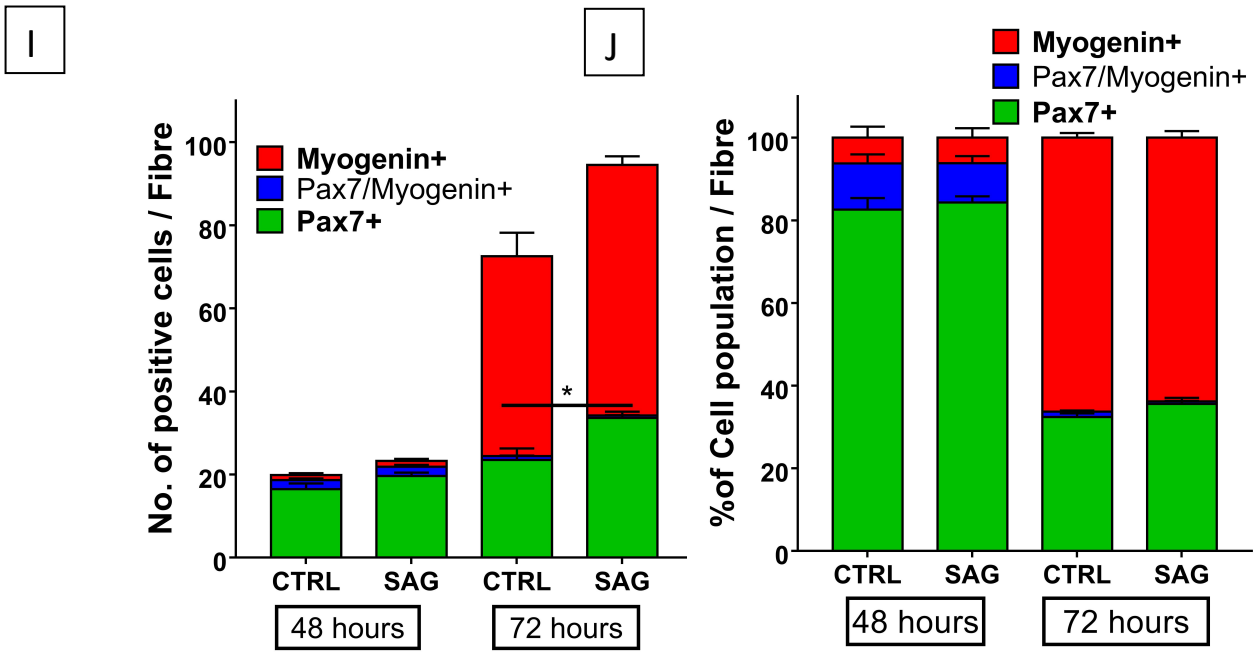

Figure 5.1: Shh upregulation increased Pax7-expressing SCs *ex vivo*.
Representative images of C57BL/6 EDL myofibres cultured for 48 hours in the presence of DMSO (control) **(A-D)** and with SAG **(A'-D')**, and 72 hours **(E-H, E'-H')** analysed by immunofluorescence using antibodies against Pax7 (green) and Myogenin (red) with nuclei counterstained with DAPI. Merged panels are shown on the right. Magnified area are indicated by arrows. Scale bar is 50µM **(I)** Quantification graph of the number of SCs expressing Pax7 (green), Myogenin (red) and Pax7 and Myogenin (blue) at 48 and 72 hours with DMSO (control) or SAG treatment. **(J)** percentage of the SCs analysed in graph E. Data are based on 3 independent experiments with 30-33 myofibres analysed per condition per time point. *P≤ 0.05, error bars are ±SEM

While the myogenin-expressing cell population is unequivocally labelling differentiating muscle progenitor cells because Pax7 and myogenin are mutually exclusive during myogenesis (Olguin et al., 2007), the Pax7-expressing cell population contains a mixture of early differentiating cells that have not yet express myogenin, in addition to cells that self-renew. This is because SCs in the *ex vivo* myofibre culture system are not synchronised.

To distinguish early differentiating from self-renewing cells, myofibres cultured for 72 hours in the presence of SAG or in control conditions were analysed by

immunofluorescence using antibodies against an earlier myogenic marker, MyoD, and against Pax7. Representative images of myofibres cultured in the presence of SAG show that cell clusters contain equal numbers of Pax7-expressing and MyoD-expressing cells, together with some double positive cells (Fig 5.2 A'-D'), whereas control cultures usually have a greater number of MyoD-positive cells than Pax7-positive cells (Fig 5.2 A-D). Quantification analyses confirms the significant increase in the number of $Pax7^+$ SCs in SAG-treated compared to control myofibres (mean= 21.28 cell versus 13.62 cells), with a concomitant decrease in the number of double positive $Pax7^+/MyoD^+$ cells (mean= 6.44 cell versus 9.94 cell) at 72 hours of culture. No difference in the number of differentiating SCs that are $MyoD^+$ only was observed between SAG-treated and control myofibres. Interestingly, the quantification of the proportion of cells present in the cultures showed that SAG treatment caused an increase in the proportion of self-renewing SCs, with 27.39% of SCs self-renewing ($Pax7^+$) compared to 18.21% SCs in the control group (p= 0.016) (Fig 5.2 F). This increase in self-renewing cells was at the expense of cells committed to the myogenic program, with only 8.55% being double positive $Pax7^+/MyoD^+$ SCs compared to 12.95% in the control group (Fig 5.2 F). Collectively, these data suggest that upregulation of Shh signalling during adult myogenesis promotes SC self-renewal.

Table 5.2 The expression of Pax7 and MyoD at 72 hours in SCs upon Shh stimulation *ex vivo.*

		Pax7+		**Pax7+ /MyoD+**		**MyoD+**		
Time (h)	**Experimental Group**	**Mean value (cell)**	**S.E.M.**	**Mean value (cell)**	**S.E.M.**	**Mean value (cell)**	**S.E.M.**	**N**
72	Control	13.62	0.99	9.94	0.99	50.46	0.008	3
	SAG-Treated	21.29*	2.45	6.44*	0.79	51.39	1.61	3

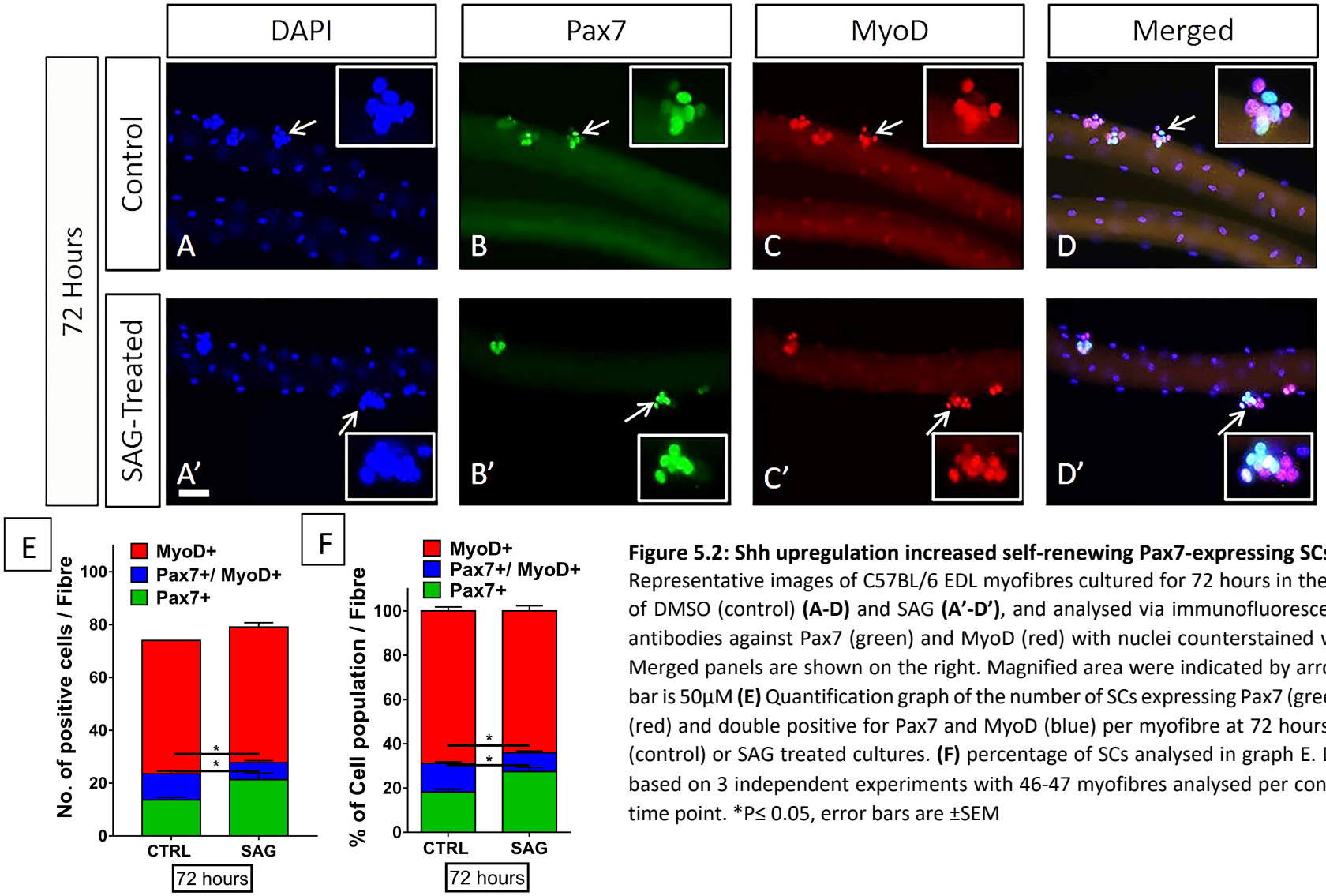

Figure 5.2: Shh upregulation increased self-renewing Pax7-expressing SCs *ex vivo*. Representative images of C57BL/6 EDL myofibres cultured for 72 hours in the presence of DMSO (control) **(A-D)** and SAG **(A'-D')**, and analysed via immunofluorescence using antibodies against Pax7 (green) and MyoD (red) with nuclei counterstained with DAPI. Merged panels are shown on the right. Magnified area were indicated by arrows. Scale bar is 50µM **(E)** Quantification graph of the number of SCs expressing Pax7 (green), MyoD (red) and double positive for Pax7 and MyoD (blue) per myofibre at 72 hours in DMSO (control) or SAG treated cultures. **(F)** percentage of SCs analysed in graph E. Data were based on 3 independent experiments with 46-47 myofibres analysed per condition per time point. *P≤ 0.05, error bars are ±SEM

5.3.2 Up-regulation of Shh signalling increases the proportion of AraC-resistant Pax7-positive SCs.

To confirm that Shh signalling controls SC self-renewal, I designed an experiment using cytosine β-D-arabinofuranoside (AraC), a chemical agent used traditionally in chemotherapy because it kills proliferating cells, and has no effect on differentiated and self-renewing cells that have exited the cell cycle (schematic diagram of experimental design, Fig 5.3 C) (Reano et al., 2017). AraC inhibits DNA replication during S-phase by forming cleavage complexes with topoisomerase I, which result in DNA fragmentation and trigger apoptosis (Reano et al., 2017). The rationale of this study was to allow SC activation and proliferation in the presence or absence of SAG, and treat cultures with AraC at a time self-renewing cells are being produced. The treatment will cause cell death of any cell engaged in the cell cycle, and leave intact self-renewing and differentiating cells. Therefore, if upregulation of Shh signalling drives cells towards self-renewal, I would expect to observe an increase in the number of Pax7-positive cells in SAG-treated cultures following AraC treatment (Fig. 5A). Thus, 100µM AraC was added to the culture medium of SAG-treated (100 nM) or control (DMSO) myofibre cultures at 60 hours. The timing of AraC treatment was chosen to avoid the period of cell amplification, which occurs in the first 48 hours of the culture, and because self-renewing SC begin emerging at 50-52 hours. Myofibres were analysed at 96 hours by immunofluorescence using antibodies against Pax7 to label self-renewing cells and against myogenin to label differentiating cells.

As observed in Fig. 5.A and 5.3B, no double positive cell ($Pax7^+$/$myogenin^+$) were detected, and clusters were smaller following AraC treatment on control and SAG-treated cultures, indicating that the addition of AraC to the culture medium has been effective in killing proliferating cells. Notably, clusters contained more $Pax7^+$ cells in SAG-treated compared to control myofibre cultures (Fig. 5.3 A). Quantification of the data showed that there was a 64.75% reduction in the number of $myogenin^+$ SCs in control cultures after AraC treatment (mean= 57.07 cell (untreated) compared to mean=20.12 cell (AraC treated) (Fig 5.3 D- E). Nonetheless, In SAG-treated cultures, AraC treatment had no effect on the total number of $Myogenin^+$ cells compared to AraC-treated control

cultures (mean= 21.85 (SAG-treated) compared to 20.12 (Control) (Fig 5.3 D-E). This indicates that when AraC was added to the cultures at 60 hours, a third of muscle progenitor cells were already fully differentiated, the remaining MPCs committed to myogenesis were still engaged in the cell cycle. It is interesting that although SAG treatment causes an increase in the number of MPCs (see Fig. 3.2), it does not affect the proportion of cells in terminal differentiation.

In contrast, I observed a significant difference in the number and percentage of Pax7-expressing cells after AraC treatment in SAG-treated myofibre cultures compared to control myofibre cultures (Fig 5.3 C, E). While there were only 1 $Pax7^+$ SC (mean= 1.38 cell) emerged after 60 hours of myofibre culture, there were more than 3 $Pax7^+$ SCs (mean= 3.39 cell) found in SAG-treated myofibre culture (Fig 5.3 D). The percentage analysis showed that while control myofibre cultures had 4.96% Pax7-expressing SCs after treatment with AraC, the SAG-treated myofibre cultures had a significant increase of Pax7-expressing SCs 12.13% (Fig 5.3 E). This finding indicates that at 60 hours when AraC was added to cultures, SAG-treated myofibres contained twice as many SCs already committed to self-renewal compared to control myofibres. Comparing with data in Figure 5.2 where there was 1.5-fold increase in $Pax7^+$ SCs, experiment with AraC treatment at 60 hours had a 2.4-fold increase, suggesting that the effect was diluted over time possibly due to the increase in overall number of SCs. This confirms that upregulation of Shh signalling promotes SC self-renewal during adult myogenesis.

Table 5.3 The expression of Pax7 and myogenin in AraC-resistant SCs upon Shh stimulation *ex vivo*.

		Pax7+		**Myogenin+**		
Time (h)	**Experimental Group**	**Mean value (cell)**	**S.E.M.**	**Mean value (cell)**	**S.E.M.**	**N**
96	Untreated	27.98	6.25	57.07	12.16	2
	CTRL +AraC	1.39	0.25	20.12	2.99	4
	SAG +AraC	3.39**	0.42	21.85	0.96	4

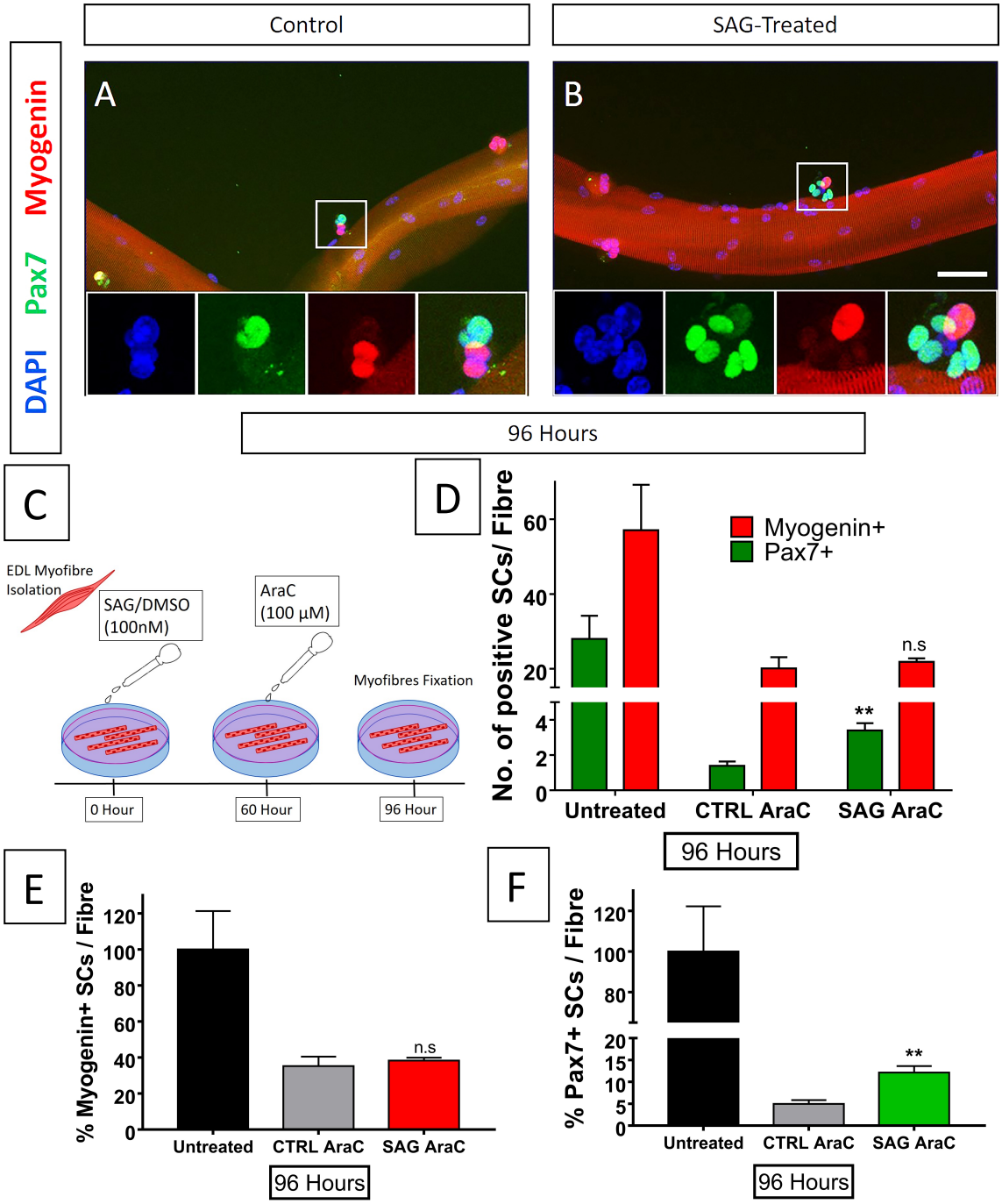

Figure 5.3: Upregulation of Shh signalling increases AraC-resistant Pax7-expressing SCs *ex vivo*. **(A-B)** Representative images of C57BL/6 EDL myofibres cultured for 96 hours in the presence of DMSO (control) or SAG, and treated with AraC at 66 hours. Fibres were analysed by immunofluorescence using antibodies against Pax7 (green) and Myogenin (red) with nuclei counterstained with DAPI. Merged panels are shown on the right. Magnified area are boxed. Scale bar is 50µM **(C)** Graph showing the quantification of the number of SCs expressing Pax7 (green) and MyoD (red) at 96 hours. Untreated group was only treated with DMSO, CTRL+AraC group had DMSO with AraC added at 66 hours and SAG +AraC group was treated with SAG with AraC added at 66 hours of culture. **(D)** percentage of Pax7-expressing SCs analysed in graph C.

(E) Percentage of Myogenin-expressing SCs analysed in graph C. Data were based on 4 independent experiments with 61-63 myofibres analysed per condition per time point. *P⩽ 0.05, **P⩽ 0.005 and error bars are ±SEM

5.3.3 Up-regulation of Shh signalling increases the proportion of self-renewing SCs harbouring a primary cilium

A recent study in the laboratory has demonstrated that primary cilia, an organelle that serves as a signalling hub, are selectively re-assembled in self-renewing SCs following cell cycle exit (Jaafar Marican et al., 2016). The organelle is usually disassembled when cell division is taking place to allow for centriole duplication and mitotic spindle formation, and re-assembled when cells exit the M phase (Anderson and Stearns, 2009; Jaafar Marican et al., 2016). Because primary cilia are also essential for the transduction of Shh signalling by controlling microtubule-dependent Smo trafficking (Goetz et al., 2009), I investigated whether the effect of SAG on SC self-renewal was accompanied by an effect on primary cilia.

Fixed myofibres were immuno-stained with antibodies against Arl13b, a marker of primary cilia, and Caveolin1 to label all SCs. Representative images of 72 hour and 96 hour-cultures show an increased number of primary cilia in SAG-treated cultures compared to control cultures (Fig 5.4 A-D). Quantification analysis shows a significant increase in the total number of SCs (caveolin^{+}) treated with SAG (mean= 80.43 cell) compared to control group (mean= 61.06 cell) at 72 hours, but not at 96 hours. Remarkably, there was a marked increase in the number of primary cilia in myofibres treated with SAG compared to control myofibres at 72 hours [mean= 19.38 primary cilia vs 10.94 primary cilia (control)] and 96 hours [mean= 35.51 primary cilia vs 15.86 primary cilia (control)]. As primary cilia were shown previously to selectively mark self-renewing SCs (Jaafar Marican et al., 2016), these observations confirm that up-regulating Shh signalling leads to an increase in cells committing to the self-renewal program and raise the interesting possibility that Shh signalling may influence cell fate choice by promoting primary cilium re-assembly.

Table 5.4 The number of primary cilia-harbouring SCs upon Shh stimulation *ex vivo.*

		Caveolin1+		Primary cilia (Arl13b)+		
Time (hours)	**Experimental Group**	**Mean value (cell)**	**S.E.M.**	**Mean value (cell)**	**S.E.M.**	**N**
72	Control	61.06	4.15	10.94	0.54	4
	SAG-Treated	80.43	4.10	19.38***	1.30	4
96	Control	72.63	9.58	15.86	0.94	4
	SAG-Treated	105.79	12.61	35.51***	2.63	4

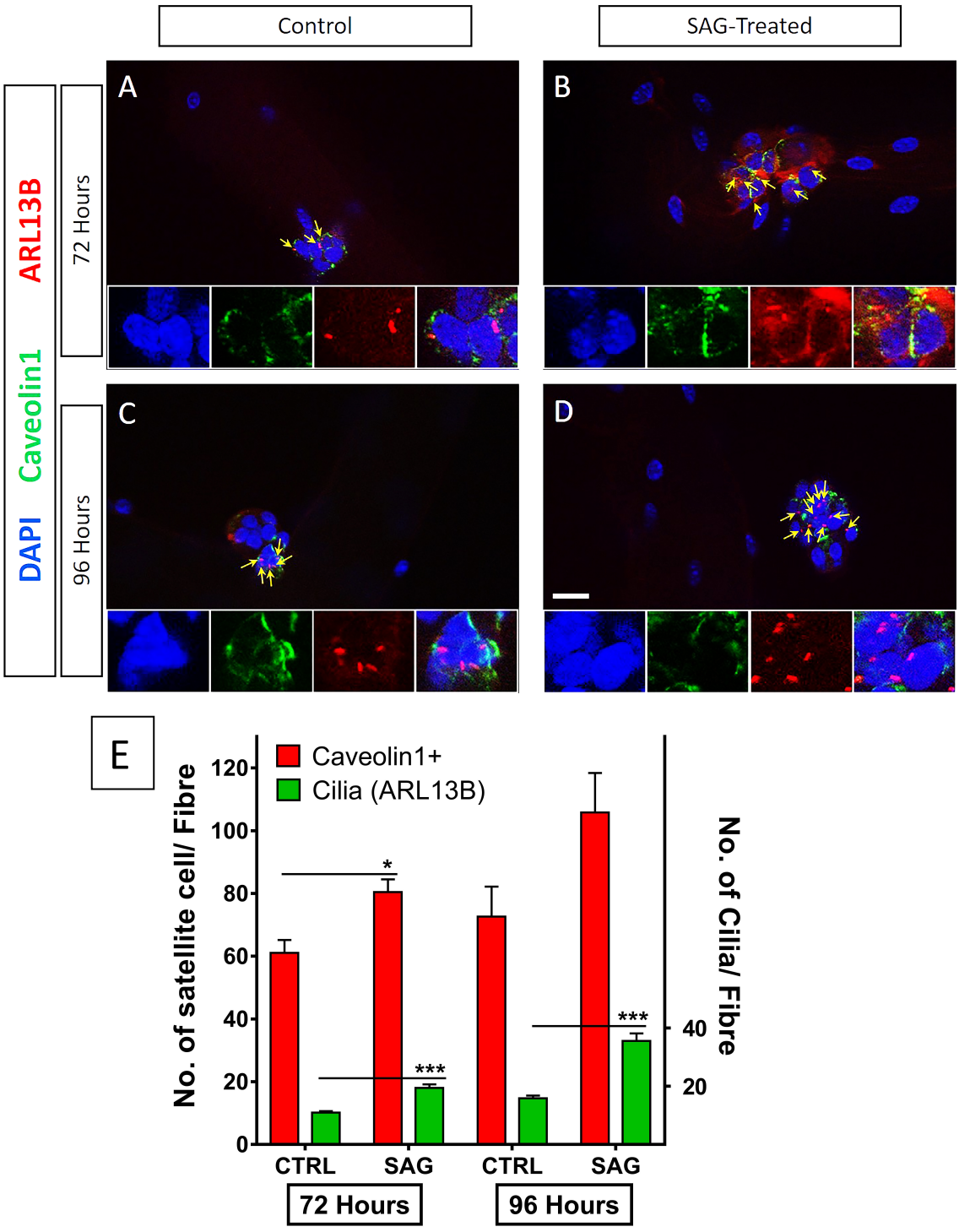

Figure 5.4: Upregulation of Shh signalling increases the number of primary cilia-associated SCs in *ex vivo* myofibre cultures.

(A-D) Representative images of C57BL/6 EDL myofibres cultured for 72 and 96 hours in the presence of DMSO (control) or SAG, and analysed by immunofluorescence using antibodies against Caveolin1 (green) and Arl13b (red) with nuclei counterstained with DAPI. Merged panels are shown on the right. Primary cilia are indicated with arrows. Scale bar is 20µM **(E)** Graph showing the quantification of the number of SCs expressing Caveolin1 (red) and the number of Arl13b^{+} primary cilia (green) per fibre cultured for 72 and 96 hours with DMSO (control) or with SAG. Data are based on 4 independent experiments with 43-64 myofibres analysed per condition per time point. ***P≤ 0.0005 and error bars are ±SEM

5.4 Discussion

In this chapter, I have shown that Shh upregulation causes an increase in self-renewing SCs using different approaches. Pax7 is the primary marker for quiescent SCs and a vital requirement in self-renewal as its expression is restricted to undifferentiated SC (Wen et al., 2012). Pax7 transcriptionally functions to downregulate MyoD and inhibit the expression of myogenin, which drives SCs differentiation during myogenesis (Olguin et al., 2007). Therefore, I used Pax7 as a marker of self-renewing SCs and MyoD or Myogenin as markers of differentiation. First, I found that there was an increase in the number of Pax7+ SCs but not myogenin+ cells at 72 hours when Shh signalling was up-regulated. However, there was no change in the proportion of Pax7+ SCs indicating that the increase in the number of Pax7+ cells (Fig 5.1) was due to a general increase in cell number (proliferative effect of Shh signalling) in the treated group without changes in the balance between self-renewing and differentiation. This result was not conclusive, because cells in myofibre cultures are not synchronised and SCs are known to have variation on the time taken to divide depending on their cell fate (Rocheteau et al., 2012). Therefore, I did a follow up experiment using MyoD, a differentiation marker that is expressed earlier than myogenin. Here, the self-renewing Pax7+ cells were segregated from the early differentiating SCs that express MyoD. Indeed, the proportion of self-renewing SCs was significantly increased at the expense of early differentiating MyoD+ SCs.

These findings were further validated by using a pharmacological agent Cytosine β-D-arabinofuranoside (AraC) that triggers cell death in cycling SCs by interfering with DNA synthesis (Reano et al., 2017). Therefore, any proliferating cell at the time of AraC treatment (60 hours) would undergo apoptosis, leaving intact SCs that have exited the cell cycle and are in either G0 reversible (quiescent) phase or G0 irreversible (differentiated) phase (reviewed in chapter 1, Fig 1.6). This experiment confirmed that Shh upregulation stimulates SCs self-renewal, as there was a 2-fold increase in the number of Pax7+ cells upon AraC treatment during myogenesis. Collectively, these observations demonstrate unequivocally that Shh upregulation leads to an increase in SC self-renewal.

Since self-renewing cells can emerge during adult myogenesis from symmetric or asymmetric cell division, one possibility is that Shh signalling may drive SC cell fate towards self-renewal by affecting cell division (Dumont et al., 2015a). If Shh signalling increases self-renewing SCs by promoting symmetric cell division, one would predict that no change in the number of myogenin+ cells but an increase in the number of Pax7+ cells would be observed. In contrast, an equal increase in the number of myogenin+ and Pax7+ cells would be expected if Shh signalling was controlling SC self-renewal by increasing asymmetric cell divisions. However, the marginal increase contributed by asymmetric cell division would potentially be masked in a large population of myogenin+ cells compared to the small population of Pax7+ self-renewing SC. Interestingly, I observed that Pax7+, but not Myogenin+ cells, increased upon SAG treatment (see Fig 5.3), suggesting that up-regulating Shh signalling could have affected symmetric cell divisions or asymmetric cell division. Although there are no evidence yet of Shh directly regulating SC self-renewal, Shh signalling has been associated with control of cell division in adult stem cells, embryonic stem cells and cancer stem cells (CSCs) (Ruiz i Altaba et al., 2002). In particular, Shh signalling was shown to increase self-renewal by shifting the mode of cell division from asymmetric to symmetric in granule neuronal progenitors (GNPs), which is the cell type implicated in the Shh-driven brain cancer medulloblastoma (Ferent et al., 2014; Tanno et al., 2017; Yang et al., 2015; Saade et al., 2017). As we know, deregulation of Shh signalling has also been implicated in skeletal muscle cancer rhabdomyosarcoma (Hahn et al., 1998). Therefore, it is a possible that similar regulatory mechanisms control symmetric and asymmetric cell division in neuronal progenitor cells and in satellite cells, and that upregulation of Shh signalling somehow impacts of the mode of cell division to promote symmetric cell division.

However, in the case of skeletal muscle, several studies have demonstrated that SCs preferentially perform asymmetric cell division to generate self-renewing SCs (Dumont et al., 2015c; Jaafar Marican et al., 2016; Kuang et al., 2007; Shinin et al., 2006). Therefore, there is also a possibility that Shh signalling promotes SCs self-renewal through asymmetric cell division. Logically, an effect on asymmetric cell division would result in an increase of both cell populations, the self-renewing SC population and the differentiating SC population. Because self-renewing SCs represent a much smaller

proportion of the entire SC progeny (approximately 5% in Fig 5.3 D) compared to differentiating SCs (approximately 40% in Fig 5.3 D), it is likely that any small increase in the number of self-renewing SCs would be more readily detected than a similar increase in differentiating cells, due to their larger number.

The mechanism by which Shh signalling could stimulate asymmetric cell division remains largely unknown. One possibility is that Shh signalling acts indirectly through another signalling pathway that controls asymmetric cell division in SCs such as Notch or Wnt signalling (Knoblich, 2008; Shinin et al., 2006). Cross-talk between Shh and Notch signalling have been reported previously (Yabut et al., 2015), although some evidence suggests that Shh signalling activates the Notch target gene *Hes1* independently of Notch ligand in mammalian stem cells (Ingram et al., 2008; Wall et al., 2009).

Shh signalling could also promote asymmetric cell division directly through an effect on one or several cell fate determinants, on proteins regulating spindle orientation or interaction with the niche (Chen et al., 2016). For example, in neural stem cells Shh inhibitory signalling through Gli3R controls the function of the cell fate determinant Numb, a protein, which is known to be expressed prior to differentiation and segregated asymmetrically during SC cell division (Shinin et al., 2006; Wang et al., 2014a). In addition, Numb also could suppress SC self-renewal via its function on Notch and Gli1 inhibitory function (Gulino et al., 2010). Thus, up-regulation of Shh signalling might be promoting SC asymmetric division through the processing of Gli3R into full-length Gli3A. However it has to be noted that while Gli3R in developing brain is driving stem cell differentiation, it supressed myogenic differentiation by repressing *Myf5* expression in developing somites, therefore suggesting a differential functions of Gli3R (McDermott et al., 2005; Wang et al., 2014a).

Finally, I carried out another experiment to visualise if the increase in SC self-renewal upon Shh stimulation was associated with the inheritance of primary cilia since Shh signalling mediates its signalling through primary cilia in vertebrates, and primary cilia mark self-renewing SC in adult muscles (Jaafar Marican et al., 2016; Rohatgi et al., 2007). Moreover, several ciliary proteins were identified to be functional during HH signalling transduction including the intraflagellar transport (IFT88) and Kinesin family member 7 (Kif7) (Davey et al., 2006; Liem et al., 2009; Liu et al., 2018). Indeed, primary

cilia and its associated mother centrosome are asymmetrically inherited by self-renewing cells during cell division (Jaafar Marican et al., 2016; Paridaen et al., 2013). Consistent with this, I observed a 2-fold increase in the number of primary cilia-expressing SCs at the end of myogenesis upon Shh upregulation. However, whether primary cilia are simply a readout for Shh signalling effect on SC self-renewal or whether Shh signalling takes a direct role in stimulating self-renewal through controlling cilia reassembly remains to be established. However, to date the function of Shh signalling in ciliogenesis remains unexplored. Nonetheless, inhibition of Hh signalling in human glioma cells resulted in the overexpression of microRNA-124 (miR-124) which is a translational inhibitor of Aurora kinase A (AURKA) (Xu et al., 2017). Aurora kinase A has a major function in primary cilia re-assembly (Liu et al., 2018), thus suggesting a possible novel function of Shh signalling in ciliogenesis to regulate the self-renewal program .

6 Up-regulation of Sonic hedgehog signalling promotes asymmetric cell division *ex vivo*.

6.1 Introduction

Stem cells are identified by their ability to simultaneously self-renew to replenish their own niche while giving rise to differentiated progenies. During muscle growth and regeneration, SCs fulfil this criterion by doing either symmetric or asymmetric cell division (reviewed in Fig 1.7, Chapter 1). Symmetric cell division is defined as the division that gives rise to two identical progenies while asymmetric cell division is the cell division that gives rise to two distinct cell fates. While symmetric cell division is adopted usually to generate transit-amplifying committed progenitor cells (MPCs), asymmetric cell division is performed to generate self-renewing SCs while giving rise to committed progenies. However, under extreme conditions such as dystrophies, SCs can undergo symmetric cell division to generate self-renewing SCs. Asymmetric cell division is regulated intrinsically by pluripotency regulators, cell fate determinants, cell polarity and mitotic spindle. While extrinsically it is regulated by the stem cell niche for example the basal lamina at the basal side of SCs (Etemadmoghadam et al., 1995; Gomez-Lopez et al., 2014; Guo and Kemphues, 1995; Januschke and Gonzalez, 2010; Rayagiri et al., 2018; Rhyu et al., 1994).

Our group reported previously that primary cilia are selectively re-assembled in self-renewing SCs (Jaafar Marican et al., 2016). This raises the interesting possibility that the re-assembly of primary cilia following cell cycle exit marks cells for self-renewal. Primary cilia present in quiescent SCs disassemble upon activation and entry into the cell cycle to allow centriole duplication during cell division (Jaafar Marican et al., 2016). Re-assembly following cell cycle exit initiates upon the recruitment of pre-ciliary vesicles to the mother centriole and the maturation of the mother centriole into a basal body (Kobayashi and Dynlacht, 2011). The subsequent fusion of pre-ciliary vesicles generates the ciliary vesicle and marks the initiation of axoneme formation and docking of the nascent primary cilium to the plasma membrane (Wang and Dynlacht, 2018). Consistent

with the primordial function of mother centrioles in cilia assembly, mother and daughter centrioles were reported to be unequally inherited during asymmetric cell division (Yamashita et al., 2007). Thus, monitoring the inheritance of mother centrioles may provide important clues of cell fate decision and primary cilia re-assembly in satellite cells.

In the previous chapter, I have shown using multiple approaches that up-regulation of Shh signalling increases SC self-renewal in the *ex vivo* myofibre culture system. This led me to ask whether Shh signalling increases SC self-renewal by altering the mode of cell division. As cell division is dictated by several factors, including cell polarity, mitotic spindle orientation, cell fate determinants and extrinsic cues from the niche, I have also investigated some of these factors to address this question.

6.1.1 Hypothesis and aim

Therefore, I hypothesized that Shh signalling promotes asymmetric cell division to generate self-renewing SCs during adult myogenesis. The aim of this chapter was to investigate the effect of Shh up-regulation on cell division orientation of SC in the *ex vivo* myofibre culture system.

6.2 Results

6.2.1 Stimulation of Shh signalling promotes cell division in the apico-basal orientation in early stage myogenesis.

In chapter 5, I showed that treatment with SAG to up-regulate Shh signalling resulted in an increase in SC self-renewal in late stage myogenesis. Although asymmetric cell division in apico-basal orientation is the preferred mode of division used by SCs to self-renew, they can also divide symmetrically in extreme environments, raising the possibility that Shh acts by promoting symmetric cell division. Therefore, using EDL myofibres isolated from C57BL/6 mice and cultured in the presence of SAG at 100nM to up-regulate Shh signalling or with the vehicle reagent DMSO as control, I studied the orientation of cell division and cell fate at 44 and 72 hours. The rationale for choosing 44 hours instead of the usual 48 hours as time point for this study is that SAG treatment induces proliferation and therefore by 48 hours, treated cultures contain clusters of cells instead of doublets normally observed in control condition. SCs were immunostained with antibodies against Pax7 and MyoD at 44 hours, and Pax7 and Myogenin at 72 hours to label differentiating SCs.

Planar oriented cell doublets (Fig 6.1 A-A') and apico-basal oriented cell doublets (Fig 6.1 B-B') could be identified at both 44 hours and 72 hours in the myofibre culture system. The doublets were categorised based on their orientation (plane) and cell fate marker expression as described in section 2.7 Chapter 2. Fig. 6.1A shows an example of symmetric planar cell division generating two differentiated daughter cells identified as myogenin-positive and Pax7-negative. Pax7 is a nuclear gene that should be localised in the nuclei and the green rings surrounding the SCs are artefacts caused by low-intensity signals. Fig. 6.1A' shows one example of symmetric planar cell division resulting in two stem daughter cells that are Pax7-positive and Myogenin-negative (presence of an artefact signal). Fig. 6.1B and 6.1B' present examples of apico-basal cell divisions either symmetric and generating two differentiated daughter cells (Fig. 6.1B) or asymmetric and generating one differentiated daughter cell and one stem daughter cell (Fig. 6.1B'). Quantification analysis of the data showed that at 44 hours there was an increase in the

percentage of apico-basal doublets with mean= 54.0% of doublets in SAG-treated myofibres compared to control with mean= 43.3% of doublets at the expense of planar doublets (mean= 46.0% of doublets in SAG treated compared to mean= 56.7% of doublets in control myofibres) (Fig 6.1 C). Despite a trend towards an increase in the number of apico-basal cell doublets at 72 hours in SAG-treated compared to control myofibres, the difference was not statistically significant (Fig 6.1 C).

However, there was no difference in the distribution of symmetric and asymmetric cell divisions in myofibres cultured for 44 hours and labelled with Pax7 and MyoD, and myofibres cultured for 72 hours and labelled with Pax7 and Myogenin. Indeed, I observed that the majority of SCs expressed both Pax7 and MyoD at 44 hours. This finding contrasts with my findings reported in the previous chapter (Fig 5.1-5.2) showing that SAG treatment causes an increase in the number of $Pax7^{+}$ self-renewing SCs in the presence of SAG. However, a major difference was that the data was collected from the total SC population, which was mainly of large cell clusters in SAG-treated cultures. Nonetheless, this study reveals that Shh up-regulation promotes cell division in an apico-basal orientation in the early phase of myogenesis.

Table 6.1 The percentage of Apico basal and Planar doublets upon Shh stimulation *ex vivo*

		Apico Basal		**Planar Doublets**		
Time (hours)	**Experimental Group**	**Mean value (%)**	**S.E.M.**	**Mean value (%)**	**S.E.M.**	**N**
44	Control	56.71	1.50	43.29	1.50	3
	SAG-Treated	46.02*	0.63	53.98*	0.63	3
72	Control	45.40	1.01	54.27	0.90	3
	SAG-Treated	39.42	2.92	60.58	2.92	3

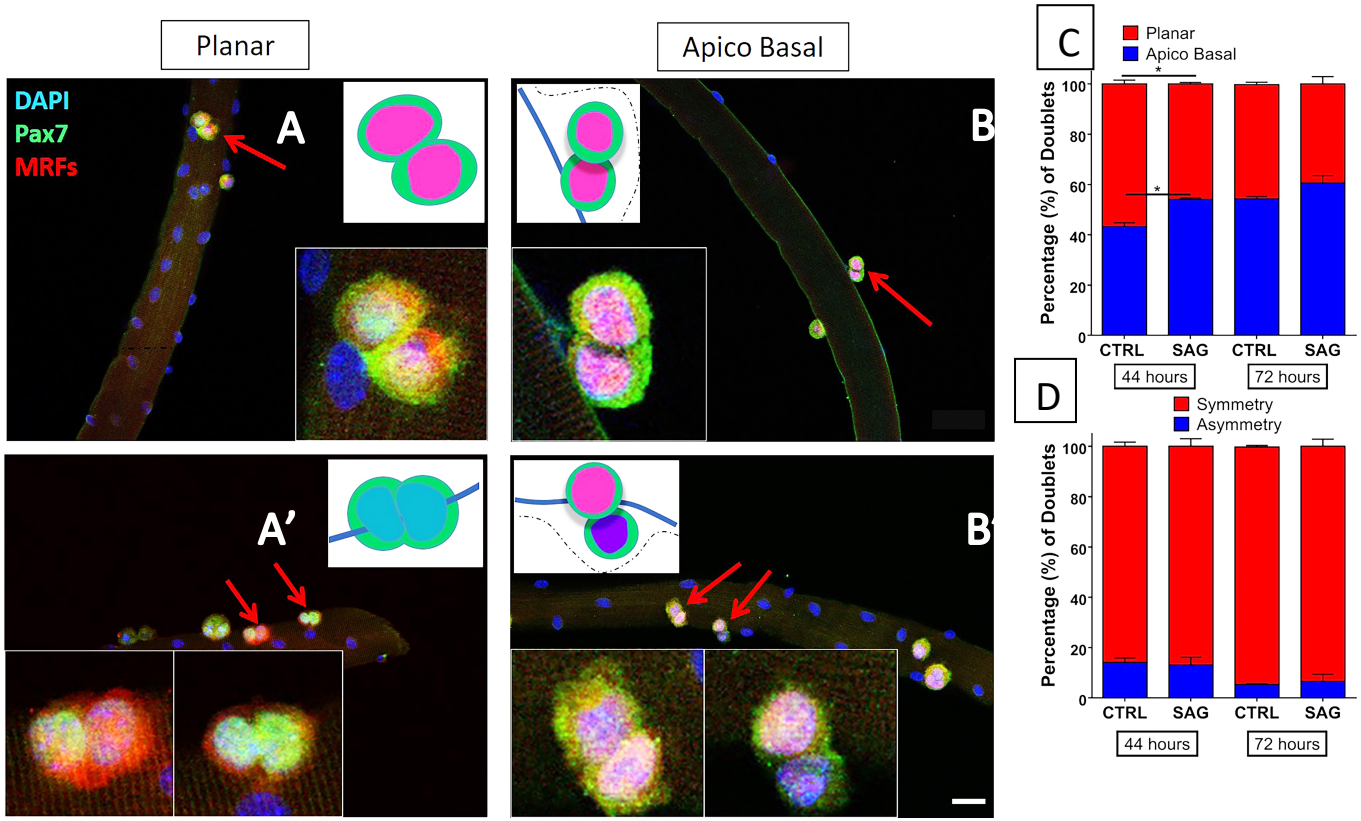

Figure 6.1: Shh upregulation increases apico-basal cell divisions *ex vivo*.
Representative images of planar cell divisions **(A-A')** and apico-basal cell divisions **(B-B')** in cultured myofibres analysed by immunofluorescence using antibodies against Pax7 (green) and MRFs (red) with nuclei counterstained with DAPI. Magnified areas are indicated by red arrows. Illustration of the doublets are shown with the images. Scale bar is 50µm **(C)** Quantification graph showing the percentage of SC doublets in planar or apico-basal orientation at 44 and 72 hours in DMSO (control) or SAG-treated myofibre cultures. **(D)** Percentage of SC doublets expressing either Pax7 or MRFs or Pax7 and MRFs symmetrically, (red bars) or Pax7 and MRFs asymmetrically (blue bars). Data are based on 3 independent experiments with 310-315 doublets analysed per condition. *P≤ 0.05, error bars are ±SEM

6.2.2 Shh signalling preferentially promotes asymmetrical distribution of centrosomal proteins during cell division in early stage myogenesis.

Data in Figure 6.1 suggest that Shh signalling affects the orientation of cell division during early myogenesis, without altering cell fate choice (MRFs). In the previous chapter (Fig 5.4), I have shown that the increase in SC self-renewal was associated with an increase in the number of primary cilia-harbouring SCs. Therefore, I investigated whether up-regulation of Shh signalling would affect mother centriole inheritance in SC doublets at early myogenesis. SCs were immunostained with antibodies against Pax7 (green) to label all SCs and Outer-Dense-Fibre2 (ODF2, red) to identify the mother centrosome. ODF2, also known as Cenexin1, is a protein of the subdistal appendages of the mother centriole (Ishikawa et al., 2005).

Representative images show different combinations of division plane and ODF2 inheritance in SC doublets at 44 hours (Fig. 6.2A-B'). SC doublets that inherited ODF2 protein asymmetrically in planar orientation are shown in panel A. Figure 6.2A' shows a symmetric distribution of ODF2 in planar cell division. Doublets in panel B illustrates an apico-basal cell division where the two daughter cells present an asymmetric distribution of ODF2 in only one daughter cell. Interestingly, the two daughter cells have different shapes with the ODF^{+} SC more elongated and the $ODF2^{-}$ SC more circular. Figure 6.2B' shows a cell doublet undergoing apico-basal cell division with a symmetric distribution of ODF2. Quantification of ODF2 distribution showed that SAG treatment increased the number and proportion of apico-basal cell divisions associated with an asymmetric distribution of mother centrioles with mean=8.34 doublets (22.5%) compared to control with mean= 4.2 doublets (11.6%) (Fig. 6.2 C,D). Notably, the overall increase apico-basal cell divisions recorded in SAG-treated cultures here (51.9% of apico basal doublets overall) mirrors the findings reported in Fig. 6.1C (56.7% apico-basal cell doublets in SAG-treated cultures). This increase was concomitant with a trend towards a decrease in symmetric planar cell divisions in SAG-treated cultures, although no significant difference was observed (p= 0.061). Thus, these data suggest that up-regulation of Shh signalling promotes SCs to divide asymmetrically in an apico-basal orientation to generate self-renewing SCs.

Table 6.2 The inheritance of ODF2-expressing mother centriole in SCs doublets at 44 hours upon Shh stimulation *ex vivo.*

	Planar symmetry		**Planar asymmetry**		**Apico Basal symmetry**		**Apico Basal asymmetry**		
Experimental Group	**Mean value (%)**	**S.E.M**	**Mean value (%)**	**S.E.M**	**Mean value (%)**	**S.E.M**	**Mean value (%)**	**S.E.M**	**N**
Control	44.60	4.69	12.70	2.17	31.14	3.67	11.57	2.67	6
SAG-Treated	34.09	1.31	13.96	2.71	29.44	3.22	22.51*	3.00	6

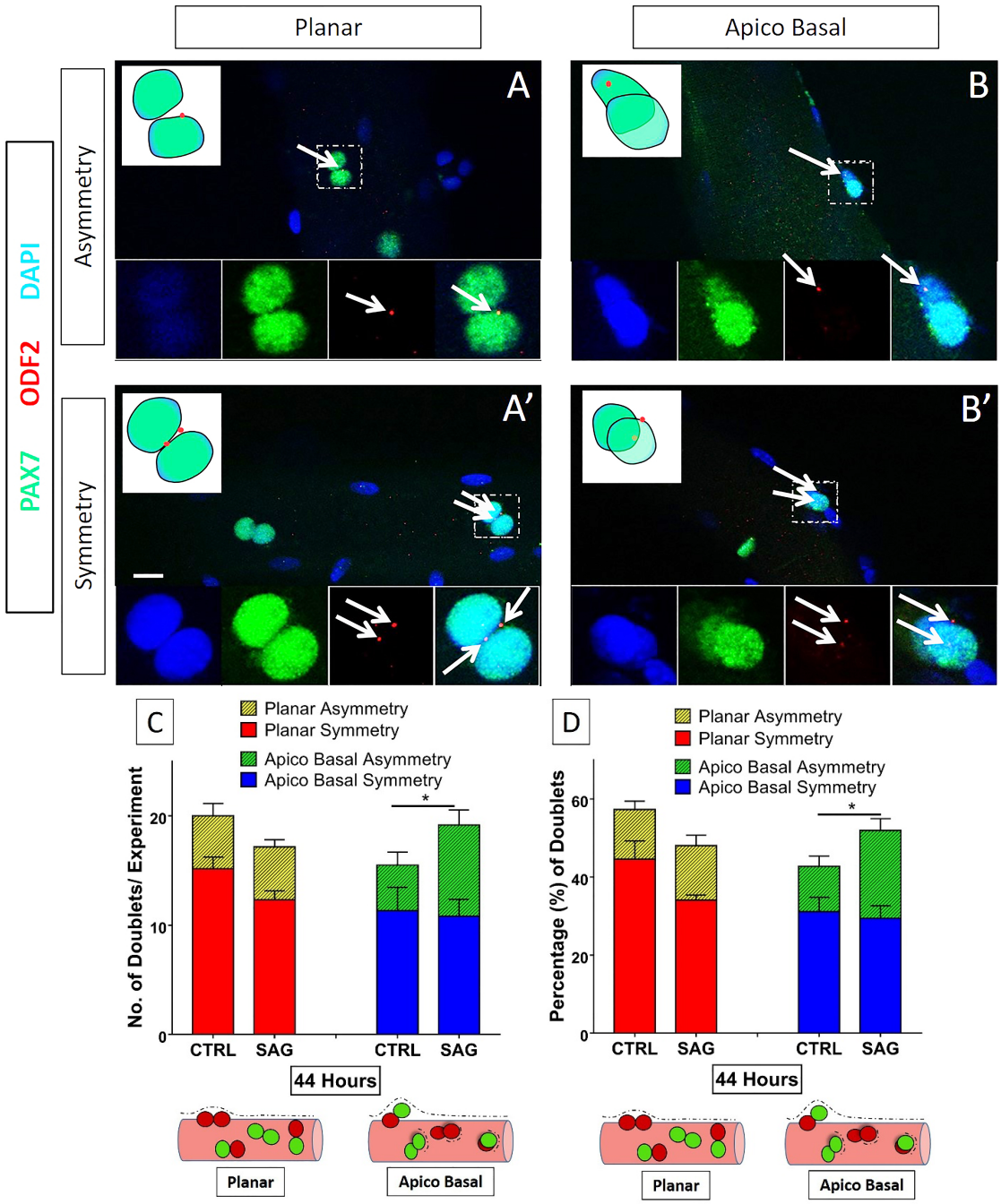

Figure 6.2: Shh upregulation increases the asymmetric inheritance of mother centrioles in apico-basal cell divisions *ex vivo*.

Representative images of asymmetric planar cell doublets **(A),** and symmetric planar cell doublets **(A')**, asymmetric apico-basal cell doublets **(B)** and symmetric apico-basal cell doublets **(B')** in myofibres cultured for 44 hours and analysed by immunofluorescence using antibodies against Pax7 (green) and ODF2 (red) with nuclei counterstained with DAPI. Illustration of the doublets are shown with the images. Magnified area are boxed and ODF2 expression is indicated by arrows. Scale bar is 10µM. **(C)** Quantification graph of the number of cell doublets dividing in planar or apico-basal orientation with asymmetric or symmetric distribution of ODF2 at 44 hours with DMSO (control) or SAG treatment. **(D)** Percentage of the SC doublets analysed in graph C. Data are based on 6 independent experiments with 357-375 doublets per condition. *P⩽ 0.05, error bars are ±SEM

Centrosomal protein CEP164 is another mother centriole protein localised in the distal appendages of mother centrioles, that is unequally distributed in asymmetric cell division. Furthermore, CEP164 (Yu et al., 2006) is involved also in centrosome migration and initiates primary cilia assembly upon mitosis (Cajanek and Nigg, 2014; Pitaval et al., 2017). Therefore, CEP164 is a relevant candidate protein to confirm my previous findings with ODF2. Fixed myofibres were immuno-stained with antibodies against CEP164 to label the mother centriole or basal body and Pax7 to label all SCs. Representative images show different combinations of division plane and CEP164 inheritance in SC doublets at 44 hours. Planar cell doublets with only one daughter cell expressing CEP164 (asymmetric doublet) are shown in panel 6.3A, and with both daughter cells expressing CEP164 (symmetric doublet) shown in panel 6.3A'. Apico-basal cell doublets with a single daughter cell inheriting CEP164 (asymmetric doublet) are shown in panel 6.3B and with equal inheritence of CEP164 (symmetric doublet) is shown in panel 6.3B'. Similar to the findings reported in Figure 6.2, daughter cells that inherited the mother centriole asymmetrically appear to be more elongated compared to daughter cells that did not inherit the mother centriole, which were more rounded.

Quantification analysis showed that there was a significant increase in the number and percentage of cell doublets with an asymmetric distribution of CEP164 either in planar cell divisions [mean=4.67 doublet (13.8%) compared to control myofibres with mean=1.00 doublet (3.5%)] or in apico-basal cell divisions [mean=8 doublet (23.5%) compared to control myofibres with mean= 3.33 doublet (10.8%)] in SAG-treated myofibres after 44 hours of culture (Fig 6.3 C-D). Interestingly, the recorded percentage of asymmetric inheritance of mother centrioles in apico-basal cell divisions using both ODF2 and CEP164 was very similar –22.5% of doublets with ODF2 versus 23.6% of doublets with CEP164 in SAG-treated myofibres culture and 11.6% of doublets (ODF2) versus 10.8% of doublets (CEP164) in control myofibre cultures. This similarity confirms the reliability of the markers. Taken together, these data confirm that up-regulation of Shh signalling has altered the balance of SCs cell division by increasing asymmetric cell division in apico-basal orientation to promote self-renewal in early myogenesis.

Table 6.3 The inheritance of CEP164-expressing mother centriole in SCs doublets at 44 hours upon Shh stimulation *ex vivo.*

	Planar symmetry		**Planar asymmetry**		**Apico Basal symmetry**		**Apico Basal asymmetry**		
Experimental Group	**Mean value (%)**	**S.E.M**	**Mean value (%)**	**S.E.M**	**Mean value (%)**	**S.E.M**	**Mean value (%)**	**S.E.M**	**N**
Control	57.71	4.09	3.45	1.99	28.03	3.69	10.82	0.47	3
SAG-Treated	44.10	2.97	13.8*	2.87	18.50	1.95	23.58***	0.80	3

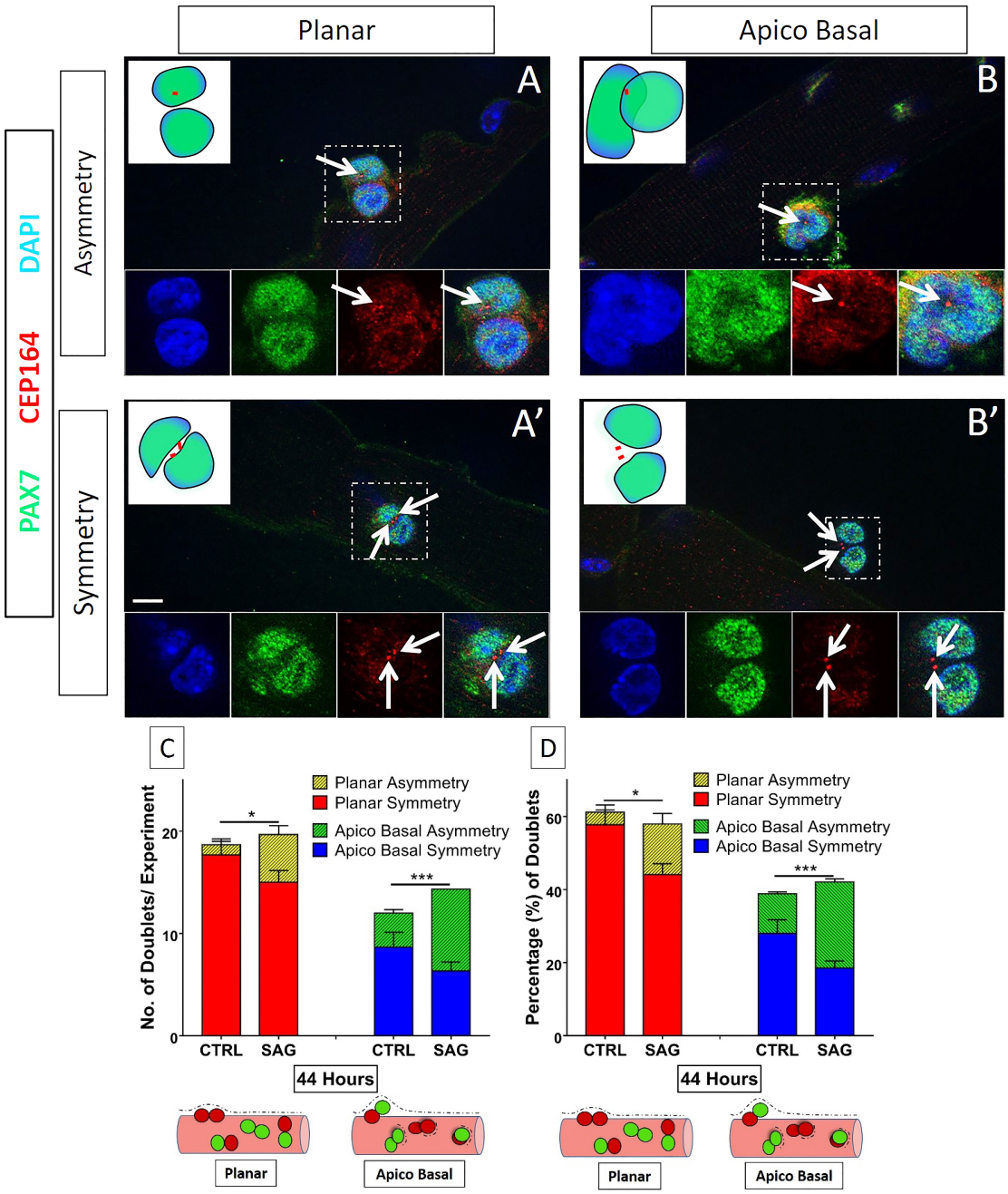

Figure 6.3: Up-regulation of Shh signalling increases the asymmetric distribution of CEP164 *ex vivo*.

Representative images of asymmetric planar cell doublets **(A),** symmetric planar cell doublets **(A')**, asymmetric apico-basal cell doublets **(B),** and symmetric apico-basal cell doublets **(B')** in cultured myofibres analysed by immunofluorescence using antibodies against Pax7 (green) and CEP164 (red) with nuclei counterstained with DAPI. Illustrations of the doublets are shown with the image. Magnified areas are boxed and CEP164 expression is indicated by arrows. Scale bar is 10µM. **(C)** Quantification graph of the number of doublets dividing asymmetrically or symmetrically in planar or apico-basal orientation at 44 hours with DMSO (control) or SAG treatment. **(D)** Percentage of SC doublets analysed in graph C. Data are based on 3 independent experiments with 166-171 doublets per condition. *P≤ 0.05, ***P≤ 0.0005 error bars are ± SEM

6.2.3 Shh signalling preferentially promotes asymmetric cell division in planar orientation in late stage myogenesis.

At the beginning of this chapter, I reported that there was no significant effect of SAG treatment on the orientation of cell division or cell fate choice at 72 hours when using Pax7 as a marker for SC self-renewal and myogenin as a marker for differentiation (Fig. 6.1). However, in chapter 5 I have shown that an overall increase in the number of self-renewing SCs in SAG-treated cultures in late stage myogenesis , and I noticed that most Pax7-expressing SCs were present in large clusters with ≥8 cells per cluster. Hence, I hypothesized that an increase in asymmetric cell divisions may have been missed at 72 hours due to the increased cell proliferation in the presence of SAG causing cells to be present in clusters and not in cell doublets, and the cell clusters not being considered in the cell division analysis. Therefore, I repeated the experiment but performing my assessment at an earlier time point at 66 hours.

Myofibres were fixed after 66 hours of culture and immune-stained with Pax7 to label self-renewing SCs and myogenin to label differentiating SCs. The representative images and the schematic diagram in Figure 6.4A show the different combinations of cell fate that were identified in the myofibre cultures after 66 hours. Cell doublets were recorded as symmetric if both daughter cells were self-renewing and expressed Pax7 only (green), or differentiating and expressed myogenin only (red) or in early differentiation and expressed both Pax7 and myogenin (yellow). In contrast, cell doublets were recorded as asymmetric if one of the daughter cell was self-renewing and expressing only Pax7 while the other daughter cell was expressing either myogenin only or expressing both Pax7 and myogenin, since Pax7 will be down regulated when Myogenin is expressed. As observed in the representative images, the majority of cell doublets identified in the control group were differentiating planar symmetric doublets, while in the SAG-treated myofibres, asymmetric cell doublets in planar plane were frequently identified (Fig 6.4B, C).

The quantification showed that there was a significant increase in the number and percentage of asymmetric cell doublets undergoing planar cell division in myofibres treated with SAG with mean=10 doublet (11.9%) compared to myofibres in control

group mean=3 doublet (4.07%) (Fig 6.4D,E). The increase was at the expense of a significant decrease in the percentage of symmetric cell doublets undergoing planar cell division in SAG-treated myofibres with mean=52.4% of doublets compared to control myofibres with mean= 71.7% of doublets (Fig 6.4 E). Interestingly, SAG treatment also resulted in an increase in the number of symmetric cell doublets that divided in an apico-basal orientation with mean= 23.7% of doublets compared to control myofibres with mean= 13.7% of doublets (Fig 6.4 E).

Surprisingly, SCs were responding to SAG treatment differently in late myogenesis compared to early myogenesis. While in the early stage of myogenesis Shh upregulation induced SCs to divide asymmetrically in both planar and apico-basal orientations, at a later stage in addition to inducing asymmetric cell divisions in a planar orientation, it promoted also symmetric cell divisions in an apico-basal orientation. In this experiment, I have not recorded the fate of the symmetric doublets, but grouping all together the three different types of symmetric doublets categorised in figure 6.4 A. This was because majority of the symmetric doublets were either differentiating double positive doublets (yellow) or differentiated doublets (red). However, because I have not formally recorded it during the experiement, there is a possibility that the treatment affected differentiation or self-renewal via symmetric division but was neglected. Nonetheless, this study showed that up-regulation of Shh signalling drives SCs to divide asymmetrically in a planar orientation to generate self-renewing SCs.

Table 6.4 The expression of Pax7 and Myogenin in SCs doublets at 66 hours upon Shh stimulation *ex vivo*.

	Planar symmetry	**Planar asymmetry**	**Apico Basal symmetry**	**Apico Basal asymmetry**	
Experim	**Mean S.E.M**	**Mean value (%) S.E.M**	**Mean value (%) S.E.M**	**Mean S.E.M**	**N**

entalGroup	**lue(%)**					**lue(%)**		
Control	71.68	2.89	4.08	0.31	18.39	3.21	5.86	0.43	3
SAG-Treated	52.39**	0.90	11.91***	0.07	28.26	3.19	7.44	1.19	3

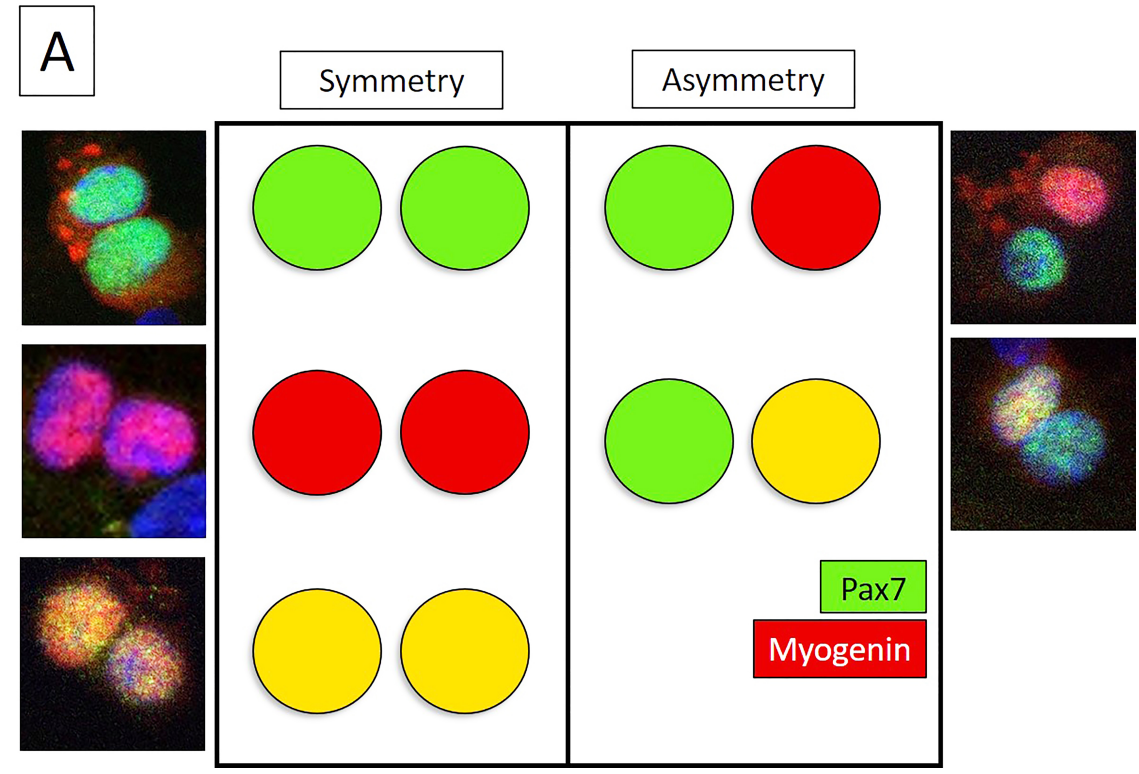
A
Symmetry
Asymmetry
Pax7
Myogenin

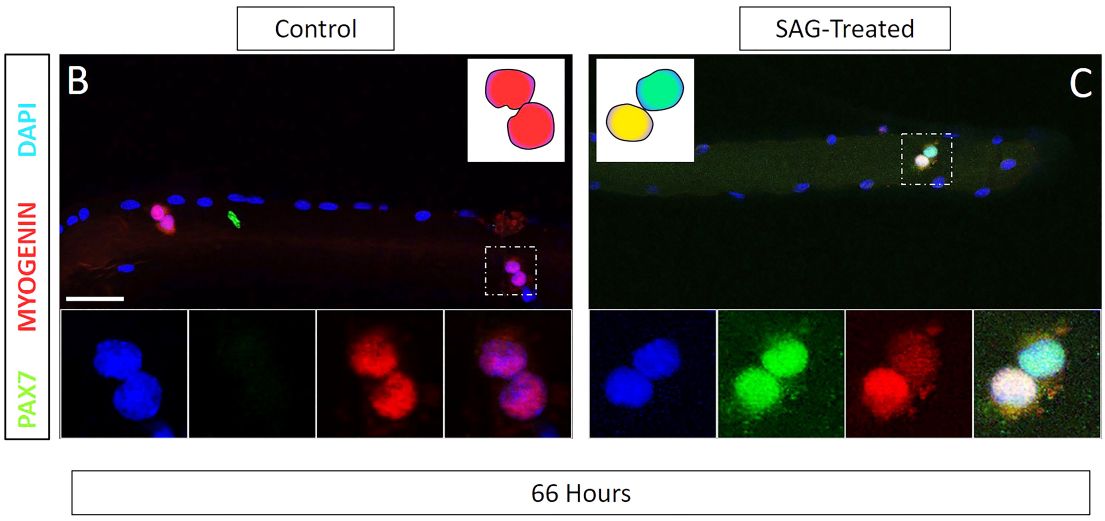
Control
SAG-Treated
B
C
DAPI
MYOGENIN
PAX7
66 Hours

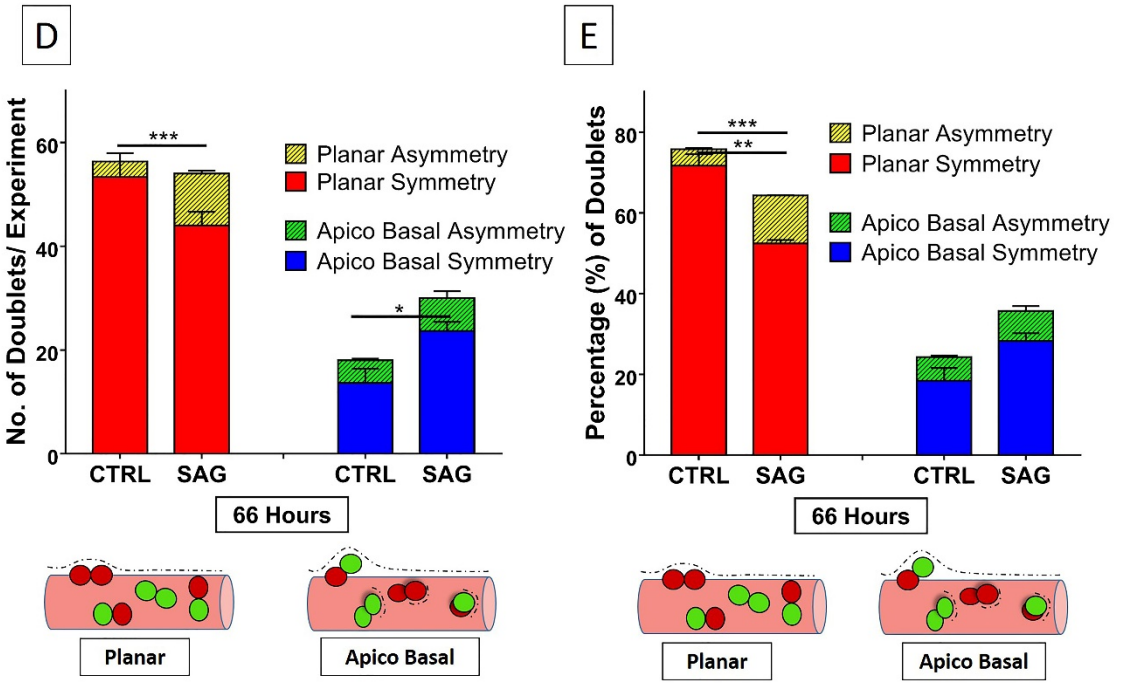

Figure 6.4: Up-regulation of Shh signalling increased asymmetric cell division in planar orientation *ex vivo*.

Schematic illustration and example images of different combinations for symmetric and asymmetric cell doublets analysed by immunofluorescence using antibodies against Pax7 (green) and Myogenin (red) with nuclei counterstained with DAPI **(A)**. Representative images of myofibres cultured for 66 hours in the presence of DMSO (control) **(B)** or SAG **(C)** and analysed with the antibodies mentioned in the schematic illustration in A. Magnified areas are indicated by boxes and simplified illustrations are shown with the images. Scale bar is 20µM **(D)** Quantification graph of the number of asymmetric or symmetric cell doublets in planar or apico-basal orientation at 66 hours in DMSO (control) or SAG-treated cultures. **(E)** Percentage of SC doublets analysed in graph D. Data are based on 3 independent experiments with 223-252 doublets analysed per condition. *P⩽ 0.05, error bars are ±SEM

6.3 Discussion

In this chapter, I have revealed using dual labeling of Pax7 and MRFs, and of mother centriole markers that up-regulation of Shh signaling increased SC self-renewal by promoting asymmetric cell division. While during early stage myogenesis Shh signalling drives asymmetric cell division in an apico-basal plane, during late stage myogenesis it increased asymmetric cell division in a planar orientation. Intracellular mechanisms of asymmetric stem cell division associated with the differential distribution of intracellular determinants have been studied extensively in *Drosophila* neuroblasts (Yu et al., 2006). One of the determinants that has emerged in recent years as a critical factor of asymmetric cell division is the distribution of the mother and daughter centrosomes. In *Drosophila* neuroblast and female germ stem cells, the daughter centrosome is preferentially inherited whereas in male germ stem cells it is the mother centrosome that is preferentially inherited (Salzmann 2014, Yamashita 2007, Januschke 2011). Knowing that the mother centrosome confers the ability to nucleate microtubules for the assembly of mitotic spindles, it is clear that the differential inheritance of centrosome will impact on the orientation of cell division. Moreover, as centrosomes are also asymmetrically inherited and confer that ability to re-assemble a primary cilium, which is essential for Shh signalling, it has been proposed in the mammalian central nervous system that asymmetric centrosome inheritance would expose cells to differential levels of Shh signalling, favoring stem cell cell fate determination (Anderson 2009, Paridaen 2013). However, the converse relationship whereby Shh signalling somehow drives asymmetric inheritance of internal determinant and stem cell fate choice has not been considered so far.

However, work on granule neuron progenitor cells (GNPs) showed that Shh signalling proliferative response required growth-associated protein 43 (GAP-43) and was mediated through PKC phosphorylation (Shen et al., 2008). Interestingly, GAP-43 associates with and positions centrosomes, thereby regulating mitotic spindle orientation during cell division hence polarizing GNPs in an apico-basal position (Mishra et al., 2008; Zhao et al., 2011). GAP-43 regulates also cell polarity via its interaction with polarity proteins Cdc42, Par6 and IQGAP1 (Gupta et al., 2010). Interestingly, Par

complex-mediated polarity also is conserved in SCs and mediates their asymmetric cell division during myogenesis (Troy et al., 2012). Importantly, Cdc42, a Rho GTPase family protein with crucial role during primary ciliogenesis, was shown to be up-regulated by Shh signaling in mouse embryonic stem cells through activation of β1-Integrin expression (Oh et al., 2018). Cdc42 interacts with an exocyst-associated protein Sec10 in zebrafish retinal cells and in renal tubular epithelial cells, and controls connecting cilia and primary cilia formation, respectively (Choi et al., 2015; Elias et al., 2015; Zuo et al., 2011). This multi-dimensional fuction of Cdc42 in establishing cell polarity and regulating ciliogenesis in a GAP-43-dependent manner may be the undiscovered bridge between Shh and asymmetric cell division.

In recent work by the Sayer's lab has reported a more direct regulatory function for Shh signaling on primary cilia (Srivastava et al., 2017). They showed that treatment with the Shh agonist purmophamine was able to reduce the length of abnormally long primary cilia in human urine-derived renal epithelial cells (HURECs) transfected with an siRNA targetting *CEP290* to mimic Joubert Syndrome (JBTS). Up-regulated Shh signalling reduced ciliary length by reducing the expression of *CDK5* (Srivastava et al., 2017). The effect was possibly transduced through Cdk5-Cyclin E complex formation (Miyajima et al., 1995) since *Cyclin E* in *Drosophila* is one of the transcriptional target of Shh pathway (Duman-Scheel et al., 2002a). However, the effects on CDK5 and primary cilia were not accompanied by an up-regulation in GLI1 expresion, thus suggesting that the non-canonical Shh pathway might be involved (Srivastava et al., 2017).

Shh signalling functions also in a combinatorial manner with other signalling pathways in regulating cell division, in particular with the Wnt and Notch signalling pathways. Notably, both Shh and Wnt signalling pathways are mediated through the primary cilium in vertebrates, and function as regulators for tissue patterning and growth during embryogenesis and are implicated in tumorigenesis (Singh et al., 2012). However, the nature and effects of the interactions between Shh and Wnt signaling are highly tissue-dependent. For instance, while in neuronal progenitor cells Shh signalling acts upstream of Wnt signalling in promoting cell cycle progression through G1 (Alvarez-Medina et al., 2009), activation of Shh signalling is crucial to downregulate Wnt signalling and promote self-renewal in cancer cell lines (Ma et al., 2015). Similarly, inhibition of

WNT signalling in SHH-dependent medulloblastoma is necessary to combat reccurence, suggesting an effect on self-renewal (Rodriguez-Blanco et al., 2017). Therefore, although direct evidence of Shh function in regulating asymmetric cell division in stem cells through the control of centrosome positioning is still lacking, it remains possible that Shh acts indirectly by controling Wnt signalling, which has been shown to regulate centrosome and mitotic spindle orientation during neurogenesis (Bielen and Houart, 2014; Habib et al., 2013). In SCs, balance between canonical and non-canonical Wnt signalling controls symmetric cell division and differentiation. Indeed, while Wnt7a has been reported to control self-renewal through planar cell polarity pathway and symmetric cell division (Bentzinger et al., 2013b; Le Grand et al., 2009), levels of β-catenin and APC have been shown to control cell cycle progression and differentiation (murphy 2014, Parisi 2015, Rudolph 2016). As the balance between canonical and non-canonical Wnt signaling operates at the level of primary cilia, at least in some tissues(), it remains possible that Shh signalling might be regulating asymmetric cell division indirectly by modulating primary cilia function and consequently Wnt signalling.

Asymmetric cell division in SCs is also regulated by Notch signalling, which controls both SC quiescence and self-renewal (Conboy and Rando, 2002; Jiang et al., 2014; Mourikis et al., 2012a). SCs seggregate Notch signalling components asymmetrically to generate self-renewing SCs expressing Notch1 and Notch3 receptors while commited MPCs express Numb, a Notch signalling antagonist (Conboy and Rando, 2002). Numb asymmetric segregation is conserved in different stem cells including in the nervous system (Knoblich, 2008; Shen et al., 2002). Theoretically, up-regulation of Shh signalling in self-renewing daughter cell promotes asymmetric distribution of Numb protein in the differentiating daughter cell to increase in asymmetric cell division, since Shh repressor protein Gli3R is required to maintain Numb expression (Wang et al., 2014b). Interestingly, Numb is known to directly regulate Hedgehog signalling by targeting the downstream pathway component Gli1 for Itch-dependent ubiquitination and degradation, which inhibits Shh response (Di Marcotullio et al., 2006). Therefore, it is possible that an interplay between between Notch (Numb) and Shh signalling causes the increase in asymmetric cell division I observed. It would be interesting to elucidate further the mechanisms by which Shh signalling drives asymmetric cell division in SCs.

7 Final Discussion

7.1 Thesis Summary

In this thesis, I investigated the effects of up-regulation of Shh signalling on satellite cell activity and adult myogenesis. I hypothesised that increasing Shh signalling in satellite cells would affect their behaviour during myogenesis and might play a role in tumour formation or promote tumour expansion in skeletal muscles. Taking advantage of *in vivo* and *ex vivo* models to study satellite cell behaviour, I have shown that the activation of Shh signalling in satellite cells via *Ptch1* gene inactivation *in vivo* or through Smoothened agonist (SAG) treatment *ex vivo* in myofibre cultures resulted in greater satellite cell proliferation during the expansion phase of myogenesis (Fig 7.1). Upregulation of Shh signalling in satellite cells also accelerated the entrance into cell cycle and their progression through the cell cycle. Further investigations revealed that the activation of Shh signalling, promoted also satellite cell self-renewal at a later stage of myogenesis (Fig 7.1). Through examining satellite cell division in cell doublets and evaluating cell fate choice, I found that Shh signalling controls asymmetric cell division in satellite cells (Fig 7.1). In combination, the impact on accelerated cell cycle progression and asymmetric cell division caused a long- term deficit in satellite cell differentiation (Fig 7.1). Together, these observations have allowed me to propose a model for the regulation of satellite cell asymmetric division to generate self-renewing satellite cells by Shh signalling (Fig. 7.1). From these studies, I conclude that Shh signalling plays an important role in the production of transit-amplifying cells and self-renewing stem cells through its coordinated control of cell division (asymmetric versus symmetric) and temporal control of the expansion phase. The significance of these findings is important, because deregulation and abnormally elevated levels of Shh signalling will affect satellite cell proliferation and self-renewal and could result in the formation or contribute to the maintenance and progression of muscle tumours.

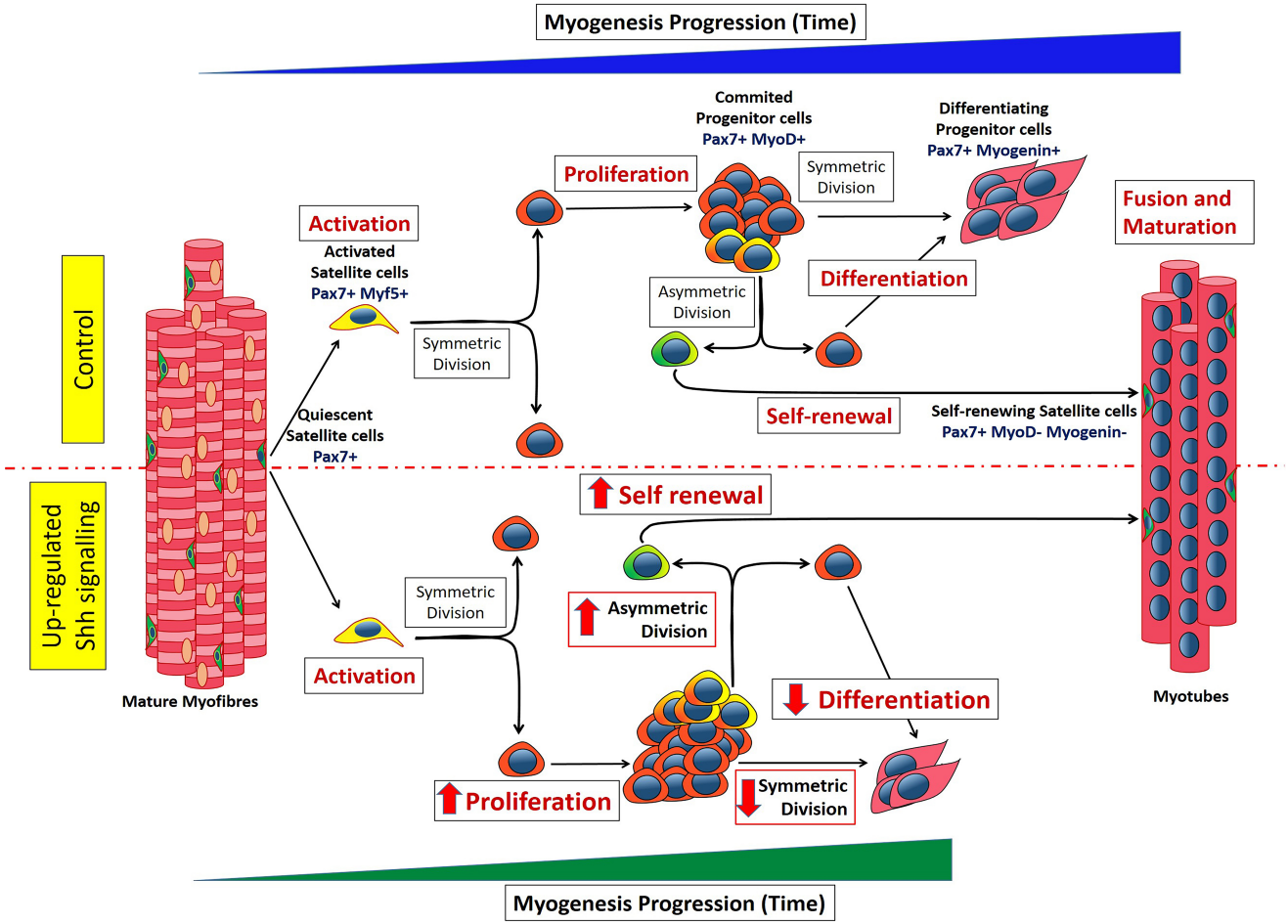

Figure 7.1: Proposed model illustrating how up-regulated Shh signalling impacts adult myogenesis.

Up-regulation of Shh signalling either exogenously via treatment with the pathway agonist smoothened agonist (SAG) or endogenously through *Ptch1* gene inactivation stimulated the proliferation of progenitor cells during muscle regeneration. Concomitantly, up-regulated Shh signalling promoted satellite cell self-renewal by driving asymmetric cell division. Increased asymmetric cell division is at the expense of symmetric division, which resulted in reduced differentiating progenitors. Accelerated myogenesis progression also affected long-term myogenic differentiation.

7.2 Shh signalling promotes satellite cell proliferation

The work I reported in this thesis identified a significant role for Shh signalling in the control of satellite cell proliferation and the expansion of muscle progenitor cells. Although several studies have previously suggested that stimulating Shh signalling has a pro-proliferative effect on myoblasts *in vitro* (Elia et al., 2007; Koleva et al., 2005b), this is the first study to test directly the effect of Shh signalling on adult satellite cells maintained in their native microenvironment and to demonstrate that the pro-proliferative effect of Shh signalling is a cell-autonomous process. Previous studies in the lab have shown that quiescent satellite cells were not responsive to Shh signalling, and that Shh response was initiated upon activation (Cruz Migoni, 2015).

Further loss-of-function approaches revealed that Shh signalling is required for the activation of SCs and their progression through S-phase of the cell cycle (Cruz Migoni, 2015). Here using gain-of-function approaches, I have confirmed this observation since I observed an accelerated entry and progression through the cell cycle when satellite cells were treated with SAG and in the Ptch1^{cKO} mice. An important question to address is the molecular mechanism by which Shh signalling controls SC activation and cell cycle progression. Shh is known to signal cells via a canonical Gli-dependent pathway and also via a non-canonical ERK-dependent pathway, both of which diverge downstream of Smo (Brechbiel et al., 2014). Previous studies by Elia et al. 2005 have suggested that Shh signalling promoted myoblast proliferation via the non-canonical Hedgehog signalling pathway, which operates through MAPK/ERK signalling (Elia et al., 2007; Jones et al., 2001b). The approaches I used to up-regulate Hedgehog signalling interfered with Ptc or Smo activity, and therefore do not allow me to distinguish between the canonical or non-canonical pathway. However, the previous work carried out in the lab that shared my conclusions used GANT61, an inhibitor of Gli activity (Cruz Migoni, 2015). This suggests that Shh signalling acts partially at least through the canonical pathway to control cell cycle progression. To uncover the molecular players acting downstream of Ptc and Smo, a gene-wide transcriptome analysis is currently under way in the lab, and should reveal potential target genes that control the cell cycle. Some crucial cell cycle regulators has been identified in other stem cell systems including *N-myc, CyclinD1,*

Cyclin D2, Cyclin E1 and *pRB* (Colvin Wanshura et al., 2011; Duman-Scheel et al., 2002a; Li et al., 2010; Oliver et al., 2003; Wang et al., 2005).

Sonic hedgehog also promotes indirectly satellite cell activation and proliferation by inducing another potent mitogen, IGF-1 (Straface et al., 2009b; Piccioni et al., 2014a). IGF-1 inhibits cyclin inhibitor cdk1b and stimulate the activity of CyclinE-Cdk2 via phosphathydilinositol 3-kinase/Akt (PI3K/Akt) pathway to induce satellite cell activation (Chakravarthy et al., 2000). The induction of IGF-1 signalling by hedgehog is a generic response rather than a muscle-specific response since it has been also observed in neuron progenitors and in osteoblasts (Rao et al., 2004; Shi et al., 2015). Both Myf5 and MyoD are the myogenic regulatory factors expressed upon satellite cell activation to induce their proliferation (Cooper et al., 1999). Together, these data confirms that Shh signalling has a distinct role in satellite cell activation and its progression through the cell cycle to expand the size of progenitor cell population during myogenesis.

7.3 Shh signalling activation deregulated myogenic differentiation program

Moreover, work on embryonic myogenesis and on myogenic cells have also shown that both *Myf5* and *MyoD* genes contain sequences for Gli-binding site (GBS) (Anderson et al., 2012; Voronova et al., 2013). However, an in vivo study using $HSA^{CreERT2}$;$Gli3^{Flox/Flox}$ to conditionally delete Gli3 in skeletal muscle discovered that the loss in Gli3 impaired myogenesis and Gli3 regulates the expression of Myf5 (Renault et al., 2013c). This finding is contradictory to the literature when we consider Gli3 as a Shh signalling repressor, but Gli3 could also be present in the cells in their activator form (full length) and therefore its uncertain whether it's the activation or inhibitition of the pathway that causes the impairment (Cruz-Migoni and Borycki, 2014; Renault et al., 2013c). Nonetheless, Gli3 deletion was shown to be pro-proliferative in that study that agrees with my findings (Renault et al., 2013c). Moreover, loss of Ptch1 that potentially up-regulated Shh signalling similar to the impact of deleting Gli3 also disrupted differentiation leading to myogenesis. Together, these data suggest an inhibitory effect

on satellite cell differentiation and adds to the paradigm of tumorigenesis whereby cells remain undifferentiated.

7.4 Shh signalling promotes self-renewal by regulating asymmetric cell division

In this thesis I reported for the first time the role of Shh signalling in regulating satellite cell self-renewal. This is an important mechanism by which Hedgehog signalling regulates stemness, and may constitute a generic mode of action of Hedgehog signalling. Indeed, Hedgehog signalling popular morphogen activity during embryonic development that dictates progenitor cell fate decision makes it a good candidate for controlling stemness (Arsic et al., 2007). In other stem cells, Shh signalling functions to maintain stemness (self-renewal) (Palma et al., 2005; Petrova and Joyner, 2014). For example in granule neuron precursor (GNP) cells, upregulation of Shh signalling increased the stem cell pool in the cerebellum by stimulating symmetric cell divisions and conversely blocking Shh signalling promoted asymmetric cell divisions as the expense of symmetric cell divisions (Yang et al., 2015). However, another recent study has reported that blocking Shh signalling in P9 mouse cerebellum randomised the orientation of cell division leading to fewer apico-basal asymmetric cell divisions, suggesting that Shh signalling has an active role in determining the orientation of cell divisions (Miyashita et al., 2017). Irrespective of the interpretation of the data, these two studies highlight that Shh signalling regulates the orientation of the cell division during mitosis and any perturbation in the signalling pathway disrupt the balance between planar and apico-basal cell divisions with consequences on cell fate decision (Miyashita et al., 2017; Yang et al., 2015). In this thesis, satellite cell self-renewal observed upon stimulation of Shh signalling is associated with a shift of division mode towards asymmetric cell division. In addition, increase in self-renewal was accompanied with an increase in primary cilia-harbouring satellite cells. Primary cilia and their associated centrioles are one of the determinants for asymmetric cell division (Borovina et al., 2010; Paridaen et al., 2013). Traditionally, the primary cilium is considered as a signalling centre where Shh signalling pathway components are either activated or inactivated, therefore influencing the read-out of the signalling pathway. However, my

results suggest another level of control whereby Shh signalling would regulate cilia assembly or maintenance, or disassembly. Consistent with this possibility, Shh signalling was recently found to regulate a centrosomal docking protein called pericentrin, which is known to recruit PKA for Gli protein processing (Saade et al., 2017). Pericentrin is an important component of the centrosome and primary cilia, and pericentrin deregulated expression has been linked to disruption of the mitotic spindle assembly, which causes dwarfism and cancer (Delaval and Doxsey, 2010).

More work is required to explore this novel area of Hedgehog function to further understand stem cell biology. More analysis on Par proteins and polarity genes would add more information to the cell division analysis done in this thesis. Interesting state-of-the-art techniques such as live imaging would also be useful in visualising the actual events that occur during cell division on cultured myofibres. In this thesis, the effect on satellite cell self-renewal was the result of an increase in asymmetric cell division, but the mechanistic regulation behind this observation has not yet been explored. Therefore, molecular studies on the Shh signalling transduction and their cross-talk with other pathways such as Wnt and Notch signalling if relevant, would be interesting.

7.5 Implications in pathologies and cancers.

The function of primary cilia and ciliary proteins as mechanosensors and as a signalling hub is not restricted to Hedgehog signalling only, but implicates other pathways including Wnt, Notch, and PDGF signalling (Liu et al., 2018). Given the importance of primary cilia in hedgehog signalling and other signalling pathways, it is therefore not surprising that defects in primary cilia assembly and deregulated expression of primary cilia components have been linked to more than 35 diseases collectively grouped as ciliopathies (Wang and Dynlacht, 2018). Ciliopathies present with in a wide-spectrum of abnormalities in many organs, including retinal degeneration, brain malformation, facial deformities, renal anomalies, liver fibrosis, central obesity, skeletal dysplasias and myotonias (Reiter and Leroux, 2017). Within the mentioned spectrum, mutations in Megf10 and Talpid3 are really interesting as they cause a

muscular phenotype (Boyden et al., 2012; Logan et al., 2011). Megf10 is expressed in satellite cells and loss-of-function causes premature differentiation and a decline in the number of self-renewing cells (Holterman et al., 2007). Conversely, overexpression of Megf10 in myoblasts inhibits myogenic differentiation and fusion leading to hyperplasia (Holterman et al., 2007). Talpid3, another protein involved in ciliogenesis and the transduction of Shh signalling, has also been investigated in satellite cells. Similar to Megf10, loss-of-function mutation in *Talpid3* results in defects in adult myogenic differentiation and defective self-renewal of satellite cells (Blackwell, 2017). Together with my own findings, these data provide compelling evidence that Shh signalling, acting through the primary cilium, controls muscle regeneration and satellite cell activity by regulating cell fate choice through the control of cell division.

Hedgehog signalling and primary cilia have both been implicated in the pathobiology of skeletal muscle tumours particularly embryonal Rhabdomyosarcoma (RMS) (Liu et al., 2016). Moreover, Shh signalling is a key regulator of cancer stem cells (CSCs) in many type of tumours including pancreatic, oesophageal, colorectal, medulloblastoma and RMS (Skoda et al., 2018). CSCs are self-propagating malignant cells that are capable of initiating tumour formation because of their stem cell-like properties and their ability to self-renew (Heiden et al., 2014). Consistent with the role of hedgehog signalling in CSCs and the role of primary cilia in hedgehog signalling, aberrant activation of hedgehog signalling caused by deregulated ciliogenesis promotes RMS pathogenesis (Fu et al., 2014). Thus, acting on the hedgehog pathway through hedgehog pathway inhibitors impairs SCS self-renewal through down-regulating *Nanog,* and limits CSCs activity in RMS models (*in vivo*) (Nitzki et al., 2011). Likewise, small peptides or agents that interfere with ciliogenesis such as ADP ribosylation factor-like GTPase 6 (Arl6) have beneficial effects on the growth of RMS cells (Liu et al., 2016). Together, these reports indicate that my findings on the role of Shh signalling in muscle stem cell self-renewal are likely to be relevant to understanding the pathobiology of rhabdomyosarcomas and muscle-associated pathologies in ciliopathies.

The data presented in this thesis highlighted the function of Shh signalling in regulating satellite cell proliferation and self-renewal. However, the study requires analyses of the tumour samples that arises from the $Ptch1^{cKO}$ or $Ptch1^{\Delta/+}$ to confirm the

implication of the mutation in RMS formation. The analyses would include histological studies and tumour markers analysis. The data on self-renewal effects *in vivo* could also be extended by doing the repeated injury analysis to challenge the replenishment of satellite cell pool over multiple rounds of injury.

7.6 Conclusion

Although there have been discrepancies in the reported functions of Shh signalling in skeletal muscles, treatment with plasmid delivering Shh ligand and Shh recombinant protein have been shown to be beneficial in improving muscle repair (Piccioni et al., 2014a; Piccioni et al., 2014b). Previous work from the lab demonstrated that inhibition of Shh signalling delayed muscle regeneration and prevented the progression of satellite cells through the cell cycle (Cruz Migoni, 2015). Here, my results support these findings by demonstrating that aberrant activation of Hedgehog signalling promotes satellite cell proliferation. Interestingly, I have also discovered that Shh signalling regulates satellite cell self-renewal through an effect on asymmetric cell division. Additional work is required to further our in-depth understanding of the role of Shh signalling in adult skeletal muscle stem cells and to establish a correlation with cancer pathogenesis. This, in turn, would shed some light on new-targeted strategies to combat this incurable disease.

References

Albini, S., Coutinho Toto, P., Dall'Agnese, A., Malecova, B., Cenciarelli, C., Felsani, A., Caruso, M., Bultman, S. J. & Puri, P. L. 2015. Brahma is required for cell cycle arrest and late muscle gene expression during skeletal myogenesis. *EMBO Rep,* 16(8)**,** pp 1037-50.

Alcedo, J., Ayzenzon, M., Von Ohlen, T., Noll, M. & Hooper, J. E. 1996. The Drosophila smoothened gene encodes a seven-pass membrane protein, a putative receptor for the hedgehog signal. *Cell,* 86(2)**,** pp 221-32.

Alexandre, C., Jacinto, A. & Ingham, P. W. 1996. Transcriptional activation of hedgehog target genes in Drosophila is mediated directly by the cubitus interruptus protein, a member of the GLI family of zinc finger DNA-binding proteins. *Genes Dev,* 10(16)**,** pp 2003-13.

Alfaro, A. C., Roberts, B., Kwong, L., Bijlsma, M. F. & Roelink, H. 2014. Ptch2 mediates the Shh response in Ptch1-/- cells. *Development,* 141(17)**,** pp 3331-9.

Allen, R. E., Sheehan, S. M., Taylor, R. G., Kendall, T. L. & Rice, G. M. 1995. Hepatocyte growth factor activates quiescent skeletal muscle satellite cells in vitro. *J Cell Physiol,* 165(2)**,** pp 307-12.

Alman, B. A. 2015. The role of hedgehog signalling in skeletal health and disease. *Nat Rev Rheumatol,* 11(9)**,** pp 552-60.

Almeida, C. F., Fernandes, S. A., Ribeiro Junior, A. F., Keith Okamoto, O. & Vainzof, M. 2016. Muscle Satellite Cells: Exploring the Basic Biology to Rule Them. *Stem Cells Int,* 2016(1078686).

Alvarez-Medina, R., Le Dreau, G., Ros, M. & Marti, E. 2009. Hedgehog activation is required upstream of Wnt signalling to control neural progenitor proliferation. *Development,* 136(19)**,** pp 3301-3309.

Amano, K., Densmore, M. J. & Lanske, B. 2015. Conditional Deletion of Indian Hedgehog in Limb Mesenchyme Results in Complete Loss of Growth Plate Formation but Allows Mature Osteoblast Differentiation. *J Bone Miner Res,* 30(12)**,** pp 2262-72.

Anderson, C., Thorsteinsdottir, S. & Borycki, A. G. 2009. Sonic hedgehog-dependent synthesis of laminin alpha1 controls basement membrane assembly in the myotome. *Development,* 136(20)**,** pp 3495-504.

Anderson, C., Williams, V. C., Moyon, B., Daubas, P., Tajbakhsh, S., Buckingham, M. E., Shiroishi, T., Hughes, S. M. & Borycki, A. G. 2012. Sonic hedgehog acts cell-autonomously on muscle precursor cells to generate limb muscle diversity. *Genes Dev,* 26(18)**,** pp 2103-17.

Anderson, C. T. & Stearns, T. 2009. Centriole age underlies asynchronous primary cilium growth in mammalian cells. *Curr Biol,* 19(17)**,** pp 1498-502.

Andrade, B. M., Baldanza, M. R., Ribeiro, K. C., Porto, A., Pecanha, R., Fortes, F. S., Zapata-Sudo, G., Campos-de-Carvalho, A. C., Goldenberg, R. C. & Werneck-de-Castro, J. P. 2015. Bone marrow mesenchymal cells improve muscle function in a skeletal muscle re-injury model. *PLoS One,* 10(6)**,** pp e0127561.

Antoniou, A., Mastroyiannopoulos, N. P., Uney, J. B. & Phylactou, L. A. 2014. miR-186 inhibits muscle cell differentiation through myogenin regulation. *J Biol Chem,* 289(7)**,** pp 3923-35.

Arensdorf, A. M., Marada, S. & Ogden, S. K. 2016. Smoothened Regulation: A Tale of Two Signals. *Trends Pharmacol Sci,* 37(1)**,** pp 62-72.

Argiles, J. M., Campos, N., Lopez-Pedrosa, J. M., Rueda, R. & Rodriguez-Manas, L. 2016. Skeletal Muscle Regulates Metabolism via Interorgan Crosstalk: Roles in Health and Disease. *J Am Med Dir Assoc,* 17(9)**,** pp 789-96.

Arnold, L., Henry, A., Poron, F., Baba-Amer, Y., van Rooijen, N., Plonquet, A., Gherardi, R. K. & Chazaud, B. 2007. Inflammatory monocytes recruited after skeletal muscle injury switch into antiinflammatory macrophages to support myogenesis. *J Exp Med,* 204(5)**,** pp 1057-69.

Arrighi, N., Lypovetska, K., Moratal, C., Giorgetti-Peraldi, S., Dechesne, C. A., Dani, C. & Peraldi, P. 2017. The primary cilium is necessary for the differentiation and the maintenance of human adipose progenitors into myofibroblasts. *Scientific Reports,* *7*(1), p.15248

Arsic, D., Beasley, S. W. & Sullivan, M. J. 2007. Switched-on Sonic hedgehog: a gene whose activity extends beyond fetal development--to oncogenesis. *J Paediatr Child Health,* 43(6)**,** pp 421-3.

Asakura, A. 2012. Skeletal Muscle-derived Hematopoietic Stem Cells: Muscular Dystrophy Therapy by Bone Marrow Transplantation. *J Stem Cell Res Ther,* Suppl 11(

Asakura, A., Seale, P., Girgis-Gabardo, A. & Rudnicki, M. A. 2002. Myogenic specification of side population cells in skeletal muscle. *J Cell Biol,* 159(1)**,** pp 123-34.

Au, Y. 2004. The muscle ultrastructure: a structural perspective of the sarcomere. *Cell Mol Life Sci,* 61(24)**,** pp 3016-33.

Aza-Blanc, P. & Kornberg, T. B. 1999. Ci: a complex transducer of the hedgehog signal. *Trends Genet,* 15(11)**,** pp 458-62.

Aza-Blanc, P., Lin, H. Y., Ruiz i Altaba, A. & Kornberg, T. B. 2000. Expression of the vertebrate Gli proteins in Drosophila reveals a distribution of activator and repressor activities. *Development,* 127(19)**,** pp 4293-301.

Beauchamp, J. R., Heslop, L., Yu, D. S., Tajbakhsh, S., Kelly, R. G., Wernig, A., Buckingham, M. E., Partridge, T. A. & Zammit, P. S. 2000. Expression of CD34 and Myf5 defines the majority of quiescent adult skeletal muscle satellite cells. *J Cell Biol,* 151(6)**,** pp 1221-34.

Bendris, N., Lemmers, B., Blanchard, J. M. & Arsic, N. 2011. Cyclin A2 mutagenesis analysis: a new insight into CDK activation and cellular localization requirements. *PLoS One,* 6(7)**,** pp e22879.

Bentzinger, C. F., Wang, Y. X., Dumont, N. A. & Rudnicki, M. A. 2013a. Cellular dynamics in the muscle satellite cell niche. *EMBO Rep,* 14(12)**,** pp 1062-72.

Bentzinger, C. F., Wang, Y. X., von Maltzahn, J., Soleimani, V. D., Yin, H. & Rudnicki, M. A. 2013b. Fibronectin regulates Wnt7a signaling and satellite cell expansion. *Cell Stem Cell,* 12(1)**,** pp 75-87.

Bi, P., McAnally, J. R., Shelton, J. M., Sanchez-Ortiz, E., Bassel-Duby, R. & Olson, E. N. 2018. Fusogenic micropeptide Myomixer is essential for satellite cell fusion and muscle regeneration. *Proc Natl Acad Sci U S A,* 115(15)**,** pp 3864-3869.

Bielen, H. & Houart, C. 2014. The Wnt Cries Many: Wnt Regulation of Neurogenesis Through Tissue Patterning, Proliferation, and Asymmetric Cell Division. *Developmental Neurobiology,* 74(8)**,** pp 772-780.

Bischoff, R. 1975. Regeneration of single skeletal muscle fibers in vitro. *Anat Rec,* 182(2)**,** pp 215-35.

Bischoff, R. 1986. Proliferation of muscle satellite cells on intact myofibers in culture. *Dev Biol,* 115(1)**,** pp 129-39.

Bischoff, R. 1990a. Cell cycle commitment of rat muscle satellite cells. *J Cell Biol,* 111(1)**,** pp 201-7.

Bischoff, R. 1990b. Interaction between satellite cells and skeletal muscle fibers. *Development,* 109(4)**,** pp 943-52.

Bischoff, R. & Heintz, C. 1994. Enhancement of skeletal muscle regeneration. *Dev Dyn,* 201(1)**,** pp 41-54.

Bitgood, M. J., Shen, L. & McMahon, A. P. 1996. Sertoli cell signaling by Desert hedgehog regulates the male germline. *Curr Biol,* 6(3)**,** pp 298-304.

Bjornson, C. R., Cheung, T. H., Liu, L., Tripathi, P. V., Steeper, K. M. & Rando, T. A. 2012. Notch signaling is necessary to maintain quiescence in adult muscle stem cells. *Stem Cells,* 30(2)**,** pp 232-42.

Blackwell, D. 2017. *The role of Talpid3 in skeletal muscle satellite cells and skeletal muscle regeneration.* online, University of East Anglia.

Blanc, R. S., Vogel, G., Chen, T., Crist, C. & Richard, S. 2016. PRMT7 Preserves Satellite Cell Regenerative Capacity. *Cell Rep,* 14(6)**,** pp 1528-1539.

Blum, J. M., Ano, L., Li, Z., Van Mater, D., Bennett, B. D., Sachdeva, M., Lagutina, I., Zhang, M., Mito, J. K., Dodd, L. G., Cardona, D. M., Dodd, R. D., Williams, N., Ma, Y., Lepper, C., Linardic, C. M., Mukherjee, S., Grosveld, G. C., Fan, C. M. & Kirsch, D. G. 2013. Distinct and overlapping sarcoma subtypes initiated from muscle stem and progenitor cells. *Cell Rep,* 5(4)**,** pp 933-40.

Borello, U., Berarducci, B., Murphy, P., Bajard, L., Buffa, V., Piccolo, S., Buckingham, M. & Cossu, G. 2006. The Wnt/beta-catenin pathway regulates Gli-mediated Myf5 expression during somitogenesis. *Development,* 133(18)**,** pp 3723-32.

Borovina, A., Superina, S., Voskas, D. & Ciruna, B. 2010. Vangl2 directs the posterior tilting and asymmetric localization of motile primary cilia. *Nat Cell Biol,* 12(4)**,** pp 407-12.

Borycki, A. G. 2013. The myotomal basement membrane: insight into laminin-111 function and its control by Sonic hedgehog signaling. *Cell Adh Migr,* 7(1)**,** pp 72-81.

Borycki, A. G., Brunk, B., Tajbakhsh, S., Buckingham, M., Chiang, C. & Emerson, C. P., Jr. 1999. Sonic hedgehog controls epaxial muscle determination through Myf5 activation. *Development,* 126(18)**,** pp 4053-63.

Borycki, A. G., Mendham, L. & Emerson, C. P., Jr. 1998. Control of somite patterning by Sonic hedgehog and its downstream signal response genes. *Development,* 125(4)**,** pp 777-90.

Bosurgi, L., Corna, G., Vezzoli, M., Touvier, T., Cossu, G., Manfredi, A. A., Brunelli, S. & Rovere-Querini, P. 2012. Transplanted mesoangioblasts require macrophage IL-10 for survival in a mouse model of muscle injury. *J Immunol,* 188(12)**,** pp 6267-77.

Bouvier, J. & Cheng, J. G. 2009. Recombineering-based procedure for creating Cre/loxP conditional knockouts in the mouse. *Curr Protoc Mol Biol,* Chapter 23(Unit 23 13.

Boyden, S. E., Mahoney, L. J., Kawahara, G., Myers, J. A., Mitsuhashi, S., Estrella, E. A., Duncan, A. R., Dey, F., DeChene, E. T., Blasko-Goehringer, J. M., Bonnemann, C. G., Darras, B. T., Mendell, J. R., Lidov, H. G., Nishino, I., Beggs, A. H., Kunkel, L. M. & Kang, P. B. 2012. Mutations in the satellite cell gene MEGF10 cause a recessive congenital myopathy with minicores. *Neurogenetics,* 13(2)**,** pp 115-24.

Brack, A. S., Conboy, I. M., Conboy, M. J., Shen, J. & Rando, T. A. 2008. A temporal switch from notch to Wnt signaling in muscle stem cells is necessary for normal adult myogenesis. *Cell Stem Cell,* 2(1)**,** pp 50-9.

Brechbiel, J., Miller-Moslin, K. & Adjei, A. A. 2014. Crosstalk between hedgehog and other signaling pathways as a basis for combination therapies in cancer. *Cancer Treatment Reviews,* 40(6)**,** pp 750-759.

Briscoe, J. 2009. Making a grade: Sonic Hedgehog signalling and the control of neural cell fate. *EMBO J,* 28(5)**,** pp 457-65.

Buckingham, M. 2001. Skeletal muscle formation in vertebrates. *Curr Opin Genet Dev,* 11(4)**,** pp 440-8.

Buglino, J. A. & Resh, M. D. 2008. Hhat is a palmitoylacyltransferase with specificity for N-palmitoylation of Sonic Hedgehog. *J Biol Chem,* 283(32)**,** pp 22076-88.

Buller, N. V. J. A., Rosekrans, S. L. & van den Brink, G. R. 2012. Self-renewal and Differentiation of Intestinal Stem Cells: Role of Hedgehog Pathway. *Stem Cells and Cancer Stem Cells: Therapeutic Applications in Disease and Injury,* 2(95-102).

Buono, R., Vantaggiato, C., Pisa, V., Azzoni, E., Bassi, M. T., Brunelli, S., Sciorati, C. & Clementi, E. 2012. Nitric oxide sustains long-term skeletal muscle regeneration by regulating fate of satellite cells via signaling pathways requiring Vangl2 and cyclic GMP. *Stem Cells,* 30(2)**,** pp 197-209.

Burkhart, D. L. & Sage, J. 2008. Cellular mechanisms of tumour suppression by the retinoblastoma gene. *Nat Rev Cancer,* 8(9)**,** pp 671-82.

Cajanek, L. & Nigg, E. A. 2014. Cep164 triggers ciliogenesis by recruiting Tau tubulin kinase 2 to the mother centriole. *Proc Natl Acad Sci U S A,* 111(28)**,** pp E2841-50.

Capetanaki, Y., Bloch, R. J., Kouloumenta, A., Mavroidis, M. & Psarras, S. 2007. Muscle intermediate filaments and their links to membranes and membranous organelles. *Exp Cell Res,* 313(10)**,** pp 2063-76.

Carmeli, E., Moas, M., Reznick, A. Z. & Coleman, R. 2004. Matrix metalloproteinases and skeletal muscle: a brief review. *Muscle Nerve,* 29(2)**,** pp 191-7.

Chakkalakal, J. V., Christensen, J., Xiang, W., Tierney, M. T., Boscolo, F. S., Sacco, A. & Brack, A. S. 2014. Early forming label-retaining muscle stem cells require p27kip1 for maintenance of the primitive state. *Development,* 141(8)**,** pp 1649-59.

Chakkalakal, J. V., Jones, K. M., Basson, M. A. & Brack, A. S. 2012. The aged niche disrupts muscle stem cell quiescence. *Nature,* 490(7420)**,** pp 355-60.

Chakravarthy, M. V., Abraha, T. W., Schwartz, R. J., Fiorotto, M. L. & Booth, F. W. 2000. Insulin-like growth factor-I extends in vitro replicative life span of skeletal muscle satellite cells by enhancing G1/S cell cycle progression via the activation of phosphatidylinositol 3'-kinase/Akt signaling pathway. *J Biol Chem,* 275(46)**,** pp 35942-52.

Chal, J. & Pourquie, O. 2017. Making muscle: skeletal myogenesis in vivo and in vitro. *Development,* 144(12)**,** pp 2104-2122.

Charge, S. B. & Rudnicki, M. A. 2004. Cellular and molecular regulation of muscle regeneration. *Physiol Rev,* 84(1)**,** pp 209-38.

Chazaud, B. 2014. Macrophages: supportive cells for tissue repair and regeneration. *Immunobiology,* 219(3)**,** pp 172-8.

Chen, C., Fingerhut, J. M. & Yamashita, Y. M. 2016. The ins(ide) and outs(ide) of asymmetric stem cell division. *Curr Opin Cell Biol,* 43(1-6.

Chen, J. F., Tao, Y., Li, J., Deng, Z., Yan, Z., Xiao, X. & Wang, D. Z. 2010a. microRNA-1 and microRNA-206 regulate skeletal muscle satellite cell proliferation and differentiation by repressing Pax7. *J Cell Biol,* 190(5)**,** pp 867-79.

Chen, J. K., Taipale, J., Young, K. E., Maiti, T. & Beachy, P. A. 2002. Small molecule modulation of Smoothened activity. *Proc Natl Acad Sci U S A,* 99(22)**,** pp 14071-6.

Chen, Y., Cardinaux, J. R., Goodman, R. H. & Smolik, S. M. 1999. Mutants of cubitus interruptus that are independent of PKA regulation are independent of hedgehog signaling. *Development,* 126(16)**,** pp 3607-16.

Chen, Y., Li, S., Tong, C., Zhao, Y., Wang, B., Liu, Y., Jia, J. & Jiang, J. 2010b. G protein-coupled receptor kinase 2 promotes high-level Hedgehog signaling by regulating the active state of Smo through kinase-dependent and kinase-independent mechanisms in Drosophila. *Genes Dev,* 24(18)**,** pp 2054-67.

Cheng, L., Alvares, L. E., Ahmed, M. U., El-Hanfy, A. S. & Dietrich, S. 2004. The epaxial-hypaxial subdivision of the avian somite. *Dev Biol,* 274(2)**,** pp 348-69.

Cheng, W., Wang, L., Yang, B., Zhang, R., Yao, C., He, L., Liu, Z., Du, P., Hammache, K., Wen, J., Li, H., Xu, Q. & Hua, Z. 2014. Self-renewal and differentiation of muscle satellite cells are regulated by the Fas-associated death domain. *J Biol Chem,* 289(8)**,** pp 5040-50.

Cheung, T. H. & Rando, T. A. 2013. Molecular regulation of stem cell quiescence. *Nat Rev Mol Cell Biol,* 14(6)**,** pp 329-40.

Chiang, C., Litingtung, Y., Lee, E., Young, K. E., Corden, J. L., Westphal, H. & Beachy, P. A. 1996. Cyclopia and defective axial patterning in mice lacking Sonic hedgehog gene function. *Nature,* 383(6599)**,** pp 407-13.

Choi, S. Y., Baek, J. I., Zuo, X., Kim, S. H., Dunaief, J. L. & Lipschutz, J. H. 2015. Cdc42 and sec10 Are Required for Normal Retinal Development in Zebrafish. *Invest Ophthalmol Vis Sci,* 56(5)**,** pp 3361-70.

Choudhry, Z., Rikani, A. A., Choudhry, A. M., Tariq, S., Zakaria, F., Asghar, M. W., Sarfraz, M. K., Haider, K., Shafiq, A. A. & Mobassarah, N. J. 2014. Sonic hedgehog signalling pathway: a complex network. *Ann Neurosci,* 21(1)**,** pp 28-31.

Christov, C., Chretien, F., Abou-Khalil, R., Bassez, G., Vallet, G., Authier, F. J., Bassaglia, Y., Shinin, V., Tajbakhsh, S., Chazaud, B. & Gherardi, R. K. 2007. Muscle satellite cells and endothelial cells: close neighbors and privileged partners. *Mol Biol Cell,* 18(4)**,** pp 1397-409.

Cifuentesdiaz, C., Nicolet, M., Goudou, D., Rieger, F. & Mege, R. M. 1993. N-Cadherin and N-Cam-Mediated Adhesion in Development and Regeneration of Skeletal-Muscle. *Neuromuscular Disorders,* 3(5-6)**,** pp 361-365.

Clevers, H., Loh, K. M. & Nusse, R. 2014. Stem cell signaling. An integral program for tissue renewal and regeneration: Wnt signaling and stem cell control. *Science,* 346(6205)**,** pp 1248012.

Collins, C. A., Olsen, I., Zammit, P. S., Heslop, L., Petrie, A., Partridge, T. A. & Morgan, J. E. 2005. Stem cell function, self-renewal, and behavioral heterogeneity of cells from the adult muscle satellite cell niche. *Cell,* 122(2)**,** pp 289-301.

Collins, C. A. & Partridge, T. A. 2005. Self-renewal of the adult skeletal muscle satellite cell. *Cell Cycle,* 4(10)**,** pp 1338-41.

Colnot, C., de la Fuente, L., Huang, S., Hu, D., Lu, C., St-Jacques, B. & Helms, J. A. 2005. Indian hedgehog synchronizes skeletal angiogenesis and perichondrial maturation with cartilage development. *Development,* 132(5)**,** pp 1057-67.

Colvin Wanshura, L. E., Galvin, K. E., Ye, H., Fernandez-Zapico, M. E. & Wetmore, C. 2011. Sequential activation of Snail1 and N-Myc modulates sonic hedgehog-induced transformation of neural cells. *Cancer Res,* 71(15)**,** pp 5336-45.

Conboy, I. M. & Rando, T. A. 2002. The regulation of Notch signaling controls satellite cell activation and cell fate determination in postnatal myogenesis. *Dev Cell,* 3(3)**,** pp 397-409.

Contreras, O., Rebolledo, D. L., Oyarzun, J. E., Olguin, H. C. & Brandan, E. 2016. Connective tissue cells expressing fibro/adipogenic progenitor markers increase under chronic damage: relevance in fibroblast-myofibroblast differentiation and skeletal muscle fibrosis. *Cell Tissue Res,* 364(3)**,** pp 647-60.

Cooper, R. N., Tajbakhsh, S., Mouly, V., Cossu, G., Buckingham, M. & Butler-Browne, G. S. 1999. In vivo satellite cell activation via Myf5 and MyoD in regenerating mouse skeletal muscle. *J Cell Sci,* 112 (Pt 17)(2895-901).

Corbit, K. C., Aanstad, P., Singla, V., Norman, A. R., Stainier, D. Y. & Reiter, J. F. 2005. Vertebrate Smoothened functions at the primary cilium. *Nature,* 437(7061)**,** pp 1018-21.

Cornelison, D. D., Olwin, B. B., Rudnicki, M. A. & Wold, B. J. 2000. MyoD(-/-) satellite cells in single-fiber culture are differentiation defective and MRF4 deficient. *Dev Biol,* 224(2)**,** pp 122-37.

Cornelison, D. D. & Wold, B. J. 1997. Single-cell analysis of regulatory gene expression in quiescent and activated mouse skeletal muscle satellite cells. *Dev Biol,* 191(2)**,** pp 270-83.

Cruz-Migoni S.B. & Borycki, A.G. 2014. Hedgehog Signalling. eLS John Wiley & Sons, Ltd (online edition). doi: 10.1002/9780470015902.a0000806.pub2

Cruz Migoni, S., B. 2015. *The role of Sonic Hedgehog signalling in satellite cell-mediated myogenesis.* PhD eThesis, The University of Sheffield.

Dagher, R. & Helman, L. 1999. Rhabdomyosarcoma: an overview. *Oncologist,* 4(1)**,** pp 34-44.

Davey, M. G., Paton, I. R., Yin, Y., Schmidt, M., Bangs, F. K., Morrice, D. R., Smith, T. G., Buxton, P., Stamataki, D., Tanaka, M., Munsterberg, A. E., Briscoe, J., Tickle, C. & Burt, D. W. 2006. The chicken talpid3 gene encodes a novel protein essential for Hedgehog signaling. *Genes Dev,* 20(10)**,** pp 1365-77.

Day, K., Shefer, G., Shearer, A. & Yablonka-Reuveni, Z. 2010. The depletion of skeletal muscle satellite cells with age is concomitant with reduced capacity of single progenitors to produce reserve progeny. *Dev Biol,* 340(2)**,** pp 330-43.

De Angelis, L., Berghella, L., Coletta, M., Lattanzi, L., Zanchi, M., Cusella-De Angelis, M. G., Ponzetto, C. & Cossu, G. 1999. Skeletal myogenic progenitors originating from embryonic dorsal aorta coexpress endothelial and myogenic markers and contribute to postnatal muscle growth and regeneration. *J Cell Biol,* 147(4)**,** pp 869-78.

De Luca, G., Ferretti, R., Bruschi, M., Mezzaroma, E. & Caruso, M. 2013. Cyclin D3 critically regulates the balance between self-renewal and differentiation in skeletal muscle stem cells. *Stem Cells,* 31(11)**,** pp 2478-91.

De Paepe, B. & De Bleecker, J. L. 2013. Cytokines and chemokines as regulators of skeletal muscle inflammation: presenting the case of Duchenne muscular dystrophy. *Mediators Inflamm,* 2013(540370).

Deato, M. D. E., Marr, M. T., Sottero, T., Inouye, C., Hu, P. & Tjian, R. 2008. MyoD Targets TAF3/TRF3 to Activate Myogenin Transcription. *Molecular Cell,* 32(1)**,** pp 96-105.

Delaney, K., Kasprzycka, P., Ciemerych, M. A. & Zimowska, M. 2017. The role of TGF-beta1 during skeletal muscle regeneration. *Cell Biol Int,* 41(7)**,** pp 706-715.

Delaval, B. & Doxsey, S. J. 2010. Pericentrin in cellular function and disease. *J Cell Biol,* 188(2)**,** pp 181-90.

Dellavalle, A., Sampaolesi, M., Tonlorenzi, R., Tagliafico, E., Sacchetti, B., Perani, L., Innocenzi, A., Galvez, B. G., Messina, G., Morosetti, R., Li, S., Belicchi, M., Peretti, G., Chamberlain, J. S., Wright, W. E., Torrente, Y., Ferrari, S., Bianco, P. & Cossu, G. 2007. Pericytes of human skeletal muscle are myogenic precursors distinct from satellite cells. *Nat Cell Biol,* 9(3)**,** pp 255-67.

Deries, M. & Thorsteinsdottir, S. 2016. Axial and limb muscle development: dialogue with the neighbourhood. *Cell Mol Life Sci,* 73(23)**,** pp 4415-4431.

Dezawa, M., Ishikawa, H., Itokazu, Y., Yoshihara, T., Hoshino, M., Takeda, S., Ide, C. & Nabeshima, Y. 2005. Bone marrow stromal cells generate muscle cells and repair muscle degeneration. *Science,* 309(5732)**,** pp 314-7.

Dhawan, J. & Rando, T. A. 2005. Stem cells in postnatal myogenesis: molecular mechanisms of satellite cell quiescence, activation and replenishment. *Trends Cell Biol,* 15(12)**,** pp 666-73.

Di Marcotullio, L., Ferretti, E., Greco, A., De Smaele, E., Po, A., Sico, M. A., Alimandi, M., Giannini, G., Maroder, M., Screpanti, I. & Gulino, A. 2006. Numb is a suppressor of Hedgehog signalling and targets Gli1 for Itch- dependent ubiquitination. *Nature Cell Biology,* 8(12)**,** pp 1415-U68.

Dick, S. A., Chang, N. C., Dumont, N. A., Bell, R. A., Putinski, C., Kawabe, Y., Litchfield, D. W., Rudnicki, M. A. & Megeney, L. A. 2015. Caspase 3 cleavage of Pax7 inhibits self-renewal of satellite cells. *Proc Natl Acad Sci U S A,* 112(38)**,** pp E5246-52.

Dorchies, O. M., Reutenauer-Patte, J., Dahmane, E., Ismail, H. M., Petermann, O., Patthey- Vuadens, O., Comyn, S. A., Gayi, E., Piacenza, T., Handa, R. J., Decosterd, L. A. & Ruegg, U. T. 2013. The anticancer drug tamoxifen counteracts the pathology in a mouse model of duchenne muscular dystrophy. *Am J Pathol,* 182(2)**,** pp 485-504.

Duman-Scheel, M., Weng, L., Xin, S. & Du, W. 2002a. Hedgehog regulates cell growth and proliferation by inducing Cyclin D and Cyclin E. *Nature,* 417(6886)**,** pp 299-304.

Dumont, N. A., Bentzinger, C. F., Sincennes, M. C. & Rudnicki, M. A. 2015a. Satellite Cells and Skeletal Muscle Regeneration. *Compr Physiol,* 5(3)**,** pp 1027-59.

Dumont, N. A., Wang, Y. X. & Rudnicki, M. A. 2015b. Intrinsic and extrinsic mechanisms regulating satellite cell function. *Development,* 142(9)**,** pp 1572-81.

Dumont, N. A., Wang, Y. X., von Maltzahn, J., Pasut, A., Bentzinger, C. F., Brun, C. E. & Rudnicki, M. A. 2015c. Dystrophin expression in muscle stem cells regulates their polarity and asymmetric division. *Nat Med,* 21(12)**,** pp 1455-63.

Duprez, D., Fournier-Thibault, C. & Le Douarin, N. 1998. Sonic Hedgehog induces proliferation of committed skeletal muscle cells in the chick limb. *Development,* 125(3)**,** pp 495-505.

Elia, D., Madhala, D., Ardon, E., Reshef, R. & Halevy, O. 2007. Sonic hedgehog promotes proliferation and differentiation of adult muscle cells: Involvement of MAPK/ERK and PI3K/Akt pathways. *Biochimica et Biophysica Acta (BBA)-Molecular Cell Research,* 1773(9)**,** pp 1438-1446.

Elias, B. C., Das, A., Parekh, D. V., Mernaugh, G., Adams, R., Yang, Z., Brakebusch, C., Pozzi, A., Marciano, D. K., Carroll, T. J. & Zent, R. 2015. Cdc42 regulates epithelial cell polarity and cytoskeletal function during kidney tubule development. *J Cell Sci,* 128(23)**,** pp 4293-305.

Emery, A. E. 2002. The muscular dystrophies. *Lancet,* 359(9307)**,** pp 687-95.

Engert, J. C., Berglund, E. B. & Rosenthal, N. 1996. Proliferation precedes differentiation in IGF-I-stimulated myogenesis. *J Cell Biol,* 135(2)**,** pp 431-40.

Etemadmoghadam, B., Guo, S. & Kemphues, K. J. 1995. Asymmetrically Distributed Par-3 Protein Contributes to Cell Polarity and Spindle Alignment in Early C-Elegans Embryos. *Cell,* 83(5)**,** pp 743-752.

Ferent, J., Cochard, L., Faure, H., Taddei, M., Hahn, H., Ruat, M. & Traiffort, E. 2014. Genetic activation of Hedgehog signaling unbalances the rate of neural stem cell renewal by increasing symmetric divisions. *Stem Cell Reports,* 3(2)**,** pp 312-23.

Ferrari, G., Cusella-De Angelis, G., Coletta, M., Paolucci, E., Stornaiuolo, A., Cossu, G. & Mavilio, F. 1998. Muscle regeneration by bone marrow-derived myogenic progenitors. *Science,* 279(5356)**,** pp 1528-30.

Fielding, R. A., Manfredi, T. J., Ding, W., Fiatarone, M. A., Evans, W. J. & Cannon, J. G. 1993. Acute phase response in exercise. III. Neutrophil and IL-1 beta accumulation in skeletal muscle. *Am J Physiol,* 265(1 Pt 2)**,** pp R166-72.

Fiore, D., Judson, R. N., Low, M., Lee, S., Zhang, E., Hopkins, C., Xu, P., Lenzi, A., Rossi, F. M. & Lemos, D. R. 2016. Pharmacological blockage of fibro/adipogenic progenitor expansion and suppression of regenerative fibrogenesis is associated with impaired skeletal muscle regeneration. *Stem Cell Res,* 17(1)**,** pp 161-9.

Fu, W., Asp, P., Canter, B. & Dynlacht, B. D. 2014. Primary cilia control hedgehog signaling during muscle differentiation and are deregulated in rhabdomyosarcoma. *Proc Natl Acad Sci U S A,* 111(25)**,** pp 9151-6.

Fukada, S., Uezumi, A., Ikemoto, M., Masuda, S., Segawa, M., Tanimura, N., Yamamoto, H., Miyagoe-Suzuki, Y. & Takeda, S. 2007. Molecular signature of quiescent satellite cells in adult skeletal muscle. *Stem Cells,* 25(10)**,** pp 2448-59.

Fukada, S., Yamaguchi, M., Kokubo, H., Ogawa, R., Uezumi, A., Yoneda, T., Matev, M. M., Motohashi, N., Ito, T., Zolkiewska, A., Johnson, R. L., Saga, Y., Miyagoe-Suzuki, Y., Tsujikawa, K., Takeda, S. & Yamamoto, H. 2011. Hesr1 and Hesr3 are essential to generate undifferentiated quiescent satellite cells and to maintain satellite cell numbers. *Development,* 138(21)**,** pp 4609-19.

Gailani, M. R., Stahle-Backdahl, M., Leffell, D. J., Glynn, M., Zaphiropoulos, P. G., Pressman, C., Unden, A. B., Dean, M., Brash, D. E., Bale, A. E. & Toftgard, R. 1996. The role of the human homologue of Drosophila patched in sporadic basal cell carcinomas. *Nat Genet,* 14(1)**,** pp 78-81.

Galli, D., Vitale, M. & Vaccarezza, M. 2014. Bone marrow-derived mesenchymal cell differentiation toward myogenic lineages: facts and perspectives. *Biomed Res Int,* 2014(762695.

Galvez, B. G., Sampaolesi, M., Brunelli, S., Covarello, D., Gavina, M., Rossi, B., Constantin, G., Torrente, Y. & Cossu, G. 2006. Complete repair of dystrophic skeletal muscle by mesoangioblasts with enhanced migration ability. *J Cell Biol,* 174(2)**,** pp 231-43.

Ganassi, M., Badodi, S., Ortuste Quiroga, H. P., Zammit, P. S., Hinits, Y. & Hughes, S. M. 2018. Myogenin promotes myocyte fusion to balance fibre number and size. *Nat Commun,* 9(1)**,** pp 4232.

Gang, E. J., Darabi, R., Bosnakovski, D., Xu, Z., Kamm, K. E., Kyba, M. & Perlingeiro, R. C. 2009. Engraftment of mesenchymal stem cells into dystrophin-deficient mice is not accompanied by functional recovery. *Exp Cell Res,* 315(15)**,** pp 2624-36.

Gautam, J., Nirwane, A. & Yao, Y. 2017. Laminin differentially regulates the stemness of type I and type II pericytes. *Stem Cell Res Ther,* 8(1)**,** pp 28.

Gawlik, K. I. & Durbeej, M. 2015. Deletion of integrin alpha7 subunit does not aggravate the phenotype of laminin alpha2 chain-deficient mice. *Sci Rep,* 5(13916.

Goel, A. J., Rieder, M. K., Arnold, H. H., Radice, G. L. & Krauss, R. S. 2017. Niche Cadherins Control the Quiescence-to-Activation Transition in Muscle Stem Cells. *Cell Rep,* 21(8)**,** pp 2236-2250.

Goetz, S. C., Ocbina, P. J. & Anderson, K. V. 2009. The primary cilium as a Hedgehog signal transduction machine. *Methods Cell Biol,* 94(199-222.

Gomez-Lopez, S., Lerner, R. G. & Petritsch, C. 2014. Asymmetric cell division of stem and progenitor cells during homeostasis and cancer. *Cell Mol Life Sci,* 71(4)**,** pp 575-97.

Gomez-Orte, E., Saenz-Narciso, B., Moreno, S. & Cabello, J. 2013. Multiple functions of the noncanonical Wnt pathway. *Trends Genet,* 29(9)**,** pp 545-53.

Gonzalez, M. N., de Mello, W., Butler-Browne, G. S., Silva-Barbosa, S. D., Mouly, V., Savino, W. & Riederer, I. 2017. HGF potentiates extracellular matrix-driven migration of human myoblasts: involvement of matrix metalloproteinases and MAPK/ERK pathway. *Skelet Muscle,* 7(1)**,** pp 20.

Gonzalez, N., Moresco, J. J., Cabezas, F., de la Vega, E., Bustos, F., Yates, J. R., 3rd & Olguin, H. C. 2016. Ck2-Dependent Phosphorylation Is Required to Maintain Pax7 Protein Levels in Proliferating Muscle Progenitors. *PLoS One,* 11(5)**,** pp e0154919.

Gopinath, S. D. & Rando, T. A. 2008. Stem cell review series: Aging of the skeletal muscle stem cell niche. *Aging Cell,* 7(4)**,** pp 590-598.

Gopinath, S. D., Webb, A. E., Brunet, A. & Rando, T. A. 2014. FOXO3 promotes quiescence in adult muscle stem cells during the process of self-renewal. *Stem Cell Reports,* 2(4)**,** pp 414-26.

Gorlin, R. J. 1995. Nevoid basal cell carcinoma syndrome. *Dermatol Clin,* 13(1)**,** pp 113-25.

Gulino, A., Di Marcotullio, L. & Screpanti, I. 2010. The multiple functions of Numb. *Exp Cell Res,* 316(6)**,** pp 900-6.

Guo, S. & Kemphues, K. J. 1995. par-1, a gene required for establishing polarity in C. elegans embryos, encodes a putative Ser/Thr kinase that is asymmetrically distributed. *Cell,* 81(4)**,** pp 611-20.

Gupta, S. K., Meiri, K. F., Mahfooz, K., Bharti, U. & Mani, S. 2010. Coordination between extrinsic extracellular matrix cues and intrinsic responses to orient the centrosome in polarizing cerebellar granule neurons. *J Neurosci,* 30(7)**,** pp 2755-66.

Gussoni, E., Soneoka, Y., Strickland, C. D., Buzney, E. A., Khan, M. K., Flint, A. F., Kunkel, L. M. & Mulligan, R. C. 1999. Dystrophin expression in the mdx mouse restored by stem cell transplantation. *Nature,* 401(6751)**,** pp 390-4.

Gustafsson, M. K., Pan, H., Pinney, D. F., Liu, Y., Lewandowski, A., Epstein, D. J. & Emerson, C. P., Jr. 2002. Myf5 is a direct target of long-range Shh signaling and Gli regulation for muscle specification. *Genes Dev,* 16(1)**,** pp 114-26.

Habib, S. J., Chen, B. C., Tsai, F. C., Anastassiadis, K., Meyer, T., Betzig, E. & Nusse, R. 2013. A localized Wnt signal orients asymmetric stem cell division in vitro. *Science,* 339(6126)**,** pp 1445-8.

Hahn, H., Wicking, C., Zaphiropoulous, P. G., Gailani, M. R., Shanley, S., Chidambaram, A., Vorechovsky, I., Holmberg, E., Unden, A. B., Gillies, S., Negus, K., Smyth, I., Pressman, C., Leffell, D. J., Gerrard, B., Goldstein, A. M., Dean, M., Toftgard, R., Chenevix-Trench, G., Wainwright, B. & Bale, A. E. 1996. Mutations of the human homolog of Drosophila patched in the nevoid basal cell carcinoma syndrome. *Cell,* 85(6)**,** pp 841-51.

Hahn, H., Wojnowski, L., Zimmer, A. M., Hall, J., Miller, G. & Zimmer, A. 1998. Rhabdomyosarcomas and radiation hypersensitivity in a mouse model of Gorlin syndrome. *Nat Med,* 4(5)**,** pp 619-22.

Han, B., Tong, J., Zhu, M. J., Ma, C. & Du, M. 2008. Insulin-like growth factor-1 (IGF-1) and leucine activate pig myogenic satellite cells through mammalian target of rapamycin (mTOR) pathway. *Mol Reprod Dev,* 75(5)**,** pp 810-7.

Hanson, J. & Huxley, H. E. 1953. Structural basis of the cross-striations in muscle. *Nature,* 172(4377)**,** pp 530-2.

Hayes, K. L., Messina, L. M., Schwartz, L. M., Yan, J., Burnside, A. S. & Witkowski, S. 2018. Type 2 diabetes impairs the ability of skeletal muscle pericytes to augment postischemic neovascularization in db/db mice. *Am J Physiol Cell Physiol,* 314(5)**,** pp C534-C544.

Heiden, K. B., Williamson, A. J., Doscas, M. E., Ye, J., Wang, Y., Liu, D., Xing, M., Prinz, R. A. & Xu, X. 2014. The sonic hedgehog signaling pathway maintains the cancer stem cell self-renewal of anaplastic thyroid cancer by inducing Snail expression. *The Journal of Clinical Endocrinology & Metabolism*.

Hellemans, J., Coucke, P. J., Giedion, A., De Paepe, A., Kramer, P., Beemer, F. & Mortier, G. R. 2003. Homozygous mutations in IHH cause acrocapitofemoral dysplasia, an autosomal recessive disorder with cone-shaped epiphyses in hands and hips. *Am J Hum Genet,* 72(4)**,** pp 1040-6.

Heredia, J. E., Mukundan, L., Chen, F. M., Mueller, A. A., Deo, R. C., Locksley, R. M., Rando, T. A. & Chawla, A. 2013. Type 2 innate signals stimulate fibro/adipogenic progenitors to facilitate muscle regeneration. *Cell,* 153(2)**,** pp 376-88.

Hindi, S. M. & Kumar, A. 2016. TRAF6 regulates satellite stem cell self-renewal and function during regenerative myogenesis. *J Clin Invest,* 126(1)**,** pp 151-68.

Hinken, A. C., Powers, J. M., Luo, G. Z., Holt, J. A., Billin, A. N. & Russell, A. J. 2016. Lack of evidence for GDF11 as a rejuvenator of aged skeletal muscle satellite cells. *Aging Cell,* 15(3)**,** pp 582-584.

Hohenester, E. & Yurchenco, P. D. 2013. Laminins in basement membrane assembly. *Cell Adh Migr,* 7(1)**,** pp 56-63.

Hollnagel, A., Grund, C., Franke, W. W. & Arnold, H. H. 2002. The cell adhesion molecule M-cadherin is not essential for muscle development and regeneration. *Mol Cell Biol,* 22(13)**,** pp 4760-70.

Holmberg, J. & Durbeej, M. 2013. Laminin-211 in skeletal muscle function. *Cell Adh Migr,* 7(1)**,** pp 111-21.

Holterman, C. E., Le Grand, F., Kuang, S., Seale, P. & Rudnicki, M. A. 2007. Megf10 regulates the progression of the satellite cell myogenic program. *J Cell Biol,* 179(5)**,** pp 911-22.

Hu, J. K., McGlinn, E., Harfe, B. D., Kardon, G. & Tabin, C. J. 2012. Autonomous and nonautonomous roles of Hedgehog signaling in regulating limb muscle formation. *Genes Dev,* 26(18)**,** pp 2088-102.

Huangfu, D. & Anderson, K. V. 2005. Cilia and Hedgehog responsiveness in the mouse. *Proc Natl Acad Sci U S A,* 102(32)**,** pp 11325-30.

Hui, C. C., Slusarski, D., Platt, K. A., Holmgren, R. & Joyner, A. L. 1994. Expression of three mouse homologs of the Drosophila segment polarity gene cubitus interruptus, Gli, Gli-2,

and Gli-3, in ectoderm- and mesoderm-derived tissues suggests multiple roles during postimplantation development. *Dev Biol,* 162(2)**,** pp 402-13.

Humke, E. W., Dorn, K. V., Milenkovic, L., Scott, M. P. & Rohatgi, R. 2010. The output of Hedgehog signaling is controlled by the dynamic association between Suppressor of Fused and the Gli proteins. *Genes Dev,* 24(7)**,** pp 670-82.

Huxley, H. E. 1957. The double array of filaments in cross-striated muscle. *J Biophys Biochem Cytol,* 3(5)**,** pp 631-48.

Huxley, H. E. & Hanson, J. 1959. The structural basis of the contraction mechanism in striated muscle. *Ann N Y Acad Sci,* 81(403-8.

Indra, A. K., Warot, X., Brocard, J., Bornert, J. M., Xiao, J. H., Chambon, P. & Metzger, D. 1999. Temporally-controlled site-specific mutagenesis in the basal layer of the epidermis: comparison of the recombinase activity of the tamoxifen-inducible Cre-ER(T) and Cre-ER(T2) recombinases. *Nucleic Acids Res,* 27(22)**,** pp 4324-7.

Ingham, P. W. 2000. How cholesterol modulates the signal. *Curr Biol,* 10(5)**,** pp R180-3.

Ingham, P. W. & Placzek, M. 2006. Orchestrating ontogenesis: variations on a theme by sonic hedgehog. *Nat Rev Genet,* 7(11)**,** pp 841-50.

Ingram, W. J., McCue, K. I., Tran, T. H., Hallahan, A. R. & Wainwright, B. J. 2008. Sonic Hedgehog regulates Hes1 through a novel mechanism that is independent of canonical Notch pathway signalling. *Oncogene,* 27(10)**,** pp 1489-500.

Ishikawa, H., Kubo, A., Tsukita, S. & Tsukita, S. 2005. Odf2-deficient mother centrioles lack distal/subdistal appendages and the ability to generate primary cilia. *Nat Cell Biol,* 7(5)**,** pp 517-24.

Jaafar Marican, N. H., Cruz-Migoni, S. B. & Borycki, A. G. 2016. Asymmetric Distribution of Primary Cilia Allocates Satellite Cells for Self-Renewal. *Stem Cell Reports,* 6(6)**,** pp 798-805.

Jakobs, P., Schulz, P., Ortmann, C., Schurmann, S., Exner, S., Rebollido-Rios, R., Dreier, R., Seidler, D. G. & Grobe, K. 2016. Bridging the gap: heparan sulfate and Scube2 assemble Sonic hedgehog release complexes at the surface of producing cells. *Sci Rep,* 6(26435.

Januschke, J. & Gonzalez, C. 2010. The interphase microtubule aster is a determinant of asymmetric division orientation in Drosophila neuroblasts. *Journal of Cell Biology,* 188(5)**,** pp 693-706.

Jash, S., Dhar, G., Ghosh, U. & Adhya, S. 2014. Role of the mTORC1 complex in satellite cell activation by RNA-induced mitochondrial restoration: dual control of cyclin D1 through microRNAs. *Mol Cell Biol,* 34(19)**,** pp 3594-606.

Jia, J., Amanai, K., Wang, G., Tang, J., Wang, B. & Jiang, J. 2002. Shaggy/GSK3 antagonizes Hedgehog signalling by regulating Cubitus interruptus. *Nature,* 416(6880)**,** pp 548-52.

Jiang, C., Wen, Y., Kuroda, K., Hannon, K., Rudnicki, M. A. & Kuang, S. 2014. Notch signaling deficiency underlies age-dependent depletion of satellite cells in muscular dystrophy. *Dis Model Mech,* 7(8)**,** pp 997-1004.

Jiang, J. & Hui, C. C. 2008. Hedgehog signaling in development and cancer. *Dev Cell,* 15(6)**,** pp 801-12.

Joe, A. W., Yi, L., Natarajan, A., Le Grand, F., So, L., Wang, J., Rudnicki, M. A. & Rossi, F. M. 2010. Muscle injury activates resident fibro/adipogenic progenitors that facilitate myogenesis. *Nat Cell Biol,* 12(2)**,** pp 153-63.

Johnson, R. L., Milenkovic, L. & Scott, M. P. 2000. In vivo functions of the patched protein: requirement of the C terminus for target gene inactivation but not Hedgehog sequestration. *Mol Cell,* 6(2)**,** pp 467-78.

Johnson, R. L., Rothman, A. L., Xie, J., Goodrich, L. V., Bare, J. W., Bonifas, J. M., Quinn, A. G., Myers, R. M., Cox, D. R., Epstein, E. H., Jr. & Scott, M. P. 1996. Human homolog of

patched, a candidate gene for the basal cell nevus syndrome. *Science,* 272(5268)**,** pp 1668-71.

Johnson, R. L. & Tabin, C. J. 1997. Molecular models for vertebrate limb development. *Cell,* 90(6)**,** pp 979-90.

Jones, A. E., Price, F. D., Le Grand, F., Soleimani, V. D., Dick, S. A., Megeney, L. A. & Rudnicki, M. A. 2015. Wnt/beta-catenin controls follistatin signalling to regulate satellite cell myogenic potential. *Skeletal Muscle,* 5(14.

Jones, N. C., Fedorov, Y. V., Rosenthal, R. S. & Olwin, B. B. 2001a. ERK1/2 is required for myoblast proliferation but is dispensable for muscle gene expression and cell fusion. *J Cell Physiol,* 186(1)**,** pp 104-15.

Jones, N. C., Fedorov, Y. V., Rosenthal, R. S. & Olwin, B. B. 2001b. ERK1/2 is required for myoblast proliferation but is dispensable for muscle gene expression and cell fusion. *Journal of Cellular Physiology,* 186(1)**,** pp 104-115.

Jones, N. C., Tyner, K. J., Nibarger, L., Stanley, H. M., Cornelison, D. D., Fedorov, Y. V. & Olwin, B. B. 2005. The p38alpha/beta MAPK functions as a molecular switch to activate the quiescent satellite cell. *J Cell Biol,* 169(1)**,** pp 105-16.

Joo, S., Lim, H. J., Jackson, J. D., Atala, A. & Yoo, J. J. 2014. Myogenic-induced mesenchymal stem cells are capable of modulating the immune response by regulatory T cells. *J Tissue Eng,* 5(2041731414524758.

Kahane, N., Ribes, V., Kicheva, A., Briscoe, J. & Kalcheim, C. 2013. The transition from differentiation to growth during dermomyotome-derived myogenesis depends on temporally restricted hedgehog signaling. *Development,* 140(8)**,** pp 1740-50.

Kassar-Duchossoy, L., Giacone, E., Gayraud-Morel, B., Jory, A., Gomes, D. & Tajbakhsh, S. 2005. Pax3/Pax7 mark a novel population of primitive myogenic cells during development. *Genes Dev,* 19(12)**,** pp 1426-31.

Khaliullina, H., Panakova, D., Eugster, C., Riedel, F., Carvalho, M. & Eaton, S. 2009. Patched regulates Smoothened trafficking using lipoprotein-derived lipids. *Development,* 136(24)**,** pp 4111-21.

Kharraz, Y., Guerra, J., Mann, C. J., Serrano, A. L. & Munoz-Canoves, P. 2013. Macrophage plasticity and the role of inflammation in skeletal muscle repair. *Mediators Inflamm,* 2013(491497.

Kharraz, Y., Guerra, J., Pessina, P., Serrano, A. L. & Munoz-Canoves, P. 2014. Understanding the process of fibrosis in Duchenne muscular dystrophy. *Biomed Res Int,* 2014(965631.

Khodabukus, A. & Baar, K. 2015. Contractile and metabolic properties of engineered skeletal muscle derived from slow and fast phenotype mouse muscle. *J Cell Physiol,* 230(8)**,** pp 1750-7.

Kikuchi, K., Rubin, B. P. & Keller, C. 2011. Developmental origins of fusion-negative rhabdomyosarcomas. *Curr Top Dev Biol,* 96(33-56.

Kim, J., Hsia, E. Y., Brigui, A., Plessis, A., Beachy, P. A. & Zheng, X. 2015a. The role of ciliary trafficking in Hedgehog receptor signaling. *Sci Signal,* 8(379)**,** pp ra55.

Kim, J. H., Jin, P., Duan, R. & Chen, E. H. 2015b. Mechanisms of myoblast fusion during muscle development. *Curr Opin Genet Dev,* 32(162-70.

Kitzmann, M., Carnac, G., Vandromme, M., Primig, M., Lamb, N. J. & Fernandez, A. 1998. The muscle regulatory factors MyoD and myf-5 undergo distinct cell cycle-specific expression in muscle cells. *J Cell Biol,* 142(6)**,** pp 1447-59.

Knoblich, J. A. 2008. Mechanisms of asymmetric stem cell division. *Cell,* 132(4)**,** pp 583-97.

Kobayashi, T. & Dynlacht, B. D. 2011. Regulating the transition from centriole to basal body. *J Cell Biol,* 193(3)**,** pp 435-44.

Koleva, M., Kappler, R., Vogler, M., Herwig, A., Fulda, S. & Hahn, H. 2005b. Pleiotropic effects of sonic hedgehog on muscle satellite cells. *Cellular and Molecular Life Sciences CMLS,* 62(16)**,** pp 1863-1870.

Kopinke, D., Roberson, E. C. & Reiter, J. F. 2017. Ciliary Hedgehog Signaling Restricts Injury-Induced Adipogenesis. *Cell,* 170(2)**,** pp 340.

Kostallari, E., Baba-Amer, Y., Alonso-Martin, S., Ngoh, P., Relaix, F., Lafuste, P. & Gherardi, R. K. 2015. Pericytes in the myovascular niche promote post-natal myofiber growth and satellite cell quiescence. *Development,* 142(7)**,** pp 1242-53.

Kotter, S., Andresen, C. & Kruger, M. 2014. Titin: central player of hypertrophic signaling and sarcomeric protein quality control. *Biol Chem,* 395(11)**,** pp 1341-52.

Kruger, M., Mennerich, D., Fees, S., Schafer, R., Mundlos, S. & Braun, T. 2001. Sonic hedgehog is a survival factor for hypaxial muscles during mouse development. *Development,* 128(5)**,** pp 743-52.

Kuang, S., Kuroda, K., Le Grand, F. & Rudnicki, M. A. 2007. Asymmetric self-renewal and commitment of satellite stem cells in muscle. *Cell,* 129(5)**,** pp 999-1010.

Kulesza, A., Burdzinska, A., Szczepanska, I., Zarychta-Wisniewska, W., Pajak, B., Bojarczuk, K., Dybowski, B. & Paczek, L. 2016. The Mutual Interactions between Mesenchymal Stem Cells and Myoblasts in an Autologous Co-Culture Model. *PLoS One,* 11(8)**,** pp e0161693.

Kuroda, K., Kuang, S., Taketo, M. M. & Rudnicki, M. A. 2013. Canonical Wnt signaling induces BMP-4 to specify slow myofibrogenesis of fetal myoblasts. *Skelet Muscle,* 3(1)**,** pp 5.

LaBarge, M. A. & Blau, H. M. 2002. Biological progression from adult bone marrow to mononucleate muscle stem cell to multinucleate muscle fiber in response to injury. *Cell,* 111(4)**,** pp 589-601.

Le Grand, F., Jones, A. E., Seale, V., Scime, A. & Rudnicki, M. A. 2009. Wnt7a activates the planar cell polarity pathway to drive the symmetric expansion of satellite stem cells. *Cell Stem Cell,* 4(6)**,** pp 535-47.

Lee, Y., Kawagoe, R., Sasai, K., Li, Y., Russell, H. R., Curran, T. & McKinnon, P. J. 2007. Loss of suppressor-of-fused function promotes tumorigenesis. *Oncogene,* 26(44)**,** pp 6442-7.

Lehman, W., Galinska-Rakoczy, A., Hatch, V., Tobacman, L. S. & Craig, R. 2009. Structural basis for the activation of muscle contraction by troponin and tropomyosin. *J Mol Biol,* 388(4)**,** pp 673-81.

Lepper, C., Conway, S. J. & Fan, C. M. 2009. Adult satellite cells and embryonic muscle progenitors have distinct genetic requirements. *Nature,* 460(7255)**,** pp 627-31.

Lepper, C. & Fan, C. M. 2012. Generating tamoxifen-inducible Cre alleles to investigate myogenesis in mice. *Methods Mol Biol,* 798(297-308.

Lepper, C., Partridge, T. A. & Fan, C. M. 2011. An absolute requirement for Pax7-positive satellite cells in acute injury-induced skeletal muscle regeneration. *Development,* 138(17)**,** pp 3639-46.

Li, F., Duman-Scheel, M., Yang, D., Du, W., Zhang, J., Zhao, C., Qin, L. & Xin, S. 2010. Sonic hedgehog signaling induces vascular smooth muscle cell proliferation via induction of the G1 cyclin-retinoblastoma axis. *Arterioscler Thromb Vasc Biol,* 30(9)**,** pp 1787-94.

Li, X., Blagden, C. S., Bildsoe, H., Bonnin, M. A., Duprez, D. & Hughes, S. M. 2004. Hedgehog can drive terminal differentiation of amniote slow skeletal muscle. *BMC developmental biology,* 4(1)**,** pp 9.

Lieber, R. L. 2002. *Skeletal muscle structure, function & plasticity : the physiological basis of rehabilitation*: Lippincott Williams&Wilkins.

Liem, K. F., Jr., He, M., Ocbina, P. J. & Anderson, K. V. 2009. Mouse Kif7/Costal2 is a cilia-associated protein that regulates Sonic hedgehog signaling. *Proc Natl Acad Sci U S A,* 106(32)**,** pp 13377-82.

Lindon, C., Montarras, D. & Pinset, C. 1998. Cell cycle-regulated expression of the muscle determination factor Myf5 in proliferating myoblasts. *J Cell Biol,* 140(1)**,** pp 111-8.

Liu, D., Wang, S., Cui, Y., Shen, L., Du, Y., Li, G., Zhang, B. & Wang, R. 2012a. Sonic hedgehog elevates N-myc gene expression in neural stem cells. *Neural Regen Res,* 7(22)**,** pp 1703-8.

Liu, H., Kiseleva, A. A. & Golemis, E. A. 2018. Ciliary signalling in cancer. *Nat Rev Cancer,* 18(8)**,** pp 511-524.

Liu, J., Sato, C., Cerletti, M. & Wagers, A. 2010. Notch signaling in the regulation of stem cell self-renewal and differentiation. *Curr Top Dev Biol,* 92(367-409.

Liu, N., Nelson, B. R., Bezprozvannaya, S., Shelton, J. M., Richardson, J. A., Bassel-Duby, R. & Olson, E. N. 2014. Requirement of MEF2A, C, and D for skeletal muscle regeneration. *Proc Natl Acad Sci U S A,* 111(11)**,** pp 4109-14.

Liu, Q. C., Zha, X. H., Faralli, H., Yin, H., Louis-Jeune, C., Perdiguero, E., Pranckeviciene, E., Munoz-Canoves, P., Rudnicki, M. A., Brand, M., Perez-Iratxeta, C. & Dilworth, F. J. 2012b. Comparative expression profiling identifies differential roles for Myogenin and p38alpha MAPK signaling in myogenesis. *J Mol Cell Biol,* 4(6)**,** pp 386-97.

Liu, X. T., Shen, Q. H., Yu, T. T., Huang, H. J., Zhang, Z. Y., Ding, J., Tang, Y., Xu, N. & Yue, S. 2016. Small GTPase Arl6 controls RH30 rhabdomyosarcoma cell growth through ciliogenesis and Hedgehog signaling. *Cell and Bioscience,* 6(

Logan, C. V., Lucke, B., Pottinger, C., Abdelhamed, Z. A., Parry, D. A., Szymanska, K., Diggle, C. P., van Riesen, A., Morgan, J. E., Markham, G., Ellis, I., Manzur, A. Y., Markham, A. F., Shires, M., Helliwell, T., Scoto, M., Hubner, C., Bonthron, D. T., Taylor, G. R., Sheridan, E., Muntoni, F., Carr, I. M., Schuelke, M. & Johnson, C. A. 2011. Mutations in MEGF10, a regulator of satellite cell myogenesis, cause early onset myopathy, areflexia, respiratory distress and dysphagia (EMARDD). *Nat Genet,* 43(12)**,** pp 1189-92.

Lozano-Velasco, E., Vallejo, D., Esteban, F. J., Doherty, C., Hernandez-Torres, F., Franco, D. & Aranega, A. E. 2015. A Pitx2-MicroRNA Pathway Modulates Cell Proliferation in Myoblasts and Skeletal-Muscle Satellite Cells and Promotes Their Commitment to a Myogenic Cell Fate. *Mol Cell Biol,* 35(17)**,** pp 2892-909.

Lyons, G. E., Ontell, M., Cox, R., Sassoon, D. & Buckingham, M. 1990. The expression of myosin genes in developing skeletal muscle in the mouse embryo. *J Cell Biol,* 111(4)**,** pp 1465-76.

Ma, J., Cheng, J., Gong, Y., Tian, L. & Huang, Q. 2015. Downregulation of Wnt signaling by sonic hedgehog activation promotes repopulation of human tumor cell lines. *Dis Model Mech,* 8(4)**,** pp 385-91.

Machida, S., Spangenburg, E. E. & Booth, F. W. 2003. Forkhead transcription factor FoxO1 transduces insulin-like growth factor's signal to p27Kip1 in primary skeletal muscle satellite cells. *J Cell Physiol,* 196(3)**,** pp 523-31.

Madhala-Levy, D., Williams, V. C., Hughes, S. M., Reshef, R. & Halevy, O. 2012. Cooperation between Shh and IGF-I in promoting myogenic proliferation and differentiation via the MAPK/ERK and PI3K/Akt pathways requires Smo activity. *J Cell Physiol,* 227(4)**,** pp 1455-64.

Malempati, S. & Hawkins, D. S. 2012. Rhabdomyosarcoma: review of the Children's Oncology Group (COG) Soft-Tissue Sarcoma Committee experience and rationale for current COG studies. *Pediatr Blood Cancer,* 59(1)**,** pp 5-10.

Martini, F. H., Nath, J. L. & Bartholomew, E. F. 2015. *Fundamentals of Anatomy & Physiology*, Tenth, Global Edition: Pearson

Mauro, A. 1961. Satellite cell of skeletal muscle fibers. *J Biophys Biochem Cytol,* 9(493-5.

Mayer, U., Saher, G., Fassler, R., Bornemann, A., Echtermeyer, F., von der Mark, H., Miosge, N., Poschl, E. & von der Mark, K. 1997. Absence of integrin alpha 7 causes a novel form of muscular dystrophy. *Nat Genet,* 17(3)**,** pp 318-23.

McCarthy, J. J., Mula, J., Miyazaki, M., Erfani, R., Garrison, K., Farooqui, A. B., Srikuea, R., Lawson, B. A., Grimes, B., Keller, C., Van Zant, G., Campbell, K. S., Esser, K. A., Dupont-Versteegden, E. E. & Peterson, C. A. 2011. Effective fiber hypertrophy in satellite cell-depleted skeletal muscle. *Development,* 138(17)**,** pp 3657-66.

McCroskery, S., Thomas, M., Maxwell, L., Sharma, M. & Kambadur, R. 2003. Myostatin negatively regulates satellite cell activation and self-renewal. *J Cell Biol,* 162(6)**,** pp 1135-47.

McDermott, A., Gustafsson, M., Elsam, T., Hui, C. C., Emerson, C. P., Jr. & Borycki, A. G. 2005. Gli2 and Gli3 have redundant and context-dependent function in skeletal muscle formation. *Development,* 132(2)**,** pp 345-57.

McElhanon, K. E. & Bhattacharya, S. 2018. Altered membrane integrity in the progression of muscle diseases. *Life Sci,* 192(166-172.

McKinney-Freeman, S. L., Jackson, K. A., Camargo, F. D., Ferrari, G., Mavilio, F. & Goodell, M. A. 2002. Muscle-derived hematopoietic stem cells are hematopoietic in origin. *Proc Natl Acad Sci U S A,* 99(3)**,** pp 1341-6.

McPherron, A. C., Huynh, T. V. & Lee, S. J. 2009. Redundancy of myostatin and growth/differentiation factor 11 function. *BMC Dev Biol,* 9(24.

McPherron, A. C., Lawler, A. M. & Lee, S. J. 1997. Regulation of skeletal muscle mass in mice by a new TGF-beta superfamily member. *Nature,* 387(6628)**,** pp 83-90.

Megeney, L. A., Kablar, B., Garrett, K., Anderson, J. E. & Rudnicki, M. A. 1996. MyoD is required for myogenic stem cell function in adult skeletal muscle. *Genes Dev,* 10(10)**,** pp 1173-83.

Merlino, G. & Helman, L. J. 1999. Rhabdomyosarcoma--working out the pathways. *Oncogene,* 18(38)**,** pp 5340-8.

Messina, G., Sirabella, D., Monteverde, S., Galvez, B. G., Tonlorenzi, R., Schnapp, E., De Angelis, L., Brunelli, S., Relaix, F., Buckingham, M. & Cossu, G. 2009. Skeletal muscle

differentiation of embryonic mesoangioblasts requires pax3 activity. *Stem Cells,* 27(1)**,** pp 157-64.

Millay, D. P., Sutherland, L. B., Bassel-Duby, R. & Olson, E. N. 2014. Myomaker is essential for muscle regeneration. *Genes & Development,* 28(15)**,** pp 1641-1646.

Minetti, G. C., Feige, J. N., Bombard, F., Heier, A., Morvan, F., Nurnberg, B., Leiss, V., Birnbaumer, L., Glass, D. J. & Fornaro, M. 2014. Galphai2 signaling is required for skeletal muscle growth, regeneration, and satellite cell proliferation and differentiation. *Mol Cell Biol,* 34(4)**,** pp 619-30.

Mishra, R., Gupta, S. K., Meiri, K. F., Fong, M., Thostrup, P., Juncker, D. & Mani, S. 2008. GAP-43 is key to mitotic spindle control and centrosome-based polarization in neurons. *Cell Cycle,* 7(3)**,** pp 348-57.

Miyajima, M., Nornes, H. O. & Neuman, T. 1995. Cyclin E is expressed in neurons and forms complexes with cdk5. *Neuroreport,* 6(8)**,** pp 1130-2.

Miyake, T., Alli, N. S. & McDermott, J. C. 2010. Nuclear function of Smad7 promotes myogenesis. *Mol Cell Biol,* 30(3)**,** pp 722-35.

Miyashita, S., Adachi, T., Yamashita, M., Sota, T. & Hoshino, M. 2017. Dynamics of the cell division orientation of granule cell precursors during cerebellar development. *Mech Dev,* 147(1-7.

Mohan, A. & Asakura, A. 2017. CDK inhibitors for muscle stem cell differentiation and self-renewal. *J Phys Fit Sports Med,* 6(2)**,** pp 65-74.

Mokalled, M. H., Johnson, A. N., Creemers, E. E. & Olson, E. N. 2012. MASTR directs MyoD-dependent satellite cell differentiation during skeletal muscle regeneration. *Genes Dev,* 26(2)**,** pp 190-202.

Molkentin, J. D. & Olson, E. N. 1996. Defining the regulatory networks for muscle development. *Curr Opin Genet Dev,* 6(4)**,** pp 445-53.

Montanaro, F., Lindenbaum, M. & Carbonetto, S. 1999. alpha-Dystroglycan is a laminin receptor involved in extracellular matrix assembly on myotubes and muscle cell viability. *J Cell Biol,* 145(6)**,** pp 1325-40.

Montarras, D., L'Honore, A. & Buckingham, M. 2013. Lying low but ready for action: the quiescent muscle satellite cell. *FEBS J,* 280(17)**,** pp 4036-50.

Moore, R. & Walsh, F. S. 1993. The cell adhesion molecule M-cadherin is specifically expressed in developing and regenerating, but not denervated skeletal muscle. *Development,* 117(4)**,** pp 1409-20.

Morin, X. & Bellaiche, Y. 2011. Mitotic spindle orientation in asymmetric and symmetric cell divisions during animal development. *Dev Cell,* 21(1)**,** pp 102-19.

Mourikis, P., Gopalakrishnan, S., Sambasivan, R. & Tajbakhsh, S. 2012a. Cell-autonomous Notch activity maintains the temporal specification potential of skeletal muscle stem cells. *Development,* 139(24)**,** pp 4536-48.

Mourikis, P., Sambasivan, R., Castel, D., Rocheteau, P., Bizzarro, V. & Tajbakhsh, S. 2012b. A critical requirement for notch signaling in maintenance of the quiescent skeletal muscle stem cell state. *Stem Cells,* 30(2)**,** pp 243-52.

Mozzetta, C., Consalvi, S., Saccone, V., Tierney, M., Diamantini, A., Mitchell, K. J., Marazzi, G., Borsellino, G., Battistini, L., Sassoon, D., Sacco, A. & Puri, P. L. 2013. Fibroadipogenic progenitors mediate the ability of HDAC inhibitors to promote regeneration in dystrophic muscles of young, but not old Mdx mice. *EMBO Mol Med,* 5(4)**,** pp 626-39.

Munsterberg, A. E., Kitajewski, J., Bumcrot, D. A., McMahon, A. P. & Lassar, A. B. 1995. Combinatorial signaling by Sonic hedgehog and Wnt family members induces myogenic bHLH gene expression in the somite. *Genes Dev,* 9(23)**,** pp 2911-22.

Murphy, M. M., Lawson, J. A., Mathew, S. J., Hutcheson, D. A. & Kardon, G. 2011. Satellite cells, connective tissue fibroblasts and their interactions are crucial for muscle regeneration. *Development,* 138(17)**,** pp 3625-37.

Murtaugh, L. C., Chyung, J. H. & Lassar, A. B. 1999. Sonic hedgehog promotes somitic chondrogenesis by altering the cellular response to BMP signaling. *Genes Dev,* 13(2)**,** pp 225-37.

Muskiewicz, K. R., Frank, N. Y., Flint, A. F. & Gussoni, E. 2005. Myogenic potential of muscle side and main population cells after intravenous injection into sub-lethally irradiated mdx mice. *J Histochem Cytochem,* 53(7)**,** pp 861-73.

Myer, A., Olson, E. N. & Klein, W. H. 2001. MyoD cannot compensate for the absence of myogenin during skeletal muscle differentiation in murine embryonic stem cells. *Dev Biol,* 229(2)**,** pp 340-50.

Nieuwenhuis, E., Motoyama, J., Barnfield, P. C., Yoshikawa, Y., Zhang, X., Mo, R., Crackower, M. A. & Hui, C. C. 2006. Mice with a targeted mutation of patched2 are viable but develop alopecia and epidermal hyperplasia. *Mol Cell Biol,* 26(17)**,** pp 6609-22.

Nitzki, F., Zibat, A., Frommhold, A., Schneider, A., Schulz-Schaeffer, W., Braun, T. & Hahn, H. 2011. Uncommitted precursor cells might contribute to increased incidence of embryonal rhabdomyosarcoma in heterozygous Patched1-mutant mice. *Oncogene,* 30(43)**,** pp 4428-36.

Nusslein-Volhard, C. & Wieschaus, E. 1980. Mutations affecting segment number and polarity in Drosophila. *Nature,* 287(5785)**,** pp 795-801.

Ogura, Y., Hindi, S. M., Sato, S., Xiong, G., Akira, S. & Kumar, A. 2015. TAK1 modulates satellite stem cell homeostasis and skeletal muscle repair. *Nat Commun,* 6(10123.

Oh, J. Y., Suh, H. N., Choi, G. E., Lee, H. J., Jung, Y. H., Ko, S. H., Kim, J. S., Chae, C. W., Lee, C. K. & Han, H. J. 2018. Modulation of sonic hedgehog-induced mouse embryonic stem cell behaviours through E-cadherin expression and integrin beta1-dependent F-actin formation. *Br J Pharmacol,* 175(17)**,** pp 3548-3562.

Olguin, H. C. & Olwin, B. B. 2004. Pax-7 up-regulation inhibits myogenesis and cell cycle progression in satellite cells: a potential mechanism for self-renewal. *Dev Biol,* 275(2)**,** pp 375-88.

Olguin, H. C., Yang, Z., Tapscott, S. J. & Olwin, B. B. 2007. Reciprocal inhibition between Pax7 and muscle regulatory factors modulates myogenic cell fate determination. *J Cell Biol,* 177(5)**,** pp 769-79.

Oliver, T. G., Grasfeder, L. L., Carroll, A. L., Kaiser, C., Gillingham, C. L., Lin, S. M., Wickramasinghe, R., Scott, M. P. & Wechsler-Reya, R. J. 2003. Transcriptional profiling of the Sonic hedgehog response: a critical role for N-myc in proliferation of neuronal precursors. *Proc Natl Acad Sci U S A,* 100(12)**,** pp 7331-6.

Ono, Y., Calhabeu, F., Morgan, J. E., Katagiri, T., Amthor, H. & Zammit, P. S. 2011. BMP signalling permits population expansion by preventing premature myogenic differentiation in muscle satellite cells. *Cell Death Differ,* 18(2)**,** pp 222-34.

Ono, Y., Masuda, S., Nam, H. S., Benezra, R., Miyagoe-Suzuki, Y. & Takeda, S. 2012. Slow-dividing satellite cells retain long-term self-renewal ability in adult muscle. *J Cell Sci,* 125(Pt 5)**,** pp 1309-17.

Otto, A., Collins-Hooper, H., Patel, A., Dash, P. R. & Patel, K. 2011. Adult skeletal muscle stem cell migration is mediated by a blebbing/amoeboid mechanism. *Rejuvenation Res,* 14(3)**,** pp 249-60.

Pagano, A. F., Brioche, T., Arc-Chagnaud, C., Demangel, R., Chopard, A. & Py, G. 2018. Short-term disuse promotes fatty acid infiltration into skeletal muscle. *Journal of Cachexia Sarcopenia and Muscle,* 9(2)**,** pp 335-347.

Pajcini, K. V., Corbel, S. Y., Sage, J., Pomerantz, J. H. & Blau, H. M. 2010. Transient inactivation of Rb and ARF yields regenerative cells from postmitotic mammalian muscle. *Cell Stem Cell,* 7(2)**,** pp 198-213.

Pallafacchina, G., Francois, S., Regnault, B., Czarny, B., Dive, V., Cumano, A., Montarras, D. & Buckingham, M. 2010. An adult tissue-specific stem cell in its niche: a gene profiling

analysis of in vivo quiescent and activated muscle satellite cells. *Stem Cell Res,* 4(2)**,** pp 77-91.

Palma, V., Lim, D. A., Dahmane, N., Sanchez, P., Brionne, T. C., Herzberg, C. D., Gitton, Y., Carleton, A., Alvarez-Buylla, A. & Ruiz i Altaba, A. 2005. Sonic hedgehog controls stem cell behavior in the postnatal and adult brain. *Development,* 132(2)**,** pp 335-44.

Pannerec, A., Marazzi, G. & Sassoon, D. 2012. Stem cells in the hood: the skeletal muscle niche. *Trends Mol Med,* 18(10)**,** pp 599-606.

Pappo, A. S., Shapiro, D. N., Crist, W. M. & Maurer, H. M. 1995. Biology and therapy of pediatric rhabdomyosarcoma. *J Clin Oncol,* 13(8)**,** pp 2123-39.

Paridaen, J. T., Wilsch-Brauninger, M. & Huttner, W. B. 2013. Asymmetric inheritance of centrosome-associated primary cilium membrane directs ciliogenesis after cell division. *Cell,* 155(2)**,** pp 333-44.

Park, S., Kim, H., Kim, K. & Roh, S. 2018. Sonic hedgehog signalling regulates the self-renewal and proliferation of skin-derived precursor cells in mice. *Cell Prolif,* e12500.

Pasut, A., Jones, A. E. & Rudnicki, M. A. 2013. Isolation and culture of individual myofibers and their satellite cells from adult skeletal muscle. *J Vis Exp,* 73)**,** pp e50074.

Peake, J. M., Neubauer, O., Della Gatta, P. A. & Nosaka, K. 2017. Muscle damage and inflammation during recovery from exercise. *J Appl Physiol (1985),* 122(3)**,** pp 559-570.

Penton, C. M., Thomas-Ahner, J. M., Johnson, E. K., McAllister, C. & Montanaro, F. 2013. Muscle side population cells from dystrophic or injured muscle adopt a fibro-adipogenic fate. *PLoS One,* 8(1)**,** pp e54553.

Pepinsky, R. B., Zeng, C., Wen, D., Rayhorn, P., Baker, D. P., Williams, K. P., Bixler, S. A., Ambrose, C. M., Garber, E. A., Miatkowski, K., Taylor, F. R., Wang, E. A. & Galdes, A. 1998. Identification of a palmitic acid-modified form of human Sonic hedgehog. *J Biol Chem,* 273(22)**,** pp 14037-45.

Petrova, R. & Joyner, A. L. 2014. Roles for Hedgehog signaling in adult organ homeostasis and repair. *Development,* 141(18)**,** pp 3445-57.

Piccioni, A., Gaetani, E., Neri, V., Gatto, I., Palladino, M., Silver, M., Smith, R. C., Giarretta, I., Pola, E., Hlatky, L. & Pola, R. 2014a. Sonic hedgehog therapy in a mouse model of age-associated impairment of skeletal muscle regeneration. *J Gerontol A Biol Sci Med Sci,* 69(3)**,** pp 245-52.

Piccioni, A., Gaetani, E., Palladino, M., Gatto, I., Smith, R. C., Neri, V., Marcantoni, M., Giarretta, I., Silver, M., Straino, S., Capogrossi, M., Landolfi, R. & Pola, R. 2014b. Sonic hedgehog gene therapy increases the ability of the dystrophic skeletal muscle to regenerate after injury. *Gene Ther,* 21(4)**,** pp 413-21.

Pickering, J., Cunliffe, V. T., Van Eeden, F. & Borycki, A. G. 2017. Hedgehog signalling acts upstream of Laminin alpha1 transcription in the zebrafish paraxial mesoderm. *Matrix Biol,* 62(58-74.

Pitaval, A., Senger, F., Letort, G., Gidrol, X., Guyon, L., Sillibourne, J. & Thery, M. 2017. Microtubule stabilization drives 3D centrosome migration to initiate primary ciliogenesis. *J Cell Biol,* 216(11)**,** pp 3713-3728.

Pola, R., Ling, L. E., Aprahamian, T. R., Barban, E., Bosch-Marce, M., Curry, C., Corbley, M., Kearney, M., Isner, J. M. & Losordo, D. W. 2003. Postnatal recapitulation of embryonic hedgehog pathway in response to skeletal muscle ischemia. *Circulation,* 108(4)**,** pp 479-485.

Porter, J. A., Ekker, S. C., Park, W. J., von Kessler, D. P., Young, K. E., Chen, C. H., Ma, Y., Woods, A. S., Cotter, R. J., Koonin, E. V. & Beachy, P. A. 1996. Hedgehog patterning activity: role of a lipophilic modification mediated by the carboxy-terminal autoprocessing domain. *Cell,* 86(1)**,** pp 21-34.

Porter, J. D., Khanna, S., Kaminski, H. J., Rao, J. S., Merriam, A. P., Richmonds, C. R., Leahy, P., Li, J., Guo, W. & Andrade, F. H. 2002. A chronic inflammatory response dominates the skeletal muscle molecular signature in dystrophin-deficient mdx mice. *Hum Mol Genet,* 11(3)**,** pp 263-72.

Powell, G. T. & Wright, G. J. 2011. Jamb and Jamc Are Essential for Vertebrate Myocyte Fusion. *Plos Biology,* 9(12)**,** pp.

Pownall, M. E., Gustafsson, M. K. & Emerson, C. P., Jr. 2002. Myogenic regulatory factors and the specification of muscle progenitors in vertebrate embryos. *Annu Rev Cell Dev Biol,* 18(747-83.

Qahar, M., Takuma, Y., Mizunoya, W., Tatsumi, R., Ikeuchi, Y. & Nakamura, M. 2016. Semaphorin 3A promotes activation of Pax7, Myf5, and MyoD through inhibition of emerin expression in activated satellite cells. *FEBS Open Bio,* 6(6)**,** pp 529-39.

Qaisar, R., Bhaskaran, S. & Van Remmen, H. 2016. Muscle fiber type diversification during exercise and regeneration. *Free Radic Biol Med,* 98(56-67.

Rajurkar, M., Huang, H., Cotton, J. L., Brooks, J. K., Sicklick, J., McMahon, A. P. & Mao, J. 2014. Distinct cellular origin and genetic requirement of Hedgehog-Gli in postnatal rhabdomyosarcoma genesis. *Oncogene,* 33(46)**,** pp 5370-8.

Rana, R., Carroll, C. E., Lee, H. J., Bao, J., Marada, S., Grace, C. R., Guibao, C. D., Ogden, S. K. & Zheng, J. J. 2013. Structural insights into the role of the Smoothened cysteine-rich domain in Hedgehog signalling. *Nat Commun,* 4(2965.

Rando, T. A. & Blau, H. M. 1994. Primary mouse myoblast purification, characterization, and transplantation for cell-mediated gene therapy. *J Cell Biol,* 125(6)**,** pp 1275-87.

Rao, G., Pedone, C. A., Del Valle, L., Reiss, K., Holland, E. C. & Fults, D. W. 2004. Sonic hedgehog and insulin-like growth factor signaling synergize to induce medulloblastoma formation from nestin-expressing neural progenitors in mice. *Oncogene,* 23(36)**,** pp 6156-62.

Rayagiri, S. S., Ranaldi, D., Raven, A., Mohamad Azhar, N. I. F., Lefebvre, O., Zammit, P. S. & Borycki, A. G. 2018. Basal lamina remodeling at the skeletal muscle stem cell niche mediates stem cell self-renewal. *Nat Commun,* 9(1)**,** pp 1075.

Reano, S., Angelino, E., Ferrara, M., Malacarne, V., Sustova, H., Sabry, O., Agosti, E., Clerici, S., Ruozi, G., Zentilin, L., Prodam, F., Geuna, S., Giacca, M., Graziani, A. & Filigheddu, N. 2017. Unacylated Ghrelin Enhances Satellite Cell Function and Relieves the Dystrophic Phenotype in Duchenne Muscular Dystrophy mdx Model. *Stem Cells,* 35(7)**,** pp 1733-1746.

Reifenberger, J., Wolter, M., Knobbe, C. B., Kohler, B., Schonicke, A., Scharwachter, C., Kumar, K., Blaschke, B., Ruzicka, T. & Reifenberger, G. 2005. Somatic mutations in the PTCH, SMOH, SUFUH and TP53 genes in sporadic basal cell carcinomas. *Br J Dermatol,* 152(1)**,** pp 43-51.

Reisz-Porszasz, S., Bhasin, S., Artaza, J. N., Shen, R., Sinha-Hikim, I., Hogue, A., Fielder, T. J. & Gonzalez-Cadavid, N. F. 2003. Lower skeletal muscle mass in male transgenic mice with muscle-specific overexpression of myostatin. *Am J Physiol Endocrinol Metab,* 285(4)**,** pp E876-88.

Reiter, J. F. & Leroux, M. R. 2017. Genes and molecular pathways underpinning ciliopathies. *Nat Rev Mol Cell Biol,* 18(9)**,** pp 533-547.

Relaix, F., Montarras, D., Zaffran, S., Gayraud-Morel, B., Rocancourt, D., Tajbakhsh, S., Mansouri, A., Cumano, A. & Buckingham, M. 2006. Pax3 and Pax7 have distinct and overlapping functions in adult muscle progenitor cells. *J Cell Biol,* 172(1)**,** pp 91-102.

Relaix, F., Rocancourt, D., Mansouri, A. & Buckingham, M. 2005. A Pax3/Pax7-dependent population of skeletal muscle progenitor cells. *Nature,* 435(7044)**,** pp 948-53.

Relaix, F. & Zammit, P. S. 2012. Satellite cells are essential for skeletal muscle regeneration: the cell on the edge returns centre stage. *Development,* 139(16)**,** pp 2845-56.

Renault, M. A., Chapouly, C., Yao, Q., Larrieu-Lahargue, F., Vandierdonck, S., Reynaud, A., Petit, M., Jaspard-Vinassa, B., Belloc, I., Traiffort, E., Ruat, M., Duplaa, C., Couffinhal, T., Desgranges, C. & Gadeau, A. P. 2013a. Desert hedgehog promotes ischemia-induced angiogenesis by ensuring peripheral nerve survival. *Circ Res,* 112(5)**,** pp 762-70.

Renault, M. A., Robbesyn, F., Chapouly, C., Yao, Q., Vandierdonck, S., Reynaud, A., Belloc, I., Traiffort, E., Ruat, M., Desgranges, C. & Gadeau, A. P. 2013b. Hedgehog-dependent regulation of angiogenesis and myogenesis is impaired in aged mice. *Arterioscler Thromb Vasc Biol,* 33(12)**,** pp 2858-66.

Renault, M. A., Vandierdonck, S., Chapouly, C., Yu, Y., Qin, G., Metras, A., Couffinhal, T., Losordo, D. W., Yao, Q., Reynaud, A., Jaspard-Vinassa, B., Belloc, I., Desgranges, C. & Gadeau, A. P. 2013c. Gli3 regulation of myogenesis is necessary for ischemia-induced angiogenesis. *Circ Res,* 113(10)**,** pp 1148-58.

Reznik, M. 1969. Thymidine-3H uptake by satellite cells of regenerating skeletal muscle. *J Cell Biol,* 40(2)**,** pp 568-71.

Rhyu, M. S., Jan, L. Y. & Jan, Y. N. 1994. Asymmetric distribution of numb protein during division of the sensory organ precursor cell confers distinct fates to daughter cells. *Cell,* 76(3)**,** pp 477-91.

Richter, E. A., Garetto, L. P., Goodman, M. N. & Ruderman, N. B. 1982. Muscle glucose metabolism following exercise in the rat: increased sensitivity to insulin. *J Clin Invest,* 69(4)**,** pp 785-93.

Riddle, R. D., Johnson, R. L., Laufer, E. & Tabin, C. 1993. Sonic hedgehog mediates the polarizing activity of the ZPA. *Cell,* 75(7)**,** pp 1401-16.

Robbins, D. J., Nybakken, K. E., Kobayashi, R., Sisson, J. C., Bishop, J. M. & Therond, P. P. 1997. Hedgehog elicits signal transduction by means of a large complex containing the kinesin-related protein costal2. *Cell,* 90(2)**,** pp 225-34.

Rocheteau, P., Gayraud-Morel, B., Siegl-Cachedenier, I., Blasco, M. A. & Tajbakhsh, S. 2012. A subpopulation of adult skeletal muscle stem cells retains all template DNA strands after cell division. *Cell,* 148(1-2)**,** pp 112-25.

Rodgers, J. T., King, K. Y., Brett, J. O., Cromie, M. J., Charville, G. W., Maguire, K. K., Brunson, C., Mastey, N., Liu, L., Tsai, C. R., Goodell, M. A. & Rando, T. A. 2014. mTORC1 controls the adaptive transition of quiescent stem cells from G0 to G(Alert). *Nature,* 510(7505)**,** pp 393-6.

Rodriguez-Blanco, J., Pednekar, L., Penas, C., Li, B., Martin, V., Long, J., Lee, E., Weiss, W. A., Rodriguez, C., Mehrdad, N., Nguyen, D. M., Ayad, N. G., Rai, P., Capobianco, A. J. & Robbins, D. J. 2017. Inhibition of WNT signaling attenuates self-renewal of SHH-subgroup medulloblastoma. *Oncogene,* 36(45)**,** pp 6306-6314.

Rohatgi, R., Milenkovic, L. & Scott, M. P. 2007. Patched1 regulates hedgehog signaling at the primary cilium. *Science,* 317(5836)**,** pp 372-6.

Rubin, B. P., Nishijo, K., Chen, H. I., Yi, X., Schuetze, D. P., Pal, R., Prajapati, S. I., Abraham, J., Arenkiel, B. R., Chen, Q. R., Davis, S., McCleish, A. T., Capecchi, M. R., Michalek, J. E., Zarzabal, L. A., Khan, J., Yu, Z., Parham, D. M., Barr, F. G., Meltzer, P. S., Chen, Y. & Keller, C. 2011. Evidence for an unanticipated relationship between undifferentiated pleomorphic sarcoma and embryonal rhabdomyosarcoma. *Cancer Cell,* 19(2)**,** pp 177-91.

Rudnicki, M. A., Le Grand, F., McKinnell, I. & Kuang, S. 2008. The molecular regulation of muscle stem cell function. *Cold Spring Harb Symp Quant Biol,* 73(323-31.

Ruiz i Altaba, A., Sanchez, P. & Dahmane, N. 2002. Gli and hedgehog in cancer: tumours, embryos and stem cells. *Nat Rev Cancer,* 2(5)**,** pp 361-72.

Saade, M., Gonzalez-Gobartt, E., Escalona, R., Usieto, S. & Marti, E. 2017. Shh-mediated centrosomal recruitment of PKA promotes symmetric proliferative neuroepithelial cell division. *Nat Cell Biol,* 19(5)**,** pp 493-503.

Saccone, V., Consalvi, S., Giordani, L., Mozzetta, C., Barozzi, I., Sandona, M., Ryan, T., Rojas-Munoz, A., Madaro, L., Fasanaro, P., Borsellino, G., De Bardi, M., Frige, G., Termanini, A., Sun, X., Rossant, J., Bruneau, B. G., Mercola, M., Minucci, S. & Puri, P. L. 2014. HDAC-regulated myomiRs control BAF60 variant exchange and direct the functional phenotype of fibro-adipogenic progenitors in dystrophic muscles. *Genes Dev,* 28(8)**,** pp 841-57.

Saladin, K. S. 2018. Part 2: Support and movement. *Anatomy & physiology : the unity of form and function.* 8th edition, International student edition. ed. New York: McGraw-Hill Education.

Salic, A. & Mitchison, T. J. 2008. A chemical method for fast and sensitive detection of DNA synthesis in vivo. *Proc Natl Acad Sci U S A,* 105(7)**,** pp 2415-20.

Sambasivan, R., Yao, R., Kissenpfennig, A., Van Wittenberghe, L., Paldi, A., Gayraud-Morel, B., Guenou, H., Malissen, B., Tajbakhsh, S. & Galy, A. 2011. Pax7-expressing satellite cells are indispensable for adult skeletal muscle regeneration. *Development,* 138(17)**,** pp 3647-56.

Sampaolesi, M., Blot, S., D'Antona, G., Granger, N., Tonlorenzi, R., Innocenzi, A., Mognol, P., Thibaud, J. L., Galvez, B. G., Barthelemy, I., Perani, L., Mantero, S., Guttinger, M., Pansarasa, O., Rinaldi, C., Cusella De Angelis, M. G., Torrente, Y., Bordignon, C., Bottinelli, R. & Cossu, G. 2006. Mesoangioblast stem cells ameliorate muscle function in dystrophic dogs. *Nature,* 444(7119)**,** pp 574-9.

Sampaolesi, M., Torrente, Y., Innocenzi, A., Tonlorenzi, R., D'Antona, G., Pellegrino, M. A., Barresi, R., Bresolin, N., De Angelis, M. G., Campbell, K. P., Bottinelli, R. & Cossu, G. 2003. Cell therapy of alpha-sarcoglycan null dystrophic mice through intra-arterial delivery of mesoangioblasts. *Science,* 301(5632)**,** pp 487-92.

Sampath, S. C., Sampath, S. C., Ho, A. T. V., Corbel, S. Y., Millstone, J. D., Lamb, J., Walker, J., Kinzel, B., Schmedt, C. & Blau, H. M. 2018. Induction of muscle stem cell quiescence by the secreted niche factor Oncostatin M. *Nat Commun,* 9(1)**,** pp 1531.

Sanchez-Hernandez, D., Sierra, J., Ortigao-Farias, J. R. & Guerrero, I. 2012. The WIF domain of the human and Drosophila Wif-1 secreted factors confers specificity for Wnt or Hedgehog. *Development,* 139(20)**,** pp 3849-58.

Sandri, M. 2008. Signaling in muscle atrophy and hypertrophy. *Physiology (Bethesda),* 23(160-70.

Sasai, N. & Briscoe, J. 2012. Primary cilia and graded Sonic Hedgehog signaling. *Wiley Interdiscip Rev Dev Biol,* 1(5)**,** pp 753-72.

Schiaffino, S. & Reggiani, C. 2011. Fiber types in mammalian skeletal muscles. *Physiol Rev,* 91(4)**,** pp 1447-531.

Schienda, J., Engleka, K. A., Jun, S., Hansen, M. S., Epstein, J. A., Tabin, C. J., Kunkel, L. M. & Kardon, G. 2006. Somitic origin of limb muscle satellite and side population cells. *Proc Natl Acad Sci U S A,* 103(4)**,** pp 945-50.

Schultz, E., Gibson, M. C. & Champion, T. 1978. Satellite cells are mitotically quiescent in mature mouse muscle: an EM and radioautographic study. *J Exp Zool,* 206(3)**,** pp 451-6.

Seale, P., Sabourin, L. A., Girgis-Gabardo, A., Mansouri, A., Gruss, P. & Rudnicki, M. A. 2000. Pax7 is required for the specification of myogenic satellite cells. *Cell,* 102(6)**,** pp 777-86.

Sebastian, S., Sreenivas, P., Sambasivan, R., Cheedipudi, S., Kandalla, P., Pavlath, G. K. & Dhawan, J. 2009. MLL5, a trithorax homolog, indirectly regulates H3K4 methylation, represses cyclin A2 expression, and promotes myogenic differentiation. *Proc Natl Acad Sci U S A,* 106(12)**,** pp 4719-24.

Seifert, A. W., Zheng, Z., Ormerod, B. K. & Cohn, M. J. 2010. Sonic hedgehog controls growth of external genitalia by regulating cell cycle kinetics. *Nat Commun,* 1(23.

Shea, K. L., Xiang, W., LaPorta, V. S., Licht, J. D., Keller, C., Basson, M. A. & Brack, A. S. 2010. Sprouty1 regulates reversible quiescence of a self-renewing adult muscle stem cell pool during regeneration. *Cell Stem Cell,* 6(2)**,** pp 117-29.

Shen, Q., Zhong, W. M., Jan, Y. N. & Temple, S. 2002. Asymmetric Numb distribution is critical for asymmetric cell division of mouse cerebral cortical stem cells and neuroblasts. *Development,* 129(20)**,** pp 4843-4853.

Shen, Y., Mishra, R., Mani, S. & Meiri, K. F. 2008. Both cell-autonomous and cell non-autonomous functions of GAP-43 are required for normal patterning of the cerebellum in vivo. *Cerebellum,* 7(3)**,** pp 451-66.

Shi, D., Reinecke, H., Murry, C. E. & Torok-Storb, B. 2004. Myogenic fusion of human bone marrow stromal cells, but not hematopoietic cells. *Blood,* 104(1)**,** pp 290-4.

Shi, Y., Chen, J., Karner, C. M. & Long, F. 2015. Hedgehog signaling activates a positive feedback mechanism involving insulin-like growth factors to induce osteoblast differentiation. *Proc Natl Acad Sci U S A,* 112(15)**,** pp 4678-83.

Shinin, V., Gayraud-Morel, B., Gomes, D. & Tajbakhsh, S. 2006. Asymmetric division and cosegregation of template DNA strands in adult muscle satellite cells. *Nat Cell Biol,* 8(7)**,** pp 677-87.

Siegel, A. L., Kuhlmann, P. K. & Cornelison, D. D. 2011. Muscle satellite cell proliferation and association: new insights from myofiber time-lapse imaging. *Skelet Muscle,* 1(1)**,** pp 7.

Singh, B. N., Doyle, M. J., Weaver, C. V., Koyano-Nakagawa, N. & Garry, D. J. 2012. Hedgehog and Wnt coordinate signaling in myogenic progenitors and regulate limb regeneration. *Dev Biol,* 371(1)**,** pp 23-34.

Sinha, M., Jang, Y. C., Oh, J., Khong, D., Wu, E. Y., Manohar, R., Miller, C., Regalado, S. G., Loffredo, F. S., Pancoast, J. R., Hirshman, M. F., Lebowitz, J., Shadrach, J. L., Cerletti, M., Kim, M. J., Serwold, T., Goodyear, L. J., Rosner, B., Lee, R. T. & Wagers, A. J. 2014. Restoring systemic GDF11 levels reverses age-related dysfunction in mouse skeletal muscle. *Science,* 344(6184)**,** pp 649-52.

Skoda, A. M., Simovic, D., Karin, V., Kardum, V., Vranic, S. & Serman, L. 2018. The role of the Hedgehog signaling pathway in cancer: A comprehensive review. *Bosn J Basic Med Sci,* 18(1)**,** pp 8-20.

Smelkinson, M. G., Zhou, Q. & Kalderon, D. 2007. Regulation of Ci-SCFSlimb binding, Ci proteolysis, and hedgehog pathway activity by Ci phosphorylation. *Dev Cell,* 13(4)**,** pp 481-95.

Squire, J. M. 2016. Muscle contraction: Sliding filament history, sarcomere dynamics and the two Huxleys. *Glob Cardiol Sci Pract,* 2016(2)**,** pp e201611.

Srivastava, R. K., Kaylani, S. Z., Edrees, N., Li, C., Talwelkar, S. S., Xu, J., Palle, K., Pressey, J. G. & Athar, M. 2014. GLI inhibitor GANT-61 diminishes embryonal and alveolar rhabdomyosarcoma growth by inhibiting Shh/AKT-mTOR axis. *Oncotarget,* 5(23)**,** pp 12151-65.

Srivastava, S., Ramsbottom, S. A., Molinari, E., Alkanderi, S., Filby, A., White, K., Henry, C., Saunier, S., Miles, C. G. & Sayer, J. A. 2017. A human patient-derived cellular model of Joubert syndrome reveals ciliary defects which can be rescued with targeted therapies. *Hum Mol Genet,* 26(23)**,** pp 4657-4667.

Straface, G., Aprahamian, T., Flex, A., Gaetani, E., Biscetti, F., Smith, R. C., Pecorini, G., Pola, E., Angelini, F. & Stigliano, E. 2009a. Sonic hedgehog regulates angiogenesis and myogenesis during post-natal skeletal muscle regeneration. *Journal of cellular and molecular medicine,* 13(8b)**,** pp 2424-2435.

Strutt, H., Thomas, C., Nakano, Y., Stark, D., Neave, B., Taylor, A. M. & Ingham, P. W. 2001. Mutations in the sterol-sensing domain of Patched suggest a role for vesicular trafficking in Smoothened regulation. *Curr Biol,* 11(8)**,** pp 608-13.

Taipale, J., Cooper, M. K., Maiti, T. & Beachy, P. A. 2002. Patched acts catalytically to suppress the activity of Smoothened. *Nature,* 418(6900)**,** pp 892-7.

Tanno, B., Leonardi, S., Babini, G., Giardullo, P., De Stefano, I., Pasquali, E., Saran, A. & Mancuso, M. 2017. Nanog-driven cell-reprogramming and self-renewal maintenance in Ptch1 (+/-) granule cell precursors after radiation injury. *Sci Rep,* 7(1)**,** pp 14238.

Tatsumi, R., Anderson, J. E., Nevoret, C. J., Halevy, O. & Allen, R. E. 1998. HGF/SF is present in normal adult skeletal muscle and is capable of activating satellite cells. *Dev Biol,* 194(1)**,** pp 114-28.

Tedesco, F. S., Gerli, M. F., Perani, L., Benedetti, S., Ungaro, F., Cassano, M., Antonini, S., Tagliafico, E., Artusi, V., Longa, E., Tonlorenzi, R., Ragazzi, M., Calderazzi, G., Hoshiya, H., Cappellari, O., Mora, M., Schoser, B., Schneiderat, P., Oshimura, M., Bottinelli, R., Sampaolesi, M., Torrente, Y., Broccoli, V. & Cossu, G. 2012. Transplantation of

genetically corrected human iPSC-derived progenitors in mice with limb-girdle muscular dystrophy. *Sci Transl Med,* 4(140)**,** pp 140ra89.

Tenzen, T., Allen, B. L., Cole, F., Kang, J. S., Krauss, R. S. & McMahon, A. P. 2006. The cell surface membrane proteins Cdo and Boc are components and targets of the Hedgehog signaling pathway and feedback network in mice. *Dev Cell,* 10(5)**,** pp 647-56.

Thomas, K., Engler, A. J. & Meyer, G. A. 2015. Extracellular matrix regulation in the muscle satellite cell niche. *Connect Tissue Res,* 56(1)**,** pp 1-8.

Thomas, M., Langley, B., Berry, C., Sharma, M., Kirk, S., Bass, J. & Kambadur, R. 2000. Myostatin, a negative regulator of muscle growth, functions by inhibiting myoblast proliferation. *J Biol Chem,* 275(51)**,** pp 40235-43.

Tiffin, N., Williams, R. D., Shipley, J. & Pritchard-Jones, K. 2003. PAX7 expression in embryonal rhabdomyosarcoma suggests an origin in muscle satellite cells. *Br J Cancer,* 89(2)**,** pp 327-32.

Torroja, C., Gorfinkiel, N. & Guerrero, I. 2004. Patched controls the Hedgehog gradient by endocytosis in a dynamin-dependent manner, but this internalization does not play a major role in signal transduction. *Development,* 131(10)**,** pp 2395-408.

Towers, M., Mahood, R., Yin, Y. & Tickle, C. 2008. Integration of growth and specification in chick wing digit-patterning. *Nature,* 452(7189)**,** pp 882-6.

Towler, M. C., Kaufman, S. J. & Brodsky, F. M. 2004. Membrane traffic in skeletal muscle. *Traffic,* 5(3)**,** pp 129-39.

Troy, A., Cadwallader, A. B., Fedorov, Y., Tyner, K., Tanaka, K. K. & Olwin, B. B. 2012. Coordination of satellite cell activation and self-renewal by Par-complex-dependent asymmetric activation of p38alpha/beta MAPK. *Cell Stem Cell,* 11(4)**,** pp 541-53.

Tukachinsky, H., Kuzmickas, R. P., Jao, C. Y., Liu, J. & Salic, A. 2012. Dispatched and scube mediate the efficient secretion of the cholesterol-modified hedgehog ligand. *Cell Rep,* 2(2)**,** pp 308-20.

Uezumi, A., Fukada, S., Yamamoto, N., Takeda, S. & Tsuchida, K. 2010. Mesenchymal progenitors distinct from satellite cells contribute to ectopic fat cell formation in skeletal muscle. *Nat Cell Biol,* 12(2)**,** pp 143-52.

Uhmann, A., Dittmann, K., Nitzki, F., Dressel, R., Koleva, M., Frommhold, A., Zibat, A., Binder, C., Adham, I., Nitsche, M., Heller, T., Armstrong, V., Schulz-Schaeffer, W., Wienands, J. & Hahn, H. 2007. The Hedgehog receptor Patched controls lymphoid lineage commitment. *Blood,* 110(6)**,** pp 1814-23.

van der Ven, P. F. & Furst, D. O. 1997. Assembly of titin, myomesin and M-protein into the sarcomeric M band in differentiating human skeletal muscle cells in vitro. *Cell Struct Funct,* 22(1)**,** pp 163-71.

Varga, T., Mounier, R., Horvath, A., Cuvellier, S., Dumont, F., Poliska, S., Ardjoune, H., Juban, G., Nagy, L. & Chazaud, B. 2016. Highly Dynamic Transcriptional Signature of Distinct Macrophage Subsets during Sterile Inflammation, Resolution, and Tissue Repair. *J Immunol,* 196(11)**,** pp 4771-82.

Varjosalo, M. & Taipale, J. 2008. Hedgehog: functions and mechanisms. *Genes Dev,* 22(18)**,** pp 2454-72.

Veenstra, V. L., Dingjan, I., Waasdorp, C., Damhofer, H., van der Wal, A. C., van Laarhoven, H. W., Medema, J. P. & Bijlsma, M. F. 2018. Patched-2 functions to limit Patched-1 deficient skin cancer growth. *Cell Oncol (Dordr)*.

von Maltzahn, J., Jones, A. E., Parks, R. J. & Rudnicki, M. A. 2013. Pax7 is critical for the normal function of satellite cells in adult skeletal muscle. *Proc Natl Acad Sci U S A,* 110(41)**,** pp 16474-9.

Voronova, A., Coyne, E., Al Madhoun, A., Fair, J. V., Bosiljcic, N., St-Louis, C., Li, G., Thurig, S., Wallace, V. A., Wiper-Bergeron, N. & Skerjanc, I. S. 2013. Hedgehog signaling regulates MyoD expression and activity. *J Biol Chem,* 288(6)**,** pp 4389-404.

Wakabayashi, T. 2015. Mechanism of the calcium-regulation of muscle contraction--in pursuit of its structural basis. *Proc Jpn Acad Ser B Phys Biol Sci,* 91(7)**,** pp 321-50.

Wall, D. S., Mears, A. J., McNeill, B., Mazerolle, C., Thurig, S., Wang, Y., Kageyama, R. & Wallace, V. A. 2009. Progenitor cell proliferation in the retina is dependent on Notch-independent Sonic hedgehog/Hes1 activity. *J Cell Biol,* 184(1)**,** pp 101-12.

Wang, H., Kane, A. W., Lee, C. & Ahn, S. 2014b. Gli3 Repressor Controls Cell Fates and Cell Adhesion for Proper Establishment of Neurogenic Niche. *Cell Reports,* 8(4)**,** pp 1093-1104.

Wang, L. & Dynlacht, B. D. 2018. The regulation of cilium assembly and disassembly in development and disease. *Development,* 145(18)**,** pp.

Wang, Y., Dakubo, G. D., Thurig, S., Mazerolle, C. J. & Wallace, V. A. 2005. Retinal ganglion cell-derived sonic hedgehog locally controls proliferation and the timing of RGC development in the embryonic mouse retina. *Development,* 132(22)**,** pp 5103-13.

Wang, Y., Wehling-Henricks, M., Samengo, G. & Tidball, J. G. 2015. Increases of M2a macrophages and fibrosis in aging muscle are influenced by bone marrow aging and negatively regulated by muscle-derived nitric oxide. *Aging Cell,* 14(4)**,** pp 678-88.

Weintraub, H., Tapscott, S. J., Davis, R. L., Thayer, M. J., Adam, M. A., Lassar, A. B. & Miller, A. D. 1989. Activation of Muscle-Specific Genes in Pigment, Nerve, Fat, Liver, and Fibroblast Cell-Lines by Forced Expression of Myod. *Proceedings of the National Academy of Sciences of the United States of America,* 86(14)**,** pp 5434-5438.

Wen, Y., Bi, P., Liu, W., Asakura, A., Keller, C. & Kuang, S. 2012. Constitutive Notch activation upregulates Pax7 and promotes the self-renewal of skeletal muscle satellite cells. *Mol Cell Biol,* 32(12)**,** pp 2300-11.

Whalen, R. G., Harris, J. B., Butler-Browne, G. S. & Sesodia, S. 1990. Expression of myosin isoforms during notexin-induced regeneration of rat soleus muscles. *Dev Biol,* 141(1)**,** pp 24-40.

Wiendl, H., Hohlfeld, R. & Kieseier, B. C. 2005. Immunobiology of muscle: advances in understanding an immunological microenvironment. *Trends Immunol,* 26(7)**,** pp 373-80.

Winbanks, C. E., Wang, B., Beyer, C., Koh, P., White, L., Kantharidis, P. & Gregorevic, P. 2011. TGF-beta regulates miR-206 and miR-29 to control myogenic differentiation through regulation of HDAC4. *J Biol Chem,* 286(16)**,** pp 13805-14.

Wong, S. P., Rowley, J. E., Redpath, A. N., Tilman, J. D., Fellous, T. G. & Johnson, J. R. 2015. Pericytes, mesenchymal stem cells and their contributions to tissue repair. *Pharmacology & Therapeutics,* 151(107-120.

Xu, L., Liu, H., Yan, Z., Sun, Z., Luo, S. & Lu, Q. 2017. Inhibition of the Hedgehog signaling pathway suppresses cell proliferation by regulating the Gli2/miR-124/AURKA axis in human glioma cells. *Int J Oncol,* 50(5)**,** pp 1868-1878.

Xynos, A., Corbella, P., Belmonte, N., Zini, R., Manfredini, R. & Ferrari, G. 2010. Bone marrow-derived hematopoietic cells undergo myogenic differentiation following a Pax-7 independent pathway. *Stem Cells,* 28(5)**,** pp 965-73.

Yablonka-Reuveni, Z., Seger, R. & Rivera, A. J. 1999. Fibroblast growth factor promotes recruitment of skeletal muscle satellite cells in young and old rats. *J Histochem Cytochem,* 47(1)**,** pp 23-42.

Yabut, O., Pleasure, S. J. & Yoon, K. 2015. A Notch above Sonic Hedgehog. *Dev Cell,* 33(4)**,** pp 371-2.

Yamada, M., Tatsumi, R., Kikuiri, T., Okamoto, S., Nonoshita, S., Mizunoya, W., Ikeuchi, Y., Shimokawa, H., Sunagawa, K. & Allen, R. E. 2006. Matrix metalloproteinases are involved in mechanical stretch-induced activation of skeletal muscle satellite cells. *Muscle Nerve,* 34(3)**,** pp 313-9.

Yamane, H., Ihara, S., Kuroda, M. & Nishikawa, A. 2011. Adult-type myogenesis of the frog Xenopus laevis specifically suppressed by notochord cells but promoted by spinal cord cells in vitro. *In Vitro Cellular & Developmental Biology-Animal,* 47(7)**,** pp 470-483.

Yamashita, Y. M., Mahowald, A. P., Perlin, J. R. & Fuller, M. T. 2007. Asymmetric inheritance of mother versus daughter centrosome in stem cell division. *Science,* 315(5811)**,** pp 518-21.

Yan, D., Wu, Y., Yang, Y., Belenkaya, T. Y., Tang, X. & Lin, X. 2010. The cell-surface proteins Dally-like and Ihog differentially regulate Hedgehog signaling strength and range during development. *Development,* 137(12)**,** pp 2033-44.

Yang, R., Wang, M., Wang, J., Huang, X., Yang, R. & Gao, W. Q. 2015. Cell Division Mode Change Mediates the Regulation of Cerebellar Granule Neurogenesis Controlled by the Sonic Hedgehog Signaling. *Stem Cell Reports,* 5(5)**,** pp 816-828.

Yao, S., Lum, L. & Beachy, P. 2006. The ihog cell-surface proteins bind Hedgehog and mediate pathway activation. *Cell,* 125(2)**,** pp 343-57.

Yennek, S., Burute, M., Thery, M. & Tajbakhsh, S. 2014. Cell adhesion geometry regulates non-random DNA segregation and asymmetric cell fates in mouse skeletal muscle stem cells. *Cell Rep,* 7(4)**,** pp 961-70.

Yu, F., Kuo, C. T. & Jan, Y. N. 2006. Drosophila neuroblast asymmetric cell division: recent advances and implications for stem cell biology. *Neuron,* 51(1)**,** pp 13-20.

Yu, Y., Qi, L., Wu, J., Wang, Y., Fang, W. & Zhang, H. 2013. Kindlin 2 regulates myogenic related factor myogenin via a canonical Wnt signaling in myogenic differentiation. *PLoS One,* 8(5)**,** pp e63490.

Yurchenco, P. D., McKee, K. K., Reinhard, J. R. & Ruegg, M. A. 2017. Laminin-deficient muscular dystrophy: Molecular pathogenesis and structural repair strategies. *Matrix Biol*.

Zammit, P. S. 2017. Function of the myogenic regulatory factors Myf5, MyoD, Myogenin and MRF4 in skeletal muscle, satellite cells and regenerative myogenesis. *Semin Cell Dev Biol,* 72(19-32.

Zammit, P. S., Carvajal, J. J., Golding, J. P., Morgan, J. E., Summerbell, D., Zolnerciks, J., Partridge, T. A., Rigby, P. W. & Beauchamp, J. R. 2004a. Myf5 expression in satellite cells and spindles in adult muscle is controlled by separate genetic elements. *Dev Biol,* 273(2)**,** pp 454-65.

Zammit, P. S., Golding, J. P., Nagata, Y., Hudon, V., Partridge, T. A. & Beauchamp, J. R. 2004b. Muscle satellite cells adopt divergent fates: a mechanism for self-renewal? *J Cell Biol,* 166(3)**,** pp 347-57.

Zammit, P. S., Heslop, L., Hudon, V., Rosenblatt, J. D., Tajbakhsh, S., Buckingham, M. E., Beauchamp, J. R. & Partridge, T. A. 2002. Kinetics of myoblast proliferation show that resident satellite cells are competent to fully regenerate skeletal muscle fibers. *Exp Cell Res,* 281(1)**,** pp 39-49.

Zammit, P. S., Relaix, F., Nagata, Y., Ruiz, A. P., Collins, C. A., Partridge, T. A. & Beauchamp, J. R. 2006. Pax7 and myogenic progression in skeletal muscle satellite cells. *J Cell Sci,* 119(Pt 9)**,** pp 1824-32.

Zhang, T., Gunther, S., Looso, M., Kunne, C., Kruger, M., Kim, J., Zhou, Y. & Braun, T. 2015. Prmt5 is a regulator of muscle stem cell expansion in adult mice. *Nat Commun,* 6(7140.

Zhao, J., Yao, Y., Xu, C., Cheng, B. & Xu, Q. 2011. Expression of GAP-43 in fibroblast cell lines influences the orientation of cell division. *Int J Dev Neurosci,* 29(4)**,** pp 469-74.

Zhao, Y., Tong, C. & Jiang, J. 2007. Hedgehog regulates smoothened activity by inducing a conformational switch. *Nature,* 450(7167)**,** pp 252-8.

Zibat, A., Missiaglia, E., Rosenberger, A., Pritchard-Jones, K., Shipley, J., Hahn, H. & Fulda, S. 2010. Activation of the hedgehog pathway confers a poor prognosis in embryonal and fusion gene-negative alveolar rhabdomyosarcoma. *Oncogene,* 29(48)**,** pp 6323-30.

Zuo, X., Fogelgren, B. & Lipschutz, J. H. 2011. The small GTPase Cdc42 is necessary for primary ciliogenesis in renal tubular epithelial cells. *J Biol Chem,* 286(25)**,** pp 22469-77.